MOLECULAR BIOMARKERS FOR RESPIRATION IN *DEHALOCOCCOIDES ETHENOGENES* AND *METHANOSPIRLLUM HUNGATEI*: COMPARING PROTEIN AND MESSENGER-RNA ABUNDANCE IN ANAEROBES

A Dissertation

Presented to the Faculty of the Graduate School

of Cornell University

In Partial Fulfillment of the Requirements for the Degree of

Doctor of Philosophy

by

Annette Ruth Rowe

August 2011

MOLECULAR BIOMARKERS FOR RESPIRATION IN *DEHALOCOCCOIDES ETHENOGENES* AND *METHANOSPIRLLUM HUNGATEI*: COMPARING PROTEIN AND MESSENGER-RNA ABUNDANCE IN ANAEROBES

Annette Ruth Rowe, Ph. D.

Cornell University 2011

One of the major limitations in environmental microbiology and bioremediation is the inability to confidently monitor microbial processes *in situ.* The detection of molecular biomarkers, molecules of biological origin that are indicative of these processes, is one promising approach. In an anaerobic, dehalorespiring and methanogenic mixed culture, biomarkers for respiration of two organisms, *Dehalococcoides ethenogenes* sp. and *Methanospirillum hungatei* sp., have been identified. Both microbes utilize hydrogen as an electron donor. Targeted absolute quantification assays of mRNA and protein biomarkers for specific respiratory enzymes—the hydrogenases HupL and FrcA, the oxidoreductase MvrD, and the reductive dehalogenases TceA, PceA , DET1559 and DET1545—have been developed and used to quantify these molecules over an array of experimental conditions. To derive transcript-respiration trends, various donors and chloroethene acceptors were continuously fed to sub-cultures at different ratios and rates. These experiments induced pseudo-steady-state respiration and mRNA biomarker levels that could then be correlated. In both *Dehalococcoides* and *Methanospirillum,* linear correlations across mRNA biomarker levels and respiration (1 - 150 μeeq/L-hr) were

observed in the following targets: MvrD and FrcA for *Methanospirillum*, and HupL and TceA for *Dehalococcoides*. Other empirical trends were observed for *Dehalococcoides* biomarkers, including trends that saturate (the reductive dehalogenases PceA and DET1559) or decline (the dehalogenases DET1545) above a respiration rate of 5 μeeq/L-hr. Insight into how mRNA expression levels affect translation of proteins was gained through quantification of peptide biomarkers. Differences in absolute abundance of proteins-per-genome for *Dehalococcoides* and *Methanospirillum* suggest that mRNA abundance is a poor predictor of protein abundance across targets within an organism and across organisms. In *Dehalococcoides,* more TceA proteins were generated per transcript (0.4 - 1.2 proteins/mRNA-hr) than other monitored biomarker targets (0.03 - 0.17 proteins/ mRNA-hr). Protein decay rates for individual enzymes were indistinguishable from cell decay, suggesting that translation rates, rather than decay rates, are controlling the differences in protein abundance. Quantification of protein abundances allowed for the calculation of enzyme-specific rate constants for enzymes of known function in *Dehalococcoides*: TceA and PceA. These *in vivo* parameters could be utilized for predicting *in situ* process rates from protein abundance and metabolite levels. In addition, these data support the utility of both mRNA and protein biomarkers, especially for inferring process rates. However, they also highlight potential problems with inferring protein abundance from mRNA data alone and emphasize the need for strong empirically-derived correlations for any newly-discovered mRNA biomarker.

BIOGRAPHICAL SKETCH

I was born in Houston Texas (a rarely admitted fact), to a cardiologist and an internist. I was saved from middle child syndrome (or at least a severe case), by being the only girl. My family moved to Wailuku, Maui in 1986 where I remained, and was educated, until I attended college at U.C. Berkeley in 1999. I am still surprised that they accepted me given my inability to take standardized tests and the fact that I was not a valedictorian in my very small high school (only 48 students in my graduating class). Nonetheless, I worked off a healthy inferiority complex developed my first year in the Berkeley dorm, and managed to graduate with honors in Molecular and Cellular biology, and with a departmental citation in Microbial biology. My interest in Environmental Microbiology started in the Lab of Dr. Loy Volkman, working with Dr. Taro Ohkawa on Bachuloviruses, the subject of one of my favorite high school books, the Cobra Event. I additionally acquired a life-long love of Fungi thanks to working with Dr. Tom Bruns and Dr. John Taylor, and still can't believe that, after field trips to redwood forests in search of chanterelles with beer and bluegrass, that I didn't stick with mycology (but work and passion don't always mix). To round out my experience as a microbiologist, I decided to work on Bacteria and Archaea for my Ph.D. I also decided to try living on the east coast for graduate school, and have only second guessed that decision in late March when the weather is unforgiving (or when my partner wants to watch a surf film).

This is dedicated to my Mom and Dad, for loving me in spite of my faults, and never failing to point them out.

And to Nahala Adams, for the reminder that the people are as important as the science…or medicine.

ACKNOWLEDGMENTS

This is a long list! Mike Booth has made the biggest contribution to my happiness and sanity (making for much better science). Without Mike or his dissertation hugs, I would not have accomplished nearly as much. If it were not for his time, care and critiques, my defense likely would not have gone so smoothly. I can't think of a better sounding board (even if he does study macro-organisms).

In the lab, all of this work was done side by side, or in collaboration with two of the most phenomenal people I have ever met: Gretchen Heavner and Cresten Mansfeldt. I have a hard time imagining doing science without them. In addition to being brilliant scientists, they are two of the most pleasant people to be around. I found myself wanting to spend my free time with them in spite of having spent long hours with them in lab. I am grateful that they indulged me, and that we can find things to talk about beyond science.

Throughout my six years in graduate school, there is no single person that I learned more from then my advisor, Ruth Richardson. At times, getting a Ph. D feels like being a stubborn teenager (and my parents can attest to the fact that I can be a pain). Thankfully, Ruth doesn't seem to hold it against me. I am grateful for the freedom and the help (not to mention the flat out hard work) she has given me throughout the years, and in particular for not playing soccer against me too often.

Thanks to Jim Gossett and Steve Zinder, for their sound advice and support. In addition to being amazing scientists, it was a pleasure to experience all the expertise they had to offer. Jim in his methodical beer brewing, and Steve in his encyclopedic knowledge of great songs on guitar, have given me things to aspire to outside the lab as well.

The best part of graduate school, hands down, has been the friends that I have

made. I came to school with one, Punita (who helped me make so many more). There are few people outside my family who have seen me grow as much, or for whom I have gotten to do the same. In lab, the BA environmental engineering women (Clo, Gabi, Gretchen, Deborah and Iman) and the men who keep us up to affirmative action standards (Cresten, Wan, Brian, Po-Hsun, Matt and Jeff) have made the environmental lab a happy and fun place to work. In life, the brewing conspiracy and extended others Ben and Gretchen Heavner, Cloelle Sausville-Giddings, Mike Booth, Heather Fullerton, Arend Van Der Zande, Cresten Mansfeldt, Maddie Galac, Sarah Short, Matt Rendina, , Ben Logsdon, Gabi and Jose Hidalgo, Vivi Ruiz and Kathryn Gardner have been the best support system a person could ask for. Thank you for all the memories and your help with life, science, and beer drinking. I'm looking forward to many more brews with you all (you're all moving to Hawaii right?).

To Dan Buckley, and Steve Zinder, I am not sure how I got selected to be a TA for the Microbial diversity course, but it is an experience that has enriched my life and motivated me to stay in science.

Last but not least to my family. Mom and Dad were my first scientific mentors, despite claims that we raised ourselves (I'm pretty sure we would have been mal-nourished, with more scars if that were true). My brothers (whom I have known all my life) surprised me both by daring to be different and daring to be normal in ways I would have never guessed. I am looking forward to more games of apples to apples, surfing trips, and making fun of mom and dad when I get back to the islands.

TABLE OF CONTENTS

LIST OF FIGURES

LIST OF TABLES

CHAPTER 1

Background and Objectives

1.A. Introduction

Microbial communites can have profound impacts on environmental systems. Methane, a common end product of anaerobic food webs, is often formed from hydrogen, formate or acetate produced by syntrophic fermenters in consortia (90, 97). This process results in an estimated one gigaton of methane formed per year from biomass degradation (2% of the carbon dioxide fixed annually on Earth) (90). In similar anaerobic consortia, microbes have been shown to impact environmental quality through the transformation of chemical pollutants (52). A pertinent example is the bioremediation of the common ground water pollutants tetrachloroethene (PCE) and trichloroethene (TCE) to non-toxic ethene through an anaerobic process called organohalide respiration (64, 66). In this respiration, the organochlorine compound acts as a terminal electron acceptor, and chloride is released from the carbon backbone. Monitoring of microbial respirations such as methanogenesis and dehalorespiration has important implications in both environmental microbiology and environmental engineering. However, the nature of systems where these processes occur, such as those undergoing *in situ* bioremediation, make monitoring difficult (21). As such, detection of biologically synthesized molecules indicative of a process or physiologic state (biomarkers) could be used to infer metabolic activity of microbes (20). Understanding the biology of key organisms is essential to determining appropriate and informative biomarkers. **This dissertation specifically seeks to address two important questions in environmental microbiology and bioremediation: 1) how can we relate on a quantitative scale what a given biomarker means for the activity of an organism, and 2)**

how can we begin to understand differential activities of organisms in complex samples by tracking multiple biomarkers in whole communities.

Biomarker targets were developed for two organisms: a chloroethene respiring organism *Dehalococcoides ethenongenes* sp. (DET) and a hydrogenotrophic methanogen *Methanospirillum hungatei* sp. (MHU). Enzyme targets were chosen based on biochemical characterization, genomic inference and previous mRNA and/or protein biomarker work. Approaches to target specific genes in the forms of DNA, RNA and proteins on an absolute scale were developed for these organisms in an anaerobic mixed culture. This dissertation is divided into three paper chapters. The first paper chapter (Chapter 2) characterizes the microbial community being studied in addition to introducing the concept of comparing mRNA biomarkers in different microbial species. Each of the subsequent chapters focuses on mRNA and protein biomarker trends, as well as the relationship between these two molecules, in a single organism. Specifically, *Dehalococcoides* biomarkers are the focus in Chapter 3 and *Methanospirillum* biomarkers in Chapter 4. A comparison of these biomarker trends is further analyzed in Chapter 4 and highlighted in the final chapter (Chapter 5) which suggests future directions of this work. The following background sections provide contextual information highlighting the importance of the proposed work to the fields of environmental microbiology and environmental engineering, as well as support for the rationale of these research questions, and the approaches taken to address them.

1.B. Environmental Contamination with Chloroethenes

Chloroethenes are among the most common ground water pollutants in the United States (64, 67). A recent survey of ground water samples performed by the United States Geological

Survey (USGS) suggested that PCE and TCE are two of the three the most common pollutants detected above the Environmental Protection Agency's minimum contaminant level (MCL) (67). Three chloroethenes (PCE, TCE and vinyl-chloride) are listed among the top 40 contaminants in the 2007 Comprehensive Environmental Response, Compensation, and Liability Act (CERCLA) 'Priority list of hazardous substances', which ranks compounds based on prevalence and risk to human health (3). Vinyl chloride (VC) is the highest priority organic contaminant, listed fourth under arsenic, lead and mercury (3). While chloroethenes can be transformed biologically, many of these transformations result in production of lesser chlorinated organic compounds, which are equally, if not more toxic (most notably VC) (48). Currently, only members of *Dehalococcoides* (DHC) have been shown to metabolize VC to non-toxic ethene (12, 17). Additionally, many DHC have been shown to metabolize other compounds with a higher degree of chlorination, such as PCBs and dioxins (2, 9, 15, 30). The distribution, pervasiveness and incidence of human exposure to chlorinated organic compounds, and in particular chloroethenes (42), illustrates the need for successful and complete remediation.

1.C. Biomarkers for Bioremediation

The National Research Council's Committee on *In Situ* Bioremediation suggests three lines of evidence for demonstrating effective bioremediation:

> '1) documented loss of contaminants from the site,
>
> 2) laboratory assays showing that microorganisms from site samples have the *potential* to transform the contaminants under the expected site conditions, and
>
> 3) one or more pieces of information showing that the biodegradation potential is *actually realized* in the field.' (20)

Although the last line of evidence is often difficult to obtain, especially *in situ*, biomarkers (also known as bioindicators) hold promise for achieving this aim (12, 63). Commonly used in medicine, environmental science, food science and industrial microbiology, biomarkers can be of use in the detection of microbial pathogens, microbial contaminants, and in some cases, microbe stress (8, 72, 77). Application of biomarkers to bioremediation often focuses on identifying and quantifying populations of organisms that contain the metabolic potential to degrade contaminants, or the metabolic genes responsible for these activities (28, 34). For certain microorganisms with limited metabolic capabilities, detection at the population level can be an appropriate indicator of specific activities. However, in metabolically versatile organisms, demonstrating genetic capacity in a microbe only provides evidence of metabolic potential (*Dehalococcoides* specific discussion in section 1.E). In these cases, extending detection from DNA to RNA and proteins has been suggested, because these molecules provide evidence of gene expression (63). RNA, though less stable and traditionally more difficult to detect than DNA, is a stronger indicator of a specific activity. Detection of specific mRNAs of interest can provide evidence of energetic investment in expression of a certain pathway, response to specific environmental conditions, or both. Given knowledge of mRNA regulation and further understanding of how these mRNAs affect abundance of functional proteins, RNA-focused approaches hold promise for assessing microbial activities, and the incidences of such studies are increasing (18, 24, 33, 49, 50). Protein biomarkers, especially in the form of enzymes that catalyze key processes, may serve as the most direct evidence of realized metabolic capability in microbes. While studies that have looked at microbial proteins from field systems are limited (10, 68, 70, 88, 93), proteomic approaches are expanding and currently include methods with the

potential to provide quantitative information about the abundance of proteins from environmental systems (88, 92).

1.D. Dehalococcoides: Obligate Dehalorespirers

At anaerobic sites contaminated with chlorinated organic compounds, detection of microbial physiologies is often focused on the *Dehalococcoides* because all known members of the DHC are obligate dehalorespirers (12, 63). However, the specific substrate ranges of DHC can vary greatly with strain (38, 47, 65). Two of the specific reductive dehalogenase (RDase) enzymes that catalyze dehalorespiration in the first isolate, *Dehalococcoides ethenogenes,* have been characterized as PceA and TceA (60, 61). These enzymes catalyze the reduction of PCE to TCE (PceA) and TCE to cDCE, cDCE to VC, and with slower kinetics, VC to ethene (TceA) (Figure 1.1). They contain characteristic motifs and operon structures that allow for identification of homologs in the sequenced genomes of other DHC strains, as well as sequence identification of RDase genes present in environmental cultures (38, 39, 46, 91). In strains capable of respiration of VC to ethene, VC RDases have been identified, either biochemically (VcrA) or genetically (BvcA) (23, 45, 71). In addition to RDases, the sequenced DHC genomes contain other genes likely involved in the process of dehalorespiration—including a variety of hydrogenase sequences (47, 65, 85). DHC require hydrogen as an electron donor. As such, the nickel-iron hydrogenase Hup has been highlighted as important in hydrogen metabolism as it is the only hydrogenase predicted to contain a periplasmic catalytic subunit (Figure 1.1) (85). Hydrogen utilization studies in pure culture DHC strains have highlighted that respiration of chlorinated compounds does not differ between cell free and whole cell assays, suggesting hydrogenase activity external to DHC cells is important for dehalorespiration (75).

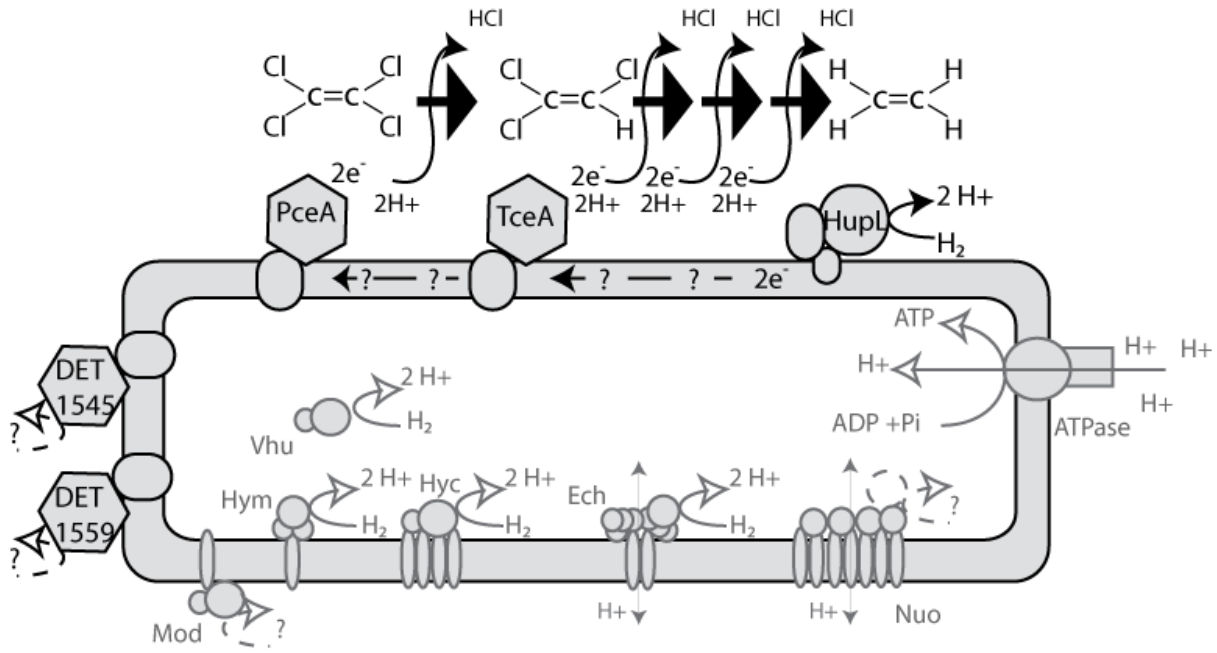

Figure 1.1. Adapted from Seshadri et al. 2005 (85), this diagram depicts respiratory proteins identified in the genome of *Dehalococcoides ethenogenes* str. 195 and detected in shotgun proteomic experiments (68, 69, Annette Rowe unpublished data). Known enzyme roles determined through either biochemical characterization (60, 61, 75) or homology to characterized protein families (47, 85) depicted with a solid line. Putative enzyme roles indicated with dashed lines. Biomarker targets outlined in black are further studied in this work.

Additionally, *hupL* is highly expressed, at both the protein and mRNA level, during reductive dechlorination (32, 69, 79) and highly conserved across strains (93-94% amino acid sequence similarity across strains). Other genes, highlighted in genomic work due to homology with electron transport chain enzymes, have been detected in both proteome and mRNA expression studies; however, the specific energy conserving pathways have not been elucidated (Figure 1.1) (32, 69, 79, Cresten Mansfelt unpublished data). Some of these putative oxidoreductases (Mod, Nuo and Fdh) are of questionable functionality due to amino acid substitutions in catalytic sites or the absence of important subunits in protein complexes (e.g., electron receiving subunit in Nuo) (85). Therefore, biomarker studies for DHC should focus predominantly on the genes with known function, as gateways to understand the respiration of chlorinated organic compounds in these organisms (32, 43, 49, 68, 69, 79, 91).

1.E. Field Biomarkers of Dehalococcoides

Application of DHC biomarkers at field sites contaminated with chloroethenes has predominantly focused on detection of populations based on bacterial clone library analysis or DHC 16S rRNA gene-specific PCR (37, 51, 62). While detection of DHC (via 16S rRNA genes) and sites undergoing complete reductive dechlorination to ethene can be correlated (37, 57), *Dehalococcoides* are often detected at sites where dechlorination has stalled at lower chlorinated ethenes like cDCE and VC (51, 58). While these studies do not report quantitative population measurements, other reports have demonstrated that DHC population size does not always correlate with the rate, fraction or type of end products of *in situ* dechlorination (82). Part of this variation likely stems from the metabolic variability amongst members of the DHC that share 97-100 percent sequence similarity in the 16S rRNA gene. Additionally, certain metabolic activities

(e.g. respiration of TCE) are shared across the different DHC groups classified based on 16S sequence similarity (Cornell, Victoria and Pinellas groups) - further highlighting the limitation of 16S rRNA gene detection. Gene specific biomarkers studies have demonstrated better correlations with specific reductive dechlorinating activity (76, 83). In Shuetz et al. 2008, an increase in *vcrA* genes (vinyl chloride reductive dehalogenase) coincided with a rise in ethene concentration (83). Nishimura et al. 2008 demonstrated that two different DHC populations were responsible for separate phases of reductive dechlorination: a *tceA*-containing population increased in abundance post treatment with a hydrogen releasing compound (HRC) (within first three months) followed by a *bvcA* containing populations (three to six months) (76). It is important to note that many reductive dehalogenases (including RDases of unknown function) are often detected at DHC containing sites undergoing remediation of chloroethenes (38, 46, 50, 91). At a field site undergoing remediation of TCE, transcripts for *tceA* were not always observed even though the gene was detected (50). In another study where *tceA* was detected at the mRNA level, abundance did not correlate with chloroethene respiration (24). In both of these studies, mRNA expression suggested that *tceA* was not the dominant RDase involved in degradation. This highlights the importance of choosing system-appropriate biomarkers as well as the potential utility of mRNA in determining the appropriateness of different targets.

1.F. Environmental Context: Obligate Community Members

There is significant evidence that an anaerobic microbial consortium is beneficial to the process of dehalorespiration (7, 35). Many of the same phylogenetic groups commonly occur with DHC both in lab studies and at field sites where bioremediation is occurring—suggesting a conserved community structure (27). Though DHC biomarkers have been highlighted and tested

in pure cultures, our biomarker studies have focused on DHC in mixed communities. As described above, DHC require hydrogen. In environmental systems, hydrogen is provided by syntrophic fermenters. Consortia members also supply growth factors and vitamins like B_{12} (and possibly methionine) that DHC are unable to synthesize (35, 40, 85). These observations highlight the importance of communities for DHC functioning and a potentially complex web of interactions. In addition to fermentations, dehalorespiration can occur in concert with other metabolisms that consume hydrogen, such as sulfate reduction, methanogenesis and acetogenesis (6, 16, 53). Competition for hydrogen has been observed in organisms with a variety of metabolic capabilities, both in lab consortia (4, 5, 6, 29, 96) and environmental settings (16, 54-56). Dechlorinators have a thermodynamic advantage over methanogens in systems fed electron donors and fermented under low hydrogen concentrations, but methanogens utilize hydrogen more rapidly at high hydrogen concentrations (87, 90). This highlights potential complications when constructing remediation strategies for environmental systems. Though many field bioremediation studies do not report methane concentrations, in certain studies methane increases were shown to coincide with enhanced reductive dechlorination (following stimulation of reductive dechlorination through vegetable oil donor amendment) (11) or even suggested to compete with reductive dechlorination (following stimulation of reductive dechlorination through excess donor addition) (58). Biomarkers for activities of multiple organisms would elucidate not only *in situ* ecology, but also organismal responses to a given feeding regime or treatment strategy. In turn, this information could be valuable in constructing efficient, as well as successful remediation strategies that mitigate undesired effects. Specifically, these strategies could minimize the growth of bacteria that are not essential to remediation activities (resulting in excess bacterial biomass in ground water) and produce endproducts such as methane—a

flammable greenhouse gas more than 20 times as potent as carbon dioxide (13)Methane concentrations from ground water as low as 1 mg/L have the potential to accumulate to explosive concentrations in poorly ventilated or confined areas, such as in the immediate vicinity of treatment zones.

1.G. Biomarkers for Methanospirillum

The majority of methanogenic species utilize hydrogen in the formation of methane from carbon dioxide (36). Two types of hydrogenotrophic methanogenesis pathways are known: one utilizes cytochromes (restricted to the *Methanosarcinales*) and one does not utilize cytochromes (all other methanogenic orders) (90). In general, methanogens without cytochromes have lower hydrogen thresholds (<10Pa), lower growth yields (up to 3 g dry weight biomass per mole CH_4) and faster minimum doubling times (as low as one hour) (90). *Methanospirillum* sp. are members of the *Methanomicrobiales* (methanogens without cytochromes) that are capable of reducing carbon dioxide to methane using hydrogen, formate or both hydrogen and formate as electron donors (31). The first step in methanogenesis involves the endergonic reaction that is driven by ferredoxin (Fd) oxidation between carbon dioxide and methanofuran (MFR) making the covalently bonded intermediate formyl-MFR (Figure 1.2, Rxn 1). This formyl group is transferred to another cofactor, tetrahydormethanopterin (H_4MPT) and then reduced to generate methyl-H_4MPT (Figure 1.2, Rxn 2-5). This methyl group is subsequently transferred to HS-coenzymeM to generate methyl-S-CoM (Figure 1.2, Rxn 6). The final step produces methane (Figure 1.2, Rxn 7), and a heterodisulfide (CoB-S-S-CoM), which in turn is reduced by heterodisulfide reductase in complex with a methyl-viologen reducing hydrogenase subunit (Figure 1.2, Rxn 8-9). Past the first step in this process, reduced F_{420} ($F_{420}H_2$) is utilized as a

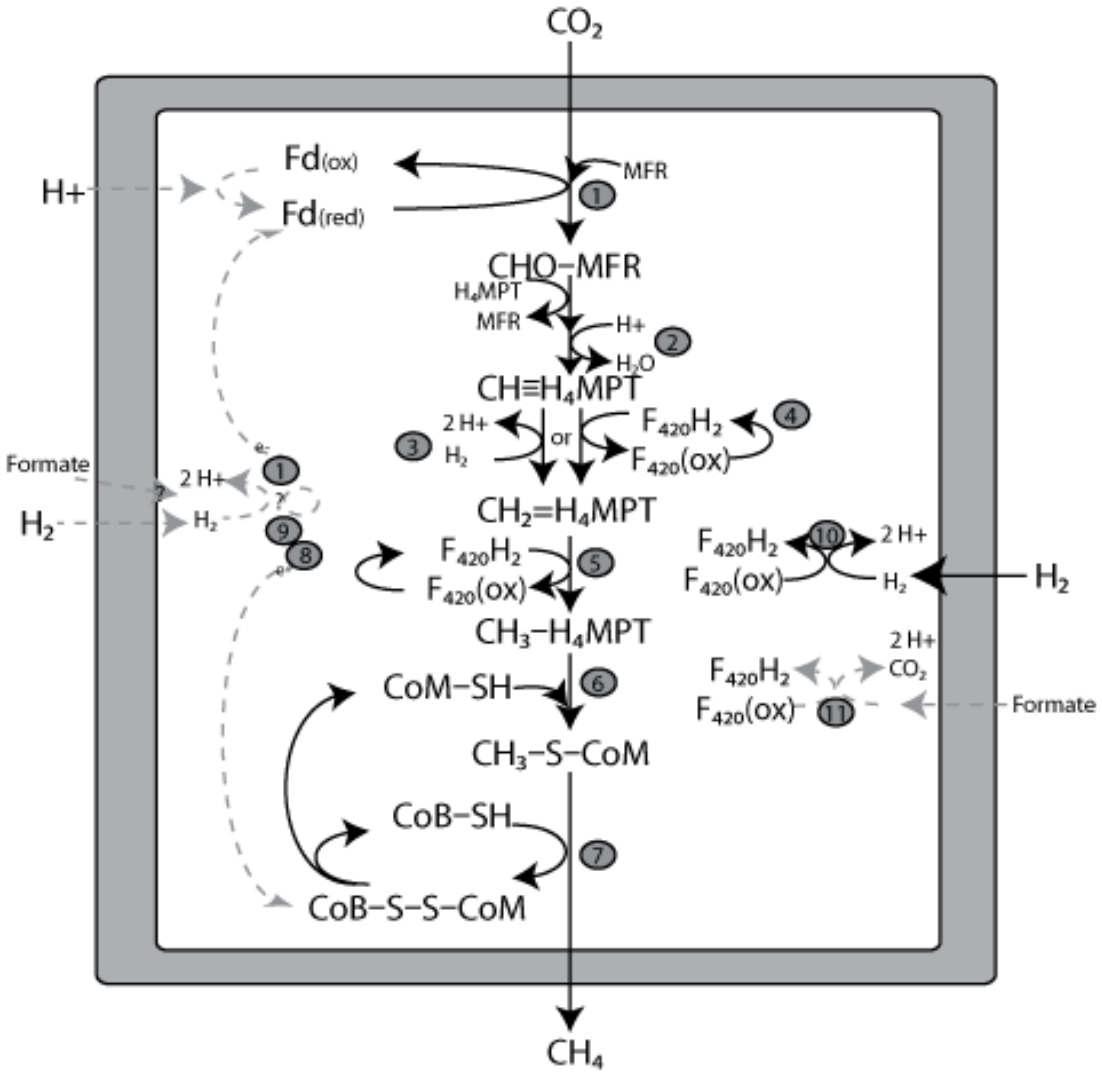

Figure 1.2. Schematic representing methanogenesis pathway in *Methanospirillum hungatei* based on genome sequence information (publically available through Integrated Microbial Genomes, http://img.jgi.doe.gov) as well as biochemical characterization in *Methanospirillum* and relatives (solid lines). Gray circle indicate specific reactions (discussed in text). Dashed lines depict hypothesized enzymatic reactions (discussed in text).

reducing agent. In many methanogens, this molecule is generated by a F_{420}-reducing hydrogenase (Frc) (Figure 1.2, Rxn 10) (86). Frc, a NiFe-hydrogenase, has been characterized in MHU (19), and was highly expressed in pure culture and co-culture with *Syntrophobacter fumaroxidans* (95). In other members of the *Methanomicrobiaes*, formate is converted to carbon dioxide and hydrogen through an F_{420}-dependent formate dehydrogenase (94) generating $F_{420}H_2$ as an intermediate (59, 90). Though many of the biochemical steps in methane formation are well characterized and conserved among methanogens (with and without cytochromes), recent insight has been gained into the biochemistry of the first and last step in methanogenesis (22, 90). In the hydrogenotrophic *Methanothermobacter marburgensis*, the importance of a methyl-viologen reducing (Mvr) (a.k.a., F_{420}-non-reducing hydrogenase) and in particular the MvrD subunit was implicated as essential to providing electrons to the last steps in methanogenesis (Figure 1.2, Rxn 9) (22, 89). Recently, Mvr was shown to form a complex with both heterodisulfide reductase (Hdr) and formylmethanofuran dehydrogenase (Fwd) (22, 44). In members of the *Methanococcales*, this Mvr-Hdr-Fwd complex includes a formate dehydrogenase (22) (Figure 1.2, Rxn 11). This protein complex couples the endergonic reduction of ferredoxin (that drives the first endergonic step in methanogenesis) with the exergonic reduction of heterodisulfide (Figure 1.2, Rxn 12) (22, 44). While it was previously thought that reverse electron transport was responsible for generating reduced Fd (which may still play a role under certain conditions) (86), this electron bifurcation reaction couples Fd reduction to a process that translocates protons across the cytoplasmic membrane, as well as regenerating essential cofactors. There is also evidence that this complex can utilize either a F_{420}-reducing hydrogenase or F_{420} directly (14, 90). Mvr-Hdr-Fwd protein complexes and their corresponding reactivity have only recently been elucidated and this activity has not yet been demonstrated in MHU.

However, many of the protein subunits highlighted in this reaction complex are present in the *Methanospirillum hungatei* JF-1 genome (Integrated Microbial Genomes; http://img.jgi.doe.gov.). The F_{420}-reducing hydrogenase (FrcA) was chosen as a biomarker because its role in hydrogen utilization for methanogenesis has been well characterized in MHU (19). Additionally, the MvrD subunit was also chosen as a biomarker due to its putative importance in the last step of methanogenesis (89), though the specific source of electrons for this reaction has not been documented.

1.H. Correlating Dehalococcoides Respiration Rate to mRNA Biomarkers

Biomarker development in this work has been conducted in a chloroethene-respiring and methanogenic mixed culture that contains *Dehalococcoides ethenogenes* str. 195 (DET). Previously in this system the expression of different functionally relevant genes for DET has been tested. These previous studies focused on RDases, specifically *pceA* and *tceA* that catalyze the dechlorination of PCE and TCE respectively (60, 61), and the putative (and often highly expressed) RDases DET1545 and DET1559, in addition to highly expressed oxidoreductases, like the annotated formate dehydrogenase *fdhA* and the hydrogenase *hupL* (described previously) (79). Quantifying transcript abundance in a pseudo-steady-state system (at steady-state with respect to respiration rate and mRNA expression in copies/mL) demonstrated that the majority of indicators observed increased linearly over a limited range of respiration rates (78, 80). However, at the highest feeding rates, this correlation lacked linearity because mRNA expression appeared to plateau or even decline at the highest feeding rates (80). Separate sets of studies with PCE (n=6), TCE (n=3) and cDCE (n=3) as electron acceptors suggested that RDase mRNAs may provide insight into the types of substrates, or even substrate concentration, respired by

organisms (78). Hydrogenases, on the other hand, provided the best information about the overall respiration rate, regardless of substrate. Though many of the mRNAs studied suggested a saturation in the up-regulation of transcription, proteins were not monitored during these experiments and it was unclear whether protein levels were similarly plateauing. Some insight may be gained from the 16S rRNA measurements in these studies. Of the twelve rate/substrate combinations tested in this previous work, the only experimental series to exhibit statistically significant changes in 16S rRNA levels per mL were the highest feeding rates (80). While some increase in rRNA abundance was expected due to an increase (79%) in DET population during this experiment, the observed growth could not compensate for the two orders of magnitude increase in 16S rRNA abundance. Though the trend between increased ribosome content per cell and growth rate has been well characterized and demonstrated in several organisms (25, 26, 81, 84), in DET, trends between growth and respiration on rRNA content are not well understood. Since translation of protein is a function of both mRNA and ribosomes, DET are potentially regulating translation of proteins through abundance of multiple types of RNA (mRNA, rRNA, tRNA, etc.). Though peptides from these biomarkers are commonly detected in mixed culture shotgun proteomic experiments, quantitative proteomic studies have been limited. Additional studies are required to further resolve RNA and protein relationships**.**

1.I. From mRNA to Protein

One potential limitation of mRNA biomarkers is knowledge of how these molecules are informative of proteins. Strong biomarkers are those functionally related to the process for which they serve as indicators. While mRNA is essential to protein production, the specifics of translation (i.e., how much protein is produced from a given mRNA and whether other factors

besides mRNA are required) for various transcripts within an organism and across organisms, has not been well characterized. Studies that have looked at global abundance of both mRNA and proteins suggest that there is significant transcript-to-transcript variation within organisms (1). Though analytical limitations may explain some of the variation, mRNA-specific differences have been shown to result in translational differences in: (1) ribosome binding and initiation, (2) elongation efficiency (based on codon or amino acid usage), and (3) stop codon effectiveness. Ribosome binding and initiation effectiveness were found to be useful in explaining variation in the mRNA-protein relationship in *Desulfovibrio*, but have been less informative in other organisms (41, 73, 74). Mechanisms of secondary regulation of mRNA have also been highlighted including mRNA silencing and mRNAs that act as sensor mRNAs. This can result in the uncoupling of mRNA synthesis and protein synthesis as has been demonstrated for the periplasmic iron binding protein gene *sfuC* in *Candidatus Pelagibacter ubique* (88). Additionally post translational regulation and/or rates of protein degradation can also affect the observed differences in the protein-mRNA correlation. Understanding this variation can have important implications for interpreting RNA biomarker expression data.

1.J. Rationale for Approach

My main focus in biomarker development has centered on monitoring mRNAs and peptides from catalytic enzymes in response to respiratory conditions. Approaches applied include: 1) monitoring of protein levels through quantitative proteomic approaches and 2) monitoring transcript levels of corresponding proteins. Direct monitoring of protein abundance is desirable because proteins are the functional unit of activity. From a biomarker perspective mRNAs and proteins have distinct benefits and drawbacks. While proteins indicate the potential

for activity, knowledge of other factors (i.e., substrate concentration) is required to assess activity from these measurements. In addition, most proteomic methods are relatively new and have yet to be standardized.

Alternatively, RNA quantification methods, specifically qRT-PCR and microarrays, are well established. Amplification of signal from RNA and DNA, opposed to proteins, allows detection of low abundance biomarkers. As RNA is a more sensitive biomarker, (i.e., shorter half life) it is less prone to residual signals that are potentially problematic for inferring instantaneous activity levels from DNA and proteins. Given that mRNAs expression is not always coupled with translation, and that currently there is no universal relationship between mRNA abundance and protein abundance, our understanding of how mRNA biomarkers function to produce proteins on a quantitative level for different organisms remains a limitation to relying on mRNA biomarkers alone.

1.K. Research Objectives

The main research goal of this work is to test the potential of organism-specific mRNA and proteins biomarkers to infer respiratory activity in complex communities. Quantification of mRNA and protein targets has focused on two hydrogen-utilizing organisms (DET and MHU) in an anaerobic mixed culture maintained on PCE and butyrate for more than twelve years.

In the first paper chapter (Chapter 2) of this dissertation, I seek to characterize the microbial community present in this system with a focus on identifying physiologies responsible for hydrogen consumption. Additionally, observations that DET, when grown in mixed culture, associate in mixed species bioflocs as well as planktonically, led me to explore the potential for heterogeneity with respect to activity in this system. Specifically, I examine the potential for

differences in transcriptional activity between these different growth forms, using mRNA biomarkers developed for the two hydrogen-consuming organisms. This work has led me to question how the differences in mRNA expression levels in addition to ribosome content could lead to differences in translation between these two hydrogen consuming organisms.

Chapter 3 extends previous DET biomarker work, by expanding the range of experimental conditions to empirically test mRNA dynamics, in addition to testing protein biomarker targets. This is the first work in DET that incorporates quantitative proteomic approaches in conjunction with mRNA work to estimate protein production from mRNA. My goals are to: 1) confirm protein production of different biomarker targets from mRNA and 2) to compare protein production rates among different mRNA biomarker targets. I also introduce this approach as a potential means to calculate *in vivo* kinetic parameters for protein biomarkers. In conjunction with metabolite data, such parameters could be used for the calculation of specific activity.

Chapter 4 focuses on MHU hydrogenase mRNAs and proteins as potential biomarkers of hydrogenotrophic methanogenesis. Shotgun proteomic work has confirmed the presence of many of MHUs putative methanogenesis enzymes, in addition MHU biomarker targets previously studied at the RNA level. I extend previous *Methanospirillum* RNA work (Chapter 2), by including an additional hydrogenase as a biomarker target (FrcA). I also develop approaches to quantify MHU respiration in the absence of acetoclastic methanogenesis in order to correlate mRNA biomarkers with MHU methane production. The final objective of this work is to compare biomarkers between DET and MHU, in order to test the feasibility of utilizing these molecules to compare respiration in complex samples. I compare how overall levels of mRNA

expression vary with respect to respiration rate between these organisms, and, in turn, how these RNA biomarker differences relate to abundance of proteins.

This work has highlighted new directions in which to focus research with respect to both *Methanospirillum* and *Dehalococcoides* biomarkers. These directions are discussed in the final chapter of this dissertation.

REFERENCES

1. **Abreu, R. d. S., L. O. Penalva, E. M. Marcotte, and C. Vogel.** 2009. Global signatures of protein and mRNA expression levels. Mol. BioSyst.. **5:**1512-1526.

2. **Adrian, L., U. Szewzyk, J. Wecke, and H. Gorisch.** 2000. Bacterial dehalorespiration with chlorinated benzenes. Nature. **408:**580-583.

3. **Agency for Toxic Substances and Disease Registry (ATSDR).** 2007 CERCLA Priority List of Hazardous Substances. http://www.atsdr.cdc.gov/cercla/07list.html

4. **Aulenta, F., A. Fina, M. Potalivo, M. P. Papini, S. Rossetti, and M. Majone.** 2005. Anaerobic transformation of tetrachloroethane, perchloroethylene, and their mixtures by mixed-cultures enriched from contaminated soils and sediments. Water Sci. and Technol. **52:**357-362.

5. **Aulenta, F., S. Rossetti, M. Majone, and V. Tandoi.** 2004. Detection and quantitative estimation of *Dehalococcoides* spp. in a dechlorinating bioreactor by a combination of fluorescent *in situ* hybridisation (FISH) and kinetic analysis. Appl. Microbiol. Biotechnol. **64:**206-212.

6. **Aulenta, F., J. M. Gossett, M. P. Papini, S. Rossetti, and M. Majone.** 2005. Comparative study of methanol, butyrate, and hydrogen as electron donors for long-term dechlorination of tetrachloroethene in mixed anerobic cultures. Biotechnol. Bioeng. **91:**743-753.

7. **Becker, J. G., G. Berardesco, B. E. Rittmann, and D. A. Stahl.** 2005. The role of syntrophic associations in sustaining anaerobic mineralization of chlorinated organic compounds. Environ. Health Perspect. **113:**310-316.

8. **Becker, P., W. Hufnagle, G. Peters, and M. Herrmann.** 2001. Detection of Differential Gene Expression in Biofilm-Forming versus Planktonic Populations of *Staphylococcus aureus* Using Micro-Representational-Difference Analysis. Appl. Environ. Microbiol. **67:**2958-2965.

9. **Bedard, D. L., K. A. Ritalahti, and F. E. Loffler.** 2007. The *Dehalococcoides* population in sediment-free mixed cultures metabolically dechlorinates the commercial polychlorinated biphenyl mixture aroclor 1260. Appl. Environ. Microbiol. **73:**2513-2521.

10. **Benndorf, D., G. U. Balcke, H. Harms, and M. von Bergen.** 2007. Functional metaproteome analysis of protein extracts from contaminated soil and groundwater. ISME J. **1:**224-234.

11. **Bennett, P., D. Gandhi, S. Warner, and J. Bussey.** 2007. *In situ* reductive dechlorination of chlorinated ethenes in high nitrate groundwater. J. Hazard. Mater. **149:**568-573.

12. **Bhatt, P., M. S. Kumar, S. Mudliar, and T. Chakrabarti.** 2007. Biodegradation of chlorinated compounds - A review. Crit. Rev. Environ. Sci. Technol. **37:**165-198.

13. **Bousquet, P., P. Ciais, J. B. Miller, E. J. Dlugokencky, D. A. Hauglustaine, C. Prigent, G. R. Van der Werf, P. Peylin, E. -. Brunke, C. Carouge, R. L. Langenfelds, J. Lathiere, F. Papa, M. Ramonet, M. Schmidt, L. P. Steele, S. C. Tyler, and J. White.** 2006. Contribution of anthropogenic and natural sources to atmospheric methane variability. Nature (London). **443:**439-443.

14. **Brodersen, J., G. Gottschalk, and U. Deppenmeier.** 1999. Membrane-bound F420H2-dependent heterodisulfide reduction in *Methanococcus voltae*. Arch. Microbiol. **171:**115-121.

15. **Bunge, M., L. Adrian, A. Kraus, M. Opel, W. G. Lorenz, J. R. Andreesen, H. Gorisch, and U. Lechner.** 2003. Reductive dehalogenation of chlorinated dioxins by an anaerobic bacterium. Nature. **421:**357-360.

16. **Chapelle, F. H., and D. R. Lovley.** 1992. Competitive Exclusion of Sulfate Reduction by Iron-Iii-Reducing Bacteria a Mechanism for Producing Discrete Zones of High-Iron Ground Water. Ground Water. **30:**29-36.

17. **Chen, G.** 2004. Reductive dehalogenation of tetrachloroethylene by microorganisms: current knowledge and application strategies. Appl. Microbiol. Biotechnol. **63:**373-377.

18. **Chin, K. J., A. Esteve-Nunez, C. Leang, and D. R. Lovley.** 2004. Direct correlation between rates of anaerobic respiration and levels of mRNA for key respiratory genes in *Geobacter sulfurreducens*. Appl. Environ. Microbiol. **70:**5183-5189.

19. **Choquet, C. G., and G. D. Sprott.** 1991. Metal Chelate Affinity-Chromatography for the Purification of the F420-Reducing (Ni,fe) Hydrogenase of Methanospirillum hungatei. J. Microbiol. Methods. **13:**161-169.

20. **Committee on *In Situ* Bioremediation, National Research Council.** 1993. *In Situ* Bioremediation: When does it work? National Acadamies Press, Washington D.C.

21. **Committee on Source Removal of Contaminants in the Subsurface, National Research Council.** 2004. Contaminants in the Subsurface: Source Zone Assessment and Remediation. National Acadamies Press, Washington DC.

22. **Costa, K. C., P. M. Wong, T. Wang, T. J. Lie, J. A. Dodsworth, I. Swanson, J. A. Burn, M. Hackett, and J. A. Leigh.** 2010. Protein complexing in a methanogen suggests electron bifurcation and electron delivery from formate to heterodisulfide reductase. Proc. Natl. Acad. Sci. U. S. A. **107:**11050-11055.

23. **Cupples, A. M., A. M. Spormann, and P. L. McCarty.** 2004. Vinyl chloride and cis-dichloroethene dechlorination kinetics and microorganism growth under substrate limiting conditions. Environ. Sci. Technol. **38:**1102-1107.

24. **Da Silva, M. L. B., and P. J. J. Alvarez.** 2008. Exploring the Correlation between Halorespirer Biomarker Concentrations and TCE Dechlorination Rates. J Environ. Eng.-Asce. **134:**895-901.

25. **Dethlefsen, L., and T. M. Schmidt.** 2005. Differences in codon bias cannot explain differences in translational power among microbes. BMC Bioinformatics. **6:**3.

26. **Dethlefsen, L., and T. M. Schmidt.** 2007. Performance of the Translational Apparatus Varies with the Ecological Strategies of Bacteria. J. Bacteriol. **189:**3237-3245.

27. **Duhamel, M., and E. A. Edwards.** 2006. Microbial composition of chlorinated ethene-degrading cultures dominated by *Dehalococcoides*. FEMS Microbiol. Ecol. **58:**538-549.

28. **El Fantroussi, S., and S. N. Agathos.** 2005. Is bioaugmentation a feasible strategy for pollutant removal and site remediation? Curr. Opin. Microbiol. **8:**268-275.

29. **Fennell, D. E., and J. M. Gossett.** 1998. Modeling the production of and competition for hydrogen in a dechlorinating culture. Environ. Sci. Technol. **32:**2450-2460.

30. **Fennell, D. E., I. Nijenhuis, S. F. Wilson, S. H. Zinder, and M. M. Haggblom.** 2004. *Dehalococcoides ethenogenes* strain 195 reductively dechlorinates diverse chlorinated aromatic pollutants. Environ. Sci. Technol. **38:**2075-2081.

31. **Ferry, J. G., P. H. Smith, and R. S. Wolfe.** 1974. *Methanospirillum*, a new genus of methanogenic bacteria, and characterization of *Methanospirillum hungatei* sp. nov. Int. J. Syst. Bacteriol. **24:**465--469.

32. **Fung, J. M., R. M. Morris, L. Adrian, and S. H. Zinder.** 2007. Expression of reductive dehalogenase genes in *Dehalococcoides ethenogenes* strain 195 growing on tetrachloroethene, trichloroethene, or 2,3-dichlorophenol. Appl. Environ. Microbiol. **73:**4439-4445.

33. **Futamata, H., S. Kaiya, M. Sugawara, and A. Hiraishi.** 2009. Phylogenetic and Transcriptional Analyses of a Tetrachloroethene-Dechlorinating "*Dehalococcoide*s" Enrichment Culture TUT2264 and Its Reductive-Dehalogenase Genes. Microbes Environ. **24:**330-337.

34. **Giddings, C. G. S., L. K. Jennings, and J. M. Gossett.** 2010. Microcosm Assessment of a DNA Probe Applied to Aerobic Degradation of cis-1,2-Dichloroethene by *Polaromonas* sp Strain JS666. Ground Water Monit. Remediat. **30:**97-105.

35. **He, J. Z., V. F. Holmes, P. K. H. Lee, and L. Alvarez-Cohen.** 2007. Influence of vitamin B-12 and cocultures on the growth of *Dehalococcoides* isolates in defined medium. Appl. Environ. Microbiol. **73:**2847-2853.

36. **Hendrickson, E. L., R. Kaul, Y. Zhou, D. Bovee, P. Chapman, J. Chung, E. C. de Macario, J. A. Dodsworth, W. Gillett, D. E. Graham, M. Hackett, A. K. Haydock, A. Kang, M. L. Land, R. Levy, T. J. Lie, T. A. Major, B. C. Moore, I. Porat, A. Palmeiri, G. Rouse,**

C. Saenphimmachak, D. Soll, S. Van Dien, T. Wang, W. B. Whitman, Q. Xia, Y. Zhang, F. W. Larimer, M. V. Olson, and J. A. Leigh. 2004. Complete genome sequence of the genetically tractable hydrogenotrophic methanogen *Methanococcus maripaludis*. J. Bacteriol. **186:**6956-6969.

37. **Hendrickson, E. R., J. A. Payne, R. M. Young, M. G. Starr, M. P. Perry, S. Fahnestock, D. E. Ellis, and R. C. Ebersole.** 2002. Molecular analysis of *Dehalococcoides* 16S ribosomal DNA from chloroethene-contaminated sites throughout north America and Europe. Appl. Environ. Microbiol. **68:**485-495.

38. **Holmes, V. F., J. Z. He, P. K. H. Lee, and L. Alvarez-Cohen.** 2006. Discrimination of multiple *Dehalococcoides* strains in a trichloroethene enrichment by quantification of their reductive dehalogenase genes. Appl. Environ. Microbiol. **72:**5877-5883.

39. **Holscher, T., R. Krajmalnik-Brown, K. M. Ritalahti, F. von Wintzingerode, H. Gorisch, F. E. Loffler, and L. Adrian.** 2004. Multiple nonidentical reductive-dehalogenase-homologous genes are common in *Dehalococcoides*. Appl. Environ. Microbiol. **70:**5290-5297.

40. **Islam, M. A., E. A. Edwards, and R. Mahadevan.** 2010. Characterizing the Metabolism of *Dehalococcoides* with a Constraint-Based Model. Plos Comp. Biol. **6:**e1000887.

41. **Jayapal, K. P., R. J. Philp, Y. Kok, M. G. S. Yap, D. H. Sherman, T. J. Griffin, and W. Hu.** 2008. Uncovering Genes with Divergent mRNA-Protein Dynamics in *Streptomyces coelicolor*. Plos One. **3:**e2097.

42. **Jia, C., J. D'Souza, and S. Batterman.** 2008. Distributions of personal VOC exposures: A population-based analysis. Environ. Int. **34:**922-931.

43. **Johnson, D. R., P. K. H. Lee, V. F. Holmes, A. C. Fortin, and L. Alvarez-Cohen.** 2005. Transcriptional expression of the tceA gene in a *Dehalococcoides*-containing microbial enrichment. Appl. Environ. Microbiol. **71:**7145-7151.

44. **Kaster, A., J. Moll, K. Parey, and R. K. Thauer.** 2011. Coupling of ferredoxin and heterodisulfide reduction via electron bifurcation in hydrogenotrophic methanogenic archaea. Proc. Natl. Acad. Sci. U. S. A. **108:**2981-2986.

45. **Krajmalnik-Brown, R., T. Holscher, I. N. Thomson, F. M. Saunders, K. M. Ritalahti, and F. E. Loffler.** 2004. Genetic identification of a putative vinyl chloride reductase in *Dehalococcoides* sp strain BAV1. Appl. Environ. Microbiol. **70:**6347-6351.

46. **Krajmalnik-Brown, R., Y. Sung, K. M. Ritalahti, F. M. Saunders, and F. E. Loffler.** 2007. Environmental distribution of the trichloroethene reductive dehalogenase gene (tceA) suggests lateral gene transfer among *Dehalococcoides*. FEMS Microbiol. Ecol. **59:**206-214.

47. **Kube, M., A. Beck, S. H. Zinder, H. Kuhl, R. Reinhardt, and L. Adrian.** 2005. Genome sequence of the chlorinated compound respiring bacterium *Dehalococcoides* species strain CBDB1. Nat. Biotechnol. **23:**1269-1273.

48. **Lee, M. D., J. M. Odom, and R. J. Buchanan.** 1998. New perspectives on microbial dehalogenation of chlorinated solvents: Insights from the field. Annu. Rev. Microbiol. **52:**423-452.

49. **Lee, P. K. H., D. R. Johnson, V. F. Holmes, J. Z. He, and L. Alvarez-Cohen.** 2006. Reductive dehalogenase gene expression as a biomarker for physiological activity of *Dehalococcoides* spp. Appl. Environ. Microbiol. **72:**6161-6168.

50. **Lee, P. K. H., T. W. Macbeth, K. S. Sorenson Jr., R. A. Deeb, and L. Alvarez-Cohen.** 2008. Quantifying Genes and Transcripts To Assess the *In Situ* Physiology of "*Dehalococcoides*" spp. in a Trichloroethene-Contaminated Groundwater Site. Appl. Environ. Microbiol. **74:**2728-2739.

51. **Lendvay, J. M., F. E. Loffler, M. Dollhopf, M. R. Aiello, G. Daniels, B. Z. Fathepure, M. Gebhard, R. Heine, R. Helton, J. Shi, R. Krajmalnik-Brown, C. L. Major, M. J. Barcelona, E. Petrovskis, R. Hickey, J. M. Tiedje, and P. Adriaens.** 2003. Bioreactive Barriers: A Comparison of Bioaugmentation and Biostimulation for Chlorinated Solvent Remediation. Environ. Sci. Technol. **37:**1422-1431.

52. **Loeffler, F. E., and E. A. Edwards.** 2006. Harnessing microbial activities for environmental cleanup. Curr. Opin. Biotechnol. **17:**274-284.

53. **Lovley, D. R., D. F. Dwyer, and M. J. Klug.** 1982. Kinetic Analysis of Competition between Sulfate Reducers and Methanogens for Hydrogen in Sediments. Appl. Environ. Microbiol. **43:**1373-1379.

54. **Lovley, D. R., and M. J. Klug.** 1983. Methanogenesis from Methanol and Methylamines and Acetogenesis from Hydrogen and Carbon Di Oxide in the Sediments of a Eutrophic Lake. Appl. Environ. Microbiol. **45:**1310-1315.

55. **Lovley, D. R., and M. J. Klug.** 1983. Sulfate Reducers can Out Compete Methanogens at Fresh Water Sulfate Concentrations. Appl. Environ. Microbiol. **45:**187-192.

56. **Lovley, D. R., and E. J. P. Phillips.** 1987. Competitive Mechanisms for Inhibition of Sulfate Reduction and Methane Production in the Zone of Ferric Iron Reduction in Sediments. Appl. Environ. Microbiol. **53:**2636-2641.

57. **Lu, X., J. T. Wilson, and D. H. Kampbell.** 2006. Relationship between geochemical parameters and the occurrence of *Dehalococcoides* DNA in contaminated aquifers. Water Resour. Res. **42:**W08427.

58. **Lu, X., J. T. Wilson, and D. H. Kampbell.** 2009. Comparison of an assay for *Dehalococcoides* DNA and a microcosm study in predicting reductive dechlorination of chlorinated ethenes in the field. Environ. Pollution. **157:**809-815.

59. **Lupa, B., E. L. Hendrickson, J. A. Leigh, and W. B. Whitman.** 2008. Formate-Dependent H-2 Production by the Mesophilic Methanogen *Methanococcus maripaludis*. Appl. Environ. Microbiol. **74:**6584-6590.

60. **Magnuson, J. K., M. F. Romine, D. R. Burris, and M. T. Kingsley.** 2000. Trichloroethene reductive dehalogenase from *Dehalococcoides ethenogenes:* Sequence of tceA and substrate range characterization. Appl. Environ. Microbiol. **66:**5141-5147.

61. **Magnuson, J. K., R. V. Stern, J. M. Gossett, S. H. Zinder, and D. R. Burris.** 1998. Reductive dechlorination of tetrachloroethene to ethene by two-component enzyme pathway. Appl. Environ. Microbiol. **64:**1270-1275.

62. **Major, D. W., M. L. McMaster, E. E. Cox, E. A. Edwards, S. M. Dworatzek, E. R. Hendrickson, M. G. Starr, J. A. Payne, and L. W. Buonamici.** 2002. Field demonstration of successful bioaugmentation to achieve dechlorination of tetrachloroethene to ethene. Environ. Sci. Technol. **36:**5106-5116.

63. **Maphosa, F., W. M. de Vos, and H. Smidt.** 2010. Exploiting the ecogenomics toolbox for environmental diagnostics of organohalide-respiring bacteria. Trends Biotechnol. **28:**308-316.

64. **McCarty, P. L.** 1997. Microbiology - Breathing with chlorinated solvents. Science. **276:**1521-1522.

65. **McMurdie, P. J., S. F. Behrens, J. A. Mueller, J. Goeke, K. M. Ritalahti, R. Wagner, E. Goltsman, A. Lapidus, S. Holmes, F. E. Loeffler, and A. M. Spormann.** 2009. Localized Plasticity in the Streamlined Genomes of Vinyl Chloride Respiring *Dehalococcoides*. Plos Genet. **5:**e1000714.

66. **Mohn, W. W., and J. M. Tiedje.** 1992. Microbial Reductive Dehalogenation. Microbiol. Rev. **56:**482-507.

67. **Moran, M. J., J. S. Zogorski, and P. J. Squillace.** 2007. Chlorinated solvents in groundwater of the United States. Environ. Sci. Technol. **41:**74-81.

68. **Morris, R. M., J. M. Fung, B. G. Rahm, S. Zhang, D. L. Freedman, S. H. Zinder, and R. E. Richardson.** 2007. Comparative proteomics of *Dehalococcoides* spp. reveals strain-specific peptides associated with activity. Appl. Environ. Microbiol. **73:**320-326.

69. **Morris, R. M., S. Sowell, D. Barofsky, S. Zinder, and R. Richardson.** 2006. Transcription and mass-spectroscopic proteomic studies of electron transport oxidoreductases in *Dehalococcoides ethenogenes*. Environ. Microbiol. **8:**1499-1509.

70. **Morris, R. M., B. L. Nunn, C. Frazar, D. R. Goodlett, Y. S. Ting, and G. Rocap.** 2010. Comparative metaproteomics reveals ocean-scale shifts in microbial nutrient utilization and energy transduction. ISME J. **4:**673-685.

71. **Muller, J. A., B. M. Rosner, G. von Abendroth, G. Meshulam-Simon, P. L. McCarty, and A. M. Spormann.** 2004. Molecular identification of the catabolic vinyl chloride reductase from *Dehalococcoides* sp strain VS and its environmental distribution. Appl. Environ. Microbiol. **70:**4880-4888.

72. **Nazaret, S., W. H. Jeffrey, E. Saouter, R. Vonhaven, and T. Barkay.** 1994. Mera Gene-Expression in Aquatic Environments Measured by Messenger-Rna Production and Hg(ii) Volatilization. Appl. Environ. Microbiol. **60:**4059-4065.

73. **Nie, L., G. Wu, and W. W. Zhang.** 2006. Correlation between mRNA and protein abundance in Desulfovibrio vulgaris: A multiple regression to identify sources of variations. Biochem. Biophys. Res. Commun. **339:**603-610.

74. **Nie, L., G. Wu, and W. Zhang.** 2006. Correlation of mRNA expression and protein abundance affected by multiple sequence features related to translational efficiency in Desulfovibrio vulgaris: A quantitative analysis. Genetics. **174:**2229-2243.

75. **Nijenhuis, I., and S. H. Zinder.** 2005. Characterization of hydrogenase and reductive dehalogenase activities of *Dehalococcoides ethenogenes* strain 195. Appl. Environ. Microbiol. **71:**1664-1667.

76. **Nishimura, M., M. Ebisawa, S. Sakihara, A. Kobayashi, T. Nakama, M. Okochi, and M. Yohda.** 2008. Detection and identification of *Dehalococcoides* species responsible for *in situ* dechlorination of trichloroethene to ethene enhanced by hydrogen-releasing compounds. Biotechnol. Appl. Biochem. **51:**1-7.

77. **Paerl, H. W., L. M. Valdes, J. L. Pickney, M. F. Piehler, J. Dyble, and P. H. Moisander.** 2003. Phytoplankton Photopigments as Indicators of Estuarine and Coastal Eutrophication. Bioscience. **53:**953-964.

78. **Rahm, B. G., and R. E. Richardson.** 2008. *Dehalococcoides*' Gene Transcripts as Quantitative Bioindicators of PCE, TCE and cDCE Dehalorespiration Rates: Trends and Limitations. Environ. Sci. Technol. **42:**5099-5105.

79. **Rahm, B. G., R. M. Morris, and R. E. Richardson.** 2006. Temporal expression of respiratory genes in an enrichment culture containing *Dehalococcoides ethenogenes*. Appl. Environ. Microbiol. **72:**5486-5491.

80. **Rahm, B. G., and R. E. Richardson.** 2008. Correlation of respiratory gene expression levels and pseudo-steady-state PCE respiration rates in *Dehalococcoides ethenogenes*. Environ. Sci. Technol. **42:**416-421.

81. **Schaechter, M. :. M., O., and N. O. Kjeldgaard.** 1958. . Dependency on Medium and Temperature of Cell Size and Chemical Composition during Balanced Growth of *Salmonella typhimurium.*. J. Gen. Microbiol. **19:**592--606.

82. **Scheutz, C., M. M. Broholm, N. D. Durant, E. B. Weeth, T. H. Jorgensen, P. Dennis, C. S. Jacobsen, E. E. Cox, J. C. Chambon, and P. L. Bjerg.** 2010. Field Evaluation of Biological Enhanced Reductive Dechlorination of Chloroethenes in Clayey Till. Environ. Sci. Technol. **44:**5134-5141.

83. **Scheutz, C., N. D. Durant, P. Dennis, M. H. Hansen, T. Jorgensen, R. Jakobsen, E. E. Cox, and P. L. Bjerg.** 2008. Concurrent Ethene Generation and Growth of *Dehalococcoides* Containing Vinyl Chloride Reductive Dehalogenase Genes During an Enhanced Reductive Dechlorination Field Demonstration. Environ. Sci. Technol. **42:**9302-9309.

84. **Schmidt, D. L.** Performance of the translational apparatus varies with the ecological strategies of bacteria. J. Bacteriol. **189:**3237-3245.

85. **Seshadri, R., L. Adrian, D. E. Fouts, J. A. Eisen, A. M. Phillippy, B. A. Methe, N. L. Ward, W. C. Nelson, R. T. Deboy, H. M. Khouri, J. F. Kolonay, R. J. Dodson, S. C. Daugherty, L. M. Brinkac, S. A. Sullivan, R. Madupu, K. T. Nelson, K. H. Kang, M. Impraim, K. Tran, J. M. Robinson, H. A. Forberger, C. M. Fraser, S. H. Zinder, and J. F. Heidelberg.** 2005. Genome sequence of the PCE-dechlorinating bacterium *Dehalococcoides ethenogenes.* Science. **307:**105-108.

86. **Shima, S., E. Warkentin, R. K. Thauer, and U. Ermler.** 2002. Structure and function of enzymes involved in the methanogenic pathway utilizing carbon dioxide and molecular hydrogen. J.Biosci. Bioeng. **93:**519-530.

87. **Smatlak, C. R., J. M. Gossett, and S. H. Zinder.** 1996. Comparative kinetics of hydrogen utilization for reductive dechlorination of tetrachloroethene and methanogenesis in an anaerobic enrichment culture. Environ. Sci. Technol.. **30:**2850-2858.

88. **Smith, D. P., J. B. Kitner, A. D. Norbeck, T. R. Clauss, M. S. Lipton, M. S. Schwalbach, L. Steindler, C. D. Nicora, R. D. Smith, and S. J. Giovannoni.** 2010. Transcriptional and Translational Regulatory Responses to Iron Limitation in the Globally Distributed Marine Bacterium *Candidatus* Pelagibacter ubique. PLoS ONE. **5:**e10487.

89. **Stojanowic, A., G. J. Mander, E. C. Duin, and R. Hedderich.** 2003. Physiological role of the F-420-non-reducing hydrogenase (Mvh) from Methanothermobacter marburgensis. Arch. Microbiol. **180:**194-203.

90. **Thauer, R. K., A. Kaster, H. Seedorf, W. Buckel, and R. Hedderich.** 2008. Methanogenic archaea: ecologically relevant differences in energy conservation. Nat. Rev. Micro. **6:**579-591.

91. **Waller, A. S., R. Krajmalnik-Brown, F. E. Loffler, and E. A. Edwards.** 2005. Multiple reductive-dehalogenase-homologous genes are simultaneously transcribed during dechlorination by Dehalococcoides-containing cultures. Appl. Environ. Microbiol. **71:**8257-8264.

92. **Werner, J. J., A. C. Ptak, B. G. Rahm, S. Zhang, and R. E. Richardson.** 2009. Absolute quantification of *Dehalococcoides* proteins: enzyme bioindicators of chlorinated ethene dehalorespiration. Environ. Microbiol. **11:**2687-2697.

93. **Wilkins, M. J., N. C. VerBerkmoes, K. H. Williams, S. J. Callister, P. J. Mouser, H. Elifantz, A. L. N'Guessan, B. C. Thomas, C. D. Nicora, M. B. Shah, P. Abraham, M. S. Lipton, D. R. Lovley, R. L. Hettich, P. E. Long, and J. F. Banfield.** 2009. Proteogenomic Monitoring of Geobacter Physiology during Stimulated Uranium Bioremediation. Appl. Environ. Microbiol. **75:**6591-6599.

94. **Wood, G. E., A. K. Haydock, and J. A. Leigh.** 2003. Function and regulation of the formate dehydrogenase genes of the methanogenic Archaeon Methanococcus maripaludis. J. Bacteriol. **185:**2548-2554.

95. **Worm, P., A. J. M. Stams, X. Cheng, and C. M. Plugge.** 2011. Growth- and substrate-dependent transcription of formate dehydrogenase and hydrogenase coding genes in Syntrophobacter fumaroxidans and Methanospirillum hungatei. Microbiology-Sgm. **157:**280-289.

96. **Yang, Y. R., and P. L. McCarty.** 1998. Competition for hydrogen within a chlorinated solvent dehalogenating anaerobic mixed culture. Environ. Sci. Technol. **32:**3591-3597.

97. **Zinder, S. H.** 1993. Physiological ecology of methanogens. *In* J. G. Ferry (ed.), Methanogenesis : ecology, physiology, biochemistry & genetics. Chapman & Hall, New York.

CHAPTER 2

Characterization of the Community Structure of a Dechlorinating Mixed Culture and Comparisons of Gene Expression in Planktonic and Biofloc-Associated *Dehalococcoides* and *Methanospirillum* species*

2.A. Abstract

This study sought to characterize bacterial and archaeal populations in a tetrachloroethene- and butyrate-fed enrichment culture containing hydrogen-consuming *Dehalococcoides ethenogenes* strain 195 and a *Methanospirillum hungatei* strain. Phylogenetic characterization of this microbial community was done via 16S rRNA gene clone library and denaturing gradient gel electrophoresis analyses. Fluorescence *in situ* hybridization was used to quantify populations of *Dehalococcoides* and *Archaea* and to examine the colocalization of these two groups within culture bioflocs. A separation technique was applied to whole-culture samples to generate sub-samples enriched in either planktonic or biofloc-associated biomass. Analysis of these sub-samples was used to assess differences in population distribution and gene expression patterns following provision of substrate. On a per-milliliter-of-culture basis, most *D. ethenogenes* genes (the hydrogenase gene *hupL*; the highly expressed gene for an oxidoreductase of unknown function, *fdhA*; the RNA polymerase subunit gene *rpoB*; and the 16S rRNA gene) showed no statistical difference in expression between planktonic and biofloc enrichments at either time point studied (1 to 2 and 6 hours post-feed). Normalization of transcripts to ribosome

Rowe, A. R., B. J. Lazar, R. M. Morris, and R. E. Richardson. 2008. Characterization of the Community Structure of a Dechlorinating Mixed Culture and Comparisons of Gene Expression in Planktonic and Biofloc-Associated "*Dehalococcoides*" and *Methanospirillum* Species. Appl. Environ. Microbiol. **74:**6709-6719.

(16S rRNA) levels supported that planktonic and biofloc-associated *D. ethenogenes* had similar gene expression profiles, with one notable exception; planktonic *D. ethenogenes* showed higher expression of *tceA* relative to biofloc-associated cells at 6 hours post-feed. These trends were compared to those for the hydrogen-consuming methanogen in the culture, *M. hungatei*. The vast majority of *M. hungatei* cells, ribosomes (16S rRNA), and transcripts of the hydrogenase subunit *mvrD* and the housekeeping gene *rpoE* were observed in the biofloc enrichments. This suggests that, unlike the comparable activity of *D. ethenogenes* from both enrichments, the planktonic *M. hungatei* population is responsible for only a small fraction of the hydrogenotrophic methanogenesis in this culture.

2.B. Introduction

Anaerobic dechlorination of chlorinated organic compounds is an important mechanism for the remediation of common groundwater pollutants (11, 58). It is now accepted that members of the *Dehalococcoides* play a crucial role in the remediation of compounds such as chloroethenes, chlorobenzenes, chloroalkanes, chlorophenols, dioxins, and polychlorinated biphenyls, in some cases dechlorinating these compounds to non-toxic endproducts (1, 2, 6, 16, 18, 26, 32, 35). While researchers have been able to isolate and perform pure culture studies of these organisms, there is significant evidence that reductive dechlorination in environmental systems and in the most robust laboratory cultures is the work of microbial consortia (4, 11). All cultured representatives of the *Dehalococcoides* require hydrogen as an electron donor (often supplied by syntrophic fermentation) and a halogenated organic as an electron acceptor. In addition, *Dehalococcoides* grow robustly in mixed cultures, likely due to currently undetermined growth factors from other community members (11, 18, 31, 34, 44). Though reductive

dechlorination is an energetically favorable process under syntrophic conditions with low hydrogen partial pressures (19, 57, 58), other, less favorable metabolic reactions such as methanogenesis and acetogenesis often occur in these communities, especially when excess hydrogen or a donor fermented at high hydrogen partial pressures is available (19, 20, 24, 38). Many methanogens depend on acetate and/or H_2, which are both utilized by *Dehalococcoides*. This suggests that competition for resources is an important interaction within dechlorinating microbial communities containing both methanogenic and *Dehalococcoides* populations.

Several studies have looked at dechlorinating microbial communities derived from both enrichment cultures and environmental systems (8, 12, 17, 21, 22, 28, 30, 33, 43, 54, 55, 64). Several distinct lineages of microorganisms, representing a variety of metabolic capabilities, are commonly found in these consortia, supporting the potential complexity of community dynamics. The Donna II enrichment culture, which has been studied previously (19, 20, 46, 48, 52, 53), is derived from the same consortium from which *Dehalococcoides ethenogenes* strain 195 (DET) was isolated (13, 14, 44, 45). In this study, the phylogenetic community structure of the Donna II enrichment culture including DET was assessed from phylogenetic analysis of bacterial and archaeal 16S rRNA gene libraries created from community DNA.

Within this heterogeneous enrichment culture, two distinct cellular attachment phases were observed: planktonic cells (individual suspended cells) and cells associated with bioflocs (suspended cell aggregates). In the Donna II culture, bioflocs (typically 10 to 100 μm in diameter) tended to contain multiple species and form around mineral precipitates from the medium. Planktonic and biofloc-associated growth forms are common in environmental microbial communities (i.e., activated sludge, marine, sediments, and groundwater) (5, 10, 41, 60). In this study, a technique for physical enrichment of these two cell attachment phases via

low-speed centrifugation was developed. Fluorescence *in situ* hybridization (FISH) with 16S rRNA-targeting probes was used to estimate the distribution of DET populations between plankton and bioflocs and to examine colocalization of DET and methanogenic *Archaea* within the bioflocs.

Potential differences in gene expression between the two attachment forms were determined for both DET and the hydrogenotrophic methanogen present in the culture, *Methanospirillum hungatei* (MHU), using quantitative reverse transcription-PCR (qRT-PCR). This method was also used to compare expression of housekeeping and hydrogenase genes between these organisms. Understanding the distribution and difference in gene expression of the two DET cell attachment phases not only is important for elucidating the ecology of these organisms; it also has implications for the use of DNA and RNA as bioindicators of *Dehalococcoides* activity. A groundwater sample, while easier and less expensive to obtain, would predominantly sample planktonic *Dehalococcoides*. Therefore, it is important to establish whether the populations and activities of the planktonic phase reflect those of the community as a whole.

2.C. Materials and Methods

2.C.1. Chemicals and Analysis of Chloroethenes

Butyric acid (99%; Acros Organics) and tetrachloroethene (PCE) (99%; Alfa Aesar) were used as culture substrates. PCE, trichloroethene (TCE), *cis*-1,2-dichloroethene (cDCE), vinyl chloride (VC), and ethene standards were constructed as previously described (53). Methane, ethene, and chlorinated ethenes were measured from headspace samples using the gas chromatography-flame ionization detector temperature program and standard construction as

described by Rahm et al. (53). Methane at high concentrations was measured by use of a gas chromatograph equipped with a thermal conductivity detector as described by Fennell et al. (20).

2.C.2. Enrichment Culture

An enrichment culture (Donna II) containing DET has been maintained for over 10 years on a low-PCE/butyrate feeding regimen described previously (20, 53). Under this regimen, the mean cell residence time in the reactors averages 80 days. Briefly, the culture is grown in a 9.1-liter stirred reactor containing 5.7 liters of culture at 30°C. PCE (110 μM) and butyric acid (440 μM) are added at a 2:1 ratio of H_2-electron equivalents (assumes that each mole of butyrate is fermented to 2 moles of hydrogenand 2 moles of acetate).

2.C.3. Culture Sampling and Cell Attachment Phase Enrichment

Liquid culture samples of 30 to 50 ml were collected via a stainless-steel valve at the reactor mouth (20, 24). Duplicate 2-ml bulk culture samples (control) for DNA and RNA were pelleted at 21,000 x *g* for 5 min at 4°C and stored at –20°C or –80°C for DNA and RNA, respectively. For all FISH and enrichment samples, large-orifice pipette tips and gentle pipetting techniques were used to minimize biofloc disruption. Enrichments for biofloc or planktonic cells were done using low-speed centrifugation (100 x *g*, 500 x *g*, and 1,000 x *g*). Alternate separation methods were tested, including gravity settling (settled for 24 h) and selective filtering through 5-μm and 12-μm polycarbonate filters.

To enrich for biofloc-associated and planktonic cells, at various time points culture samples (2-ml aliquots) were distributed into microcentrifuge tubes (eight for RNA, eight for DNA, and two for FISH). Enriched plankton and biofloc regions were created by centrifugation at 1,000 x *g* for 10 min at 4°C. For each sample type (RNA, DNA, and FISH), the uppermost 0.5 ml (plankton enriched) was pooled to create a 4-ml (for DNA and RNA) or 1-ml (for FISH)

plankton-enriched sample. An additional 0.5 ml was discarded, leaving a 1-ml biofloc-enriched region in each tube. Two of these samples were pooled. The biofloc enrichment concentrated bioflocs from 2 ml of culture into 1 ml. In order to convert back to values on a per-milliliter culture basis, data from biofloc-enriched samples were multiplied by a correction factor (0.5). All pooled enrichment samples for DNA and RNA extraction were immediately pelleted at 21,000 x *g* for 5 min at 4°C and stored at –20°C for DNA or at –80°C for RNA. FISH samples for each sample (control, plankton enriched, and biofloc enriched) were immediately fixed in an equal amount of filter-sterilized phosphate-buffered saline (PBS)-buffered (pH 7) 4% paraformaldehyde solution (EM Sciences) for 6 to 12 hours at 4°C (27, 47). After fixation, a subsample was removed for assessment of attachment phase separation (see below). In order to disrupt biofloc structures for ease of counting, samples were briefly sonicated with a sonic dismembrator (Fisher Scientific model no. 100 at a setting of 5 for 5 half-second pulses). Twenty-microliter fixed samples were dispersed in 25 ml of sterile PBS and were then vacuum filtered onto black polycarbonate membrane filters of known filtration area (diameter, 25 mm; pore size, 0.22 μm) (type Poretics; Osmonics, Inc.) supported by binder-free glass fiber support filters (25 mm, 1 μm; type A/B extra thick; Pall).

2.C.4. Assessment of Cell Attachment Phase Separation

For each sample type (i.e., control, plankton enriched, or biofloc enriched), a 20-μL sample was spotted onto coated slides as described below in order to obtain a qualitative assessment of biofloc prevalence. The quality of enrichment using the low-speed centrifugation method was based on biofloc prevalence in at least 100 randomly selected fields of DAPI (4',6'-diamidino-2-phenylindole)-stained cells from each enrichment. Quality and reproducibility of separation were based on nine replicate separation experiments.

2.C.5. Nucleic Acid Extraction

For the first bacterial clone library construction, DNA was extracted using the bead-beating, phenol-chloroform protocol of Dojka et al. (15) without the addition of poly(A). Raw DNA was passed through a Chromaspin 1000 column (Clontech) to remove DNA fragments smaller than 1,000 bp. All subsequent DNA extractions were performed using the Microbial DNA isolation kit (MoBio Laboratories) according to the manufacturers' instructions.

RNA extractions were performed within 48 hours of sampling using the bacterial protocol of the RNeasy minikit (Qiagen) with modifications and DNase treatments as previously described (53). Luciferase RNA was added to samples to be used as a measure of overall recovery efficiency as described previously (36). RNA was quantified using the RNA 6000 Nano Assay on the Agilent 2100 Bioanalyzer (Agilent Technologies).

2.C.6. 16S rDNA Amplification, Clone Library Construction, and Sequencing

One archaeal and three bacterial rRNA gene clone libraries were developed from DNA extracted from the Donna II enrichment culture. Bacterial 16S rRNA gene primers 8F (5'-AGA GTT TGA TCC TGG CTC AG) and 1492R (5'-GC[C/T] TAC CTT GTT ACG ACT T) were used as previously reported (22, 54) with annealing temperatures of 53°C and 55°C. Archaeal 16S rRNA gene primers 1Af (5'-TCY GKT TGA TCC YGS CRG AG) and 1100Ar (5'TGG GTC TCG CTC GTT G) were used as previously described (29). 16S rRNA gene clone library construction and restriction fragment length polymorphism type screening were performed as described previously (22, 54). All cloning was performed using a TOPO TA cloning kit with DH5 α-T1 chemically competent cells (Invitrogen). Clones for each bacterial restriction fragment length polymorphism type were sequenced using the M13 forward and reverse primers. In some cases, a third internal primer (the bacterial 515F primer, 5'-GTG CCA GC [A/C] GCC GCG

GTA A) was employed in order to obtain full sequences (22). Sequencing reactions were carried out using BigDye terminator chemistry according to the manufacturer's instructions (Applied Biosystems) and analyzed at the Cornell Biotechnology Resource Center using an Applied Biosystems automated 3730 DNA analyzer. Sequence assembly was performed using SeqBuilder software (Lasergene). ChimeraCheck through the Ribosomal Database Project (http://rdp8.cme.msu.edu/html/analyses.html) or through the Bellerophon server (http://foo.maths.uq.edu.au/~huber/bellorophon.pl) was performed on the assembled sequences. BLAST searches (http://www.ncbi.nlm.nih.gov/BLAST/) were run to obtain putative phylogenetic affiliations and assign more informative names to the sequences. Retrieved sequences were then aligned with a 16S rRNA gene database maintained by the Ribosomal Database Project (http://rdp.cme.msu.edu) using ARB (http://www.arb-home.de) (42).

For assessment of lineage or classification of publicly available sequences from chloroethene-reducing enrichment cultures, microcosms, and field studies, as well as the Donna II enrichment culture, the Classifier function available through the Ribosomal Database Project (http://rdp.cme.msu.edu/classifier/classifier.jsp) was used. This function, a naïve Bayesian rRNA classifier, was developed to assess taxonomy from domain to genus with confidence estimates for each assignment (62). A 90% confidence level was used as a cutoff for determination of phylogenetic assignment.

2.C.7. Denaturing Gradient Gel Electrophoresis

To ensure completeness of the community composition observed in clone library analysis, denaturing gradient gel electrophoresis (DGGE) was performed in triplicate on DNA samples used for clone library construction. PCRs (40-µL reaction mixtures) were carried out as described by Nakatsu et al. (49) using bacterial primers PRBA338F (amended with a 40-bp GC

region at the 5' end) and PRUN518R, designed to target the V3 region. Archaeal DGGE primers PARCH340F (with a 5' GC tag) and PARCH519R, designed to target the archaeal V3 region, were also used (49). Reaction programs consisted of 9 min at 94°C; followed by 30 cycles of 94°C for 30 s, 55°C for 30 s, and 72°C for 30 s; followed by a 7-min extension period at 72°C. DGGE was carried out using the D-code system (Bio-Rad). PCR products were resolved on an 8% (wt/vol) polyacrylamide gel using 1x Tris-acetate-EDTA buffer with a denaturing gradient from 35% to 55% denaturant (40% [wt/vol] formamide and 7 M urea). Gels were visualized using Sybr green (Molecular Probes). Bands excised for sequencing were run on a second DGGE gel under the same conditions to ensure purity. Sequences were obtained using DGGE primers without GC flanking regions. Sequencing reactions were carried out as described for the 16S rRNA gene clone library, which provided 150 to 300 bp of sequence information.

2.C.8. FISH, *Dehalococcoides* Probe Analysis, and Fluorescence Microscopy

Sixty-six *Dehalococcoides* and 8,794 total 16S rRNA sequences were aligned using the ARB sequence analysis package (42) to design two new *Dehalococcoides* specific probes (see Table A1.2 in Appendix I). *Dehalococcoides*-targeting probes (two from this study along with Dhe1259degR [63] and Dhe201R [50]) were evaluated with a mechanistic FISH model based on the thermodynamics of nucleic acid hybridization as described by Yilmaz et al. (65). All probes were labeled with Cy3. Probe intensity was tested for both individual and probe combinations. Cell images were captured with an Olympus BX61 fluorescence microscope equipped with a Cooke SensiCam high-performance charge-coupled device digital camera, filter sets appropriate for DAPI and Cy3, and Intelligent Imaging Innovations Slidebook software, version 3.0.10.15. Exposure times were 1 second for probed samples (Cy3) and 100 milliseconds for DAPI.

Hybridization reactions were performed as described previously (27, 47) with the following modifications. Air-dried filters were stored with desiccant at –20°C prior to hybridization. Quarter membrane sections were pretreated by dipping filters in 0.2 M HCl for 10 minutes, followed by a 2-min wash with PBS to reduce background fluorescence (51). Hybridizations were then performed at 37°C for 16 hours in hybridization buffer with the desired probe(s). Control hybridization reactions, stringency washes, and DAPI counterstaining were employed as described previously (47), except for a 48°C dissociation temperature. Hybridization and wash buffers were made as described by Yang and Zeyer (63); however, 20% formamide (EM Science) was used in all hybridizations. All probes were filter sterilized through 0.2-µm-pore filters to a final concentration of 2 ng/µL. Cell counts were performed on images captured via fluorescence microscopy with a minimum of 10 fields (field area of 5,292 μm^2) per duplicate samples. Cell count microscopy was carried out on an Olympus BX-50 at the Cornell Microscope Imaging Facility at a magnification of x630.

2.C.9. Multiplex FISH for Visualizing Bioflocs

The FISH protocol described above was amended to facilitate observation of biofloc architecture and associations. Ethanol-cleaned slides were coated by being dipped in a warmed (70°C) gelatin-chromium solution of 0.1% gelatin and 0.01% chromium (III) potassium sulfate (Aldrich) (3). Twenty microliters of fixed samples was spotted with large-orifice pipette tips onto gelatin-chromium-coated slides over a circular area of approximately 1 cm in diameter. Cell spots were allowed to air dry and then dipped sequentially in 50%, 80%, and 95% ethanol for 3 minutes each. Slides were air dried again and either hybridized as described above, DAPI stained, or stored at –20°C until hybridization. Multiplexing with differentially labeled probes (Cy3 for Dhe1259/Dhe201 and fluorescein for ARCH915) was employed in the hybridization of preserved

bioflocs. A Leica confocal TCS SP2 microscope system was used to collect z-series stacks (z-step size of 0.12 μm) from 60 images of both Cy3 (excitation range, 510 to 560 nm; emission range, >590 nm) and fluorescein (excitation range, 460 to 500 nm; emission range, 512 to 542 nm) channels.

2.C.10. Reverse Transcription and Quantitative PCR

RNA and DNA were extracted from two replicate separation experiments. From the replicate RNA pools, cDNA was synthesized from 0.2 μg of RNA using the iScript cDNA synthesis kit (Bio-Rad) with random hexamers as primers according to the instructions of the supplier. Primers targeting DET genes *rpoB* (DET0603 on the DET genome), *hupL* (DET0110), *fdhA* (DET0187), and *tceA* (DET0079) were developed previously (25, 53). DET primers targeting the 16S rRNA genes (2) were also used. Quantitative PCR (qPCR) primers were designed for the 16S rRNA genes of the two Donna II methanogens obtained from clone library sequencing, *Methanospirillum hungatei* (MHU16S F/R, 5'-AGT AAC ACG TGG ACA ATC TGC CCT and 5'-ACT CAT CCT GAA GCG ACG GAT CTT) and a *Methanosaeta* sp. (Ms16S F/R, 5'-GGG GTA GGG GTG AAA TCT TGT AAT CCT and 5'-CGG CGT TGA ATC CAA TTA AAC CGC A), using PrimerQuest available through IDT (Coralville, IA).

Expression of DET and MHU hydrogenase and RNA polymerase subunit genes was used for comparison between organisms. Because the genome sequence of the culture-specific *Methanospirillum* population was not known, in order to determine hydrogenase sequences for the *Methanospirillum* sp. present in our culture, degenerate hydrogenase primers for methyl viologen-reducing hyrdrogenases subunit D (*mvrD*) in methanogens were designed using orthologous *mvrD* sequences. PCR products were cloned and sequenced (as described for the 16S rRNA gene clone library) and used to design primers appropriate for qPCR for the *mvrD* gene

present in the Donna II culture (D2mvrh F/R, 5'-TGT TCG TAT GCA GGT GCT GAC CTT-3' and 5'-ACC ATC TGC ACC CTC AAC AAA TGC-3' (accession no. EU498366). Using the sequence available for the *Methanospirillum hungatei* JF-1 *rpoE* gene (YP_504275), a qPCR primer set was designed using PrimerQuest as described above (Msp rpoE-F/R, 5'-TCA GTC TTG GAC CGA TTG ATG CGA-3' and 5'-TCA CGA GGT TCA CGT TCG TTG AGA-3').

All qPCRs were performed using the iCycler iQ Multicolor real-time PCR detection system (Bio-Rad). Triplicate qPCRs for each sample were constructed along with standard curves (log DNA concentration versus cycle threshold) as described by Rahm et al. (53). *Methanospirillum hungatei* JF-1 and *Methanosaeta thermophila* CALS-1 pure-culture DNA samples were quantified using PicoGreen assays (Invitrogen) and converted to genome copies using molecular weights of the published genomes. Dilutions were used as standards for the 16S rRNA gene copies of Donna II methanogens as well as *Methanospirillum* sp. *rpoE* and *mvrD* copies using the iCycler method. Luciferase DNA stock (Promega) was used to generate standard curves for quantification of recovered transcripts as described by Johnson et al. (36). qPCR conditions and melt curve analysis were described previously (53). Methanogen primer sets used the same qPCR program as described for DET with a 60°C annealing temperature.

2.C.11. Statistical Analysis

Statistical tests were performed using JMP statistical software. The statistical significance of gene expression data was determined using an unpaired *t* test in addition to analysis of variance to determine experimental effects on these values. F tests were done to ensure that there was no statistically significant difference in variance between the gene expression values being compared.

2.C.12. Nucleotide Sequence Accession Numbers

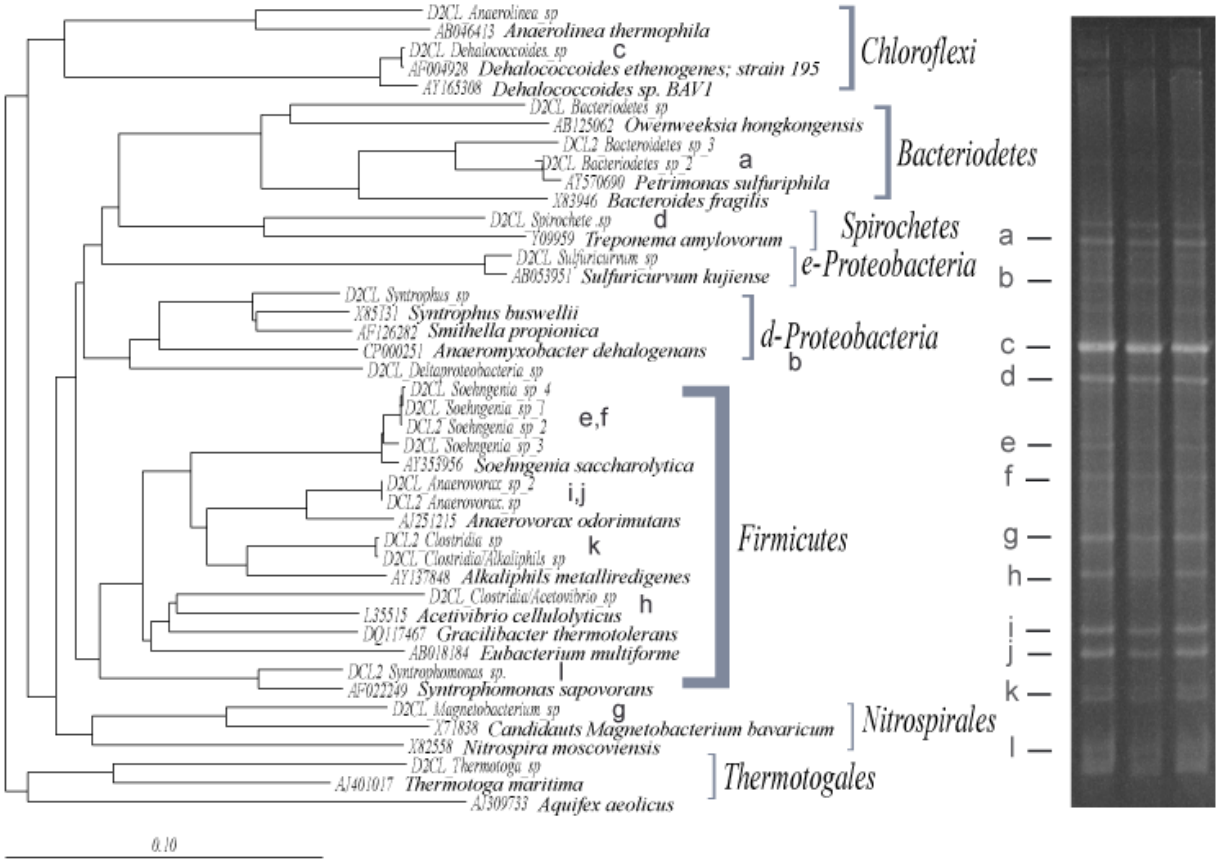

Figure 2.1. Phylogenetic tree (left) containing sequences from Donna II enrichment clone library (sequences designated D2CL_) and from cultured representatives. This unrooted tree was constructed from a 770-bp alignment using ARB with a Kimura correction parameter. Brackets indicate higher order taxonomic groupings. Lowercase letters correspond to matching sequences obtained from DGGE bands (right). Certain bands matched more than one sequence (i.e., b matched multiple δ-Proteobacteria).

The sequences determined in this study have been submitted to GenBank under accession numbers EU498367 to EU498393.

2.D. Results

2.D.1. Phylogenetic Analysis of Donna II Enrichment Culture.

The phylogenetic structure of the Donna II enrichment culture was determined through the classification of archaeal and bacterial 16S rRNA gene clone libraries and DGGE profiling (Figure 2.1). Cumulative analysis of clone libraries suggests that there are around 18 bacterial and archaeal operational taxonomic units present in the culture. In order to ensure that we were observing all the major members of the Donna II enrichment culture, we employed a second community characterization method, DGGE, on replicate DNA extractions. Replicate extracts produced a consistent profile (Figure 2.1). Sequences obtained from dominant bands (bands a through l in Figure 2.1) matched sequences from the Donna II bacterial clone libraries.

In the archaeal clone library, *Methanosarcinales* and *Methanomicrobiales* were the only two phylogenetic groups represented. The nearest cultured organisms were an acetotrophic methanogen (a *Methanosaeta* sp.) (97% identity over 1,060 bp) and a hydrogenotrophic methanogen (*Methanospirillum hungatei* JF-1) (98% identity over 1015 bp). DGGE using *Archaea*-specific primers resulted in two bands. One band matched a *Methanosaeta* sp., while the other produced a short sequence similar to sequences in many organisms in the *Methanomicrobia*, including *Methanospirillum* (data not shown).

2.D.2. *Dehalococcoides* Probe Comparison.

In order to enumerate populations of *Dehalococcoides ethenogenes* strain 195, we aimed to improve FISH for this organism. The previously published probe Dhe1259degR (64) produced the highest value for average fluorescence intensity, followed by Dhe201R, Dhe137R, and

Dhe619R (see Table A1.2 in Appendix I). With actively dechlorinating cells, attempts to increase signal intensity through probe combinations did not improve signal intensity above that of Dhe1259degR used alone; however, incorporation of a second probe, Dhe201, did improve detection of starved cells (percent DET to DAPI, 21% ± 15% with Dhe1259degR alone versus 65% ± 8% with Dhe1259 and Dhe201R combined). This combination was used subsequently for cell enumeration.

2.D.3. Enumeration of Specific Populations via FISH.

FISH with DAPI counterstaining was employed as a method to simultaneously visualize and quantify both *Dehalococcoides* (DET in this culture) and archaeal (methanogens in this culture) populations. Counts for three time points in a batch feeding cycle (pre-feed, 6 hr [active dechlorination; PCE to VC], and 16 hr [cometabolic dechlorination; VC to ethene]) (53) showed that the total culture population ranged from 6.3×10^8 to 9.9×10^8 cells per ml, with an average of 7.9×10^8 cells per ml across all time points. DET and archaeal cells averaged 60.1% ± 18.1% and 10.9% ± 5.7% of the total cells, respectively. Based on these techniques, any growth observed during one dechlorination cycle (110 μM PCE) is within the error of the measurements.

In addition to FISH with dispersed culture samples, multiplex FISH was employed on spotted culture samples to examine localization of the DET and *Archaea* within the bioflocs that are common in this culture (Figure 2.2). Archaeal and DET cells were consistently observed in close association around black medium precipitates.

2.D.4. Separation and Enumeration of Cells in Plankton-Enriched and Biofloc-Enriched Samples.

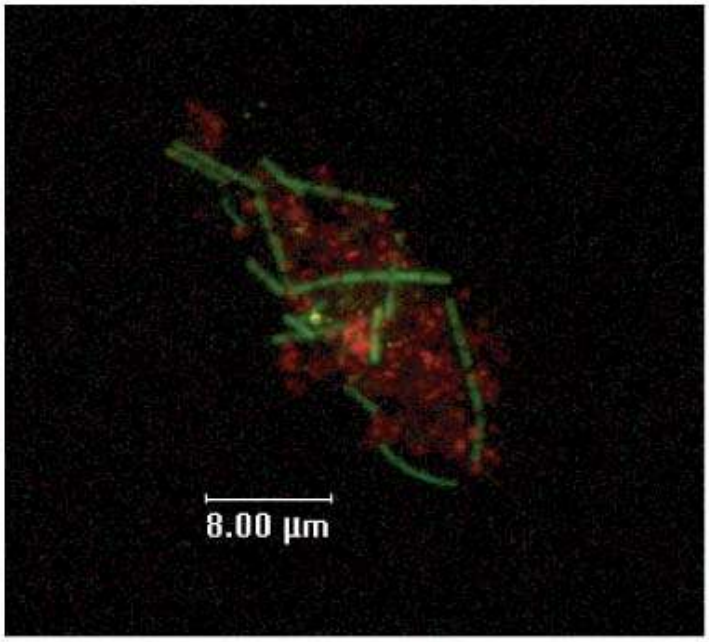

Figure 2.2. Microscopic field of view with a typical biofloc multiplexed with both Arch915R (green) and Dhe201R/1259degR (red).

When observing the bioflocs using FISH on bulk culture, it was noted that some cells were located outside of these bioflocs (planktonic cells). We describe these as two distinct cellular attachment phases: planktonic and biofloc associated. A low-speed centrifugation separation technique was developed to separate Donna II culture samples into plankton-enriched and biofloc-enriched samples. Quality of enrichment was assessed through microscopy on DAPI-stained spotted cells. Of the centrifuge speeds tested (100 x *g*, 500 x *g*, and 1,000 x *g*), 1,000 x *g* for 10 min produced the most complete separations. Other techniques were not as successful at enriching these two phases: the gravity settling separation technique yielded poorer separation of bioflocs, and size exclusion filtering attempts were unsuccessful because bioflocs became sheared under the vacuum pressure (data not shown). Biofloc prevalence counts over the course of nine centrifugation separation experiments suggested that this technique produces a significant and consistent reduction in the number of bioflocs in plankton-enriched samples. The average percentages of fields with bioflocs for the control, plankton-enriched, and biofloc-enriched samples were 76% ± 13%, 17% ± 8%, and 88% ± 8%, respectively. Qualitatively, the bioflocs detected in the plankton-enriched samples were smaller than those in the bulk (control) or biofloc-enriched samples (data not shown). However, since separation was not absolute, the terms "biofloc enriched" and "plankton enriched" are used throughout this report.

Cell counts via DAPI staining and DET counts via use of Dhe201R/Dhe1259degR were determined for samples of bulk culture (control), plankton-enriched, and biofloc-enriched samples at 2 hours and 6 hours post-feed (Figure 2.3). In terms of percentage of total cells per given microscopic analysis, the plankton-enriched samples were enriched for DET (78% ± 6%), while the biofloc-enriched samples (53.4% ± 1%) contained a lower percentage of DET relative

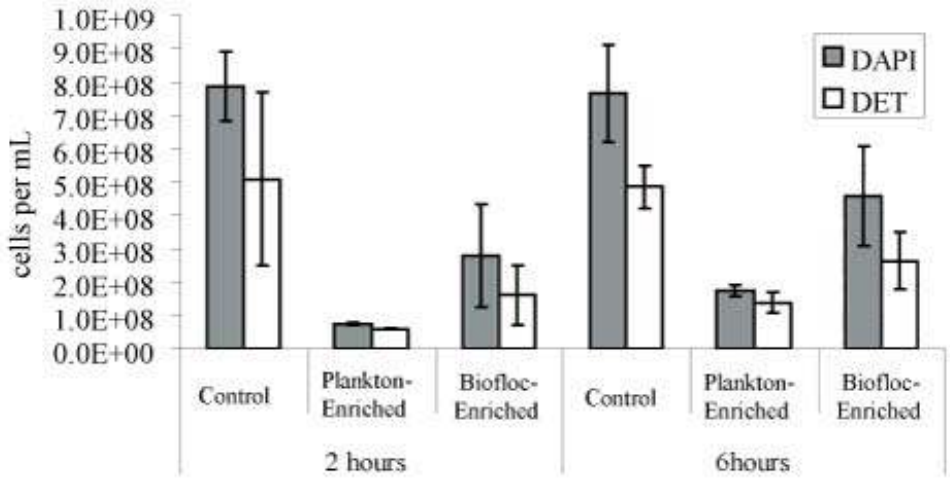

Figure 2.3. Summary of DAPI and *Dehalococcoides*-specific (DET) cell counts for control or untreated culture, planktonic enrichment and biofloc enrichments at 2 and 6 hours post-feed.

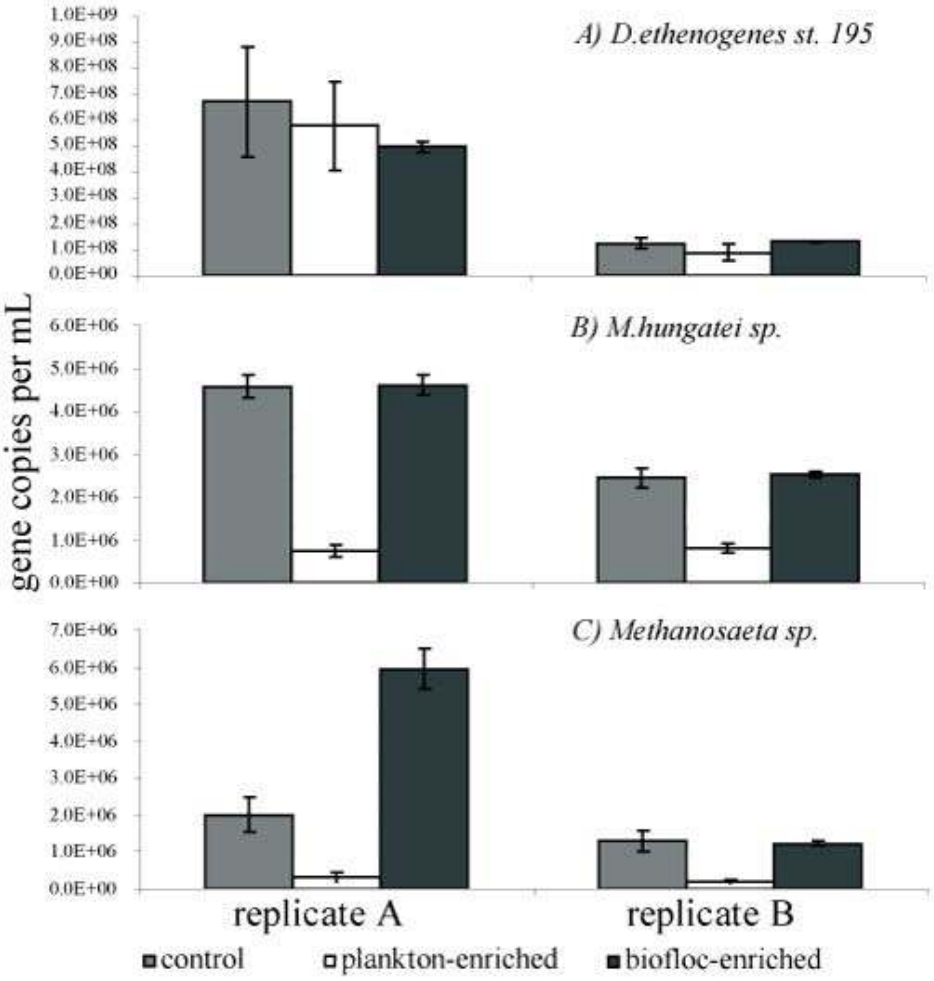

Figure 2.4. Genome copies present in each enrichment (control, planktonic, or biofloc), of each biological replicate experiment measured via: (A) *Dehalococcoides ethenogenes* 16S rDNA copies, (B) *Methanospirillum hungatei. rpoE* gene copy numbers, and (C) *Methanosaeta sp* 16S rDNA copies. Panels A and B represent known single-copy genes whereas panel C represents a gene potentially present in multiple copies per genome. Error bars represent standard errors of values from two separate DNA extractions.

to control samples (64.2% ± 2%). qPCR was also used as a technique for enumerating DET populations. Both FISH and qPCR suggest that DET cells in the culture are equally distributed between cell locations (Figure 2.3 and 2.4). Direct comparison of FISH and qPCR numbers on duplicate samples showed an average ratio of qPCR numbers to FISH numbers of 1.8 ± 1.5. Removal of a qPCR outlier two standard deviations above the mean resulted in a ratio of 1.3 ± 0.6. In subsequent studies examining gene expression in the different cell attachment phases, qPCR was used for quantification of populations due to the simplicity of the assay relative to FISH. Also, the processing and quantification biases are similar to those of quantitative reverse transcription-PCR (the method employed for assaying gene expression levels).

During gene expression experiments, DET population numbers determined by qPCR of 16S rRNA gene copies for the control culture over two time points averaged 6.7 x 10^8 and 1.3 x 10^8 per ml for replicates A and B, respectively (Figure 2.4A). In general, the qPCR estimates for all enrichments in replicate A were higher than those for in replicate B (Figure 2.4B) As in earlier studies with FISH and qPCR, an equal distribution of DET cells between biofloc and planktonic enrichments (averaging 47 and 53%, respectively) was noted on both of these dates. Unlike DET, methanogenic cells (both *Methanosaeta* sp. and *Methanospirillum*) were present predominantly in biofloc enrichments (Figure 2.4B and 2.4C). This matched previously observed FISH assays on bulk culture, where few archaeal cells were observed outside bioflocs (data not shown).

2.D.5. Gene Expression in Planktonic and Biofloc-Associated *Dehalococcoides*

Gene expression levels in planktonic and biofloc-associated DET were compared at two time points after provision of PCE and butyrate, specifically, 1 to 2 hours and 6 hours (Figure

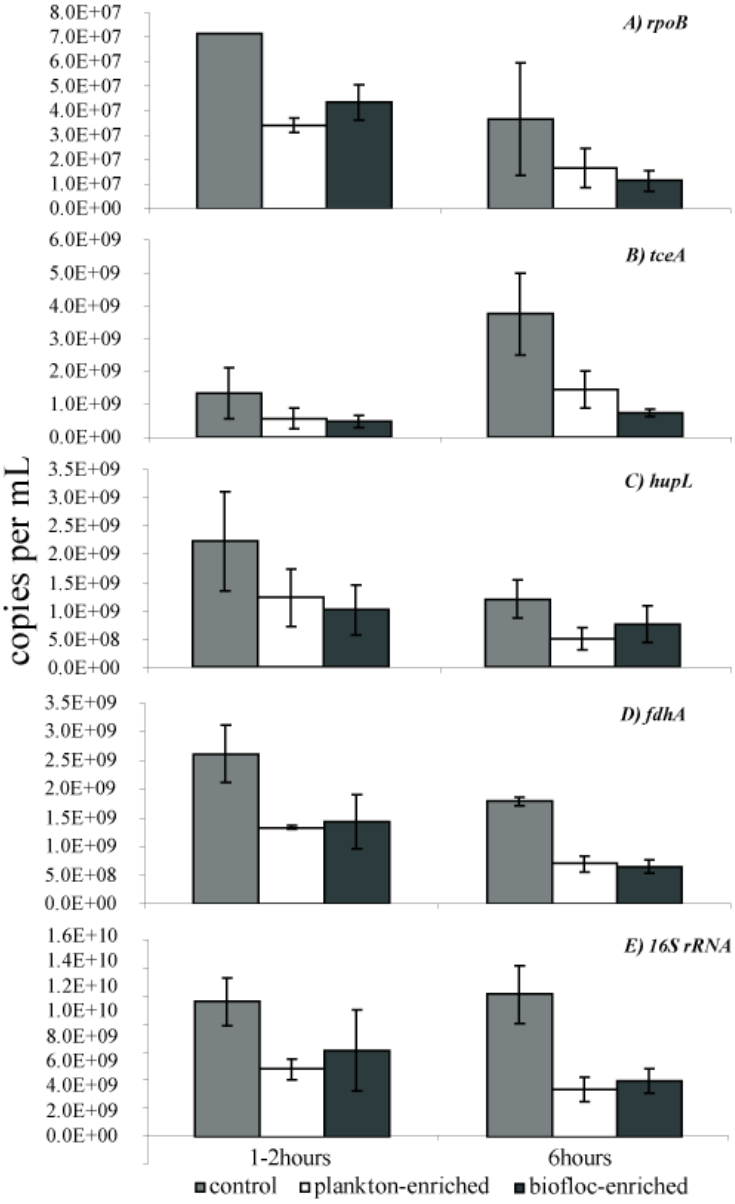

Figure 2.5. Average gene expression values for *Dehalococcoides ethenogenes* st. 195 on a per milliliter enrichment basis (control, planktonic, or biofloc) at 1 to 2 hours and 6 hours post-feed for: (A) *rpoB*, (B) *tceA*, (C) *hupL*, and (D) *fdhA*, as well as (E) 16S rRNA copies (ribosome copies). Error bars represent standard error of values from replicate experiments.

2.5). The 6-hour time point was selected based on recent studies in our laboratory showing that this time point is during active dehalorespiration of the chlorinated ethenes and is also a point at which a variety of respiratory genes were upregulated in whole-culture samples (53). The general expression trends in the control culture and enrichments showed that the hydrogenase gene *hupL*, an annotated formate dehydrogenase gene (*fdhA*), and an RNA polymerase gene (*rpoB*) were more highly expressed at early (1 to 2 hr) time points postfeeding, while expression levels of the reductive dehalogenase gene *tceA* was higher at 6 hours post-feed. Comparing planktonic and biofloc enrichments, there was no statistically significant difference (within one standard deviation) in the relative expression of *rpoB*, *hupL*, or *fdhA* between the enrichments at either time point (Figure 2.5A, 2.5C, and 2.5D). However, expression of the reductive dehalogenase gene *tceA* at 6 hours was higher in planktonic enrichments ($1.5 \times 10^9 \pm 5.6 \times 10^8$) than in biofloc enrichments ($7.5 \times 10^8 \pm 1.1 \times 10^8$) (Figure 2.5B) ($P = 0.0004$). Testing for the effect of experiment by analysis of variance suggested an effect of experimental replicate on per-milliliter culture data ($P < 0.0001$), though this did not detract from the significant difference in the *tceA* expression mean mentioned above. The effect of experiment is likely a result of minor differences in the starting culture between different separation experiments.

To look more closely at any differences in relative expression of different genes in the two attachment phases, transcript data were normalized to 16S rRNA copies from the same RNA pool (Figure 2.6). Using rRNA as an internal normalizing factor minimized any variability due to slight differences in cell density or cell lysis across replicates; the effect test suggested no effect of experiment for rRNA normalized values ($P = 1.00$). Normalized values support the trends noted earlier in essence, twofold higher relative expression of *tceA* at 6 hours in planktonic cells (0.36 *tceA* transcript per ribosome, versus 0.16 *tceA* transcript per ribosome for biofloc-

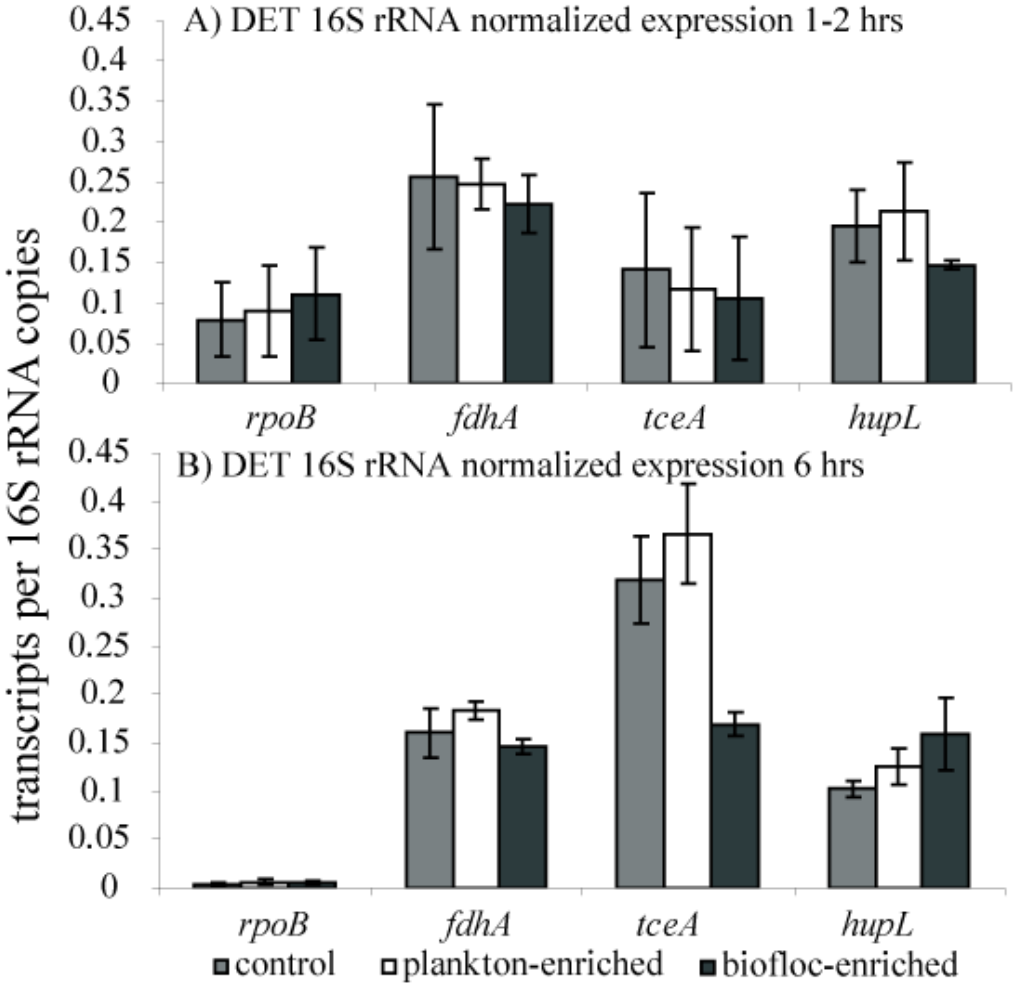

Figure 2.6. 16S rRNA normalized gene expression for *Dehalococcoides ethenogenes* strain 195 (A) 1 to 2 hours post-feed and (B) 6 hours post-feed for each enrichment (control, planktonic, or biofloc). Error bars represent standard error of replicate experiments.

associated cells [$P < 0.0001$]). Only slight differences in ribosome-normalized transcript abundance were observed between planktonic and biofloc-enriched DET for *rpoB* or *fdhA* at either time point. On a per-cell basis, the numbers of 16S rRNA (ribosome) copies per DNA gene copies (48 ± 32 per cell) were not statistically higher or lower in either enrichment.

2.D.6. Planktonic and Biofloc-Associated *Methanospirillum*

As a hydrogenotrophic methanogen, *Methanospirillum hungatei* competes with *Dehalococcoides* for electron equivalents (19). Transcripts of MHU functional genes in RNA pools from the same enrichments were also studied. Primers for the well-conserved delta subunit of the methyl viologen-reducing hydrogenase (*mvrD*) were designed. This non-coenzyme F_{420} hydrogenase subunit has been shown to interact with (provide electrons to) heterodisulfide reductase, an enzyme involved in the last step in methanogenesis (9). The sequences recovered from clone sequencing (EU498366) were most closely related to *Methanospirillum hungatei* JF-1 (YP_503279) (100% identity over 186 bp of *mvrD*).

Given that the majority of *M. hungatei* cells were present in biofloc enrichments (Figure 2.4B), detection of larger numbers of transcripts for the housekeeping gene *rpoE* and the gene *mvrhD* in the biofloc enrichment was expected (Figure 2.7). For *mvrD* but not *rpoE*, a very strong dependence on time was observed, with *mvrD* showing a strong increase (~10-fold) between the early and late time points. A lag time in the onset of *mvr*D expression has been previously observed in our lab and corresponds to a lag in the onset of methane accumulation in batch cultures (data not shown). Ribosome-normalized expression data did not show any difference between enrichments (data not shown). On a per-cell basis, plankton-enriched *M. hungatei* contained $8.5 \times 10^3 \pm 2.5 \times 10^3$ ribosomes and biofloc-enriched cells contained

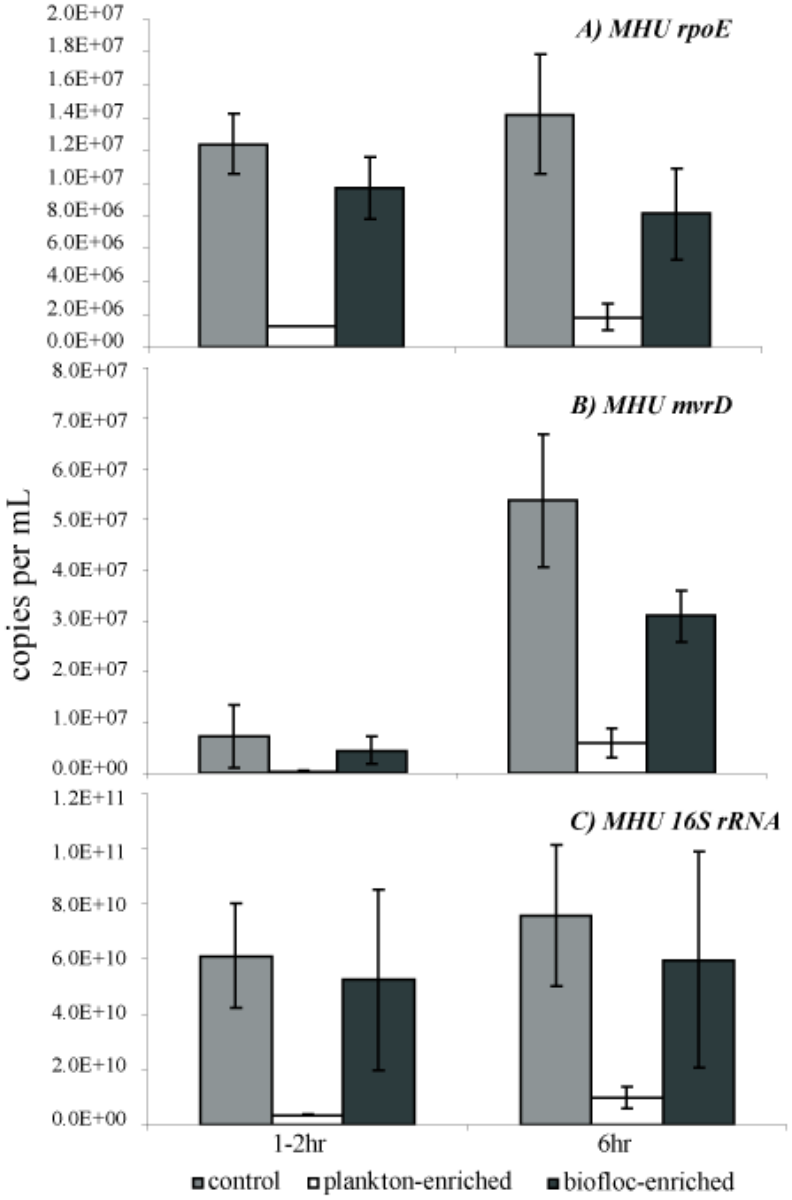

Figure 2.7. Average gene expression values for *Methanospirillum sp.* on a per mL enrichment basis (control, planktonic, or biofloc) at 1 to 2 hours and 6 hours post-feed for: (A) *rpoE*, and (B) *mvrD*, as well as (C) 16S rRNA copies (ribosome copies). Error bars represent standard error of values from replicate experiments.

significantly more, with $1.4 \times 10^4 \pm 3.6 \times 10^3$ ribosomes per DNA copy. MHU in both attachment phases contained ribosome densities over 2 orders of magnitude higher than those in DET cells on a per-cell basis.

2.E. Discussion

The Donna II enrichment culture containing *Dehalococcoides ethenogenes* strain 195 has been the subject of many previously published studies. This report presents the first phylogenetic characterization of the bacterial and archaeal groups in Donna II. From the bacterial libraries, representatives were found from the *Firmicutes*, *Delta-*/*Epsilonproteobacteria*, *Bacteriodetes*, *Nitrospirales*, *Thermotogales*, *Spirochetes*, and *Chloroflexi*. Each of these taxa has been previously observed in chloroethene-reducing communities. However, considering the diversity within many of these phyla and classes, we sought to assess the similarity within representatives of these groups, which showed conservation at the family level and even the genus level for certain operational taxonomic units (see Table A1.1 in Appendix I). The *Clostridia* were represented in all studied clone libraries. Within the class certain families were favored, especially the *Clostridiaceae*. While phylogeny cannot completely inform function and many of these representative groups are physiologically diverse, the similar phylogenetic structure of these communities suggests that the potential roles of these operational taxonomic units in chloroethene-degrading communities are likely conserved. For the Donna II enrichment culture, it has previously been shown that butyrate is converted to hydrogen and acetate (19, 20). This conversion is a microbially mediated process which involves one if not several organisms in the culture. Candidate syntrophic fermenters are different members of the *Firmicutes*, the *Bacteroidetes*, and some of the *Delta-*/*Epsilonproteobacteria* (7).

Though we cannot yet determine the specific organisms responsible for all metabolic processes occurring in this culture, two functions that we know occur and have been able to associate with the appropriate phylogenies are methanogenesis (via hydrogenotrophic *Methanospirillum* and acetoclastic *Methanosaeta*) and reductive dechlorination (via *Dehalococcoides)*. The detection of a single DET phylotype in our culture is consistent with previous *Dehalococcoides*-specific DGGE analyses (18). While the clone library results illuminate which archaeal and bacterial taxa are present, they do not provide insights into the relative or absolute populations.

The distribution and localization of DET and archaeal (methanogenic) populations was studied using both FISH and qPCR. Methanogens tended to form long strands of cells around the exteriors of bioflocs, while DET cells were more evenly distributed within bioflocs (Figure 2.2) as well as between biofloc and planktonic phases. It is unknown how or why DET associates in these different phases, though each growth form is likely to have benefits, with planktonic cells having more access to soluble nutrients and biofloc cells better access to nutrients provided by other organisms. It has been postulated that spatial orientation is important in syntrophic communities, as it facilitates the transfer of metabolites between organisms (in this case between butyrate fermenters and hydrogen consumers) (59). As such, different environmental conditions may favor one attachment phase over another; however, further study of culturing conditions and growth of these organisms in different phases would help determine the factors controlling attachment phase. Additional multiplex FISH studies targeting putative fermenters will further illuminate the association of the various syntrophic populations in bioflocs.

A direct comparison of absolute numbers of DET cells suggested that, in general, qPCR values were higher and more variable than FISH estimates, i.e., 1.8 ± 1.5 times higher, or 1.3 ±

0.6 times higher excluding an outlier (2.5 x 10^9 per ml), which is twice the highest total cell density observed by DAPI during these experiments. While the errors for these ratios are large (stemming from the fact they are a combination of two values, each with large associated errors), they suggest that in general qPCR reports higher values than FISH. Both qPCR and FISH are subject to their own biases. qPCR is a measure of DNA copies and can both over- and underestimate viable populations. Overestimation can be the result of individual cells containing multiple copies just before cell division as well as contributions from dead or inactive cells. On the other hand, poor cell lysis or DNA recovery can lead to an underestimation of populations via qPCR. FISH does not specifically discriminate between live and dead cells, but inactive cells are likely difficult to detect using FISH due to a low ribosome content. The discrepancies between these two methods, as they are commonly used to measure biomass, suggest that further investigation of factors that affect variability in these methods is needed. It also suggests that the method of quantification should be taken into account when considering reported values.

In this study, we showed that even active DET cells contain a small number of ribosomes (48 ± 32 ribosomes per cell) compared to MHU (14,000 ± 3600 ribosomes per cell). Given that these values are a ratio of assays for two different nucleotides (RNA/DNA), each of which is subject to different biases and associated errors, the large standard deviations are not surprising. Even considering these large standard deviations, there is a dramatic difference in per-cell ribosome content between MHU and DET. These differences are likely a function of size. DET cells are flattened cocci approximately 0.5 μm in diameter and 0.2 μm thick (44), giving a biovolume of 40 nm^3 (based on cylindrical volume $\pi r^2 h$). *M. hungatei* JF1 cells are long spiral chains of 0.4 to 0.5 μm in diameter and can range from 7.4 to 10 μm in length (7), with an approximate biovolume of 1,400 to 1,900 nm^3, or approximately 40 times the volume of DET.

Though cell populations given by DNA copies suggest that methanogens are far less numerous organisms, in terms of ribosomes per milliliter of control culture (Figure 2.5E and 2.7C), there are approximately six times more MHU ribosomes than DET ribosomes. This prevalence of methanogens in terms of biovolume is not surprising considering that this culture is given butyrate in excess of what is required to reduce the supplied PCE to ethene. In a typical feeding cycle, a similar number of moles of electron equivalents go to the production of methane (approximately 250 μmol methane per liter of culture from both *Methanosaeta* and *Methanospirillum*) as go to reducing PCE (approximately 288 μmol VC plus ethene per liter culture), specifically, 2.0 and 2.3 milli-electron equivalents per liter of culture based on respective end product productions (data not shown). Population numbers given by qPCR may suggest that methanogens are only minor members of the community. However, in terms of biovolume in the culture, ribosomes per milliliter, and portion of electron equivalents that are converted to end products, they are on par with the dechlorinators.

Overall gene expression levels and ribosome contents in DET cells from each cell attachment phase were similar for most targets investigated. One exception was the planktonic DET's higher expression of *tceA*, which encodes the TCE reductive dehalogenase in DET and has shown promise as a specific bioindicator of TCE respiration at contaminated field sites (36, 37, 39, 40, 61). Given that no other differences in gene expression were observed between the DET in planktonic and biofloc enrichments (similar overall transcriptional activity), this result suggests differential expression of *tceA* in different cell locations. Though specific factors controlling reductive dehalogenase expression have yet to be elucidated, the differences in expression trends for different reductive dehalogenases suggest tight transcriptional control (25, 40, 52, 53, 61). In the case of bioflocs, mass transfer of an exogenously supplied chlorinated

substrate or other small molecules (e.g., vitamins) may explain the resulting lower expression of *tceA* in the biofloc-associated cells relative to the planktonic cells. As bioflocs are presumed to be a major site of butyrate fermentation to hydrogen, one would expect biofloc-associated DET to experience higher hydrogen partial pressures. However, no statistical difference in hydrogenase expression between planktonic and biofloc associated DET was noted. This could be due to a lack of sensitivity in our assay (incomplete separation and/or variation in the method) obscuring true differences. However, previous studies with DET showed very little difference in expression of *hupL* in DET grown in 0.1 atm versus 10^{-4} to 10^{-5} atm hydrogen partial pressures (46).

The strong temporal trend for the MHU gene *mvrD* (but not for the housekeeping gene *rpoE*) may be explained by the nature of hydrogen production in this culture via interspecies hydrogen transfer. In this culture, butyrate is fermented to hydrogen and acetate, with hydrogen levels stabilizing near 10^{-5} atmospheres after 2 to 3 hours (19, 20, 57). These studies have reported that hydrogen thresholds for methanogens are higher than those for DET. The delayed expression of *mvrD* may be tied to the accumulation of hydrogen above a threshold level for gene induction at somewhere between 2 and 6 hours post-feed. Under different culturing conditions, differences in distribution of populations and/or gene expression between enrichments may become more or less pronounced for either DET or MHU.

For the MHU populations, the biofloc-associated cells were the predominant contributors to overall gene transcript levels. In terms of number of transcripts per milliliter, MHU had 1 or 2 orders of magnitude fewer transcripts than DET, depending on the gene (Figure 2.6). The corresponding ratios of transcripts to ribosomes for MHU (all bellow 10^{-3}) were also at least an order of magnitude lower than those for DET. The greater number of ribosomes and fewer transcripts per milliliter of enrichment for MHU compared to DET suggest that these two

organisms may have different translational strategies. As MHU harbors more ribosomes than DET, it may require fewer transcripts to maintain its protein pool. Further work that examines the relationship between transcript abundance and ribosome content in combination with the quantification of protein pools will further our understanding of the expression differences between these organisms.

The activity of planktonic *Dehalococcoides* populations along with their small size and tolerance for low hydrogen partial pressures may explain why organisms from *Dehalococcoides*-containing enrichment cultures, such as the commercially available KB-1™, are so successful for bioaugmentation. Though growth of *Dehalococcoides* organisms in mixed communities is more robust, dispersal in an aquifer is likely dominated by planktonic rather than biofloc-associated *Dehalococcoides*. To assess the activity of *Dehalococcoides* in an environmental setting, it has been suggested that DNA copies or mRNA transcripts could be useful bioindicators of *in situ* dehalorespiration. Since these organisms can be found in association with other organisms (biofloc) or as planktonic cells in environmental settings, it is important to establish what differences may exist in gene copies and gene expression between these attachment phases. Our data suggest that, though some differences in gene expression exist, no cell attachment phase appears to be significantly more or less transcriptionally active than the other. This suggests that the activity of planktonic *Dehalococcoides* cells in groundwater samples, which are easier and less costly to obtain than soil cores, should reflect broader activity of *Dehalococcoides* in the subsurface. However, additional studies where mRNA transcript levels in groundwater and soil samples are directly compared at active bioremediation sites are needed.

2.F. Acknowledgement

Co-authors in this work were Brendan J. Lazar, Robert M. Morris, and Ruth E. Richardson. We sincerely thank L.Safak Yilmez, Daniel R. Noguera and their lab, for their analysis of probe hybridization free energies displayed in supplementary table one. For assistance with lab techniques and trouble-shooting we thank Laura Jennings, Emily Warren and especially Brian Rahm. Special thanks to Janice E. Thies for use of laboratory equipment and supplies, and Angelika Rumberger for her technical expertise and help with DGGE. Thanks to Steve Zinder for supplying methanogen pure cultures and general assistance and advice throughout the project. This work was supported through a Biogeochemistry and Environmental Biocomplexity IGERT small grant (DGE 0221658) and Department of Defense Army Research Office Grant W911NF-07-1-0249. Thanks as well to the National Science Foundation's Graduate Research Fellowship.

REFERENCES

1. **Adrian, L. and H. Goerisch.** 2002. Microbial transformation of chlorinated benzenes under anaerobic conditions. Res. Microbiol. **153:**131-137.

2. **Adrian, L., S. K. Hansen, J. M. Fung, H. Gorisch, and S. H. Zinder.** 2007. Growth of *Dehalococcoides* strains with chlorophenols as electron acceptors. Environ. Sci. Technol. **41:**2318-2323.

3. **Amann, R. I., L. Krumholz, and D. A. Stahl.** 1990. Fluorescent-Oligonucleotide Probing of Whole Cells for Determinative Phylogenetic and Environmental Studies in Microbiology. J. Bacteriol. **172:**762-770.

4. **Becker, J. G., G. Berardesco, B. E. Rittmann, and D. A. Stahl.** 2005. The role of syntrophic associations in sustaining anaerobic mineralization of chlorinated organic compounds. Environ. Health Perspect. **113:**310-316.

5. **Becker, P., W. Hufnagle, G. Peters, and M. Herrmann.** 2001. Detection of Differential Gene Expression in Biofilm-Forming versus Planktonic Populations of *Staphylococcus aureus* Using Micro-Representational-Difference Analysis. Appl. Environ. Microbiol. **67:**2958-2965.

6. **Bedard, D. L., K. A. Ritalahti, and F. E. Loffler.** 2007. The *Dehalococcoides* population in sediment-free mixed cultures metabolically dechlorinates the commercial polychlorinated biphenyl mixture aroclor 1260. Appl. Environ. Microbiol. **73:**2513-2521.

7. **Boone, D. R., R. W. Castenholz, and G. M. Garrity**(*ed.*).2001. Bergey's manual of systematic bacteriology; Systematic bacteriology. Springer, New York.

8. **Bowman, K. S., W. M. Moe, B. A. Rash, H. S. Bae, and F. A. Rainey.** 2006. Bacterial diversity of an acidic Louisiana groundwater contaminated by dense nonaqueous-phase liquid containing chloroethanes and other solvents. FEMS Microbiol. Ecol. **58:**120-133.

9. **Brodersen, J., G. Gottschalk, and U. Deppenmeier.** 1999. Membrane-bound $F_{420}H_2$-dependent heterodisulfide reduction in *Methanococcus voltae*. Arch. Microbiol. **171:**115-121.

10. **Busch, P. L. and W. Stumm.** 1968. Chemical interactions in the aggregation of bacteria bioflocculation in waste treatment. Environ. Sci. Technol. **2:**49-53.

11. **Chen, G.** 2004. Reductive dehalogenation of tetrachloroethylene by microorganisms: current knowledge and application strategies. Appl. Microbiol. Biotechnol. **63:**373-377.

12. **Dennis, P. C., B. E. Sleep, R. R. Fulthorpe, and S. N. Liss.** 2003. Phylogenetic analysis of bacterial populations in an anaerobic microbial consortium capable of degrading saturation concentrations of tetrachloroethylene. Can. J. Microbiol. **49:**15-27.

13. **Distefano, T. D., J. M. Gossett, and S. H. Zinder.** 1992. Hydrogen as an electron donor for dechlorination of tetrachloroethene by an anaerobic mixed culture. Appl. Environ. Microbiol. **58:**3622-3629.

14. **Distefano, T. D., J. M. Gossett, and S. H. Zinder.** 1991. Reductive Dechlorination of High Concentrations of Tetrachloroethene to Ethene by an Anaerobic Enrichment Culture in the Absence of Methanogenesis. Appl. Environ. Microbiol. **57:**2287-2292.

15. **Dojka, M. A., P. Hugenholtz, S. K. Haack, and N. R. Pace.** 1998. Microbial Diversity in a Hydrocarbon- and Chlorinated-Solvent-Contaminated Aquifer Undergoing Intrinsic Bioremediation. Appl. Environ. Microbiol. **64:**3869-3877.

16. **Duhamel, M. and E. A. Edwards.** 2007. Growth and yields of dechlorinators, acetogens, and methanogens during reductive dechlorination of chlorinated ethenes and dihaloelimination of 1,2-dichloroethane. Environ. Sci. Technol. **41:**2303-2310.

17. **Duhamel, M. and E. A. Edwards.** 2006. Microbial composition of chlorinated ethene-degrading cultures dominated by *Dehalococcoides*. FEMS Microbiol. Ecol. **58:**538-549.

18. **Duhamel, M., K. Mo, and E. A. Edwards.** 2004. Characterization of a highly enriched *Dehalococcoides*-containing culture that grows on vinyl chloride and trichloroethene. Appl. Environ. Microbiol. **70:**5538-5545.

19. **Fennell, D. E. and J. M. Gossett.** 1998. Modeling the production of and competition for hydrogen in a dechlorinating culture. Environ. Sci. Technol. **32:**2450-2460.

20. **Fennell, D. E., J. M. Gossett, and S. H. Zinder.** 1997. Comparison of butyric acid, ethanol, lactic acid, and propionic acid as hydrogen donors for the reductive dechlorination of tetrachloroethene. Environ. Sci. Technol. **31:**918-926.

21. **Flynn, S. J., F. E. Loffler, and J. M. Tiedje.** 2000. Microbial community changes associated with a shift from reductive dechlorination of PCE to reductive dechlorination of cis-DCE and VC. Environ. Sci. Technol. **34:**1056-1061.

22. **Freeborn, R. A., K. A. West, V. K. Bhupathiraju, S. Chauhan, B. G. Rahm, R. E. Richardson, and L. Alvarez-Cohen.** 2005. Phylogenetic analysis of TCE-dechlorinating consortia enriched on a variety of electron donors. Environ. Sci. Technol. **39:**8358-8368.

23. **Freedman, D. L. and J. M. Gossett.** 1991. Biodegradation of Dichloromethane and its Utilization as a Growth Substrate Under Methanogenic Conditions. Appl. Environ. Microbiol. **57:**2847-2857.

24. **Freedman, D. L. and J. M. Gossett.** 1989. Biological Reductive Dechlorination of Tetrachloroethylene and Trichloroethylene to Ethylene Under Methanogenic Conditions. Appl. Environ. Microbiol. **55:**2144-2151.

25. **Fung, J. M., R. M. Morris, L. Adrian, and S. H. Zinder.** 2007. Expression of reductive dehalogenase genes in *Dehalococcoides ethenogenes* strain 195 growing on tetrachloroethene, trichloroethene, or 2,3-dichlorophenol. Appl. Environ. Microbiol. **73:**4439-4445.

26. **Futamata, H., N. Yoshida, T. Kurogi, S. Kaiya, and A. Hiraishi.** 2007. Reductive dechlorination of chloroethenes by *Dehalococcoides*-containing cultures enriched from a polychlorinated-dioxin-contaminated microcosm. ISME J. **1:**471-479.

27. **Gloeckner, F. O., R. Amann, A. Alfreider, J. Pernthaler, R. Psenner, K. Trebesius, and K. H. Schleifer.** 1996. An *in situ* hybridization protocol for detection and identification of planktonic bacteria. Syst. Appl. Microbiol. **19:**403-406.

28. **Gu, A. Z., B. P. Hedlund, J. T. Staley, S. E. Strand, and H. D. Stensel.** 2004. Analysis and comparison of the microbial community structures of two enrichment cultures capable of reductively dechlorinating TCE and cis-DCE. Environ. Microbiol. **6:**45-54.

29. **Hales, B. A., C. Edwards, D. A. Ritchie, G. Hall, R. W. Pickup, and J. R. Saunders.** 1996. Isolation and identification of methanogen-specific DNA from blanket bog feat by PCR amplification and sequence analysis. Appl. Environ. Microbiol. **62:**668-675.

30. **Harkness, M. R., A. A. Bracco, M. J. Brennan, K. A. Deweerd, and J. L. Spivack.** 1999. Use of bioaugmentation to stimulate complete reductive dechlorination of trichloroethene in dover soil columns. Environ. Sci. Technol. **33:**1100-1109.

31. **He, J. Z., V. F. Holmes, P. K. H. Lee, and L. Alvarez-Cohen.** 2007. Influence of vitamin B-12 and cocultures on the growth of *Dehalococcoides* isolates in defined medium. Appl. Environ. Microbiol. **73:** 2847-2853.

32. **Hoelscher, T., H. Goerisch, and L. Adrian.** 2003. Reductive dehalogenation of chlorobenzene congeners in cell extracts of *Dehalococcoides* sp. strain CBDB1. Appl. Environ. Microbiol. **69:**2999-3001.

33. **Hohnstock-Ashe, A. M., S. M. Plummer, R. M. Yager, P. Baveye, and E. L. Madsen.** 2001. Further biogeochemical characterization of a trichloroethene-contaminated fractured dolomite aquifer: Electron source and microbial communities involved in reductive dechlorination. Environ. Sci. Technol. **35:**4449-4456.

34. **Holmes, V. F., J. Z. He, P. K. H. Lee, and L. Alvarez-Cohen.** 2006. Discrimination of multiple *Dehalococcoides* strains in a trichloroethene enrichment by quantification of their reductive dehalogenase genes. Appl. Environ. Microbiol. **72:**5877-5883.

35. **Holoman, T. R. P., M. A. Elberson, L. A. Cutter, H. D. May, and K. R. Sowers.** 1998. Characterization of a defined 2,3,5,6-tetrachlorobiphenyl-ortho-dechlorinating microbial community by comparative sequence analysis of genes coding for 16S rRNA. Appl. Environ. Microbiol. **64:**3359-3367.

36. **Johnson, D. R., P. K. H. Lee, V. F. Holmes, and L. Alvarez-Cohen.** 2005. An internal reference technique for accurately quantifying specific mRNAs by real-time PCR with a application to the tceA reductive dehalogenase gene. Appl. Environ. Microbiol. **71:**3866-3871.

37. **Johnson, D. R., P. K. H. Lee, V. F. Holmes, A. C. Fortin, and L. Alvarez-Cohen.** 2005. Transcriptional expression of the tceA gene in a *Dehalococcoides*-containing microbial enrichment. Appl. Environ. Microbiol. **71:**7145-7151.

38. **Kassenga, G., J. H. Pardue, W. M. Moe, and K. S. Bowman.** 2004. Hydrogen thresholds as indicators of dehalorespiration in constructed treatment wetlands. Environ. Sci. Technol. **38:**1024-1030.

39. **Krajmalnik-Brown, R., Y. Sung, K. M. Ritalahti, F. M. Saunders, and F. E. Loffler.** 2007. Environmental distribution of the trichloroethene reductive dehalogenase gene (tceA) suggests lateral gene transfer among *Dehalococcoides*. FEMS Microbiol. Ecol. **59:**206-214.

40. **Lee, P. K. H., D. R. Johnson, V. F. Holmes, J. Z. He, and L. Alvarez-Cohen.** 2006. Reductive dehalogenase gene expression as a biomarker for physiological activity of *Dehalococcoides* spp. Appl. Environ. Microbiol. **72:**6161-6168.

41. **Logan, B. E. and J. R. Hunt.** 1987. Advantages to Microbes of Growth in Permeable Aggregates in Marine Systems. Limnol. Oceanogr. **32:**1034-1048.

42. **Ludwig, W., O. Strunk, R. Westram, L. Richter, H. Meier, Yadhukumar, A. Buchner, T. Lai, S. Steppi, G. Jobb, W. Forster, I. Brettske, S. Gerber, A. W. Ginhart, O. Gross, S. Grumann, S. Hermann, R. Jost, A. Konig, T. Liss, R. Lussmann, M. May, B. Nonhoff, B. Reichel, R. Strehlow, A. Stamatakis, N. Stuckmann, A. Vilbig, M. Lenke, T. Ludwig, A. Bode, and K. H. Schleifer.** 2004. ARB: a software environment for sequence data. Nucleic Acids Res. **32:**1363-1371.

43. **Macbeth, T. W., D. E. Cummings, S. Spring, L. M. Petzke, and K. S. Sorenson.** 2004. Molecular characterization of a dechlorinating community resulting from *in situ* biostimulation in a trichloroethene-contaminated deep, fractured basalt aquifer and comparison to a derivative laboratory culture. Appl. Environ. Microbiol. **70:**7329-7341.

44. **Maymo Gatell, X., Y. T. Chien, J. M. Gossett, and S. H. Zinder.** 1997. Isolation of a bacterium that reductively dechlorinates tetrachloroethene to ethene. Science. **276:**1568-1571.

45. **Maymo Gatell, X., V. Tandoi, J. M. Gossett, and S. H. Zinder.** 1995. Characterization of an H-2-utilizing enrichment culture that reductively dechlorinates tetrachloroethene to vinyl chloride and ethene in the absence of methanogenesis and acetogenesis. Appl. Environ. Microbiol. **61:**3928-3933.

46. **Morris, R. M., S. Sowell, D. Barofsky, S. Zinder, and R. Richardson.** 2006. Transcription and mass-spectroscopic proteomic studies of electron transport oxidoreductases in *Dehalococcoides ethenogenes*. Environ. Microbiol. **8:**1499-1509.

47. **Morris, R. M., M. S. Rappe, E. Urbach, S. A. Connon, and S. J. Giovannoni.** 2004. Prevalence of the *Chloroflexi*-related SAR202 bacterioplankton cluster throughout the mesopelagic zone and deep ocean. Appl. Environ. Microbiol. **70:**2836-2842.

48. **Morris, R. M., J. M. Fung, B. G. Rahm, S. Zhang, D. L. Freedman, S. H. Zinder, and R. E. Richardson.** 2007. Comparative proteomics of *Dehalococcoides* spp. reveals strain-specific peptides associated with activity. Appl. Environ. Microbiol. **73:**320-326.

49. **Nakatsu, C. H., V. Torsvik, and L. Ovreas.** 2000. Soil community analysis using DGGE of 16S rDNA polymerase chain reaction products. Soil Sci. Soc. Am. J. **64:**1382-1388.

50. **Nielson, R. B.** 1999. PhD Thesis. University of California, Berkeley, Berkeley, CA.

51. **Pernthaler, A. and R. Amann.** 2004. Simultaneous fluorescence *in situ* hybridization of mRNA and rRNA in environmental bacteria. Appl. Environ. Microbiol. **70:**5526-5533.

52. **Rahm, B. G. and R. E. Richardson.** 2008. Correlation of Respiratory Gene Expression Levels and Pseudo-Steady-State PCE Respiration Rates in *Dehalococcoides ethenogenes*. Environ. Sci. Technol. **42:**416-421.

53. **Rahm, B. G., R. M. Morris, and R. E. Richardson.** 2006. Temporal expression of respiratory genes in an enrichment culture containing *Dehalococcoides ethenogenes*. Appl. Environ. Microbiol. **72:**5486-5491.

54. **Richardson, R. E., V. K. Bhupathiraju, D. L. Song, T. A. Goulet, and L. Alvarez-Cohen.** 2002. Phylogenetic characterization of microbial communities that reductively dechlorinate TCE based upon a combination of molecular techniques. Environ. Sci. Technol. **36:**2652-2662.

55. **Rossetti, S., L. L. Blackall, M. Majone, P. Hugenholtz, J. J. Plumb, and V. Tandoi.** 2003. Kinetic and phylogenetic characterization of an anaerobic dechlorinating microbial community. Microbiology-Sgm **149:**459-469.

56. **Seshadri, R., L. Adrian, D. E. Fouts, J. A. Eisen, A. M. Phillippy, B. A. Methe, N. L. Ward, W. C. Nelson, R. T. Deboy, H. M. Khouri, J. F. Kolonay, R. J. Dodson, S. C. Daugherty, L. M. Brinkac, S. A. Sullivan, R. Madupu, K. T. Nelson, K. H. Kang, M. Impraim, K. Tran, J. M. Robinson, H. A. Forberger, C. M. Fraser, S. H. Zinder, and J. F. Heidelberg.** 2005. Genome sequence of the PCE-dechlorinating bacterium *Dehalococcoides ethenogenes*. Science **307:**105-108.

57. **Smatlak, C. R., J. M. Gossett, and S. H. Zinder.** 1996. Comparative kinetics of hydrogen utilization for reductive dechlorination of tetrachloroethene and methanogenesis in an anaerobic enrichment culture. Environ. Sci. Technol. **30:**2850-2858.

58. **Smidt, H. and W. M. de Vos.** 2004. Anaerobic Microbial Dehalogenation. Annu Rev Microbiol. 2004;58:43-73.

59. **Stams, A. J. M.** 1994. Metabolic Interactions between Anaerobic-Bacteria in Methanogenic Environments. Anton. Leeuw. Int. J. G. **66:**271-294.

60. **Thiele, J. H., M. Chartrain, and J. G. Zeikus.** 1988. Control of Interspecies Electron Flow during Anaerobic-Digestion - Role of Floc Formation in Syntrophic Methanogenesis. Appl. Environ. Microbiol. **54:**10-19.

61. **Waller, A. S., R. Krajmalnik-Brown, F. E. Loffler, and E. A. Edwards.** 2005. Multiple reductive-dehalogenase-homologous genes are simultaneously transcribed during dechlorination by *Dehalococcoides*-containing cultures. Appl. Environ. Microbiol. **71:**8257-8264.

62. **Wang, Q., G. M. Garrity, J. M. Tiedje, and J. R. Cole.** 2007. Naive Bayesian Classifier for Rapid Assignment of rRNA Sequences into the New Bacterial Taxonomy. Appl. Environ. Microbiol. **73:**5261-5267.

63. **Yang, Y. R. and J. Zeyer.** 2003. Specific detection of *Dehalococcoides* species by fluorescence *in situ* hybridization with 16S rRNA-targeted oligonucleotide probes. Appl. Environ. Microbiol. **69:**2879-2883.

64. **Yang, Y. R., M. Pesaro, W. Sigler, and J. Zeyer.** 2005. Identification of microorganisms involved in reductive dehalogenation of chlorinated ethenes in an anaerobic microbial community. Water Res. **39:**3954-3966.

65. **Yilmaz, L. S. and D. R. Noguera.** 2004. Mechanistic approach to the problem of hybridization efficiency in fluorescent *in situ* hybridization. Appl. Environ. Microbiol. **70:**7126-7139.

CHAPTER 3

Absolute quantification of *Dehalococcoides* protein and mRNA biomarkers for dehalorespiration: implications for inferring protein production and protein-specific kinetic parameters

3.A. Abstract

Well-selected and tested microbial biomarkers could provide critical insight into *in situ* microbial activities, such as organochlorine respiration. Analyses of available *Dehalococcoides* genomes and metagenomes have suggested candidate biomarkers that were previously tested at the RNA and DNA level. However, quantitative protein work has been limited and correlations between protein abundance and RNA abundance have not yet been investigated. To this aim, transcript and protein abundances of different *Dehalococcoides* metabolic genes were quantified over a variety of continuous feeding conditions. Transcript levels of the dehalogenase, TceA, and the hydrogenase, HupL, were positively correlated with respiration rates ranging from 1.5 to 280 μeeq per L-hr with no effect of chloroethenes or electron donor (n=24). Other targets tested demonstrated saturating or declining mRNA levels at respiration rates above 5 μeeq per L-hr. Below a respiration threshold (~1 μeeq per L-hr), mRNA biomarkers illustrated first-order, specific-decay coefficients of 0.03 to 0.06 per hour. Confirmation of protein production from corresponding mRNAs was performed using relative and targeted quantitative mass spectrometry-based proteomic approaches. Net protein production in batch and continuously fed cultures suggest that the mRNA translation rate is greater for TceA (0.4 to 1.2 protein molecules per mRNA-hr in continuous feed cultures), than HupL, or the dehalogenases PceA and DET1545 (all within 0.03 to 0.17 protein molecules per mRNA-hr in continuous feed cultures). For a given

target, protein production did not always correlate with mRNA abundance alone. However, accounting for rRNA content at different growth conditions demonstrated better correlations with protein abundance and production (e.g., TceA 5.2 x 10^{-8} to 5.6 x 10^{-8} protein molecules-mL per mRNA-rRNA-hour for continuous feed cultures). This targeted proteomic approach, in conjunction with pseudo-steady state substrate data, was also used for calculation of *in vivo* enzyme-specific rate constants for dehalogenases of previously confirmed function. Maximum *in vivo* enzyme-specific rate constants were 2.1 and 0.13 attamole per mole enzyme per hour for PceA and TceA, respectively. These data support the utility of both mRNA and protein biomarkers, especially for inferring process rates, but highlight potential problems with inferring protein abundance from mRNA data alone.

3.B. Introduction

Microbes catalyze many environmentally relevant processes, including the transformation or degradation of chemical pollutants. Chlorinated organic compounds, in particular the chloroethenes, make up a common and compelling group of environmental contaminants. Extensive use and poor disposal of chloroethenes, such as tetrachloroethene (PCE) and trichloroethene (TCE), has led to their wide spread distribution and made them the most common groundwater pollutants in the United States (38, 40). Members of the group *Dehalococcoides* were the first isolated organisms to generate ethene from these contaminants through dehalorespiration (37). Various strains have been shown to respire myriad chlorinated contaminants, in addition to the chloroethenes (4, 8, 16, 37). Because of this proclicity, members of the *Dehalococcoides* have become target organisms for implementation of bioremediation in ecosystems that have been affected by chlorinated organic compounds.

Detection of biomarkers (biologically synthesized molecules indicative of a process or physiologic state) has been suggested as a method for documenting *in situ* activity of *Dehalococcoides* (10, 28, 36, 50). Correlations have been drawn between the presence of the *Dehalococcoides* 16S ribosomal RNA gene and the generation of ethene in ecosystems remediating chloroethenes (13, 20, 30, 32, 35). However, depending on the abundance and/or specific activity of endemic *Dehalococcoides,* variation in rates and respiration end products (cDCE, VC, Ethene) has been observed (13, 30, 35). Genomic comparisons of *Dehalococcoides* strains with 97-100 percent ribosomal gene similarity vary considerably with respect to key metabolic enzymes (27, 39), further supporting metabolic variability between strains and suggesting that 16S rRNA genes offer limited resolution as a biomarker of specific respiratory capability. In addition to requiring halogenated organics as electron acceptors, *Dehalococcoides* require hydrogen as an electron donor. HupL, the only *Dehalococcoides* hydrogenase predicted to contain a periplasmic catalytic subunit (55), has been shown to be abundant at the protein level in several strains and is likely responsible for respiratory hydrogen uptake (21, 23, 41, 44). On the other end of the electron transport chain, reductive dehalogenases (RDases) that catalyze the reduction of a chlorine-carbon bond have been biochemically characterized for chloroethene-reducing enzymes TceA, PceA, VcrA, as well as a chlorobenzene-reducing enzyme CbrA (2, 3, 21, 23, 33, 34, 43). RDase homologs of TceA, VcrA, and BvcA (another putative VC RDase) are commonly monitored and detected at field sites undergoing remediation of TCE or PCE (12, 22, 29, 45, 51, 54). However, in studies where mRNA abundance was monitored in conjunction with DNA, gene presence has not always been linked to gene expression (11, 29).

As a result, *Dehalococcoides* biomarker research is currently focusing on gene expression, rather than gene presence, through detection of RNA and protein biomarkers (9, 18,

25, 28, 36, 41, 42, 59). Work with a mixed culture containing *Dehalococcoides ethenogenes* strain 195 (DET) highlighted up-regulation in five of the 19 putative RDases encoded in the genome (TceA, DET0162, PceA, DET1545, and DET1559) (48) following PCE batch feed. In other mixed cultures, high transcript levels of homologs to TceA (6, 28, 58), PceA (6) and DET1545 (19, 29, 58) have been demonstrated in addition to culture-specific RDases BvcA (26) and VcrA (43, 58). At a field sight undergoing TCE bioremediation, homologs of DET1545 (FtLewis 1638/CBDB1_1638) and *bcvA* were the dominant RDases represented in RDase cDNA clone libraries (29). Shotgun proteomics in DET was used to confirm presence of all but one (DET0162 containing a premature stop codon) of the high transcript level RDase targets in addition to the hydrogenase HupL (41, 42). In a continuous feed system developed to monitor mRNA expression levels under the condition of steady state respiration, DET pseudo-steady state expression increased linearly with respiration with the following exception. At the highest respiration rates tested (at or near the V_{max}), the response of mRNA (in copies per milliliter culture) appeared to saturate for many DET transcripts, coinciding with an increase in 16S rRNA abundance. This saturation in mRNA concentration, despite more rapid respiration, suggested only a limited correlation range for mRNA and respiration. Additionally, these observations raised interest in whether corresponding protein levels are also saturating. Determining whether protein production increases or saturates under these conditions could help resolve relationships between mRNA and protein biomarker levels. Although biomarker proteins have been previously detected, the functional relevance of mRNA expression levels on protein levels has yet to be demonstrated. Additionally, protein quantification would test the utility of inferring rates from protein biomarkers.

There are three interrelated objectives in the present study. The first aim was to resolve empirical relationships between mRNA biomarker levels and pseudo-steady state dehalorespiration rates over a wide range (n=24) of feeding conditions. The second aim was to determine how protein abundance changes with respiration rate. Utilizing both of these datasets, the effect of RNA levels (mRNA and rRNA) on absolute protein production for corresponding biomarkers was assessed. Additionally, this work elucidated net decay rates of mRNA, DNA and protein biomarkers in *Dehalococcoides* under starvation conditions. The last aim was to utilize quantitative proteomics and metabolite data to calculate *in vivo* enzyme-specific rate constants that could potentially be used to infer *in situ* rates from field protein and metabolite data.

3.C. Materials and Methods

3.C.1. Experimental Conditions and Analysis of Metabolites

A six-liter batch reactor containing an anaerobic mixed culture has been maintained on 110 μM PCE and 440 μM butyrate (1:2 ratio of H_2 eeqs assumes 2 H_2 per butyrate fermented) fed on a 3-4 day interval, as previously described (15, 49). Subcultures were constructed in 160-mL serum vials with 100 mL culture volume and a 60-mL headspace. Experimental conditions altered respiration rate, hydraulic residence time and substrates (outlined in Table A2.1, Appendix II) using batch and continuous feeding regimes of both electron donors (ED) and electron acceptors (EA). Respiration was quantified from headspace samples using a gas chromatograph (GC) (Perkin-Elmer) equipped with a flame ionizing detector (FID), as previously described (49). Hydrogen levels were quantified using a GC equipped with a reduced gas detector (RGD) (Trace Analytical) unless concentrations were above 1.5 μmoles nominal

(0.5 μM Cw), in which case a GC equipped with a thermal conductivity detector (TCD) was used, as previously described (56).

3.C.2. Extraction of Nucleic Acids and Proteins

Nucleic acid extractions for qPCR or qRT-PCR were performed on 2-mL culture samples. Samples were pelleted (21,000 *g*, 5 min, 4^{o}C) and stored at -80^{o}C for less than 7 days. Cell lysis was performed as described previously (52) using lysozyme, β-mercaptoethanol and rigorous vortexing. Isolation and clean up of RNA and DNA were performed according to the Qiagen AllPrep RNA/DNA mini prep kit (Qiagen).

Protein extractions were performed from 30-50 mL culture cell pellets (14,000 *g*, 10 min) via lysis by French press (8000 lb/in^2), denaturation in SDS and urea, and reduction to 50 μL volume (final concentration 500 mM phosphate, 4 M urea and 0.1% SDS, pH 8.0) by SpeedVac, as previously described (59). From a subset of French-pressed samples, 200 μL (equating to 2 mL of culture) of cell lysate was collected for qPCR and cleaned by the UltraClean^{TM} Microbial DNA Isolation Kit (MoBio) without bead beating (direct DNA extraction).

3.C.3. Bulk and Targeted (qPCR and qRT PCR) Nucleic Acid Quantification

Total DNA was quantified using the Quant-iT^{TM} Picogreen® double stranded DNA assay (Invitrogen). Prior to qPCR, all DNA samples were diluted 1 to 10. RNA samples were run on the Agilent 2100 BioAnlyzer (Agilent) to assess quality and quantity of extracted RNA. DNase treatment, cDNA synthesis, qPCR setup and qPCR run conditions were performed as described in (47, 50). Primers and annealing temperatures used in this study are listed in Supplemental Table A2.2. Analysis of qPCR data was performed as outlined in (47), utilizing luciferase mRNA as an internal reference standard (24). Raw fluorescence data was used to calculate R_0

values using the DART (data analysis for real time) method (46, 53), and plasmid or pure culture DNA standard curves for each target were used to convert R_0 to copies.

3.C.4. Proteome Sample Preparation

For iTRAQ™ protein assays, one hundred micrograms of total protein (quantified using the Agilent 2100 BioAnalyzer Protein 230 Kit) from samples fed at different rates were digested with trypsin (Sequencing grade, Promega) according to the iTRAQ™ reagent labeling protocol (Applied Biosystems). For analysis of protein decay, equivalent culture volumes (~5 mL of culture) were also digested and labeled according to the iTRAQ™ protocol. A single control (time zero culture sample) was labeled with the 114 isobaric tag. Protein pools for targeted quantitative proteomics (via multiple reaction monitoring) were quality-checked through SDS-PAGE electrophoresis alongside a *E.coli* K12 protein standard (supplied by the Cornell Proteomic facility). From each protein sample, 10 to 20 μg of total protein was treated with 1 mM tris(2-carboxyethyl)phosphine (TCEP HCL) at 37°C for one hour, followed by 50 mM iodoacetamide in the dark for 15 min. This alkylation reaction was quenched using free L-cysteine. Prior to digestion with trypsin (Mass spectrometry grade, Promega) at 37°C for 12-14 hours, the concentration of urea and SDS were diluted to 0.4 M and 0.1%, respectively.

3.C.5. Mass Spectrometry for iTRAQ™ Labeled Samples

Analysis of relative protein abundance utilized iTRAQ™ (Applied Biosystems) isobaric tagging of digest samples. Labels corresponding to reporter ion masses of 114 (control sample), and 115 through 117 (experimental samples) were combined into one protein pool for shotgun proteomic analysis. Strong cation exchange (Agilent 1100 HPLC with UV detector), generation of ten fractions and desalting of fractions via SPE (Waters SepPak C18 cartridge; 1mL of 75% ACN eluent) methods were described in (59). Shotgun proteomic analyses via nLC-MS/MS were

performed as described in (41, 42, 59). Identification of proteins, and statistical analysis of identification (Prot. scores) as well as iTRAQ^{TM} ratios, and error factors were determined using ProteinPilot 2.0 (ABSciex) as described previously (59). Spectra were searched against a custom database combining all publically available sequenced *Dehalococcoides,* methanogen and *Firmicute* genomes, in addition to community-specific metagenomic sequences available for this culture (JGI) as of December 2009.

3.C.6. Targeted Quantitative Proteomics of Mixed Culture Peptides.

Biomarker peptides for targeted proteomic experiments via multiple reaction monitoring (MRM) were selected based on detection in previous shotgun proteomic experiments. Selection of target transition ions was performed in MRMPilot 2.0 (ABSciex) (listed in Table 3.1). Each MRM, in addition to previously developed MRM targets (59), was confirmed via MRM-triggered information dependant acquisition (IDA) on control protein samples (described below).

Clean up of digested peptides followed the protocol outlined above and in (59). Aliquots (1.5 to 3 µL) were then injected into the nLC-MS/MS for MRM-IDA-mode and subsequent normal MRM mode analyses. nLC-MS/MS was also performed as previously described (59), using a hybrid triple quadrupole linear ion trap, 4000 Q Trap (Applied Biosystems, MA). MRM-IDA analysis was used for validation of selected fragment ion pairs prior to MRM quantitative analysis. In MRM-IDA, MS/MS transition ions were monitored as in normal MRM mode, but positive detection triggered linear ion trapping of parent ions followed by MS/MS scanning. Spectra were checked to confirm peptide ID.

Synthetic peptide standards for MRM targets (listed in Table 3.1) were obtained (purified >95%, Bio Basic Inc., Ontario). A dilution series of synthetic peptides were constructed in a background matrix of peptides extracted from aerobic soil mixed culture as described previously

Table 3.1. *Dehalococcoides ethenogenes* str. 195 peptides targets for MRM analysis including sequence, molecular weight, parent ion mass (+charge state), fragment ion mass (+1 charge) and corresponding protein. The average coefficient of variation (CV) for each peptide from a given sample run in triplicate or quadruplicate analysis runs. All peptide sequences were checked against the NCBI database to ensure specificity to members of the *Dehalococcoides.*

DET Gene ID	Protein Name	Target Name	Peptide	MW	Parent ion m/z (Q1)	Fragment ion m/z (Q3)	Parent ion charge state	Quantification limit (fmol per µg total protein)	CV based on quantified level per sample
DET0079	TCE reductive dehalogenase	TceA 1	DEWWASENPIR	1407.5	701.9	786.4	2+	10	33.7
					701.9	972.5	2+		
		TceA 2	VSSIIEPR	900.05	450.8	514.4	2+	10	40.8
					450.8	714.4	2+		
DET0110	[Ni/Fe] hydrogenase, group 1, large subunit	HupL 1	IEATVDGGEVK	1117.23	559.4	804.4	2+	10	18.7
					559.4	875.5	2+		
		HupL 2	DNDNPFELVR	1218.3	609.8	760.5	2+	10	27.6
					609.8	874.5	2+		
DET0318	PCE reductive dehalogenase	PceA 1	YQGTPEDNLR	1192	596.9	743.4	2+	1	22.1
					596.9	901.4	2+		
		PceA 2	YFGGEDVGALELDDK	1627.74	814.3	1317	2+	1	41.4
					814.3	860.5	2+		
DET0604	DNA-directed RNA polymerase, beta' subunit	RpoC	FATSDLNDLYR	1314	658	793.4	2+	10	9.6
					658	995.5	2+		
					658	1167.6	2+		
DET0990	Ribosomal protein L7/L12	DET rp L7/12 1	ALEAAGATIEIK	1186.38	593.8	731.4	2+	20	55.1

					593.8	802.5	2+		
		DET rp L7/L12 2	TVIELSELVK	1130.36	565.8	930.6	2+	20	67.3
					565.8	817.5	2+		
DET0997	Translation elongation factor Tu	DET EF-TU 1	ILDSAEPGDAVGLLLR	1638.9	547.1	571.4	3+	50	64.3
					547.1	1010.6	3+		
					820	856.5	2+		
					820	1010.6	2+		
		DET EF-TU 2	NSFPGDEIPIVR	1343.51	672.3	995.6	2+	50	60.8
					672.3	898.6	2+		
DET1407	Putative S-layer protein, BNR/Asp-box repeat domain protein	S-Layer 1	FDNIGILEWNADK	1534	767.9	1045.5	2+	400	57.44
					767.9	875.4	2+		
		S-Layver 2	VNTANSTSEWFPAVFTTVK	2099	700.4	862.5	3+	1000	88.9
					700.4	765.5	3+		
DET1428	Co-chaperonin GroEL	GroEL 1	AQIEETESAFDR	1395	698.4	1196.5	2+	20	24.4
					698.4	1083.5	2+		
		GroEL 2	GYISAYFVTDPGR	1445.6	723.5	1112.5	2+	20	67.9
					723.5	954.5	2+		
					486.8	802.4	3+		
DET1545	Reductive dehalogenase, putative	DET1545 1	LYTLTPEYGAPGR	1437.6	719.4	846.4	2+	1	33.2
					719.4	1161.6	2+		
					719.4	620.4	2+		
		DET1545 2	TASNYPGYTYR	1292.38	646.8	756.4	2+	2	58
					646.8	659.4	2+		
					646.8	919.5	2+		
DET1559	Reductive dehalogenase, putative	DET1559	DDASSVHEIVK	1199	600.3	488.3	2+	20	99
					600.3	476.2	2+		

(7, 59). A standard curve was generated for each MRM analysis run and analyzed in duplicate. Four MRM analysis runs were performed over a four month period (March 2010 through June 2010). Standard and sample analyses were performed using MultiQuant 2.0 (ABISciex). Peptide quantities reported are averaged from all injections over this period. Limits of quantification were set at ten times the background noise level (reported in Table 3.1).

3.C.7. Calculation of Protein-Specific Kinetic Parameters

Respiration rates and metabolite levels for PCE fed experiments were used to calculate kinetic parameters for the enzyme PceA. TCE and cDCE fed experimental data were used for TceA parameters. Experimental datasets were limited to those where electron donor was stoichiometrically non-limiting (but not necessarily kinetically non-limiting) and substrates were above the GC-FID detection limit (approximately 20-40 nM dissolved concentration). Quantified enzyme levels (X_{enzyme}) were based on average or experiment-specific protein per mL measurements determined by MRM assays. Nonlinear regression was used to solve for K_S (nmoles per L) and k_{max} (attamole per protein-hr), based on substrate conversion rates (nmoles per hr) and average substrate concentration C_w (nmoles per L). Inclusion of a correction for hydrogen limitation was included as the equation below depicts, based on previously calculated $K_{S(H2)}$ and hydrogen threshold (14).

$$\text{Substrate conversion Rate} = -\frac{k_{max}\ X_{enzyme}\ C_{w\,EA}}{K_{S(EA)} + C_{w\,EA}} \times \frac{\left(C_{w(H2)} - H_{2\,threshold}\right)}{K_{S(H2)} + \left(C_{w(H2)} - H_{2\,threshold}\right)}$$

3.C.8. Statistical Analysis

Basic statistical analyses were performed using Microsoft Excel. T tests were used to calculate P-values. Analysis of variance and 95 percent confidence intervals were calculated

using Jmp 8. Nonlinear least squares analysis of kinetic parameters was performed with R statistical software package.

3.D. Results and Discussion

3.D. 1. Nucleic acid Biomarker Levels in Continuous-Feed Reactors

To relate *Dehalococcoides* biomarkers to respiration rates, sub-cultures were taken from an anaerobic mixed culture and amended with a variety of EDs (butyrate, hydrogen, yeast extract, fermented yeast extract, lactate, none [endogenous decay]) and chloroethene EAs (PCE, TCE, cDCE). The majority of treatments were continuously fed both ED and EA in order to produce a steady state respiration rate (experimental parameters listed in Table A2.1, Appendix II). Monitoring abundance of targeted nucleic acids demonstrated that over the course of these experiments (up to one hydraulic residence time) nucleic acid biomarkers maintained a pseudo-steady-state (PSS) concentration across replicate cultures (examples depicted in Figure 3.1). This steady state results after cells transfer from a non-respiring to a respiring state, which occurs shortly after the onset of respiration (in the batch system within the first hour of feeding/respiration, see Appendix II Figure A2.1). *Dehalococcoides* cell density within reactors did not statistically change over the majority of treatments (examples depicted in Figure 3.1). Estimates of net growth were calculated using 16S rDNA copies monitored in the reactor and in wasted culture samples (Table A2.1). With these experiments we extend previous work (47, 50) by pairing different EDs and EAs at different ratios and at different feeding rates (0.9 to 280 μeeq per L-hr).

3.D.2. Correlations between mRNA Biomarkers and Respiration

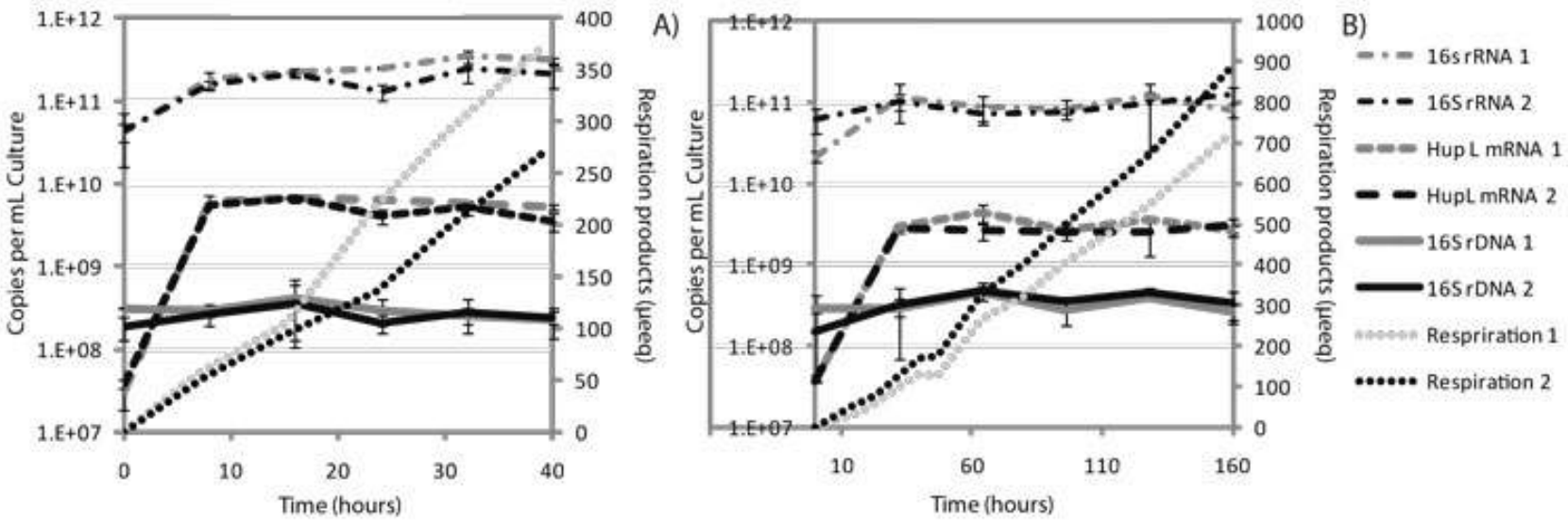

Figure 3.1. Nucleic acid biomarkers from replicate pseudo-steady state reactors fed PCE at approximately 120 µeeq per L-hour (A) and 40 µeeq per L-hour (B). Respiration end products for these reactors also displayed (right axis). Data depicts one hydraulic residence time for each feeding rate: 40 and 160 hours respectively. Error bars represent standard deviations of triplicate extractions.

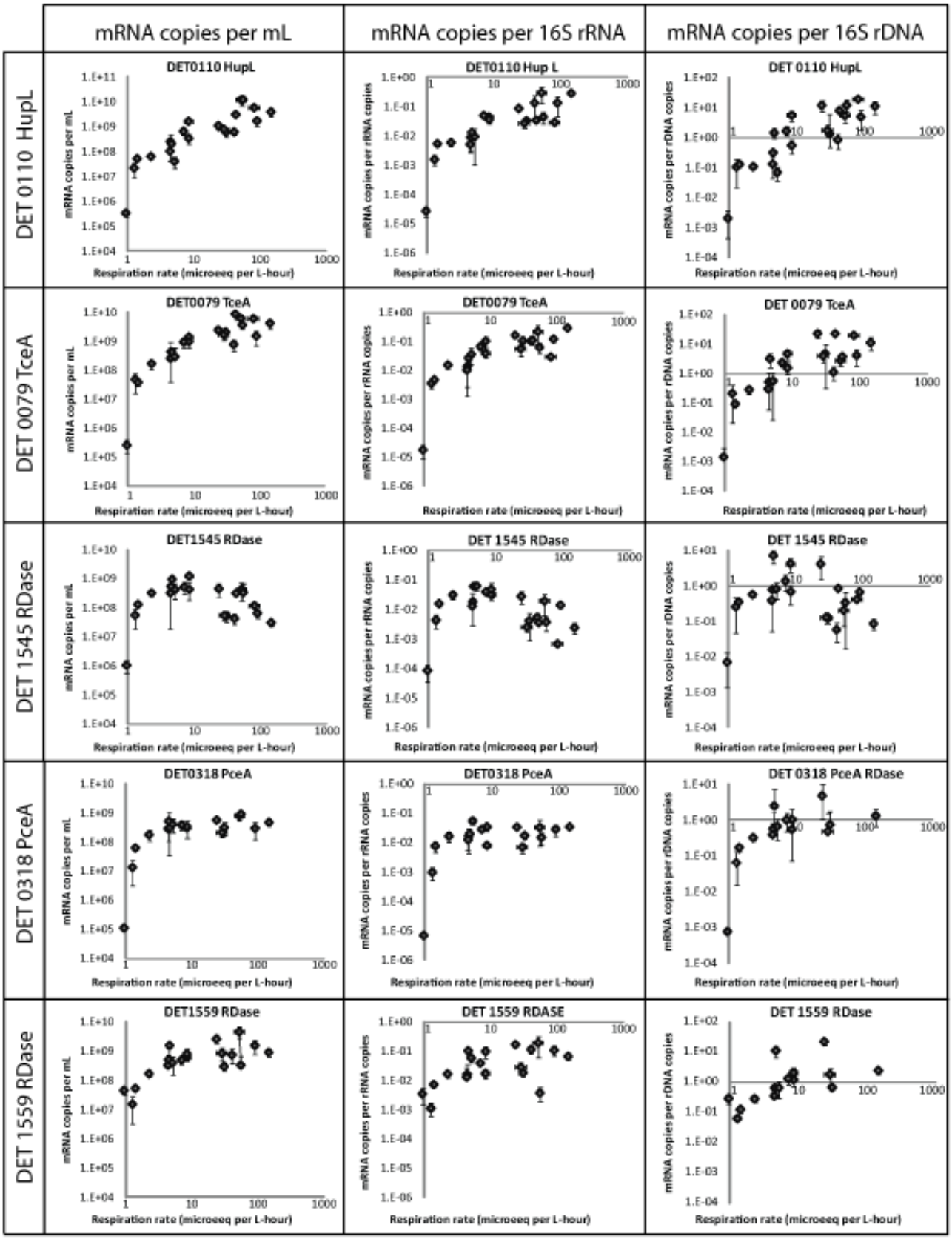
mRNA copies per mL
mRNA copies per 16S rRNA
mRNA copies per 16S rDNA
DET 0110 HupL
DET 0079 TceA
DET 1545 RDase
DET 0318 PceA
DET 1559 RDase
DET0110 HupL
DET0110 Hup L
DET 0110 HupL
DET0079 TceA
DET 0079 TceA
DET1545 RDase
DET 1545 RDase
DET 1545 RDase
DET0318 PceA
DET0318 PceA
DET 0318 PceA RDase
DET1559 RDase
DET 1559 RDASE
DET 1559 RDase
mRNA copies per mL
mRNA copies per rRNA copies
mRNA copies per rDNA copies
Respiration rate (microeeq per L-hour)

Figure 3.2. Pseudo-steady state mRNA concentrations vs. steady-state respiration rates of specific DET targets: hydrogenase DET0110 HupL, reductive dehalogenases DET0079 TceA, DET1545, DET0318 PceA, and DET1559. Transcripts reported on a per mL (left), per 16S rRNA copy (center) and a per 16S rDNA copy (right) basis. Error bars represent standard error of average respiration rates between replicates (X-error bars) and standard deviations of PSS mRNA measurements over time for replicate reactors (Y-error bars), including error in ribosome and/or DNA measurements for different normalizations.

Candidate biomarkers from DET demonstrate a variety of trends in terms of pseudo-steady-state abundance in response to respiration rate (Figure 3.2). On log-log plots these trends include: nearly linear relationships over the full range of feeding conditions (TceA and HupL), a relationship that plateaus at a low respiration rate (PceA and DET1559), and an inverted u-shaped trend peaking at a low rate (DET1545) (Figure 3.2). Observed patterns were independent of the type of ED or EA provided (Figure A2.2, Appendix II). Cell density did not change significantly over the course of most experiments. However, cell density can vary between experiments, as well as among different *Dehalococcoides* containing cultures and environmental samples. To make trends more comparable and applicable to other systems, measurements of mRNA were also normalized either to an internal RNA marker (16S rRNA copies) or genome copies (single copy 16S rRNA gene) extracted from the same sample. These normalizations demonstrate that similar overall trends are maintained on a per unit cell basis.

Positive trends between mRNA per 16S rRNA copies and respiration rate (1.5-280 μeeq per L-hr) were linear on a log-log scale (power relationship) for TceA and HupL (Figure 3.2), producing correlation scores of 0.83 and 0.85 respectively. Deviations from the linear trends for these targets were noted at the highest respiration rates where variability increased, especially with respect to variation in per cell ribosome content (per mL 16S rRNA data, See Appendix II Figure A2.2A). A notable exception to the general positive correlations was observed in the putative RDase DET1545, where peak expression occurred at low to moderate respiration rates (near 5 μeeq per L-hr) and significantly decreased with increased respiration (negative correlation observed within this region) (Figure 3.2). Though functional characterization of this protein has yet to be performed, DET1545 is a highly conserved RDase that has previously been detected at field sites, adding to its potential utility as a field biomarker. In PceA and DET1559,

the observed saturation response occurred at relatively low respiration rates (near 5 μeeq per L-hour) resulting in poor correlation scores over the full range of respiration rates ($R<0.5$). For the majority of transcripts monitored (except DET1559), the lowest experimental feeding rate tested (0.9 μeeq per L-hr) resulted in expression patterns similar to endogenous mRNA decay (Figure A2.1) suggesting this respiration rate was below a threshold for investment in mRNA production (data excluded from correlation analysis). DET1559 was the only target at this respiration rate that did not follow the exponential decay trend, but rather maintained initial transcript levels (consistent with previous observations (50)).

3.D.3. mRNA Biomarker Decay

It has been documented in other systems that transcripts are detected during periods of inactivity or cell stress (5, 17). In this work, transcripts were detected during periods of limited or no activity, as in un-amended cultures. However, exponential decay of these targets was observed over time. Exponential decay of transcripts per DNA copy has previously been observed in TceA transcripts at 0.11 per hour, followed by a slower decay (0.01 per hour) once mRNA reaches a background level (around 10^{-1} per gene after 48 hours) (28). Our observations are consistent with this result in that, after PCE is completely consumed in batch fed reactors, mRNA degradation occurs rapidly, initially at 0.06 per hour for TceA (per mL culture decay rates in Figure A2.1, per 16S rDNA decay rates in Table 3.2). A slower decay (endogenous) occurs at approximately one third the rate after TceA reached an mRNA concentration of 10^6 copies per mL culture (less than 10^{-1} transcripts per 16S rDNA copy). Similar initial decay rates per 16S rDNA (0.028-0.054 per hour, Table 3.2) and endogenous rates (0.014-0.009 per hour, Table 3.2) were seen in the other transcripts we monitored. These data suggest mRNA half-lives range from 10 to 24 hours for DET in mixed communities. Transcript abundance and decay

Table 3.2. *Dehalococcoides ethenogenes* str. 195 mRNA biomarker targets and annotation. First-order specific decay coefficients calculated from regression of Ln (mRNA copies per 16SrDNA copies) vs. time (hours). Raw data (per mL) displayed in Appendix II Figure A2.1 for mRNA degradation post PCE feed (starting ~6 hours post-feed, active) and post purge (3 days post-feed, endogenous).

DET Gene ID	Gene Name	Annotation	mRNA per 16S rDNA Specific Decay Coefficient, hour^{-1} (active)	R^2	mRNA per 16S rDNA Specific Decay Coefficient, hour^{-1} (endogenous)	R^2
DET_DE16S	16S rRNA	16S ribosomal RNA				
DET0110	HupL	[Ni/Fe] hydrogenase, group 1, large subunit (EC:1.12.99.6)	0.054	0.91	0.009	0.8
DET0079	TceA	TCE reductive dehalogenase	0.062	0.82	0.011	0.65
DET0318	PceA	PCE reductive dehalogenase	0.035	0.92	0.01	0.54
DET1545	DET1545	reductive dehalogenase, putative	0.028	0.96	0.013	0.81
DET1559	DET1559	reductive dehalogenase, putative	0.054	0.8	0.014	0.88

trends highlight the necessity of understanding quantitative relationships to infer activity from these molecules.

3.D.4. Relative Abundance of Protein Biomarkers with Respiration

While these biomarker targets have all been detected in previous proteomic experiments (41, 42, 59, Annette Rowe unpublished data), studies have not yet examined how protein levels change with respiration rate and corresponding mRNA level. Using an isobaric tagging approach (iTRAQ^{TM}) to determine relative protein abundances, it was demonstrated that relative protein levels of metabolic genes TceA and HupL matched the corresponding mRNA trends. These proteins increased in response to PSS feeding conditions over moderate respiration rates (~10-50 μeeq per L-hr) (Figure 3.3). Although DET1545 protein follows the mRNA trend of lower abundance at higher respiration rates, fewer peptides for DET1545 and DET1559 were detected for these targets than TceA and HupL, resulting in larger 95% confidence intervals on iTRAQ^{TM} ratios. This experiment spanned the region where PceA mRNA plateaus, and though PceA protein was observed to increase, the relative increase (~0.5 fold increase) was lower than those observed for HupL and TceA (>2 fold increases). DET structural and house-keeping proteins (GroEL, EF-TU, rpL7/L12, and a putative S-layer protein) also increased with respiration rate, suggesting a higher DET cell abundance per μg protein. Normalizing to structural DET targets like the S-Layer cell wall protein or the L7/L12 ribosomal protein to account for potential increases in cell biomass showed no statistically significant differences (DATA not shown). None-the-less these iTRAQ^{TM} data suggest that DET proteins follow the same general trend as mRNA at moderate respiration rates.

3.D.5. Reproducibility in Absolute Quantification of DET Proteins

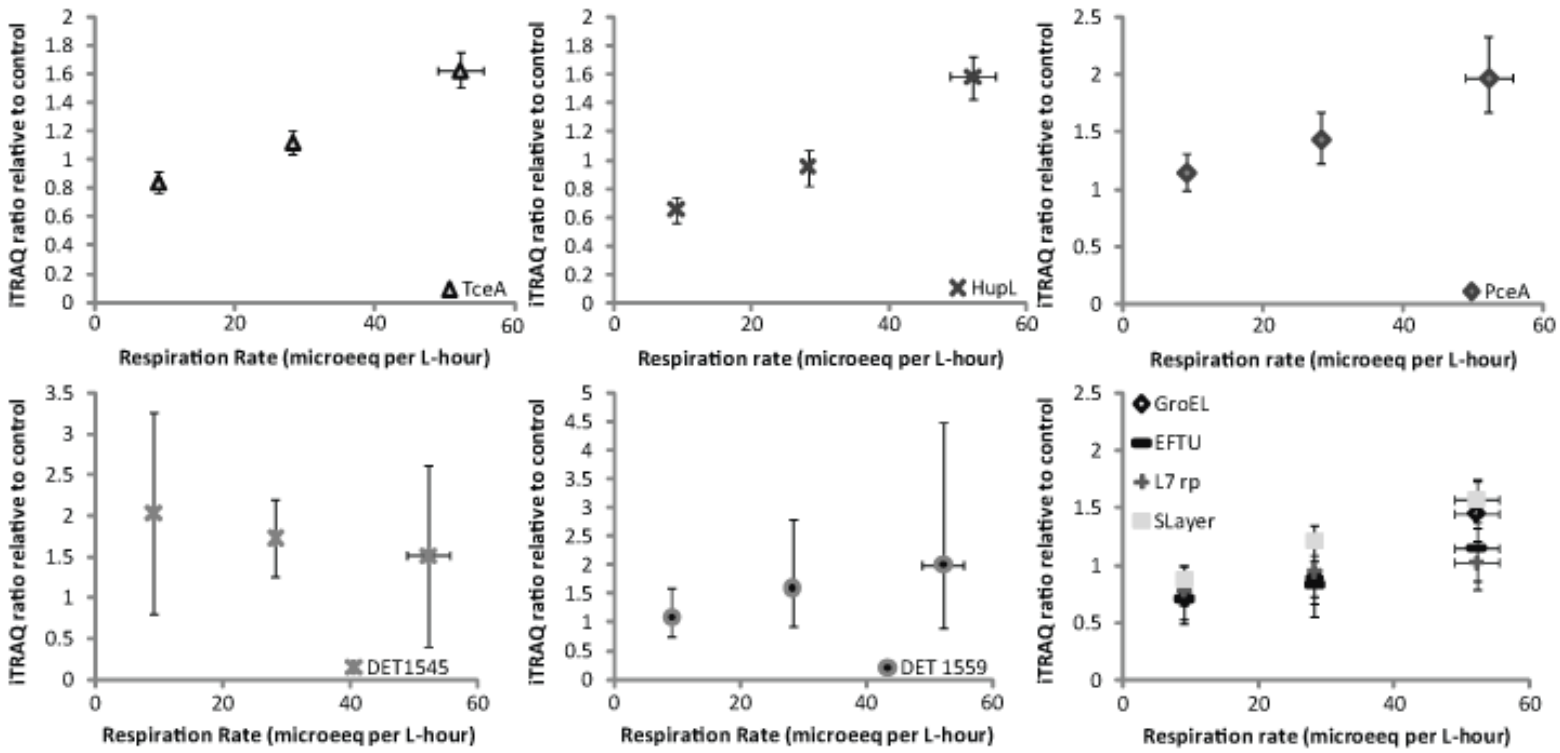

Figure 3.3. Relative protein abundance for DET targets assessed using iTRAQ™ isobaric tags. One hundred µg of total protein from four mixed culture extracts were labeled with different isobaric tags including a control sample taken from a time zero culture control sample (labeled with 114 reporter ion). Relative protein abundance is based on ratio of peak areas of iTRAQ™ tags for samples fed 9, 28, and 52 µeeq PCE per L-hr relative to control sample. Error bars reflect 95% confidence intervals based on reporter ion ratios for all spectra matching the protein.

To obtain absolute protein quantification, multiple peptides from candidate biomarkers were chosen for analysis via MRM (Table 3.1). This peptide-centric approach has previously been utilized to quantify *Dehalococcoides* proteins (59). All peptide identities were confirmed on base culture (time zero) samples using MRM-IDA analysis. In addition, potential sources of variability in sample quantification introduced by sample injection, tryptic protein digestion, protein extraction, and/or analysis run to analysis run variation have been tested (see Appendix II Table A2.3). Variability was greatest across protein extraction replicates (CV= 34 -50%) while injection replicates showed the lowest coefficients of variation (11-34%). Each sample peptide level reported is the average of data accumulated from three to four MRM runs and across all injection and digestion replicates.

Abundances for individual peptides normalized to 16S rDNA are reported to estimate values per cell. Generally peptide abundances agree for different proteins. However, abundance of individual peptides for some targets differ significantly and often reproducibly; most notably for HupL in time zero samples (Figure 3.4A, Figure A2.3). While there are many potential reasons for this including biological (e.g., post-translational modifications) and abiotic factors (e.g., variable losses or recovery of peptides), these can't be distinguished in this work. In our previous work, peptide abundance per 16S rDNA was calculated based on DNA isolated from an aliquot of French cell press lysates ("direct extraction" (59)). These direct extraction values suggested lower 16S rDNA abundance when compared with copies determined from DNA extracted from a parallel cell pellet, potentially due to DNA shearing during French press lysis. For this reason we use values from parallel DNA extractions. In support of this choice, the summed abundance of quantified protein targets was compared to previously reported DET per cell total protein mass (37). This demonstrated that MRM quantified proteins (n=7) would

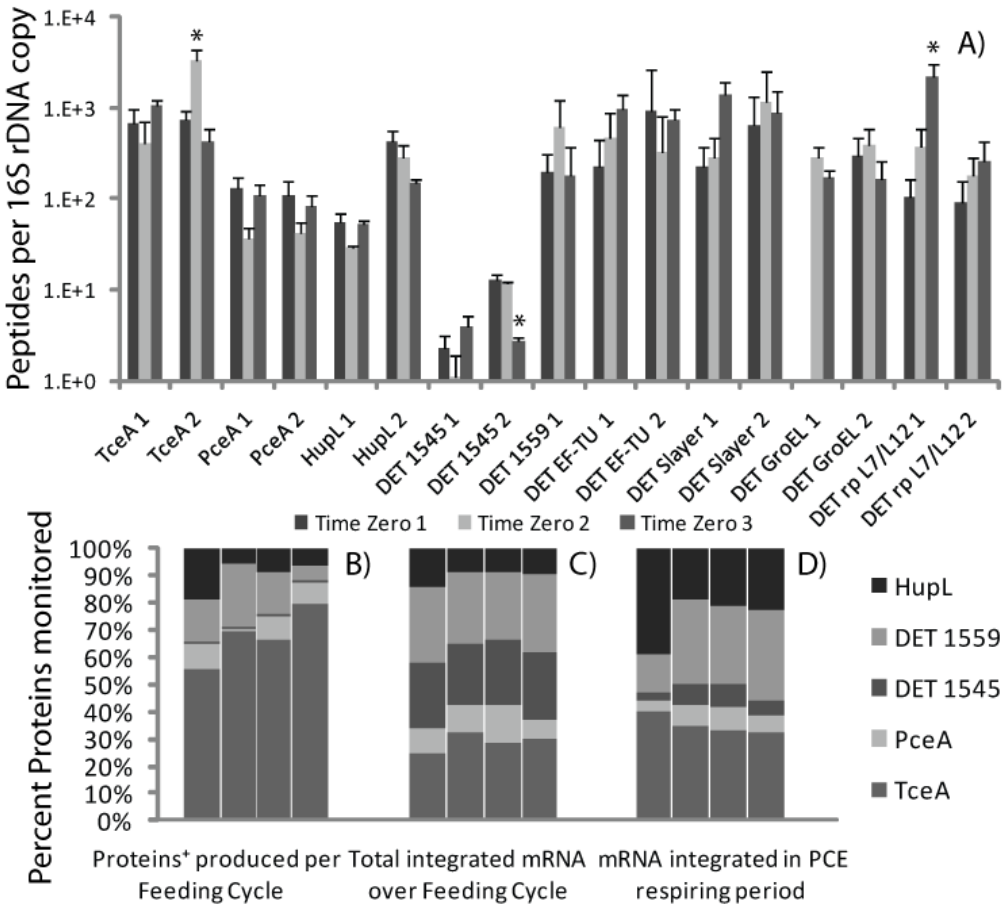

Figure 3.4. Absolute protein abundance in biological replicates of time-zero culture samples (from 6 L reactor pre-batch feeding cycle) of DET peptides based on three to four MRM runs (A). Error bars indicate standard deviations of average transition ion measurements for each peptide over replicate MRM runs. Comparison of total net protein production of selected DET metabolic targets for a batch reactor feeding cycle for triplicate time zero samples (B) and total integrated mRNA expression in four replicates for either the complete feeding cycle (C) or solely during respiratory period (six hours post-feed) (D). Data presented in terms of percent of total targets for which mRNA and proteins were quantified. Replicates are represented by individual bars for measurements over weeks of sampling.

account for >50% of the total protein biomass using the direct extraction method (see Appendix II Table A2.4). Using the parallel extraction, 1.65% of the DET proteome was quantified. Given that only a few DET proteins are monitored by this approach, and many of the unmonitored proteins are potentially also highly abundant, the parallel extraction approach was used for calculating all per 16S rDNA values.

3.D.6. Consistency of DET per cell Protein Biomarker Levels

Few statistically significant differences were noted in our time-zero culture proteome over a six month period (Figure A2.3A and Figure 3.4A). For these samples treated under the same experimental or growth condition, using DNA copies as a correction for cell density helped account for the variation in peptide abundance observed on a per µg total protein basis. Cell density varied among these time points (Time Zero 1-3: $3.6 \times 10^8 \pm 7 \times 10^7$, $1.2 \times 10^9 \pm 2 \times 10^8$, $3.7 \times 10^8 \pm 1 \times 10^8$ 16SrDNA copies per mL). Statistically significant variation (P-value of <0.001) was observed in individual time-zero samples normalized to 16S rDNA numbers in a few peptides (TceA 2, DET1545 2, and DET rp L7/12 1) (Figure3.4A). However, these differences were not upheld in the second peptide measured for the corresponding protein. The ranked order abundance of metabolic targets based on average ± standard error of peptide measurements (two per protein) was: TceA (1095 ± 337 proteins per 16S rDNA), followed by HupL (167 ± 121), PceA (85 ± 8), and DET1545 (6.7 ± 4.2) (Figure 3.4A). Only one peptide for DET1559 (329 ± 142 proteins per 16S rDNA) could be quantified. The methionine group in DET1559 2-WQGTPEEGSNMITQALR standards was oxidized during processing, limiting confidence in DET1559 quantification. In general, house-keeping proteins were more abundant than metabolic targets with the exception of TceA. For the targets that overlap between this work and previous data (59), the rank order of DET targets is conserved with the exception of PceA,

which was more abundant on average in this study, but statistically indistinguishable from HupL. In earlier work, DET1545 and DET1559 were below the peptide detection limits of 71 to 780 proteins per cell and 68 to 480 proteins per cell, respectively (59). In this study detection limits were substantially lower, especially for DET1545.

3.D.7. Comparisons between Protein Production and mRNA Abundance

Net protein production per batch feeding cycle estimates were determined from baseline (time-zero) culture protein profiles (Figure 3.4A). The time zero protein profile is the result of regular and repeated batch feeding and wasting conditions (described in methods). Given the previously reported cell yield (1.8×10^8 per μmole Cl^- respired (50)), approximately 5.2×10^{11} cells per feeding cycle incorporating 0.07 per day cell decay (two PCE/butyrate batch feeds followed by 10% wasting) are expected to be produced, which is within the range of measured waste cell biomass (2×10^{11} to 6×10^{11} cells in 600 mL). As protein production is a function of mRNA transcript levels, we compared the total time-integrated mRNA transcript abundance for a given target measured over the course of a batch feed (raw data in Figure A2.1) with net proteins produced based on MRM measurements of time zero protein quantities. On a percentage basis (relative to the subset of DET metabolic targets measured), the proportion of integrated mRNA transcript levels do not match the percentage of net proteins produced in the batch feeding cycle (Figure 3.4B&C). Notably, TceA is similar in mRNA abundance to targets like HupL and PceA, but is eight to ten times higher in protein abundance and, consequently, net protein produced. Even though DET1545 and DET1559 have similar mRNA expression patterns, their abundance at the protein level is quite different. As the majority of respiration and transcription occurs within the first six hours after PCE and butyrate addition followed by mRNA decay (Figure A2.1), transcript abundance integrated only over the first six hours was

also compared (Figure 3.4B&D). The disconnect between the percentage of mRNA produced during the respiratory period and net proteins produced remains. These discrepancies could be a result of differences in translation efficiency of mRNA (e.g., TceA has a higher ribosome binding efficiency) and/or from differences in protein degradation rates.

3.D.8. Individual Protein Decay Rates

Insight into cell decay was obtained through iTRAQ^{TM} labeling of peptides generated from equivalent culture volumes of samples starved for substrates over different time periods. Proteins were modeled with exponential decay, with rates ranging from 0.04 to 0.08 per day, but there were no statistically significant differences in decay rates among highlighted DET proteins (see Appendix II Figure A2.4A). These decay measurements tracked with normal cell decay as measured from both decline in max dechlorination rate (0.05 per day, Supplemental Figure A2.4B) and degradation of 16S rDNA copies over time ranging from 0.07 to 0.09 per day (Figure A2.4C). TceA protein decay was on the higher end of the observed rates (0.08 per day). Given these results, the abundance of TceA does not appear to be the result of a slower decay rate than other DET targets, suggesting translation efficiency is higher for TceA transcripts compared to other DET transcripts.

3.D.9. Net Production of Proteins in Pseudo-Steady-State Experiments

The protein profiles measured for duplicate reactors fed at two different rates, PCE 40 (respiration 42-48 μeeq PCE per L-hr) and PCE 120 (respiration 70-100 μeeq PCE per L-hr), showed no statistically significant differences in biomarker peptides per 16S rDNA copy (Figure 3.5A), or per μg total protein (Figure A2.3). Different feeding rates resulted in significantly different growth rates and hydraulic residence times. As no dilution was observed in these reactors in terms of proteins and/or 16S rDNA copies (Figure 3.1), net protein production

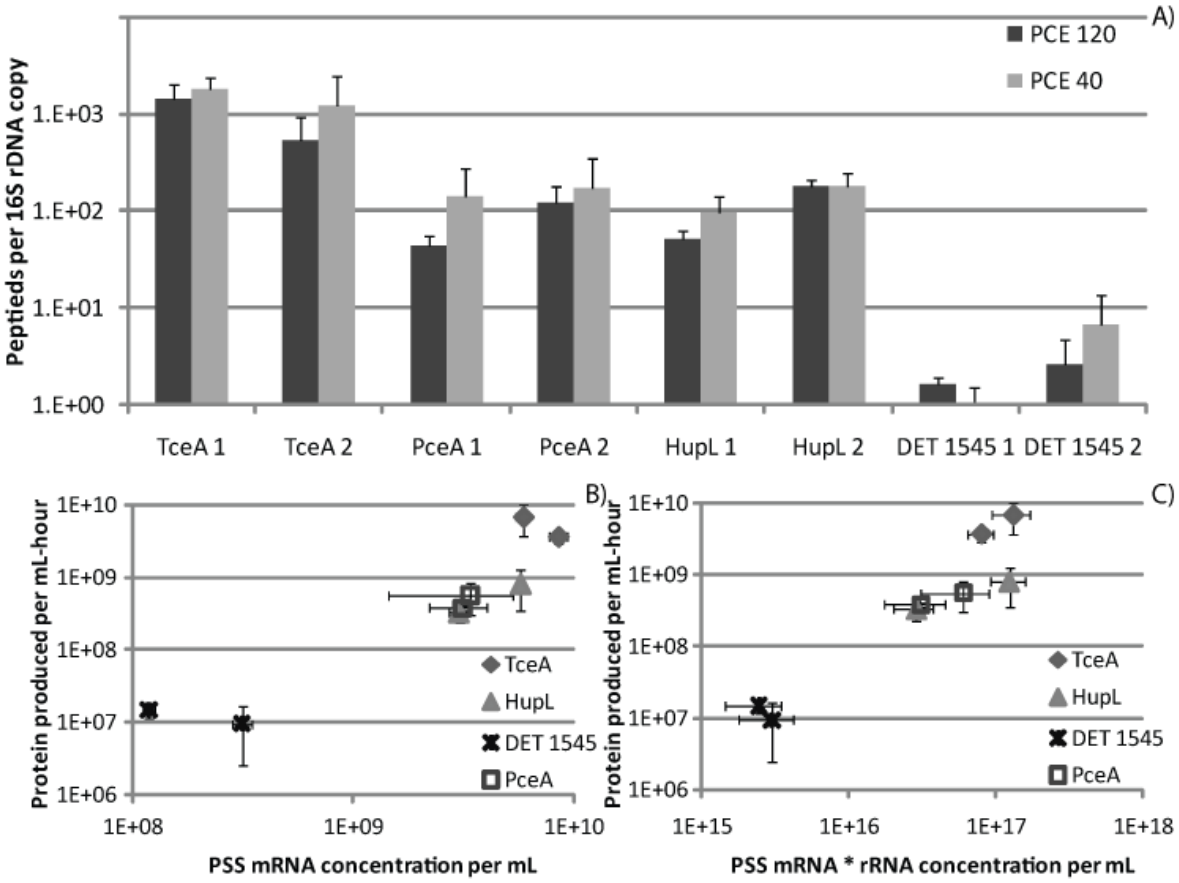

Figure 3.5. Absolute protein abundance in final time point samples for pseudo-steady-state reactors run at two feeding rates for one hydraulic residence time (A). Error bars indicate standard errors of average peptide measurement over replicate MRM runs. Net protein production rate for each of these experiments is plotted against either steady-state mRNA concentration (B) or steady-state mRNA*rRNA concentration (C). Y-error bars indicate standard error of protein abundance based on multiple peptides. X-error bars represent standard deviations in pseudo-steady state RNA levels across replicate cultures.

matches the wasting rate. This allows comparisons of mRNA concentration (mRNA per mL) and net protein production rates (protein per mL-hr) in the PSS system. In plots of PSS mRNA concentrations against net protein production rates (Figure 3.5B), HupL and PceA are clustered on the graph suggesting similar correlations between proteins per hour and mRNA levels. Though the concentration of mRNA is similar between HupL and TceA, the net production rates of TceA are four to ten times higher than that of HupL or PceA. Ratios of TceA proteins produced per mRNA-hr were 1.2 & 0.43 compared to 0.14 & 0.10 for HupL and 0.16 & 0.12 for PceA in PCE 120 and PCE 40 experiments, respectively. In addition, DET1545, though lower in terms of overall mRNA abundance, also suggests a lower ratio of proteins per mRNA-hr (0.12-0.03). Trends across targets in the amount of protein per mRNA were consistent with batch observations. Notably, net protein production increased for TceA at the higher feeding rate even though mRNA abundance did not increase between PCE 40 and PCE 120. The ribosome content, however, increased significantly between these experiments (~2 fold, Figure 3.1) and looking at mRNA abundance multiplied by ribosome content helped resolve positive trends with net production of protein for most targets (Figure 3.5C)—specifically TceA and DET1545. Net protein production of TceA was still greater than other targets.

3.D.10. Enzyme-Specific Kinetics for TceA and PceA

Given that few differences in enzyme proteins per cell were observed over a variety of experimental conditions and respiration rates (Figure 3.4A, Figure 3.5A), we were able to calculate rate constants for the enzymes known to convert PCE to TCE (DET0318, PceA) and TCE to cDCE/cDCE to VC (DET0079, TceA) (33, 34). Nonlinear regressions of per-enzyme respiration rates, based on average enzyme levels (enzyme protein/cell * cell/mL) compared with average substrate levels allowed estimation of *in vivo* Michaelis-Menten rate parameters (see

Table 3.3. Enzyme-specific kinetic parameters calculated for *Dehalococcoides ethenogenes* str. 195 enzymes TceA and PceA. Calculations based on average measured enzyme proteins per cell, then used 16S rDNA copies measured for individual experiments, as well as respiration rates and average substrate concentrations measured during pseudo-steady-state experiments (listed in Table A2.1).

		Estimates incorporating H_2 limitation		**Estimates ignoring H_2 limitation**	
Enzyme	**Reaction**	k_{max} ± std error (attamol /mol enz/h)	Ks ± std error (nM)	k_{max} ± std error (attamol /mol enz/h)	Ks ± std error (nM)
PceA	(PCE→TCE)	2.15±0.19	7950±2830	1.44±0.19	38000±11700
TceA	(TCE→cDCE)	0.13±0.007	182±47	0.03±0.002	185±45
TceA	(cDCE→VC)	0.13±0.008	2930±1200	0.15±0.01	7760±3400

Appendix II Figure A2.5, Table 3.3). These calculations also considered hydrogen as a second potential limiting substrate when inferring rate parameters. Based on the average PceA content per cell over all experiments (90 proteins per 16S rDNA), the k_{max} is 2.1 attamole per mole PceA per hour. TceA, which is more abundant on a per cell basis (~1000 proteins per 16S rDNA), has a slightly lower k_{max} for conversion of TCE and cDCE, calculated at 0.13 attamole per mole TceA per hour for both substrates. Given that under continuous butyrate feeding conditions hydrogen levels were rarely observed above 0.1 μM (C_w), hydrogen levels measured during these experiments were used to correct reaction rates for hydrogen limitation according to the previously presented model (14). These values are generally higher than the rates observed during biochemical characterization (33, 34), which were 0.13, 0.03 and 0.07 attamole per mole enzyme per hour for PceA, TceA (TCE to cDCE) and TceA (cDCE to VC), respectively. These previously reported assays were performed post extraction and purification of these oxygen-sensitive proteins, and there is potential that some loss of activity occurred due to processing. These differences could also be the result of *in vivo* vs. *in vitro* activity. Alternatively, absolute protein recovery is potentially less than 100 percent, and larger values for protein abundance would result in lower k_{max} values. Incorporating estimates of protein recovery could lead to the generation of lower rates than these estimates, and potentially will be an important component for field applicability of quantification of proteins via the MRM approach. We previously quantified differences between metabolic proteins like TceA and PceA in different strains of *Dehalococcoides* (59). Enzyme-specific kinetic parameters may help to resolve differences between rates of reaction observed between strains with different protein profiles or strains with variable proteomes. Experiments in other cultures and at field sites will be important for determining broader applicability of these rate parameters.

3.D.11. Summary and Implications

This work has resolved empirical relationships between PSS mRNA expression levels and respiration rates for different biomarker targets in a member of the *Dehalococcoides.* These respiration biomarker relationships were tested over a range of electron donors and electron acceptors. RNA has the potential to be an important environmental biomarker in that it is much more sensitive to environmental conditions and metabolic activities of organisms than DNA (10). As illustrated by decay studies, mRNAs decayed at rates around 24 times faster than those measured for DNA and proteins.

One of the potential limitations of mRNA as a biomarker has been highlighted in recent studies that demonstrate mechanisms of uncoupling between mRNA expression and protein production (e.g., RNA silencing and sensor mRNAs (57, 61)). As such, in conjunction with mRNA expression patterns, protein abundance from these experiments has been quantified, demonstrating that biomarker mRNA abundance influences production of the corresponding protein. However, the quantitative relationships between mRNA and protein production were not equivalent across transcripts as highlighted by differences in protein abundance between similarly expressed transcripts (e.g., TceA and HupL). At very high respiration rates protein production increased despite similar mRNA levels. The influence of ribosome levels helped explain differences in net protein production within a given target (specifically for TceA). In other organisms, transcript abundance has been shown to be a poor predictor of protein abundance when global proteomes and transcriptomes were compared (1, 31). Our data illustrates on an absolute scale that mRNA is a modest predictor of protein abundance within a given target, but lacks predictability across biomarkers. This further highlights the importance of understanding quantitative relationships between biomarkers and physiological processes.

In addition to being useful for the investigation of protein-mRNA relationships, absolute protein abundances proved useful for the calculation of *in vivo* enzyme kinetic parameters. Nonlinear regression analyses estimated specific k_{max} values for TceA and PceA. These parameters will be further tested on other *Dehalococcoides* strains. Currently, there is a limited body of work on recovering enzyme biomarkers from field samples (7, 60). Although more work is required to test the utility of enzymes as useful biomarkers, including testing recovery of these proteins from field settings, these targets hold promise for circumventing limitations with nucleic acid biomarkers, and, combined with geochemical data, could potentially become an important group of biomarkers for *in situ* rates of processes such as dehalorespiration.

3.E. Acknowledgements

I would like to acknowledge co-authors for this work: Gretchen Heavner, Cresten Mansfelt, Jeffery Werner, and Ruth Richardson. We would also like to acknowledge Celeste Ptak and Sheng Zhang at the Cornell Proteomics and Mass Spectrometry core facility for proteomic sample analysis. Thanks to James Gossett and Stephen Zinder for their expert advice and editorial comments for this manuscript. This work was funded through research grants from the National Science Foundation CBET Program (CBET-0731169) and the Department of Defense Army Research Office (W911NF-07-1-0249).

REFERENCES

1. **Abreu, R. d. S., L. O. Penalva, E. M. Marcotte, and C. Vogel.** 2009. Global signatures of protein and mRNA expression levels. Mol. BioSyst. **5:**1512-1526.

2. **Adrian, L., and H. Goerisch.** 2002. Microbial transformation of chlorinated benzenes under anaerobic conditions. Res. Microbiol. **153:**131-137.

3. **Adrian, L., S. K. Hansen, J. M. Fung, H. Gorisch, and S. H. Zinder.** 2007. Growth of *Dehalococcoides* strains with chlorophenols as electron acceptors. Environ. Sci. Technol. **41:**2318-2323.

4. **Adrian, L., U. Szewzyk, J. Wecke, and H. Gorisch.** 2000. Bacterial dehalorespiration with chlorinated benzenes. Nature. **408:**580-583.

5. **Amos, B. K., K. M. Ritalahti, C. Cruz-Garcia, E. Padilla-Crespo, and F. E. Loeffler.** 2008. Oxygen effect on *Dehalococcoides* viability and biomarker quantification. Environ. Sci. Technol. **42:**5718-5726.

6. **Behrens, S., M. F. Azizian, P. J. McMurdie, A. Sabalowsky, M. E. Dolan, L. Semprini, and A. M. Spormann.** 2008. Monitoring abundance and expression of "*Dehalococcoides*" species chloroethene-reductive dehalogenases in a tetrachloroethene-dechlorinating flow column. Appl. Environ. Microbiol. **74:**5695-5703.

7. **Benndorf, D., G. U. Balcke, H. Harms, and M. von Bergen.** 2007. Functional metaproteome analysis of protein extracts from contaminated soil and groundwater. ISME J. **1:**224-234.

8. **Bunge, M., L. Adrian, A. Kraus, M. Opel, W. G. Lorenz, J. R. Andreesen, H. Gorisch, and U. Lechner.** 2003. Reductive dehalogenation of chlorinated dioxins by an anaerobic bacterium. Nature. **421:**357-360.

9. **Chow, W. L., D. Cheng, S. Wang, and J. He.** 2010. Identification and transcriptional analysis of trans-DCE-producing reductive dehalogenases in *Dehalococcoides* species. ISME J. **4:**1020-1030.

10. **Cupples, A. M.** 2008. Real-time PCR quantification of *Dehalococcoides* populations: Methods and applications. J. Microbiol. Methods. **72:**1-11.

11. **Da Silva, M. L. B., and P. J. J. Alvarez.** 2008. Exploring the Correlation between Halorespirer Biomarker Concentrations and TCE Dechlorination Rates. J. Environ. Eng.-Asce. **134:**895-901.

12. **Daprato, R. C., F. E. Loffler, and J. B. Hughes.** 2007. Comparative analysis of three tetrachloroethene to ethene halorespiring consortia suggests functional redundancy. Environ. Sci. Technol. **41:**2261-2269.

13. **Ellis, D. E., E. J. Lutz, J. M. Odom, R. J. Buchanan, C. L. Bartlett, M. D. Lee, M. R. Harkness, and K. A. DeWeerd.** 2000. Bioaugmentation for Accelerated *In Situ* Anaerobic Bioremediation. Environ. Sci. Technol. **34:**2254-2260.

14. **Fennell, D. E., and J. M. Gossett.** 1998. Modeling the production of and competition for hydrogen in a dechlorinating culture. Environ. Sci. Technol.. **32:**2450-2460.

15. **Fennell, D. E., J. M. Gossett, and S. H. Zinder.** 1997. Comparison of butyric acid, ethanol, lactic acid, and propionic acid as hydrogen donors for the reductive dechlorination of tetrachloroethene. Environ. Sci. Technol. **31:**918-926.

16. **Fennell, D. E., I. Nijenhuis, S. F. Wilson, S. H. Zinder, and M. M. Haggblom.** 2004. *Dehalococcoides ethenogenes* strain 195 reductively dechlorinates diverse chlorinated aromatic pollutants. Environ. Sci. Technol. **38:**2075-2081.

17. **Fletcher KE , Costanza J , Cruz-Garcia C , Ramaswamy NS , Pennell KD , Loffler FE.** 2011. Effects of elevated temperature on *Dehalococcoides* dechlorination performance and DNA and RNA biomarker abundance. Environ. Sci. Technol. **45:**712-718.

18. **Fung, J. M., R. M. Morris, L. Adrian, and S. H. Zinder.** 2007. Expression of reductive dehalogenase genes in *Dehalococcoides ethenogenes* strain 195 growing on tetrachloroethene, trichloroethene, or 2,3-dichlorophenol. Appl. Environ. Microbiol. **73:**4439-4445.

19. **Futamata, H., S. Kaiya, M. Sugawara, and A. Hiraishi.** 2009. Phylogenetic and Transcriptional Analyses of a Tetrachloroethene-Dechlorinating "*Dehalococcoides*" Enrichment Culture TUT2264 and Its Reductive-Dehalogenase Genes. Microbes Environ. **24:**330-337.

20. **Hendrickson, E. R., J. A. Payne, R. M. Young, M. G. Starr, M. P. Perry, S. Fahnestock, D. E. Ellis, and R. C. Ebersole.** 2002. Molecular analysis of *Dehalococcoides* 16S ribosomal DNA from chloroethene-contaminated sites throughout north America and Europe. Appl. Environ. Microbiol. **68:**485-495.

21. **Hoelscher, T., H. Goerisch, and L. Adrian.** 2003. Reductive dehalogenation of chlorobenzene congeners in cell extracts of *Dehalococcoides* sp. strain CBDB1. Appl. Environ. Microbiol. **69:**2999-3001.

22. **Holscher, T., R. Krajmalnik-Brown, K. M. Ritalahti, F. von Wintzingerode, H. Gorisch, F. E. Loffler, and L. Adrian.** 2004. Multiple nonidentical reductive-dehalogenase-homologous genes are common in *Dehalococcoides*. Appl. Environ. Microbiol. **70:**5290-5297.

23. **Jayachandran, G., H. Gorisch, and L. Adrian.** 2004. Studies on hydrogenase activity and chlorobenzene respiration in *Dehalococcoides* sp strain CBDB1. Arch. Microbiol. **182:**498-504.

24. **Johnson, D. R., P. K. H. Lee, V. F. Holmes, and L. Alvarez-Cohen.** 2005. An internal reference technique for accurately quantifying specific mRNAs by real-time PCR with a application to the tceA reductive dehalogenase gene. Appl. Environ. Microbiol. **71:**3866-3871.

25. **Johnson, D. R., P. K. H. Lee, V. F. Holmes, A. C. Fortin, and L. Alvarez-Cohen.** 2005. Transcriptional expression of the tceA gene in a *Dehalococcoides*-containing microbial enrichment. Appl. Environ. Microbiol. **71:**7145-7151.

26. **Krajmalnik-Brown, R., T. Holscher, I. N. Thomson, F. M. Saunders, K. M. Ritalahti, and F. E. Loffler.** 2004. Genetic identification of a putative vinyl chloride reductase in *Dehalococcoides* sp strain BAV1. Appl. Environ. Microbiol. **70:**6347-6351.

27. **Kube, M., A. Beck, S. H. Zinder, H. Kuhl, R. Reinhardt, and L. Adrian.** 2005. Genome sequence of the chlorinated compound respiring bacterium *Dehalococcoides* species strain CBDB1. Nat. Biotechnol. **23:**1269-1273.

28. **Lee, P. K. H., D. R. Johnson, V. F. Holmes, J. Z. He, and L. Alvarez-Cohen.** 2006. Reductive dehalogenase gene expression as a biomarker for physiological activity of *Dehalococcoides* spp. Appl. Environ. Microbiol. **72:**6161-6168.

29. **Lee, P. K. H., T. W. Macbeth, K. S. Sorenson Jr., R. A. Deeb, and L. Alvarez-Cohen.** 2008. Quantifying Genes and Transcripts To Assess the *In Situ* Physiology of "*Dehalococcoides*" spp. in a Trichloroethene-Contaminated Groundwater Site. Appl. Environ. Microbiol. **74:**2728-2739.

30. **Lendvay, J. M., F. E. Loffler, M. Dollhopf, M. R. Aiello, G. Daniels, B. Z. Fathepure, M. Gebhard, R. Heine, R. Helton, J. Shi, R. Krajmalnik-Brown, C. L. Major, M. J. Barcelona, E. Petrovskis, R. Hickey, J. M. Tiedje, and P. Adriaens.** 2003. Bioreactive Barriers: A Comparison of Bioaugmentation and Biostimulation for Chlorinated Solvent Remediation. Environ. Sci. Technol. **37:**1422-1431.

31. **Lu, P., C. Vogel, R. Wang, X. Yao, and E. M. Marcotte.** 2007. Absolute protein expression profiling estimates the relative contributions of transcriptional and translational regulation. Nat. Biotechnol. **25:**117-124.

32. **Lu, X., J. T. Wilson, and D. H. Kampbell.** 2006. Relationship between geochemical parameters and the occurrence of *Dehalococcoides* DNA in contaminated aquifers. Water Resour. Res. **42:**W08427.

33. **Magnuson, J. K., M. F. Romine, D. R. Burris, and M. T. Kingsley.** 2000. Trichloroethene reductive dehalogenase from *Dehalococcoides ethenogenes*: Sequence of tceA and substrate range characterization. Appl. Environ. Microbiol. **66:**5141-5147.

34. **Magnuson, J. K., R. V. Stern, J. M. Gossett, S. H. Zinder, and D. R. Burris.** 1998. Reductive dechlorination of tetrachloroethene to ethene by two-component enzyme pathway. Appl. Environ. Microbiol. **64:**1270-1275.

35. **Major, D. W., M. L. McMaster, E. E. Cox, E. A. Edwards, S. M. Dworatzek, E. R. Hendrickson, M. G. Starr, J. A. Payne, and L. W. Buonamici.** 2002. Field demonstration of successful bioaugmentation to achieve dechlorination of tetrachloroethene to ethene. Environ. Sci. Technol. **36:**5106-5116.

36. **Maphosa, F., W. M. de Vos, and H. Smidt.** 2010. Exploiting the ecogenomics toolbox for environmental diagnostics of organohalide-respiring bacteria. Trends Biotechnol. **28:**308-316.

37. **Maymo Gatell, X., Y. T. Chien, J. M. Gossett, and S. H. Zinder.** 1997. Isolation of a bacterium that reductively dechlorinates tetrachloroethene to ethene. Science. **276:**1568-1571.

38. **McCarty, P. L.** 1997. Microbiology - Breathing with chlorinated solvents. Science. **276:**1521-1522.

39. **McMurdie, P. J., S. F. Behrens, J. A. Mueller, J. Goeke, K. M. Ritalahti, R. Wagner, E. Goltsman, A. Lapidus, S. Holmes, F. E. Loeffler, and A. M. Spormann.** 2009. Localized Plasticity in the Streamlined Genomes of Vinyl Chloride Respiring *Dehalococcoides*. Plos Genet. **5:**e1000714.

40. **Moran, M. J., J. S. Zogorski, and P. J. Squillace.** 2007. Chlorinated solvents in groundwater of the United States. Environ. Sci. Technol. **41:**74-81.

41. **Morris, R. M., J. M. Fung, B. G. Rahm, S. Zhang, D. L. Freedman, S. H. Zinder, and R. E. Richardson.** 2007. Comparative proteomics of *Dehalococcoides* spp. reveals strain-specific peptides associated with activity. Appl. Environ. Microbiol. **73:**320-326.

42. **Morris, R. M., S. Sowell, D. Barofsky, S. Zinder, and R. Richardson.** 2006. Transcription and mass-spectroscopic proteomic studies of electron transport oxidoreductases in *Dehalococcoides ethenogenes*. Environ. Microbiol. **8:**1499-1509.

43. **Muller, J. A., B. M. Rosner, G. von Abendroth, G. Meshulam-Simon, P. L. McCarty, and A. M. Spormann.** 2004. Molecular identification of the catabolic vinyl chloride reductase from *Dehalococcoides* sp strain VS and its environmental distribution. Appl. Environ. Microbiol. **70:**4880-4888.

44. **Nijenhuis, I., and S. H. Zinder.** 2005. Characterization of hydrogenase and reductive dehalogenase activities of *Dehalococcoides ethenogenes* strain 195. Appl. Environ. Microbiol. **71:**1664-1667.

45. **Nishimura, M., M. Ebisawa, S. Sakihara, A. Kobayashi, T. Nakama, M. Okochi, and M. Yohda.** 2008. Detection and identification of *Dehalococcoides* species responsible for *in situ* dechlorination of trichloroethene to ethene enhanced by hydrogen-releasing compounds. Biotechnol. Appl. Biochem. **51:**1-7.

46. **Peirson, S. N., J. N. Butler, and R. G. Foster.** 2003. Experimental validation of novel and conventional approaches to quantitative real-time PCR data analysis. Nucl. Acids Res. **31:**e73.

47. **Rahm, B. G., and R. E. Richardson.** 2008. *Dehalococcoides*' Gene Transcripts as Quantitative Bioindicators of PCE, TCE and cDCE Dehalorespiration Rates: Trends and Limitations. Environ. Sci. Technol. Environ. Sci. Technol. **42:**5099-5105.

48. **Rahm, B. G., S. Chauhan, V. F. Holmes, T. W. Macbeth, K. S. J. Sorenson, and L. Alvarez-Cohen.** 2006. Molecular characterization of microbial populations at two sites with differing reductive dechlorination abilities. Biodegradation. **17:**523-534.

49. **Rahm, B. G., R. M. Morris, and R. E. Richardson.** 2006. Temporal expression of respiratory genes in an enrichment culture containing *Dehalococcoides ethenogenes*. Appl. Environ. Microbiol. **72:**5486-5491.

50. **Rahm, B. G., and R. E. Richardson.** 2008. Correlation of respiratory gene expression levels and pseudo-steady-state PCE respiration rates in *Dehalococcoides ethenogenes*. Environ. Sci. Technol. **42:**416-421.

51. **Ritalahti, K. M., J. K. Hatt, V. Lugmayr, L. Henn, E. A. Petrovskis, D. M. Ogles, G. A. Davis, C. M. Yeager, C. A. Lebron, and F. E. Loeffler.** 2010. Comparing On-Site to Off-Site Biomass Collection for *Dehalococcoides* Biomarker Gene Quantification To Predict *In Situ* Chlorinated Ethene Detoxification Potential. Environ. Sci. Technol. **44:**5127-5133.

52. **Rowe, A. R., B. J. Lazar, R. M. Morris, and R. E. Richardson.** 2008. Characterization of the Community Structure of a Dechlorinating Mixed Culture and Comparisons of Gene Expression in Planktonic and Biofloc-Associated "*Dehalococcoides*" and *Methanospirillum* Species. Appl. Environ. Microbiol. **74:**6709-6719.

53. **Schefe, J., K. Lehmann, I. Buschmann, T. Unger, and H. Funke-Kaiser.** 2006. Quantitative real-time RT-PCR data analysis: current concepts and the "novel gene expression CT difference" formula. J Mol. Med. **84:**901-910.

54. **Scheutz, C., N. D. Durant, P. Dennis, M. H. Hansen, T. Jorgensen, R. Jakobsen, E. E. Cox, and P. L. Bjerg.** 2008. Concurrent Ethene Generation and Growth of Dehalococcoides Containing Vinyl Chloride Reductive Dehalogenase Genes During an Enhanced Reductive Dechlorination Field Demonstration. Environ. Sci. Technol. **42:**9302-9309.

55. **Seshadri, R., L. Adrian, D. E. Fouts, J. A. Eisen, A. M. Phillippy, B. A. Methe, N. L. Ward, W. C. Nelson, R. T. Deboy, H. M. Khouri, J. F. Kolonay, R. J. Dodson, S. C. Daugherty, L. M. Brinkac, S. A. Sullivan, R. Madupu, K. T. Nelson, K. H. Kang, M. Impraim, K. Tran, J. M. Robinson, H. A. Forberger, C. M. Fraser, S. H. Zinder, and J. F. Heidelberg.** 2005. Genome sequence of the PCE-dechlorinating bacterium Dehalococcoides ethenogenes. Science. **307:**105-108.

56. **Smatlak, C. R., J. M. Gossett, and S. H. Zinder.** 1996. Comparative kinetics of hydrogen utilization for reductive dechlorination of tetrachloroethene and methanogenesis in an anaerobic enrichment culture. Environ. Sci. Technol. **30:**2850-2858.

57. **Smith, D. P., J. B. Kitner, A. D. Norbeck, T. R. Clauss, M. S. Lipton, M. S. Schwalbach, L. Steindler, C. D. Nicora, R. D. Smith, and S. J. Giovannoni.** 2010. Transcriptional and Translational Regulatory Responses to Iron Limitation in the Globally Distributed Marine Bacterium *Candidatus Pelagibacter ubique*. PLoS One. **5:**e10487.

58. **Waller, A. S., R. Krajmalnik-Brown, F. E. Loffler, and E. A. Edwards.** 2005. Multiple reductive-dehalogenase-homologous genes are simultaneously transcribed during dechlorination by *Dehalococcoides*-containing cultures. Appl. Environ. Microbiol. **71:**8257-8264.

59. **Werner, J. J., A. C. Ptak, B. G. Rahm, S. Zhang, and R. E. Richardson.** 2009. Absolute quantification of *Dehalococcoides* proteins: enzyme bioindicators of chlorinated ethene dehalorespiration. Environ. Microbiol. **11:**2687-2697.

60. **Wilkins, M. J., N. C. VerBerkmoes, K. H. Williams, S. J. Callister, P. J. Mouser, H. Elifantz, A. L. N'Guessan, B. C. Thomas, C. D. Nicora, M. B. Shah, P. Abraham, M. S. Lipton, D. R. Lovley, R. L. Hettich, P. E. Long, and J. F. Banfield.** 2009. Proteogenomic Monitoring of *Geobacter* Physiology during Stimulated Uranium Bioremediation. Appl. Environ. Microbiol. **75:**6591-6599..

61. **Zhang WW, Li F, Nie L.** 2010. Integrating multiple 'omics' analysis for microbial biology: application and methodologies. Microbiology-Sgm. **156:**287-301.

CHAPTER 4

Respiratory biomarkers for *Methanospirillum* in a dechlorinating mixed culture: correlation with methanogenesis rates and quantitative comparisons with *Dehalococcoides*

4.A. Abstract

Respiration biomarkers for a hydrogenotrophic methanogen, *Methanospirillum hungatei* sp.), were developed and tested on a population growing in a mixed culture containing syntrophic fermenters, organochlorine respirers (*Dehalococcoides ethenogenes*), and acetoclastic methanogens in addition to *M. hungatei*. Mixed-culture proteomic work confirmed the presence of hydrogenase biomarker targets and the majority of other putative methanogenesis enzymes in this population. Quantification of mRNA expression of FrcA, a hydrogen utilizing Coenzyme F_{420}-reducing hydrogenase, and MvrD, an iron sulfur protein that transfers electrons to heterodisulfide reductase, an enzyme that regenerates coenzyme B for the last step in methanogenesis, correlated with *M. hungatei* respiration (linear correlation score R = 0.96 for both targets on a log-log scale across respiration rates over two orders of magnitude). While both of these targets correlated with activity, the average abundance of MvrD transcripts was two orders of magnitude lower than FrcA transcripts, regardless of the type of electron donor provided and/or presence of electron acceptors for other physiologies. Comparing levels of *M. hungatei* and *D. ethenogenes* biomarkers in mixed culture suggest different overall abundances of biomarker mRNA. Under normal batch feeding conditions (2:1 butyrate to PCE fed in terms of hydrogen eeqs), *M. hungatei* biomarkers and the *D. ethenogenes* NiFe-hydrogenase HupL demonstrated increased mRNA levels after provision of substrates (peaking at 1 h for HupL and 3 h for MHU biomarkers). Peak mRNA expression was higher in FrcA (1.5×10^{10} copies per mL

culture) than both HupL (3.2×10^9 copies per mL culture) and MvrD (1.5×10^8 copies per mL culture). When donor ratios are limited, *M. hungatei* FrcA transcript abundance drops below *D. ethenogenes*, consistent with existing thermodynamic and experimental evidence that *D. ethenogenes* outcompetes *M. hungatei* at low hydrogen partial pressures.

Inferring the relative importance of observed expression trends between *D. ethenogenes* and *M. hungatei* is difficult given their distinct phylogenetic, as well as physiological differences in terms of size and ribosome content. Protein translation rates, as a function of transcript level, could differ substantially across organisms. Basal hydrogenase protein levels of the consistently maintained Donna II batch culture were quantified to gain insight into how mRNA expression trends correlate with protein abundance. Multiple reaction monitoring, a targeted quantitative proteomic approach, was used to measure *M. hungatei* and *D. ethenogenes* specific biomarker peptides to ascertain average levels. Statistically similar per-cell abundances of both *M. hungatei* and *D. ethenogenes* protein biomarkers were observed: 167 ± 120, 60 ± 1and 42 ± 14 proteins per genome copy for HupL, FrcA, and MvrD, respectively. This implies that mRNA expression levels are not informative of protein levels within an organism (between MvrD and FrcA) or across organisms (HupL vs. MvrD or FrcA). This suggests that the strength of a particular mRNA biomarker target relies upon empirically-established quantified trends with activity (such as respiration) as well as detection limits for biomarker quantification.

4.B. Introduction

In anaerobic environments, methanogenesis serves as a major terminal electron accepting process driving the degradation of organic biomass (42). Although the majority of environmentally produced methane is consumed by methane oxidizers, the portion of methane

that escapes to the atmosphere (~0.4 Gigatons a year (42)) acts as a potent greenhouse gas, 20 times more potent than carbon dioxide (3). Methane also serves as an important energy source. As such, synthesis and collection of methane has many important industrial applications, including anaerobic digestion. The productivity of anaerobic digesters communities has been linked to phylogenetic composition (44), though currently we have limited resolution with respect to specific methanogenic activities (acetoclastic vs. hydrogenotrophic methanogenesis) in mixed communities. Monitoring methanogenic activities could have important applications for facilitating industrial processes or better understanding methanogenesis in environmental systems.

Phylogenetically, all methanogens are members of the Euryarchaeota, and the majority of species can utilize hydrogen for the reduction of carbon dioxide (CO_2) to methane (CH_4) (42). In environmental systems, hydrogen is usually supplied through the activity of syntrophic fermentors (43), and consumption of hydrogen and other fermentation end products drives organic compound catabolism that would not otherwise be thermodynamically favorable (36). Many organisms with the ability to consume hydrogen often coexist in these communities and, under certain conditions, have even been shown to compete when hydrogen is limited. This interaction has been documented in both environmental ecosystems (5, 23-26) and laboratory settings (38, 39, 48). A pertinent example is illustrated by competition between dehalorespiring *Dehalococcoides* species and hydrogenotrophic methanogens (1, 10, 38, 48). As successful bioremediation is often dependent on the activities of dehalorespiring organism, many remediation approaches that include biostimulation (potentially in conjunction with bioaugmentation) supply electron donors in excess of what is required for remediation. This can result in two undesired effects: accumulation of excess biomass in ground-water systems and the

production of the flammable greenhouse gas, methane. In some cases, competition with methanogens has been implicated in incomplete or stalled remediation (27).

Molecular biomarkers for *in situ* microbial activities could be employed at such remediation sites and other environmental systems for monitoring of specific physiological processes, such as methanogenesis and dehalorespiration. As members of the *Dehalococcoides* are actively utilized in the bioremediation of chlorinated organic compounds, several studies have focused on development of *Dehalococcoides* biomarkers and their application to field sites undergoing remediation (8). Relationships between the abundance of mRNA biomarkers and respiration have been the subject of several studies (31, 33, Chapter 3). Characterizing similar relationships in other hydrogen-consuming organisms will allow for assessing differential activities between organisms, and will potentially prove useful for understanding the ecology of these systems, as well as for facilitating cost effective and/or efficient remediation.

In an anaerobic, methanogenic and dehalorespiring community (Donna II) maintained on PCE and butyrate, syntrophically produced hydrogen is consumed by both *Dehalococcoides ethenogenes* (DET) and *Methanospirillum hungatei* (MHU) (10, 11, 34). In DET, several candidate biomarkers have been tested including several reductive dehalogenases, enzymes that catalyze reduction of chlorine-carbon bonds, and the well conserved and highly expressed NiFe-hydrogenase HupL, thought to be important for hydrogen oxidation for reductive dechlorination (28, 29, 37). As hydrogen is the electron donor for which *Dehalococcoides* and *Methanospirillum* compete, enzymes involved in hydrogen utilization were the focus of this biomarker work. In hydrogenotrophic methanogenesis, the deazaflavin F_{420} serves as an important electron carrier. In MHU, an F_{420}-reducing NiFe hydrogenase (Frc) has been shown to oxidize hydrogen for the reduction of F_{420} (6). Though formate dehydrogenases also have the

ability to reduce F_{420} in the conversion of formate to CO_2 (46), there is currently no evidence of formate production in the Donna II culture. Hydrogen production, however, has been confirmed (11). Many methanogens contain a hydrogen utilizing methylenetetrahydromethanopterin reductase (Hmd), a unique non-metal containing hydrogenase (Figure 4.1, Reaction 3), in addition to an F_{420}-dependent methylenetetrahydromethanopterin dehydrogenase (Mtd) (Figure 4.1, Reaction 4), both of which can catalyze the reduction of CH-H_4MPT to CH_2-H_4MPT. Though Hmd utilizes hydrogen directly, MHU is not annotated to contain this enzyme. The last step in methanogenesis has previously been shown to utilize a methyl-viologen reducing hydrogenase (Mvr) (4, 41). MHU contains one of the important subunits (MvrD), that has been linked to shuttling electrons to heterodisulfide reductase (Hdr) for the regeneration of CoM-SH and CoB-SH from heterodisulfide (Figure 4.1, Reaction 8) (41). The oxidative subunit that supplies electrons to MvrD has yet to be identified.

In this work, mixed culture proteomics was used to highlight important respiratory enzymes present in MHU, as well as confirm the presence of MHU biomarker targets, MvrD and FrcA that are more extensively studied. FrcA has been shown to be highly transcribed during exponential growth experiments in pure culture as well as co-culture with *Syntrophobacter fumaroxidans* (47). Previous mRNA expression work with MvrD in the Donna II culture has highlighted that this transcript is up regulated during PCE and butyrate feeding conditions (34). These studies have qualitatively suggested that these targets may serve as viable biomarkers, though previous culturing conditions did not allow for direct comparison of MHU biomarker abundance and respiration rates (due to the transient respiration rates observed in batch cultures and/or the prevalence of acetoclastic methane production under butyrate fed conditions). As such, the first goal of this work was to develop respiration-biomarker relationships for MHU

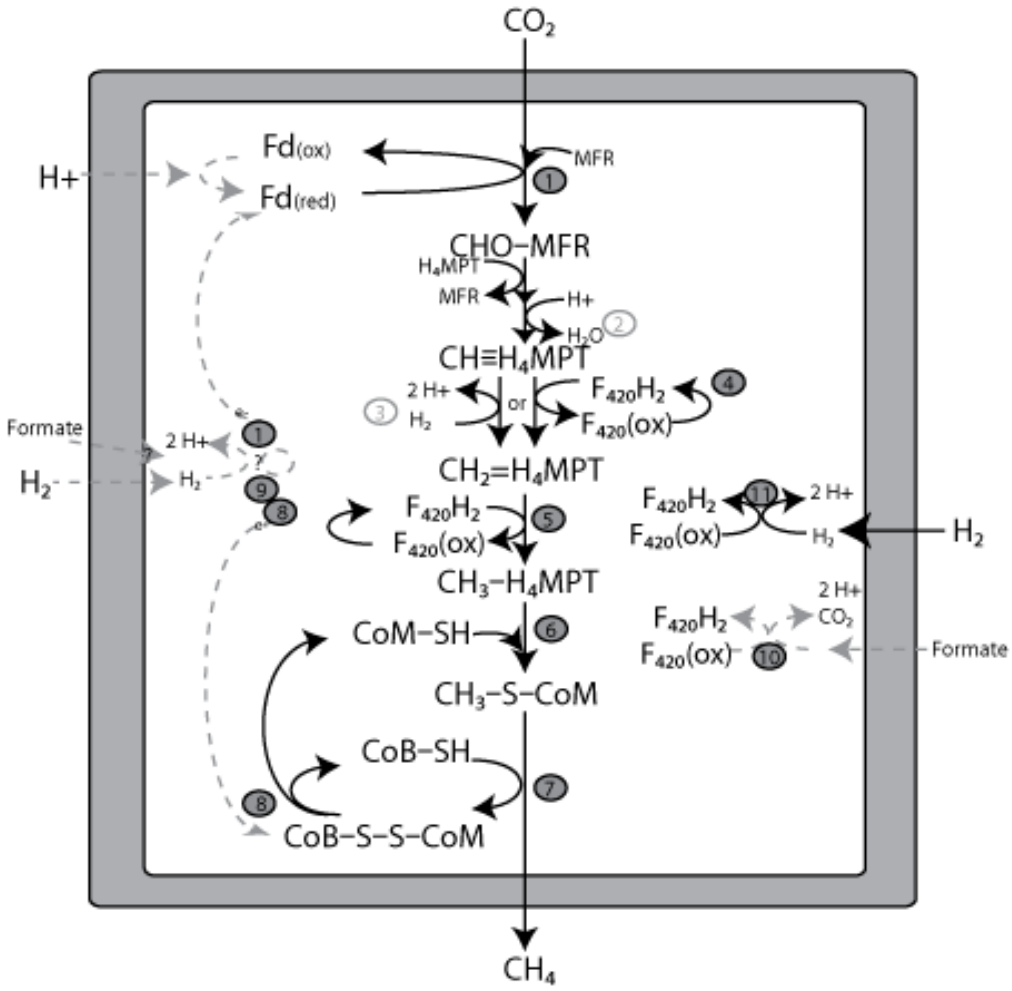

Figure 4.1. Schematic of MHU methanogenesis pathway. Specific cofactors utilized are abbreviated: methanofuran (MFR), Ferredoxin (Fd), tetrahydromethanopterin (H_2MPT), Coenzyme F_{420} (F_{420}), Coenzyme M (CoM) and Coenzyme B (CoB). Reduced redox state is indicated by (red) or H_2 and oxidized by (ox). Enzymes involved in catalysis of these reactions are indicated with numbers in grayed in circle indicating detection in shotgun proteomic experiments. White circles with gray outlines and numbers (2-3) indicate either formylmethanofuran-tetrohydromethanopterin formyltransferase, F_{420}-independent methylenetetrahydromethanopterin dehydrogenase which were not detected in the mixed culture proteome. Numbers also listed with corresponding enzymes in Table 4.1. Reactions 1 and 8 are potentially coupled, and form a complex with currently unknown oxidative subunit. This and other putative reactions (formate oxidation to F_{420} and reverse electron transport reduction of Fd) are highlighted with gray dashed arrows.

targets in the Donna II mixed culture. Quantification of mRNA expression was monitored with respect to hydrogenotrophic methanogenesis. Observed MHU mRNA-respiration relationships were then compared with previously quantified DET mRNA-respiration relationships (over similar respiratory ranges in terms of μeeq per L-hour). The goal of this comparison was to test the viability of using respective DET and MHU mRNA biomarker abundances for inter-organism comparisons of activity. The last goal of this work was to compare protein abundance of MHU and DET biomarker targets using a targeted quantitative proteomic approach. This information was used to assess biomarker mRNA-protein relationship, both within a given organism and across microorganisms.

4.C. Materials and Methods

4.C.1. Experimental Conditions and Analysis of Metabolites

An anaerobic mixed culture (Donna II) was maintained on tetrachloroethene (PCE) and butyrate in a six-liter batch reactor as previously described (11) (listed in Table A3.1). Methane was quantified from headspace samples using a gas chromatograph (GC) (Perkin-Elmer) equipped with a flame ionizing detector (FID) for levels below 33 μmoles per 160 mL serum vial (run conditions described in Smatlack et al. (38)). The thermal conductivity detector (TCD) was utilized at higher methane levels as described previously (38). Hydrogen was quantified from headspace samples via GC-TCD if above 0.5 μM aqueous concentration (C_w), and below this level using a reduced gas detector (RGD) (Trace Analytical) as described previously (11)). Quantification of chloroethenes was also performed using the GC-FID (run conditions described previously (32)). Quantification of organic acids from 0.2μm-filtered (PTFE coated syringe filters) liquid samples was performed on an ion chromatograph (IC) (Dionex). Samples were run

via isocratic 5-mM sodium hydroxide gradient through an AS-1100 column (Dionex) with a total run time of 30 min (5 min ramp to 80 mM sodium hydroxide at the end of each run). For each experimental set, organic acid standards were run for butyrate, formate, propionate and acetate ranging from 1 μM to 10mM in filtered basal salts medium (BSM, (11)). The detection limit for most organic acids was 10 μM, with the exception of formate which had a 1 μM detection limit.

4.C.2. Experimental Conditions

The majority of experiments were performed on subcultures constructed in serum vials with 100 mL culture volume and a 60 mL headspace. Experimental conditions involved batch and continuous feeding regimes as previously described (31, 32) of both electron donors (hydrogen, butyrate, lactate) with or without PCE. Bicarbonate was provided by media (BSM) and CO_2 in head space gas mix (70%N_2/30%CO_2). Conditions were varied to alter respiration rate (outlined in Table A3.1). Soluble substrates were dissolved in BSM at the desired electron equivalence (eeq) ratios and added to cultures via syringe pump (31). Constant mixing was maintained using stirbars.

Hydrogen additions were performed in two different modes: batch addition to headspace or through diffusion. Hydrogen levels kept above one hundred times the reported K_s (0.5 μM) for methanogenesis in this culture (38) were maintained with bulk hydrogen additions to the headspace. Alternately, a slow rate of hydrogen addition was generated in serum vials through the diffusion of hydrogen across low-density polyethylene (LDPE) 3/8-in. OD × 1/4-in. ID × 0.062-in. wall tubing (Freelin-Wade 1J-074). Construction and use of hydrogen diffusion tubes was performed as described previously for oxygen permeability experiments (14), substituting hydrogen for oxygen. In brief, tubing was cut to equivalent lengths of approximately 6.5 cm and sealed with barbed-end PVC plugs, maintaining a 5 cm internal length (volume 1.6 mL). This

internal volume was filled with either 66 μmoles of H_2 or N_2 (as a control). Abiotic control samples were used to calculate rates of hydrogen diffusion in basal salts media (BSM) for each hydrogen addition experiment.

To a subset of cultures continuously fed butyrate, methyl fluoride (MF) was added as a selective inhibitor of acetoclastic methanogenesis (12). MF at a partial pressure of 1 kPa has previously been shown to selectively inhibit acetoclastic methanogenesis without affecting syntrophic interactions in an anaerobic mixed culture including acetogenic, sulfate-reducing and fermentative bacteria (18). Greater partial pressures (5 kPa) may inhibit hydrogenotrophic methanogenesis (18). MF (Sigma) was measured in cultures via GC-FID (using standard chloroethene run conditions described above) and maintained at a minimum partial pressure of 1 kPa, but below 5 kPa in microcosm headspace.

4.C.3. Extraction of Nucleic Acids and Proteins

Nucleic acid extractions for quantitative PCR (qPCR) or quantitative reverse transcription PCR (qRT-PCR) were performed on two mL of culture sampled at selected time points over the course of each experiment. Samples were pelleted at 21,000 *g* for five min at 4^{o}C. Supernatant was removed and samples were stored at -80^{o}C until extraction, which occurred within one to seven days of sampling using the Qiagen Allprep RNA/DNA mini prep kit (Qiagen). Cell lysis was performed as described previously (34) using lysozyme, β-mercaptoethanol and rigorous vortexing. Isolation and cleanup of RNA and DNA were performed according to the manufacturers protocol (Qiagen).

Protein extractions were performed on pellets obtained from 30 -50 mL experimental samples. Cells were pelleted at 14,000 *g* for ten min. Lysis by French press and extraction of proteins was performed as described previously (45). Proteins were concentrated to a 50 μL

volume (final concentration 500mM phosphate, Urea 4M and 0.1% SDS, pH 8.0) using a Savant SpeedVac (Thermo Fisher) prior to quantification.

4.C.4. Bulk and Targeted (qPCR and qRT PCR) Nucleic Acid Quantification

Total DNA was quantified using the Quant-iT^{TM} Picogreen® double stranded DNA assay (Invitrogen). Prior to qPCR, all DNA samples were diluted one to ten. RNA samples were run on the Agilent 2100 BioAnlyzer (Agilent) to assess both quality of the RNA extractions, as well as amount recovered. Each RNA sample was diluted to 25 ng per µL and was treated with DNase (Fisher Scientific), then converted to cDNA using the BioRad iScript^{TM} select kit and random hexamers (BioRad). Depending on the transcript being quantified, cDNA was diluted either one to five or one to ten1:10. qPCR primers and annealing temperatures used in this study are listed in Table 4.1 (primer design discussed below). Forty-cycle qPCR runs were performed on a BioRad iCycler with annealing temperature appropriate to each primer set (as described in Fung et al. (13). Pure or mixed culture bulk DNA, or target-specific plasmids were used to generate standards. Analysis of qPCR data was performed as outlined previously (31, 33) utilizing luciferase mRNA as an internal reference standard for calculation of efficiency (19). Raw fluorescence data was used to calculate R_0 values using the DART method (30, 35). Average expression levels in continuous feed experiments were calculated using all time points past four hours ($n \geq 3$ time points).

4.C.5. *Methanospirillum* Primer Design

Degenerate primers for methanogen hydrogenases were used to obtain MHU-specific sequences from the Donna II mixed community via clone libraries as described previously (34). Hydrogenase subgroups targeted were the energy-conserving hydrogenase (EchA), the methyl-viologen reducing hydrogenase subunit D (MvrD) and the nickel-iron hydrogenase large subunit

(F_{420}-reducing, FrcA). Cloned sequences generated in this analysis matched the *Methanospirillum hungatei* JF-1 genome with 90- 99 percent nucleotide identity, with the exception of Ech which only produced *Dehalococcoides ethenogenes* str. 195 sequences. All sequences were later confirmed in the Donna II metagenome (IMG-M/ER) and were utilized to design quantitative PCR primers for Donna II MHU biomarker targets (Table 4.1) using PrimerQuest available through IDT (www.idtdna.com). Primers were also tested with JF-1 pure culture DNA extracts and cloned amplicons (data not shown). Metagenomic sequencing of this community suggests high homology and synteny between the Donna II MHU population and *Methanospirillum hungatei* JF-1, a strain consisting of four ribosomal gene copies (data not shown). An assumption of four 16S rRNA gene copies per genome was therefore made to determine estimates of genome or cell copies.

4.C.7. Protein Quantification and Proteome Sample Preparation

Protein pools to be analyzed via multiple reaction monitoring (MRM) were first assessed with SDS-PAGE gel electrophoresis alongside five micrograms of an *E. coli* K12 protein standard (Cornell Proteomics Facility) to assess quality of proteins. The amount of total protein was quantified using a serial dilution of each protein sample and the Quant-iT^{TM} protein assay (Invitrogen). Ten to twenty micrograms of protein were then treated with 1 mM TCEP HCL (tris(2-carboxyethyl)phosphine) as a reducing agent for one hour at 37^{o}C, followed by 50 mM iodoacetamide as an alkylating agent for 15 min in the dark at room temperature. The alkylation reaction was quenched using either free L-cysteine or excess DTT. Prior to digestion with trypsin (Mass spectrometry grade, Promega) at 37^{o}C for 12-14 hours, the concentration of urea and sodium dodecyl sulfate (SDS) were diluted to approximately 0.4 M and 0.1%, respectively.

4.C.8. Shotgun Proteome Analysis

Table 4.1. RNA and DNA biomarker targets for DET and MHU. Gene loci based on *Dehalococcoides ethenogenes* str. 195 or *Methanospirillum hungatei* str. JF1, along with gene name and annotation based on information from IMG (http://img.jgi.doe.gov.) are listed. Primer sequences used for quantitative PCR reported along with annealing temperature and reference.

Organism	**Gene Locus**	**Gene Name**	**Annotation/ IMG term**	**Primer Sequence**	**Annealing temp for qPCR**	**Reference**
Dehalococcoides ethenogenes .	DET_DE16S	16S rRNA	16S ribosomal RNA	GGAGCGTGTGGTTTAATTCGATGC (sense) GCCCAAGATATAAAGGCCATGCTG (anti-sense)	60^{O}C	(13)
	DET0110	HupL	[Ni/Fe] hydrogenase, group 1, large subunit (EC:1.12.99.6)	TGACGTTATTGCAGTAGCTGAGT (sense) CACACCATAGCTGAGCAGGTT (anti-sense)	55^{O}C	(13)
	DET1545	DET 1545	reductive dehalogenase, putative	ATACTTACCGGTCAAGGGCGTTAG (sense) ATGGTCACGATGTTCCTGGGTAAG(anti-sense)	60^{O}C	(13)
Methanospirillum hungatei	MHUN_R001 MHUN_R027 MHUN_R068 MHUN_R072	16S rRNA	16S ribosomal RNA	AGTAACACGTGGACAATCTGCCCT (sense) ACTCATCCTGAAGCGACGGATCTT (anti-sense)	60^{O}C	(34)
	MHUN2332	FrcA	nickel-dependent hydrogenase, large subunit, Coenzyme F420-reducing hydrogenase, alpha subunit (EC 1.12.98.1)	AGGTCAGCCTTGAAGATGCAGACT (sense) TTCTTGAACTGAACCAGACGGGCA (anti-sense)	60^{O}C	This publication
	MHUN1839 MHUN1842	MvrD	methyl-viologen-reducing hydrogenase, delta subunit, F420-non-reducing hydrogenase, subunit D (EC 1.8.98.1)	TGTTCGTATGCAGGTGCTGACCTT (sense) ACCATCTGCACCCTCAACAAATGC (anti-sense)	60^{O}C	(34)

Peptide fractionation (n = 10 fractions) and shotgun proteomics analysis via MudPIT-nLC-MS/MS were performed as described previously (45). Identification of proteins, and statistical analysis of identification including ProtScores were determined using ProteinPilot™ 2.0 (45). Spectra were searched against a custom database combining all publicly-available sequenced *Dehalococcoides,* methanogen, and *Firmicutes* genomes, in addition to community-specific metagenomic sequences available for this culture (JGI) as of December 2009. Each peptide identified was assigned a confidence level by ProteinPilot™'s scoring algorithm (up to a maximum of 99%). This peptide can contribute scores to proteins identified where the contribution = -log(1-confidence/100). The sum of scores of all peptides uniquely assigned to a particular protein (not claimed by another target) are used by ProteinPilot™ to generate the Unused ProtScore. For each protein identified, the amino acid sequence was searched against the Blast2GO database to determine Gene Ontology (GO) information and Enzyme Commission (EC) numbers (15).

4.C.9. Multiple Reaction Monitoring for Quantification of Biomarkers

Peptides for targeted proteomic experiments were selected based on detection in previous shotgun proteomic experiments. Analysis of peptides, including selection of target transition ions (parent ion/fragment ion pairs) was performed in MRMpilot 2.0 (ABSciex). Selected targets including parent and fragment ion mass to charge ratios (m/z) are listed in Table 4.2. Each target was confirmed via MRM-IDA (Chapter 3) on time zero control protein samples.

Clean up of digested peptides followed the protocol outlined previously (45), with the exception that strong cation exchange cleanup was performed as described previously for MudPIT-nLC-MS/MS (45) using the Agilent 1100 HPLC prior to solid phase extraction (SepPak C18 cartridge, Waters, Milford, MA; 1 mL 75% ACN eluent). Purified peptides were dried and

Table 4.2. DET and MHU peptides chosen for targeted-proteomic quantification via MRM. For each peptide, molecular weight (MW), parent ion m/z and fragment ion m/z are reported along with the charge state. Average response factors based on duplicate standard curves. Coefficient of variation (CV) in response factor based on four analysis runs over the course of four months. Protein concentrations on a per genome copy basis are reported along with standard deviations.

DET Gene ID	Target Name	Peptide	MW	Parent ion (Q1)	charge	Transition ion (Q3)	Response Factor (log Peak Area vs. log Concentration)	Response factor CV(%)	Average D2 concentration (proteins per genome copy)	St.Dev
DET0110	HupL 1	IEATVDGGEVK	1117.2	559.4	2+	804.4	1.02	8	46	15
				559.4	2+	875.5	0.98	9		
	HupL 2	DNDNPFELVR	1218.3	609.8	2+	760.5	1.14	6	287	140
				609.8	2+	874.5	1.10	6		
DET0990	DET rpL7/12 1	ALEAAGATIEIK	1186.3	593.8	2+	731.4	1.02	12	240	190
				593.8	2+	802.5	0.94	17		
	DET rpL7/L12 2	TVIELSELVK	1130.3	565.8	2+	930.6	1.19	20	177	86
				565.8	2+	817.5	1.18	20		
DET0997	DET EF-TU 1	ILDSAEPGDAVGLLLR	1638.9	547.1	3+	571.4	1.20	18	558	384
				547.1	3+	1010.6	1.19	15		
				820.0	2+	856.5	1.20	18		
				820.0	2+	1010.6	1.19	15		
	DET EF-TU 2	NSFPGDEIPIVR	1343.5	672.3	2+	995.6	1.05	1	663	312
				672.3	2+	898.6	1.08	1.6		
MHUN1842	MvrD 1	ELGPSPIK	839.99	420.7	2+	598.4	1.08	7	56	41
				420.7	2+	444.3	0.94	22		

	MvrD 2	IQYPPTVR	973.15	487.4	2+	472.2	1.03	4.5	28	17
				487.4	2+	569.3	1.04	5		
MHUN2332	FrcA 1	VVEVSPTTR	987.13	494.3	2+	789.4	1.05	6.7	61	28
				494.3	2+	660.4	1.00	11		
	FrcA 2	VNDAGIIER	985.52	493.8	2+	587.3	0.99	9.6	59	28
				493.8	2+	773.4	0.95	22		
MHU0654	MHU rp L12AE	GAAPAAAAAEEAPA EDK	1539.6	770.5	2+	559.3	1.03	7.4	14	*
				770.5	2+	888.4	1.02	7.9		
MHU1601	MHU rp L7AE	ALEAVEAAR	929.05	465.3	2+	545.3	1.04	13	458	232
				465.3	2+	745.4	1.00	6		
MHUN1592	MHU EF1a 1	SDVGALLK	801.95	401.7	2+	600.4	1.04	4.1	56	53
				401.7	2+	501.3	1.01	8.3		

*Less than three data points above the detection limit

reconstituted in 40 to 80 µL 2% ACN, 0.45 % formic acid/0.002% heptafluorobutyric acid. Aliquots (1.5 to 3 µL) were injected on the nLC-MS/MS for MRM-IDA mode and subsequent normal MRM mode analyses.

nLC-MS/MS was performed as described in previously (45). SCX-desalted samples were analyzed using a hybrid triple quadrupole linear ion trap, 4000 Q Trap (Applied Biosystems). MRM-IDA analysis was used for validation of selected transition ion pairs prior to MRM quantitative analysis (described in Chapter 3).

Synthetic peptide standards for MRM targets (listed in Table 4.2) were obtained as purified (>95%), lyophilized solids (Bio Basic Inc.), and were reconstituted to 2000 pmol per µL in 0.5% formic acid with 2% ACN and stored at -80º C. Dilution series of synthetic peptides were constructed in a background matrix of peptides extracted from aerobic soil mixed culture as described previously (2, 45). Standard curves were generated for each MRM run and analyzed in duplicate for each run. Four MRM analysis runs were performed over a four month period (March 2010 through June 2010). Analysis of retention times and peak areas in standards and samples was performed using MultiQuanti™ 2.1 (ABISciex).

4.C.10. Statistical Analysis

Basic statistical analyses for quantitative PCR data, microarray data, and mRNA-respiration rate correlations were performed using Microsoft Excel. Shotgun proteomic data was processed with Protein Pilot™ 2.0 and targeted MRM data was analyzed in Multiquant™ 2.1 and further statistical analyses were calculated using Jmp 8.

4.D. Results and Discussion

4.D.1. Methanogenesis Proteins Detected by Shotgun Proteomics

Shotgun proteomic analyses from an anaerobic mixed culture (Donna II) growing on PCE and butyrate were used to elucidate potential protein biomarkers for methanogenesis from *Methanospirillum hungatei* (Table 4.3). Out of 516 proteins identified with a ProtScore greater than two (equivalent to at least one 99 % confidence peptide) in the community as a whole, 55 were homologous to MHU sequences from either the *M. hungatei* JF-1 genome (IMG), MHU-associated Donna II metagenomic sequences (JGI) or both (Supplemental Table A3.2). Of these 55 proteins, 24 were methanogenesis-associated (assigned to Methanogenesis Gene Ontology pathway). Enzymes critical to the highlighted reactions in methanogenesis were identified (Figure 4.1, Table 4.3). Only one enzymatic step, catalyzed by formylmethanofuran-tetrohydromethanopterin formyltransferase (Ftr), was not detected in proteomic analysis (Figure 4.1, Reaction 2). Proteins important to the consumption of hydrogen were detected, including a coenzyme F_{420}-reducing hydrogenase (Frc, A, B and G subunits). An F_{420}-independent methylenetetrahydromethanopterin dehydrogenase, was not detected via proteomic analysis (Figure 4.1, Reaction 3) suggesting that Mtd (Reaction 4) performs this catalytic step in the Donna II MHU population, and that F_{420} is required. Proteins that form a complex important for supplying electrons to regenerate coenzyme B for the last step in methanogenesis (7, 20) were also identified: the methyl-viologen reducing hydrogenase subunit D (MvrD) (Figure 4.1, Reaction 9), heterodisulfide reductase (Hdr) subunits A and B (Reaction 8), and formylmethanofuran dehydrogenase (Fmd) subunits A-C and F (Reaction 1). Identification of these proteins suggests that MHU utilizes the proposed electron bifurcation pathway, however the specific subunit responsible for oxidation of hydrogen has yet to be identified in MHU (47). Evidence in other methanogens suggests that formate (7) or reduced F_{420} (mediated through

Table 4.3. Proteins identified in MHU methanogenesis pathway via shotgun proteomics. Reaction numbers correspond to pathway displayed in Figure 1. Each gene locus is relative to the *Methanospirillum hungatei* JF-1 genome (img.doe.gov) with corresponding gene name, annotation, and enzyme commission number. Enzyme subunits listed separately. ProtScores are determined by ProteinPilot™ 2.0 software and are indicative of sum of contributing high confidence peptides (see methods for further details). Other MHU proteins detected highlighted in Supplemental Table A2.2 along with further G.O. information and additional gene information.

Reaction Number	Gene Locus	Gene Name	Annotation/IMGterm	Unused ProtScore (only assigned to one target)	ProtScore (total peptides detected)	%Coverage (95 confidence peptides)
1	Mhun_1835	FmdF	4Fe-4S ferredoxin, iron-sulfur binding/formylmethanofuran dehydrogenase, subunit F (EC 1.2.99.5)	5.83	5.83	11.1
	Mhun_1988	FmdB	formylmethanofuran dehydrogenase, subunit B (EC 1.2.99.5)	3.92	3.92	7.9
	Mhun_1989	FmdA	Amidohydrolase 3/formylmethanofuran dehydrogenase, subunit A (EC 1.2.99.5)	2.15	2.15	1.8
	Mhun_1990	FmdC	formylmethanofuran dehydrogenase, subunit C (EC 1.2.99.5)	4.47	4.47	8.3
	Mhun_1981	FmdC	formylmethanofuran dehydrogenase, subunit C (EC 1.2.99.5)	2.01	2.6	2.7
4	Mhun_2255	Mtd	F420-dependent methylenetetrahydromethanopterin dehydrogenase/methylenetetrahydromethanopterin dehydrogenase (EC 1.5.99.9)	14.98	14.98	28.2
5	Mhun_2257	Hmd/Mer	Coenzyme F420-dependent N(5),N(10)-methenyltetrahydro-methanopterin/methylenetetrahydromethanopterin reductase (EC 1.5.99.11)	15.99	15.99	16.2
6	Mhun_2174	MtrA	tetrahydromethanopterin S-methyltransferase, subunit A/G (EC 2.1.1.86)	2.77	2.91	4.4
	Mhun_2175	MtrH	N5-methyltetrahydromethanopterin/tetrahydromethanopterin S-methyltransferase, subunit H (EC 2.1.1.86)	10.1	10.1	15.6
7	Mhun_2148	McrA	Coenzyme-B sulfoethylthiotransferase/methyl-coenzyme M reductase, alpha subunit (EC 2.8.4.1)	23.05	25.06	22.2

	Mhun_2144	McrB	methyl-coenzyme M reductase, beta subunit (EC 2.8.4.1)	14.4	15.7	17.7
	Mhun_2147	McrG	methyl-coenzyme M reductase, gamma subunit (EC 2.8.4.1)	22.25	22.25	58.1
8	Mhun_1838	HdrA	4Fe-4S ferredoxin, iron-sulfur binding/CoB--CoM heterodisulfide reductase subunit A	6.39	6.39	3.6
	Mhun_1837	HdrB	CoB--CoM heterodisulfide reductase subunit B	5.16	5.16	8.8
9	Mhun_1839	MvrD	methyl-viologen-reducing hydrogenase, delta subunit/F420-non-reducing hydrogenase subunit D (EC 1.8.98.1)	-	2.1	5.7
	Mhun_1842	MvrD	methyl-viologen-reducing hydrogenase, delta subunit/F420-non-reducing hydrogenase subunit D (EC 1.8.98.1)	2.1	2.1	5.7
10	Mhun_1813	FdhA	formate dehydrogenase, alpha subunit (F420) (EC 1.2.99.-)	-	3.47	2.6
	Mhun_1814	FdhB	formate dehydrogenase, beta subunit/ coenzyme F420 hydrogenase/dehydrogenase beta subunit-like (EC 1.2.99.-)	2.17	2.53	2.2
	Mhun_2020	FdhB	formate dehydrogenase, beta subunit/ coenzyme F420 hydrogenase/dehydrogenase beta subunit-like (EC 1.2.99.-)	9.94	16.56	9.2
	Mhun_2021	FdhA	formate dehydrogenase, alpha subunit (F420) (EC 1.2.99.-)	3.27	3.28	2.1
	Mhun_2023	FdhA	formate dehydrogenase, alpha subunit (F420) (EC 1.2.99.-)	16.76	16.83	10.4
11	Mhun_2332	FrcA	nickel-dependent hydrogenase, large subunt/ coenzyme F420-reducing hydrogenase, alpha subunit (EC 1.12.98.1)	10.6	10.6	12.6
	Mhun_2329	FrcB	coenzyme F420-reducing hydrogenase, beta subunit/ coenzyme F420 hydrogenase/dehydrogenase beta subunit-like (EC 1.12.98.1)	5.77	5.77	10.8
	Mhun_2330	FrcG	coenzyme F420-reducing hydrogenase, gamma subunit (EC 1.12.98.1)	4	4	8.0

MvrD) (4) can potentially serve as electron donors to Hdr as well, which may account for the lack of homologs of the oxidative subunits MvrA and MvrG in MHU. There was strong proteomic evidence for methyl-coenzyme M reductase (A, B and C subunits) which catalyzes the final release of methane (Figure 4.1, Reaction 7).

Peptides indicative of three of the five MHU FdhA genes were also detected (Table 4.1). However, for Mhun_1833 and Mhun_3238, the only peptides detected are conserved with other FdhA loci (Mhun_1813) and therefore could not be conclusively identified. Though detection of Fdh genes confirms the ability of these organisms to metabolize formate, formate has never been detected in liquid culture extracts analyzed via IC (i.e., <1 μM). Hydrogen and acetate are commonly detected, and are thought to be the dominant fermentation endproducts of butyrate fermentation in the Donna II mixed culture. Other hydrogen-utilizing enzymes that have been implicated as important for methanogenesis generally (42), or in MHU specifically (47), were not detected in this work: the energy-conserving hydrogenases, EchA and EchB, and the membrane bound hydrogenase, Mbh. Based on their importance in providing reducing equivalents into the respiratory pathway, identification in the proteome and previous mRNA expression work (34, 47) the MHU biomarker targets FrcA, which has previously been characterized (6), and MvrD, thought to be essential in shuttling electrons for the last step in methanogenesis (4, 20, 41), were quantified in mRNA and protein expression studies.

4.D.2. Biomarker mRNA Expression in Batch Culture

DET and MHU rapidly initiate mRNA expression of respiration-associated hydrogenases when batch fed PCE and butyrate in mixed culture (Figure 4.2A and 4.2B). No statistically significant differences were observed in 16S rDNA or rRNA levels on a per mL basis for either organism over the time course of the batch feed, though MHU ribosome content (per mL culture)

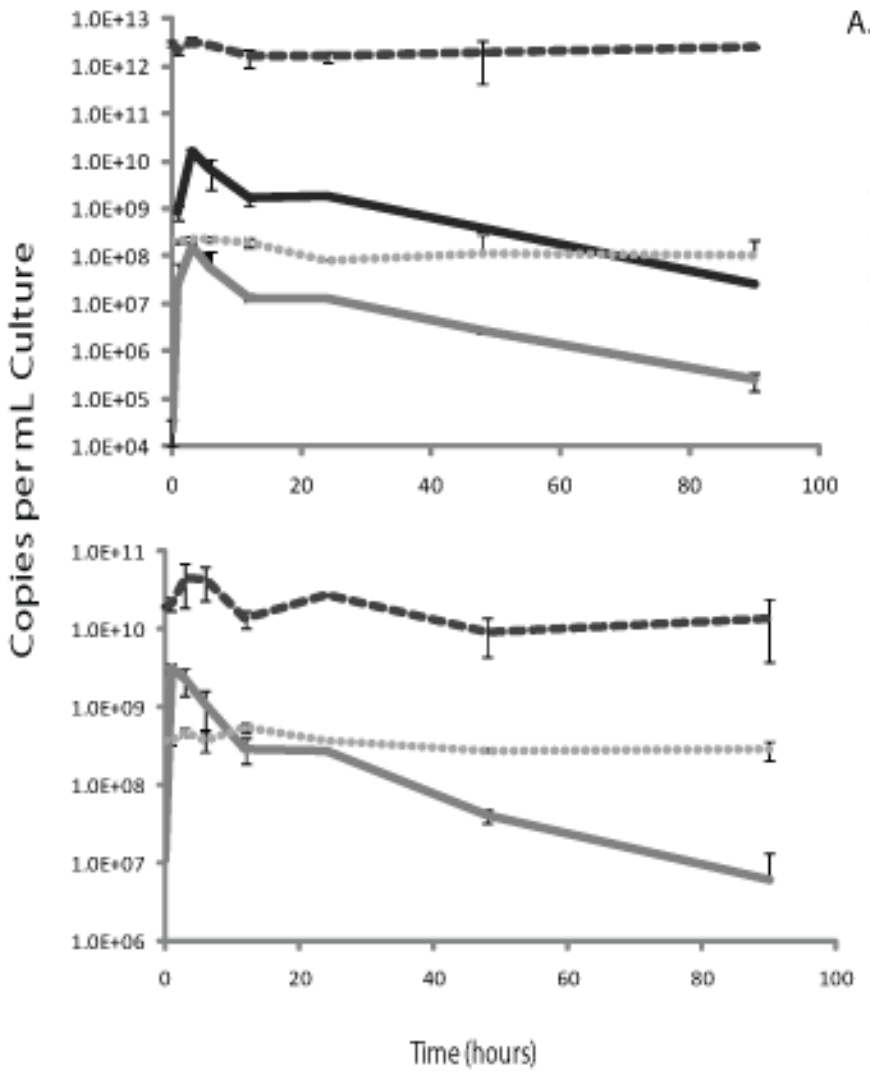
Copies per mL Culture
1.0E+13
1.0E+12
1.0E+11
1.0E+10
1.0E+09
1.0E+08
1.0E+07
1.0E+06
1.0E+05
1.0E+04
0
20
40
60
80
100
Average FrcA
Average MvrD
Average 16S rRNA
Average 16S rDNA/4
1.0E+11
1.0E+10
1.0E+09
1.0E+08
1.0E+07
1.0E+06
Average HupL
Average 16S rRNA
Average 16S rDNA
Time (hours)

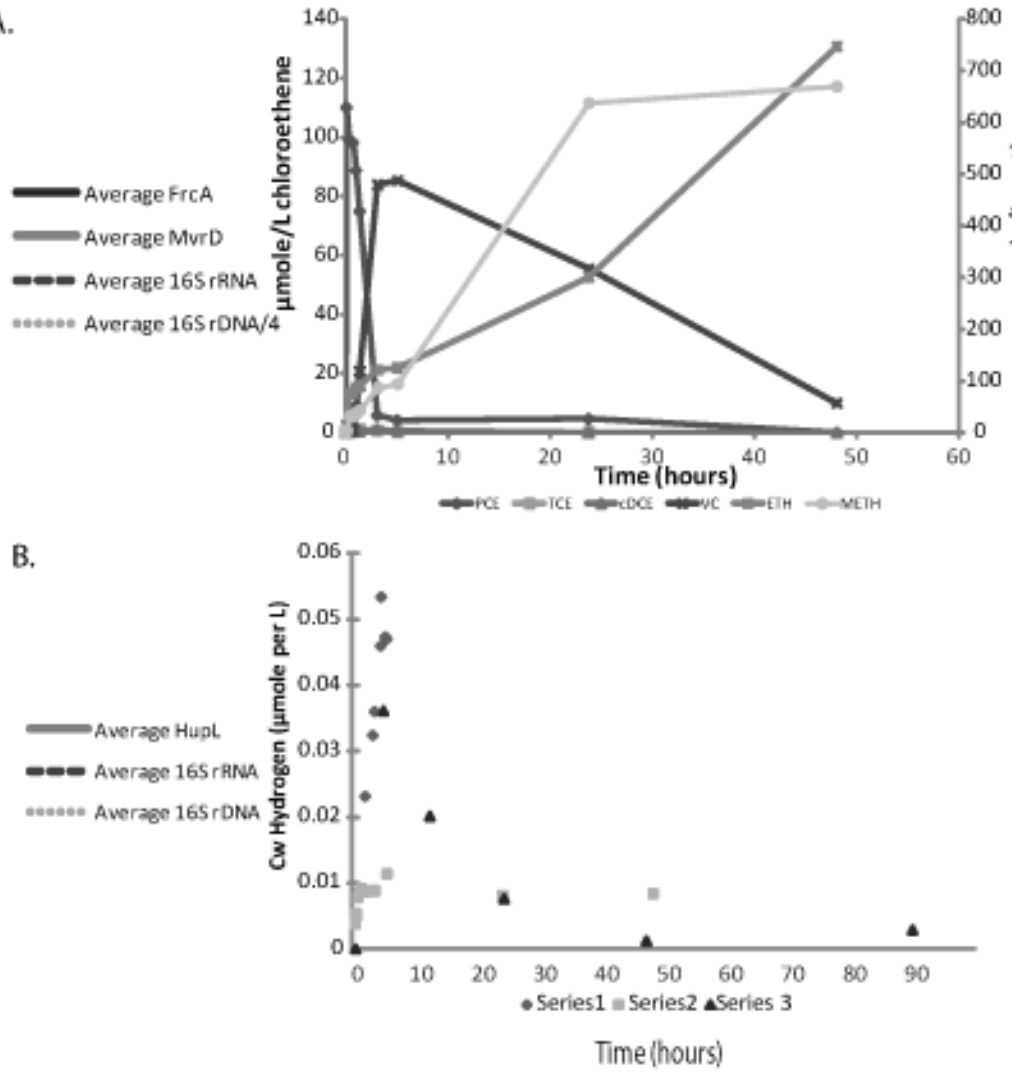
A.
µmole/L chloroethene
140
120
100
80
60
40
20
0
800
700
600
500
400
300
200
100
0
0
10
20
30
40
50
60
Time (hours)
PCE
TCE
cDCE
VC
ETH
METH
B.
Cw Hydrogen (µmole per L)
0.06
0.05
0.04
0.03
0.02
0.01
0
0
10
20
30
40
50
60
70
80
90
Series1
Series2
Series 3
Time (hours)

Figure 4.2. RNA and DNA biomarkers levels for MHU(A) and DET (B) over 90 hours post batch substrate additions of PCE (110 µmole per L) and Butyrate (440 µmole per L) in the Donna II mixed culture. Error bars indicated the standard deviation of four samples taken per time point. Monitored chloroethenes and methane over the time-course following batch feeding are presented as nominal concentration per L culture (C) in addition to the dissolved hydrogen concentration for replicate batch feeds (D). $C_w = H_2$ concentration in water at equilibrium with headspace readings.

was nearly 80 times the DET ribosome content (Figure 4.2A and 4.2B). In this system, syntrophic fermenters convert butyrate to hydrogen and acetate (molar ratio of 1:2:2 for butyrate:hydrogen:acetate). These fermentation products support the reduction of PCE to vinyl chloride and ethene via dehalorespiration, the reduction of carbon dioxide to methane and conversion of acetate to methane and carbon dioxide (Figure 4.2C). Batch conditions result in a burst of hydrogen early in the feeding cycle (peaking at 4 hours) (Figure 4.2D). The up-regulation of mRNAs from both DET and MHU suggests both organisms are responsive to respiratory conditions within this time frame, although the peak in HupL's expression is consistently earlier than MHU targets (Figure 4.2). Increases in expression after butyrate and PCE amendments, earlier up-regulation in HupL and the overall difference in mRNA abundance between DET HupL and MHU MvrD have previously been noted (34), but this work monitors expression at many more time points. Although MHU total population levels have increased since these reports, consistent ratios of MvrD expression to 16S rRNA were observed during this batch work and the previous reports (~1-2 x 10^{-4} mRNA copies per 16S rRNA) (34). Extending the previous work, these results demonstrate a similar overall pattern (spike and decay) in expression between MHU biomarkers and the DET hydrogenase HupL. Higher abundance of MHU biomarker FrcA was noted compared to MvrD and HupL (Figure 4.2A and 4.2B). The peak of DET HupL expression suggested one-fifth the peak transcript level (3.2 x 10^{9} copies per mL culture) seen for MHU FrcA (1.6 x 10^{10} copies per mL culture). At maximum, MvrD expression was two orders of magnitude lower in abundance than FrcA (1.5 x 10^{8} vs. 1.6 x 10^{10} copies per mL culture for MvrD and FrcA, respectively). Total time-integrated abundance of biomarkers over the full 90 hours differed similarly. This highlights the difference in transcript levels between MHU biomarkers themselves.

4.D.3. Degradation of mRNA Biomarkers

Following peak transcriptional activity, MHU biomarkers demonstrated exponential decay as has previously been described in DET (Figure 4.3A and 4.3B) (21, 22, Chapter 3). Similar levels of mRNA decay (transcripts per mL) were observed (decay rates of 0.057 to 0.069 per hour) in DET and MHU. No statistically significant decay in ribosome abundance was observed in MHU (0.002 per hour for 90 hours, $R^2 = 0.45$), or DET over this time period (0.014 per hour for 90 hours, $R^2 = 0.49$). Initial decay rates represent an active period of decay, which is followed by slower endogenous decay rates after 120 hours. Using transcripts-per-16S rDNA copy measurements to correct for cell decay, endogenous rates of 0.01 to 0.02 per hour were noted for transcripts in both organisms during this endogenous decay period (Figure 4.3C). Ribosome content did not decay significantly on a per 16S rDNA copy basis, in either DET or MHU during this 160 hour time period post purge (120 to 280 hours post feed) (data not shown). Decay in 16S rDNA for MHU (0.001 per hour or 0.03 per day) is on average less than half the measured DET rate (0.003 per hour or 0.07 per day). This cell decay rate likely does not reflect true cell decay for MHU, as methanogenesis is fueled by endogenous decay of other culture biomass over this time period. Though some differences were observed among these different DET and MHU biomarkers, these results suggest the mRNA and DNA decay occur in similar time frames for these organisms.

4.D.4. Pseudo-Steady State *Methanospirillum* Biomarkers

Traditional Donna II culturing conditions result in methane produced from acetoclastic and hydrogenotrophic methanogenesis. Mixed-culture biokinetic models suggest that 20% of

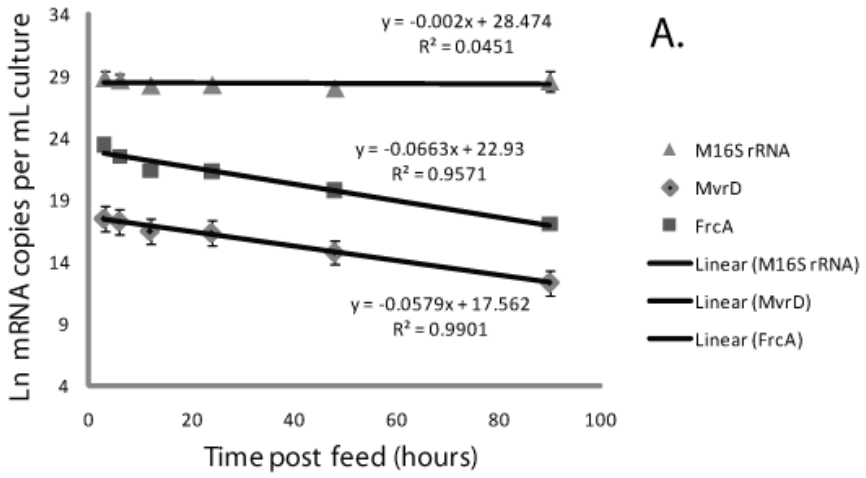
A.
y = -0.002x + 28.474
R² = 0.0451
y = -0.0663x + 22.93
R² = 0.9571
y = -0.0579x + 17.562
R² = 0.9901
Ln mRNA copies per mL culture
Time post feed (hours)
M16S rRNA
MvrD
FrcA
Linear (M16S rRNA)
Linear (MvrD)
Linear (FrcA)

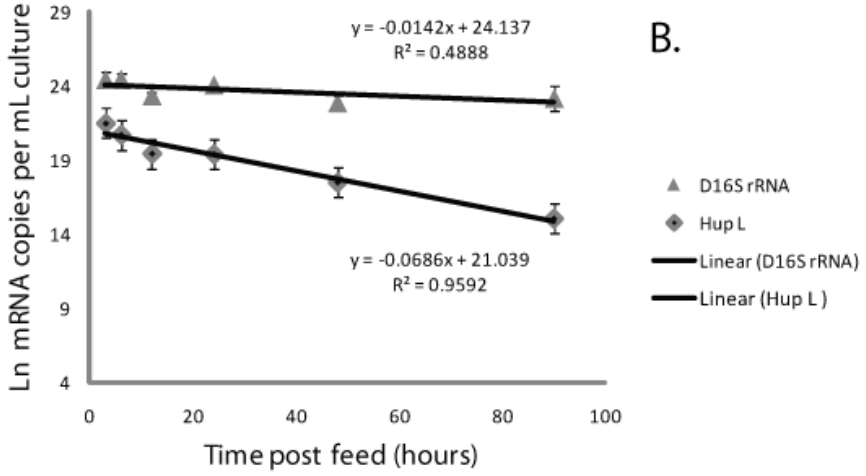
B.
y = -0.0142x + 24.137
R² = 0.4888
y = -0.0686x + 21.039
R² = 0.9592
Ln mRNA copies per mL culture
Time post feed (hours)
D16S rRNA
Hup L
Linear (D16S rRNA)
Linear (Hup L)

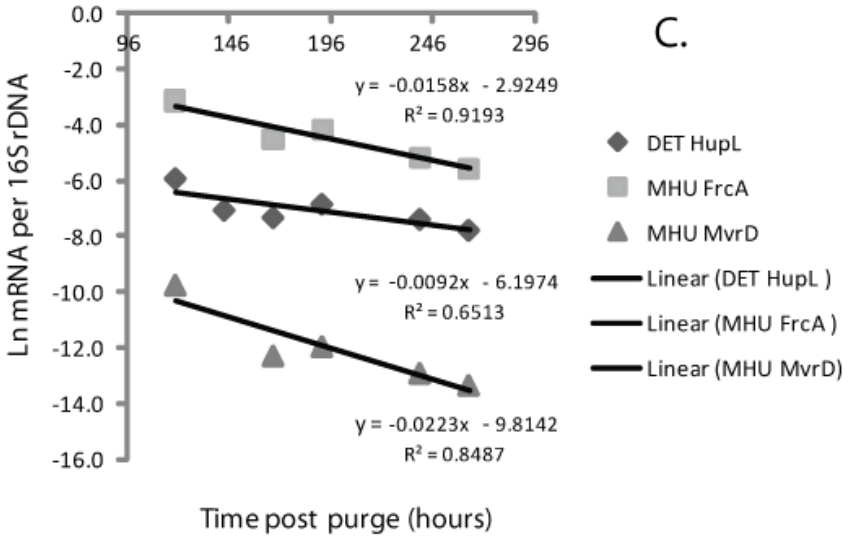
C.
y = -0.0158x - 2.9249
R² = 0.9193
y = -0.0092x - 6.1974
R² = 0.6513
y = -0.0223x - 9.8142
R² = 0.8487
Ln mRNA per 16S rDNA
Time post purge (hours)
DET HupL
MHU FrcA
MHU MvrD
Linear (DET HupL)
Linear (MHU FrcA)
Linear (MHU MvrD)

Figure 4.3. Active decay in transcript abundance post batch feed in PCE and butyrate cultures. Ln of transcript abundance for MHU biomarker targets (A) and DET biomarker targets (B) starting 3-6 hours post feed plotted against time. Slopes indicate first-order decay coefficients. Error bars indicated the standard deviation of four samples per time point (n=4). Endogenous decay rates calculated post purge of end products (starting at 96 hours post batch feed) (C). Ln of transcript abundance per 16S rDNA copy for each organism is plotted against time for calculating decay coefficients. Error bars indicate standard deviation of biological replicates (n=3).

the methane produced from butyrate fermentation (or 10% under normal butyrate and PCE feeding conditions where half the produced hydrogen is consumed by dehalorespirers) is attributable to MHU (10, Gretchen Heavner, unpublished data). The balance would normally come from acetoclastic methanogenesis. However, in order to more accurately assess relationships between MHU biomarker abundance and MHU respiration rate, experiments were performed such that only MHU was significantly producing methane.

4.D.4A. Continuous Hydrogen Addition

Two feeding conditions for hydrogen were employed to generate steady-state methanogenesis rates in MHU; both conditions resulted in a pseudo-steady state level of MHU biomarker expression within eight hours (Figure A3.1, Appendix III). Maintaining a high hydrogen level via headspace additions (average C_w = 100 μM hydrogen) resulted in a maximum methanogenesis rate of 167 ± 8μeeq per L-hr (7.6 x 10^{-10} μeeq per cell-hr). In other experiments, a slow rate of hydrogen addition was generated utilizing diffusion of hydrogen through LDPE tubes, which resulted in a hydrogen addition of 1.4 ± 0.2 μmoles per cm-hr (Figure A3.1B). This addition rate generated an average hydrogen C_w of 0.28 ± 0.08 μM (Figure A3.1B). In addition to a lower respiration rate, lower overall expression levels of both MHU mRNA biomarkers were observed in these hydrogen feeding experiments: average expression of 2.5 ± 0.6 x 10^6 and 8.3 ± 2.1 x 10^7 copies per mL for MvrD and FrcA, respectively, with slow hydrogen addition versus 2.4 ± 1.7 x 10^8 and 5.2 ± 3.6 x 10^{10} copies per mL for MvrD and FrcA, under excess hydrogen conditions.

4.D.4B. Continuous Butyrate Additions

Rates of hydrogenotrophic methanogenesis under butyrate feeding conditions were determined through inhibition of acetoclastic methanogenesis with fluoromethane (MF) (see

Appendix III, Figure A3.2) (18). Subcultures fed butyrate, acetate, and no donor, with and without MF supported our supposition that acetoclastic methanogenesis (by a *Methanosaeta* spp. in this culture) was inhibited under experimental MF concentrations (Figure A3.2A). Hydrogenotrophic methanogenesis rates were statistically equivalent in hydrogen-only amendments with or without MF suggesting MF did not inhibit MHU under these conditions (data not shown). About 18% of the methane produced in butyrate-only cultures was observed in the cultures amended with MF (25 μmoles of methane in MF-treated butyrate cultures at 24 hours compared to 140 μmoles in butyrate-only) (Figure A3.2A), supporting previous and current modeling efforts suggesting the MHU population generates approximately 20% of culture methane (10). Methane levels in the acetate + MF control were comparable to endogenous levels in no donor controls (Figure A3.2A). Between butyrate treatments with and without MF, transcript levels of MHU targets were not statistically different, though expression of FrcA and MvrD followed the same trend in terms of relative abundance of the different transcripts (MvrD less abundant overall) (Figure A3.2B). These data suggest that MHU expression was unaffected by the addition of MF and that the rate of methanogenesis observed in MF + Butyrate amended cultures is attributable to MHU respiration specifically.

4.D.5. Correlating Biomarker Gene Expression with Methanogenesis

The pseudo-steady state levels of MHU transcripts from the hydrogen and butyrate/MF experiments generated a strong correlation with respect to rate of hydrogenotrophic methanogenesis (R^2 of 0.93 for a linear fit of log respiration, log copies per mL for each transcript) (Figure 4.4A). Respiration rates over which these correlations were observed spanned two orders of magnitude (Figure 4.4). Because the density of methanogens (observed in terms of 16S rDNA copies) has been observed to vary over time, and because the abundance of organisms

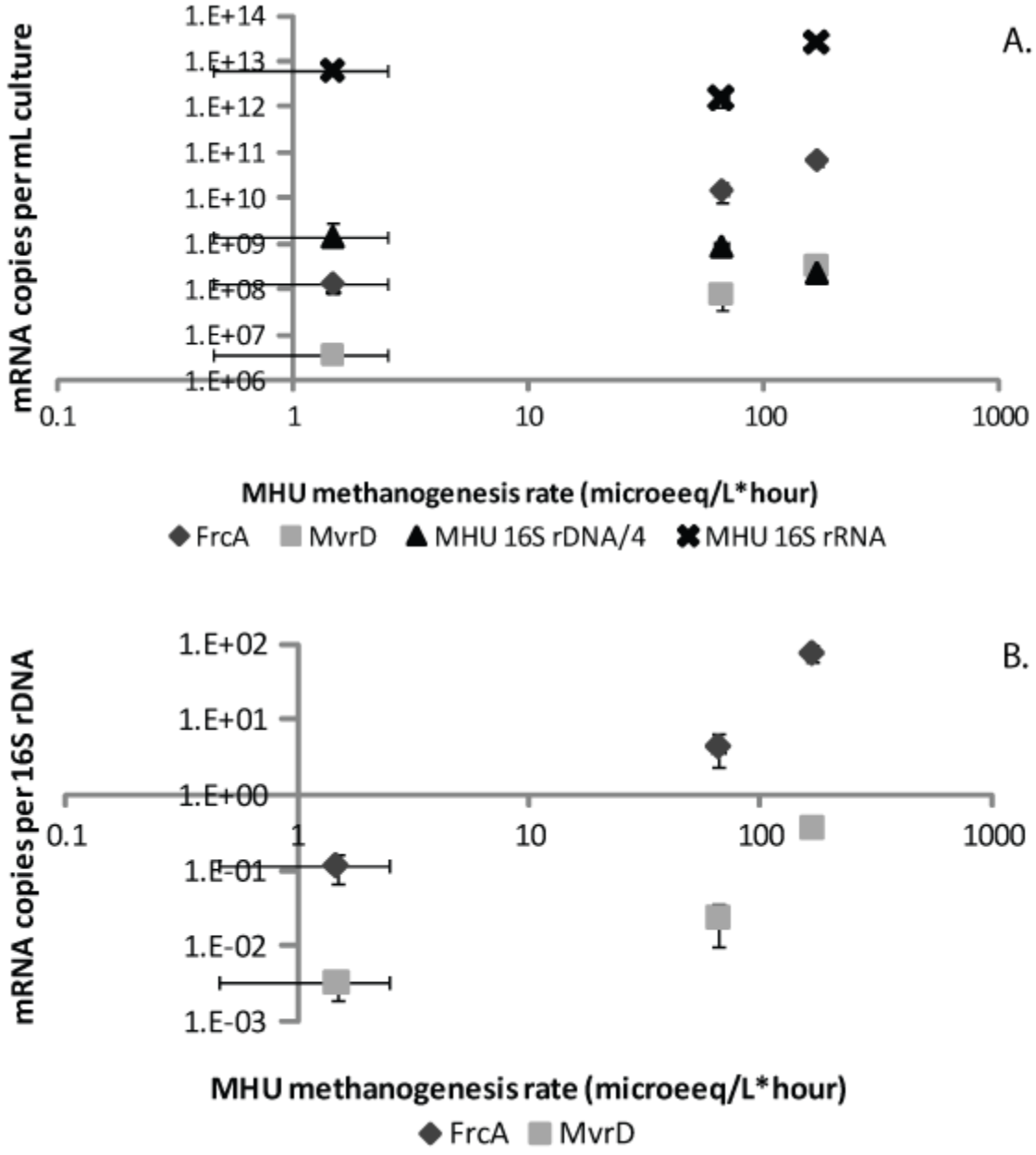

Figure 4.4. Average pseudo-steady state expression level of MHU biomarker targets for hydrogen only experiments and butyrate plus methyl fluoride (MF) experiments compared to respiration rate. PSS transcript levels as mRNA copies per mL culture (A) and normalized mRNA copies per 16S rDNA copy (B). Error bars are standard errors of biological replicates for either transcript abundance (y-error bars) or respiration rates (x-error bars).

differs in different cultures and in environmental systems, normalization of transcript abundance to various cellular markers was performed. Normalization to 16S rRNA has previously been used as an internal control to account for variability in total RNA recovery (34). However, ribosome content was observed to increase significantly at the highest rates tested (data not shown), coinciding with growth/respiration rate increase, as has been demonstrated in many organisms (9). As such, rRNA normalizations generated trends that decreased in expression at the highest respiration rates (data not shown), suggesting that fluctuations in ribosome content make it a poor internal normalizing factor for these organisms. Normalization of MvrD and FrcA levels to MHU 16S rDNA resulted in linear trends with respiration, similar to those observed on a per mL culture basis (Figure 4.4B).

Due to the link between hydrogen production and methanogenesis, and previously described associations between hydrogenase expression and hydrogen in members of *Methanococcales,* and *Methanosarcinales* (16, 17, 47), MHU biomarker levels were compared with measured aqueous hydrogen concentrations. PSS experiments fed a variety of electron donors, and chloroethene electron acceptors at different rates and ED to EA ratios (experimental conditions listed in Table A3.1), demonstrated only a weak relationship between MHU mRNA biomarkers and hydrogen level (Figure A3.3, Appendix III). However, high variability in measured hydrogen levels over time may obscure trends that exist at low hydrogen concentrations. The range of average aqueous hydrogen concentrations measured for most of these experiments was limited to 0.01-0.2 μM. As hydrogen levels dissolved in liquid media are calculated from headspace measurements, there is potential that these levels do not reflect biologically relevant concentrations, especially comparing experiments where hydrogen was provided exogenously with those where hydrogen was provided by syntrophic fermentation.

As previously noted, methane produced under these conditions is the result of both hydrogenotrophic and acetoclastic methanogenesis, and so cannot be attributed solely to MHU. None-the-less, in mixed culture PSS experiments a strong correlation between mRNA expression for MHU biomarkers and total methanogenesis was observed although the trend was offset from the MHU-only experimental trend (data not shown). Assuming MHU methanogenesis was 20% of total methanogenesis under butyrate-fed conditions or 10% if a chloroethene electron acceptor for dehalorespiration was also provided, the trend lines become indistinguishable (Figure 4.5). This further supports the trend between MHU biomarker expression and respiration.

Under all experimental conditions, MvrD transcript levels were statistically lower (up to two orders of magnitude) than FrcA levels, although the overall response patterns were similar at the mRNA level. This observation was supported by other work in *M. hungatei* JF-1, where expression of Frc (MHUN_2332) was 3 to 430 times higher than any other metabolic target monitored including: five formate dehydrogenase genes (Fdh) as well as other hydrogenases, Ech (MHUN_1745) and Mbh (MHUN_2590) (47). MvrD was not monitored in this work, however work in our system (selected qPCR studies) suggest that FdhA homologs are expressed at similar levels to MvrD. In butyrate-fed continuous feeding conditions, time zero FdhA levels were $2.8x10^5 \pm 8x10^4$ per mL compared to $2.1x10^5 \pm 5x10^4$ per mL for MvrD, and these levels increased to statistically similar PSS levels upon butyrate addition: $1.1x10^8 \pm 7x10^7$ per mL for FdhA and $7.9x10^7 \pm 4.5x10^7$ per mL for MvrD. In Worm et al. (47), MHU hydrogenase expression was monitored under hydrogen-fed, formate-fed and co-cultured conditions (with *Syntrophobacter fumaroxidans*), which has previously been shown to produce both hydrogen and formate during propionate fermentation (40). No differential regulation of Frc or Fdh genes (with the exception

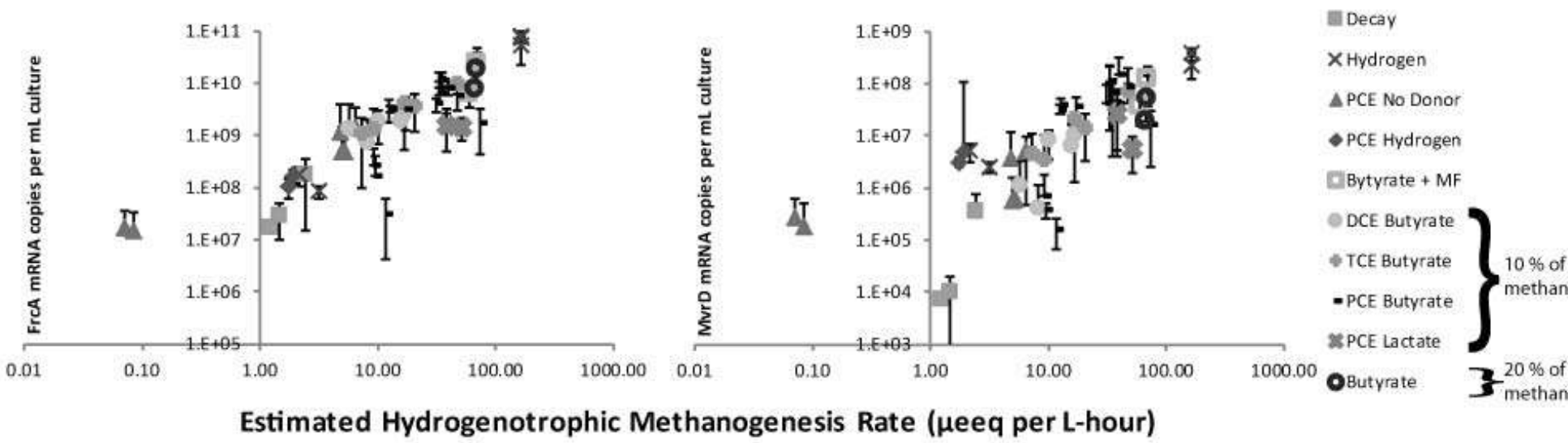

Figure 4.5. Pseudeo-steady state mRNA levels for FrcA (left) and MvrD (right) across estimated hydrogenotrophic (MHU) methanogenesis calculated as follows. For chloroethenes and butyrate fed cultures, rate was estimated to be 10% of the total. If chloroethenes were omitted from butyrate feed, rates were estimated to be 20% of the total. For Hydrogen, PCE hydrogen and butyrate plus methyl fluoride amendments, all methane was attributed to hydrogenotrophic methanogenesis. It was also estimated that the majority of methane from no donor and decay experiments stems from hydrogen. Error bars represent the standard deviation of PSS mRNA levels over time for individual reactors. Specific experimental parameters listed in Table A3.1, Appendix III.

of one Fdh homolog (MHUN_2023) were noted for these conditions suggesting that regulation of the majority of these genes is not controlled solely by formate or hydrogen level (47).

4.D.6. Comparing *Dehalococcoides* to *Methanospirillum* mRNA Expression in PSS Experiments

Given that hydrogen equivalents from excess donor provided are converted to methane (CO_2 reducing methanogens are not electron-acceptor limited under the N_2/CO_2 headspace), this results in relatively similar respiration rates in DET and MHU for experimental conditions where butyrate is provided in a 2:1 ratio to PCE (on a H_2 eeq basis). In addition, for biomarker and respiration relationships drawn for DET's HupL (Figure A3.5) and MHU's MvrD and FrcA (Figure 4.4), similar scales of mRNA responsiveness (two to three orders of magnitude change in transcript copies per mL culture basis) were observed over the range of respiration rates tested (1 to 150 μeeq per L-hour). However, the absolute values of these trends differ among biomarker targets, both within and across organisms, ranging from 10^9 to 10^{11} per mL for MHU FrcA, 10^7 to 10^{10} per mL for DET HupL, and $5x10^6$ to $5x10^8$ per mL for MHU MvrD. Linear trends for log mRNA copies vs. log respiration rate (power relationship) generated the following slopes: DET HupL 1.1, MHU FrcA 1.3 and MHU MvrD 0.8. As these are likely within a similar statistical range, it suggests that these biomarkers have similar responsiveness over the range or respiration rates tested. These trends (and slopes) were supported by 16S rDNA normalizations (Figure 4.4B for MHU and Figure A3.5B for DET).

Biomarker relationships were also responsive to relative changes in respiration under donor-limited conditions. In PCE/hydrogen and PCE/half-butyrate experiments, where ED to EA ratios were 0.5 to 1 or lower, the abundances of hydrogenase transcripts show comparatively higher expression in DET than in MHU. Specifically, pseudo-steady-state levels of DET HupL

and MHU FrcA were 1.64 x 10^9 ± 2.45 x 10^8 and 1.3 x 10^8 ± 3.71 x 10^7 copies per mL culture for hydrogen diffusion experiments amended with PCE at a rate of 10 μeeq per L- hour. Similarly, in the half-butyrate experiments, FrcA levels were 6.91 x 10^8± 3.21 x 10^8 compared with HupL levels at 3.94 x 10^9 ± 1.44 x 10^9 copies per mL culture. Interestingly, in an experimental replicate for which the addition of PCE was halted due to syringe blockage, an increase in the expression MHU biomarkers was observed (Figure A3.4, Appendix III). Reductive dechlorination slowed in the affected subculture, and methane production increased slightly following this reduction in PCE (Figure A3.E-F). Hydrogen levels did not statistically change among the triplicate reactors (data not shown), nor did DET expression of HupL (Figure A3.4D). However, other DET targets were affected. In particular, a putative reductive dehalogenase enzyme (DET1545) that has previously been reported to be up-regulated under low PCE feeding conditions followed the same marked increase in gene expression, as was observed in MHU targets (Figure A3.4A-C). Mixed culture microarray assays support qRT-PCR trends observed in MHU and DET mRNA expression (Figure A3.5). Although FrcA and HupL were not statistically different in terms of absolute fluorescence for donor-limited PCE fed experiments, without PCE, HupL expression decrease coincides with FrcA and MvrD increases. FrcA was consistently an order of magnitude higher than MvrD in all mixed culture microarray experiments, in terms of absolute fluorescence intensity.

As DET and MHU are dramatically different in terms of size, cell volume and surface area, differences in abundance of biomarker mRNA and rRNAs are not surprising. Because of the differences in ribosome content of these organisms there is potential that these transcripts result in very different amounts of proteins produced. As such, DET and MHU hydrogenase

proteins were quantified to shed light on potential differences in DET and MHU hydrogenase protein pools.

4.D.7. Quantification of *Methanospirillum* and *Dehalococcoides* Proteins

Shotgun proteomic data (Table 4.3, Table A3.2, other data not shown), were utilized for the design of quantitative assays for selected biomarker peptide targets (Table 4.2). Previously, absolute quantification of HupL via MRM analysis was performed (45, Chapter 3). In addition to DET MRM targets, MHU MRM targets were confirmed with MRM triggered IDA analysis. Peptide standards in four separate analysis runs over a four month period resulted in consistent response factors for each peptide analyzed with an average CV of 11% (Table 4.2). The reported peptide values are a result of three base culture samples over a six month period. All samples were taken three days after batch feed of butyrate and PCE on a 2:1 hydrogen eeq basis. These data are reported on a per genome copy basis. Some of the variability is potentially the result of differences in culture biomass. Differences in populations of DET and MHU have been noted across time zero samples 1-3: $3.6 \times 10^8 \pm 7 \times 10^7$, $1.2 \times 10^9 \pm 2 \times 10^8$, $3.7 \times 10^8 \pm 1 \times 10^8$ genome copies per mL for DET and $2.1 \times 10^8 \pm 5 \times 10^7$, $1.0 \times 10^9 \pm 2 \times 10^8$, $2.1 \times 10^8 \pm 5 \times 10^7$ genome copies per mL for MHU. These values were used to convert protein abundances to per-genome values.

DET and MHU contain similar hydrogenase abundances (within an order of magnitude) per μg total protein, as well as per genome copy basis (estimated by one 16S rDNA copy for DET and four copies for MHU) in base culture samples (Figure 4.6). The average HupL abundance (167 ± 120 per genome copy) was slightly higher than the average abundance of MvrD (42 ± 14per genome) and FrcA (60 ± 1 per genome). However, the difference in

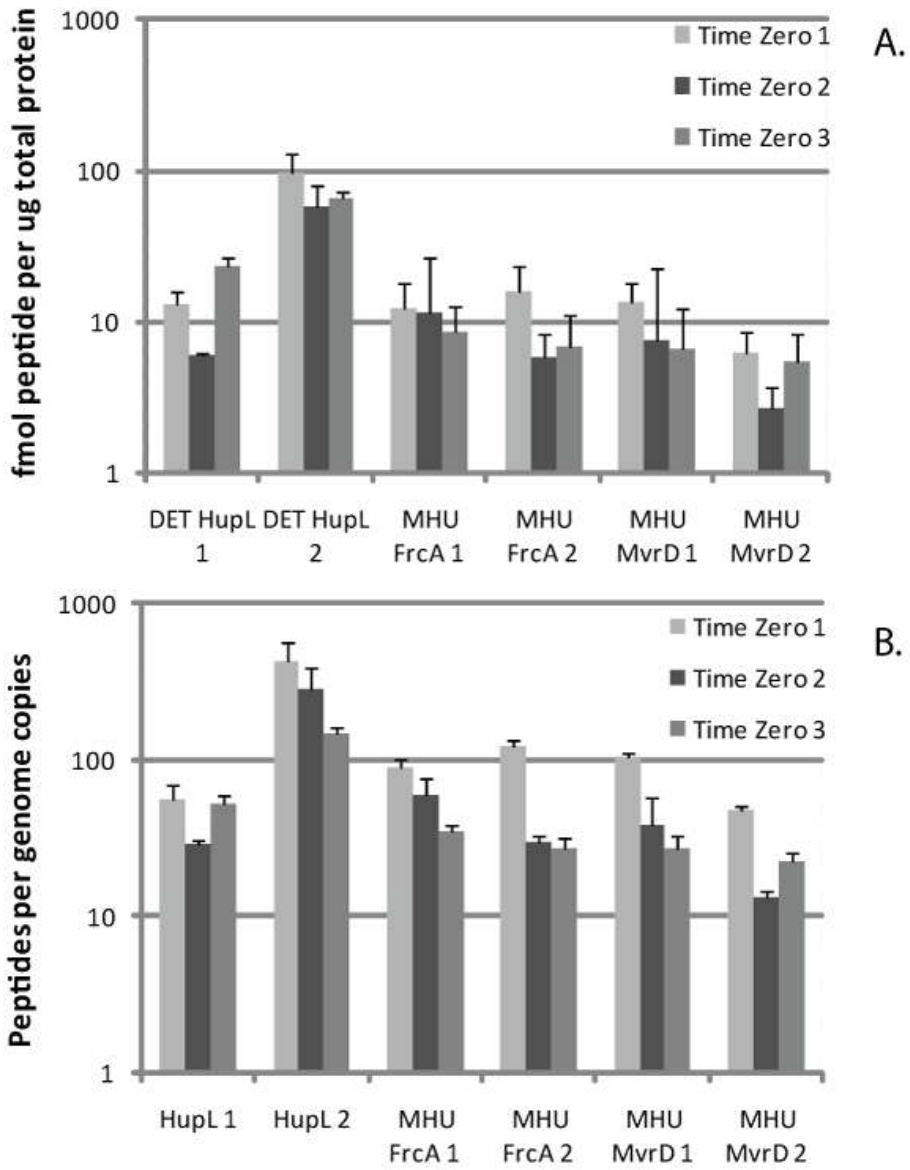

Figure 4.6. Average peptide abundance per µg total protein quantified via MRM analysis of triplicate mixed culture time zero protein samples (A). Peptides correspond to specific peptides (listed in Table 4.2) for DET and MHU hydrogenases. Normalized peptide abundances to genome copies (estimated with a single 16SrDNA copy for DET and 4 x 16S rDNA copies for MHU) was utilized to assess per cell protein abundances (B). Each measurement is the result of four different MRM analysis runs. Error bars represent standard deviations of replicate measurements.

abundance between the two HupL peptides measured make these trends statistically insignificant. In spite of differences that have been noted in mRNA expression between MvrD and FrcA, similar protein abundance of these biomarkers was observed in the culture MHU population. As these protein profiles result from batch feeding conditions (mRNA trends illustrated in Figure 4.2), time-integrated mRNA of these two different MHU transcripts over three days (MvrD- $1.13 \times 10^{9} \pm 4.3 \times 10^{8}$ total mRNA copies*hr per mL and FrcA-$1.27 \times 10^{11} \pm 2.9 \times 10^{10}$ total mRNA copies-hr per mL) illustrates the degree of difference between mRNA expression of these targets. Interestingly, DET time-integrated mRNA abundance is intermediate to these two biomarkers ($2.46 \times 10^{10} \pm 4.26 \times 10^{8}$ total mRNA copies-hour per mL). This suggests that on a per mRNA basis, compared to FrcA, more HupL polypeptides are generated per mRNA, which is surprising given the previously noted differences in ribosome content. However, potentially more MvrD polypeptides are produced on a per mRNA basis than either HupL or FrcA. This suggest differences in the net protein production of MvrD and FrcA which potentially stems from differences in mRNA translation, differences in rates of decay , and/or rates of protein turnover. It is difficult to distinguish among these different mechanisms that affect protein abundance. Previous work looking at protein decay, predominately in DET, demonstrated minimal decay (0.03 per day) in MHU proteins over the 30 day time period tested, not distinguishable from measured cell decay (0.03 to 0.04 per day). However, neither MvrD nor FrcA were specifically detected in this experimental dataset. HupL demonstrated a decay rate that was statistically indistinguishable from cell decay. More work is required to confirm these trends and potentially resolve some of the variability observed. Further work looking at decay and production of these specific proteins could highlight potential factors that are controlling differences in observed protein levels.

4.D.8. Conclusions

mRNA biomarkers showed tractable trends with respiration but overall levels were not consistent for targets within one organism or across organisms. This work highlights the potential for utilizing mRNA to assess differences in activity. Applying these quantitative trends could be used for monitoring an individual population's activities in a complex community. However, currently the scope of these trends is limited and likely to be informative only for these specific organisms and targets. Differences in the overall abundance relationships between DET and MHU mRNA biomarkers and either respiration or protein abundance highlights that no universal trends can be assumed. This supports the importance of establishing biomarker relationships before interpreting trends across different biomarkers and/or across organisms.

4.E. Acknowledgements

I would like to acknowledge co-authors for this work: Gretchen Heavner, Cresten Mansfelt and Ruth Richardson. We would also like to acknowledge Celeste Ptak and Sheng Zhang at the Cornell Proteomics and Mass Spectrometry core facility for proteomic sample analysis. Thanks to James Gossett and Stephen Zinder for their expert advice and editorial comments for this manuscript. Much of this work was funded through the IGERT funded Biogeochemistry and Environmental Biocomplexity small grant program (DGE 0221658). This work was funded through research grants from the National Science Foundation CBET Program (CBET-0731169) and the Department of Defense Army Research Office (W911NF-07-1-0249).

REFERENCES

1. **Ballapragada, B. S., H. D. Stensel, J. A. Puhakka, and J. F. Ferguson.** 1997. Effect of hydrogen on reductive dechlorination of chlorinated ethenes. Environ. Sci. Technol. **31:**1728-1734.

2. **Benndorf, D., G. U. Balcke, H. Harms, and M. von Bergen.** 2007. Functional metaproteome analysis of protein extracts from contaminated soil and groundwater. ISME J. **1:**224-234.

3. **Bousquet, P., P. Ciais, J. B. Miller, E. J. Dlugokencky, D. A. Hauglustaine, C. Prigent, G. R. Van der Werf, P. Peylin, E. -. Brunke, C. Carouge, R. L. Langenfelds, J. Lathiere, F. Papa, M. Ramonet, M. Schmidt, L. P. Steele, S. C. Tyler, and J. White.** 2006. Contribution of anthropogenic and natural sources to atmospheric methane variability. Nature (London). **443:**439-443.

4. **Brodersen, J., G. Gottschalk, and U. Deppenmeier.** 1999. Membrane-bound F420H2-dependent heterodisulfide reduction in Methanococcus voltae. Arch. Microbiol. **171:**115-121.

5. **Chapelle, F. H., and D. R. Lovley.** 1992. Competitive Exclusion of Sulfate Reduction by Iron-Iii-Reducing Bacteria a Mechanism for Producing Discrete Zones of High-Iron Ground Water. Ground Water. **30:**29-36.

6. **Choquet, C. G., and G. D. Sprott.** 1991. Metal Chelate Affinity-Chromatography for the Purification of the F420-Reducing (Ni,fe) Hydrogenase of Methanospirillum-Hungatei. J. Microbiol. Methods. **13:**161-169.

7. **Costa, K. C., P. M. Wong, T. Wang, T. J. Lie, J. A. Dodsworth, I. Swanson, J. A. Burn, M. Hackett, and J. A. Leigh.** 2010. Protein complexing in a methanogen suggests electron bifurcation and electron delivery from formate to heterodisulfide reductase. Proc. Natl. Acad. Sci. U. S. A. **107:**11050-11055.

8. **Cupples, A. M.** 2008. Real-time PCR quantification of *Dehalococcoides* populations: Methods and applications. J. Microbiol. Methods. **72:**1-11.

9. **Dethlefsen, L., and T. M. Schmidt.** 2007. Performance of the Translational Apparatus Varies with the Ecological Strategies of Bacteria. J. Bacteriol. **189:**3237-3245.

10. **Fennell, D. E., and J. M. Gossett.** 1998. Modeling the production of and competition for hydrogen in a dechlorinating culture. Environ. Sci. Technol. **32:**2450-2460.

11. **Fennell, D. E., J. M. Gossett, and S. H. Zinder.** 1997. Comparison of butyric acid, ethanol, lactic acid, and propionic acid as hydrogen donors for the reductive dechlorination of tetrachloroethene. Environ. Sci. Technol. **31:**918-926.

12. **Frenzel, P., and U. Bosse.** 1996. Methyl fluoride, an inhibitor of methane oxidation and methane production. FEMS Microbiol. Ecol. **21:**25-36.

13. **Fung, J. M., R. M. Morris, L. Adrian, and S. H. Zinder.** 2007. Expression of reductive dehalogenase genes in Dehalococcoides ethenogenes strain 195 growing on tetrachloroethene, trichloroethene, or 2,3-dichlorophenol. Appl. Environ. Microbiol. **73:**4439-4445.

14. **Gossett, J. M.** 2010. Sustained Aerobic Oxidation of Vinyl Chloride at Low Oxygen Concentrations. Environ. Sci. Technol. **44:**1405-1411.

15. **Gotz, S., J. M. Garcia-Gomez, J. Terol, T. D. Williams, S. H. Nagaraj, M. J. Nueda, M. Robles, M. Talon, J. Dopazo, and A. Conesa.** 2008. High-throughput functional annotation and data mining with the Blast2GO suite. Nucleic Acids Res. **36:**3420-3435.

16. **Guss, A. M., G. Kulkarni, and W. W. Metcalf.** 2009. Differences in Hydrogenase Gene Expression between Methanosarcina acetivorans and Methanosarcina barkeri. J. Bacteriol. **191:**2826-2833.

17. **Hendrickson, E. L., A. K. Haydock, B. C. Moore, W. B. Whitman, and J. A. Leigh.** 2007. Functionally distinct genes regulated by hydrogen limitation and growth rate in methanogenic Archaea. Proc. Natl. Acad. Sci. U. S. A. **104:**8930-8934.

18. **Janssen, P. H., and P. Frenzel.** 1997. Inhibition of methanogenesis by methyl fluoride: Studies of pure and defined mixed cultures of anaerobic bacteria and archaea. Appl. Environ. Microbiol. **63:**4552-4557.

19. **Johnson, D. R., P. K. H. Lee, V. F. Holmes, and L. Alvarez-Cohen.** 2005. An internal reference technique for accurately quantifying specific mRNAs by real-time PCR with a application to the tceA reductive dehalogenase gene. Appl. Environ. Microbiol. **71:**3866-3871.

20. **Kaster, A., J. Moll, K. Parey, and R. K. Thauer.** 2011. Coupling of ferredoxin and heterodisulfide reduction via electron bifurcation in hydrogenotrophic methanogenic archaea. Proc. Natl. Acad. Sci. U. S. A. **108:**2981-2986.

21. **Lee, P. K. H., D. R. Johnson, V. F. Holmes, J. Z. He, and L. Alvarez-Cohen.** 2006. Reductive dehalogenase gene expression as a biomarker for physiological activity of Dehalococcoides spp. Appl. Environ. Microbiol. **72:**6161-6168.

22. **Lee, P. K. H., T. W. Macbeth, K. S. Sorenson Jr., R. A. Deeb, and L. Alvarez-Cohen.** 2008. Quantifying Genes and Transcripts To Assess the In Situ Physiology of "*Dehalococcoides*" spp. in a Trichloroethene-Contaminated Groundwater Site. Appl. Environ. Microbiol. **74:**2728-2739.

23. **Lovley, D. R., D. F. Dwyer, and M. J. Klug.** 1982. Kinetic Analysis of Competition between Sulfate Reducers and Methanogens for Hydrogen in Sediments. Appl. Environ. Microbiol. **43:**1373-1379.

24. **Lovley, D. R., and S. Goodwin.** 1988. Hydrogen Concentrations as an Indicator of the Predominant Terminal Electron-Accepting Reactions in Aquatic Sediments. Geochim. Cosmochim. Acta. **52:**2993-3004.

25. **Lovley, D. R., and M. J. Klug.** 1983. Methanogenesis from Methanol and Methylamines and Acetogenesis from Hydrogen and Carbon Di Oxide in the Sediments of a Eutrophic Lake. Appl. Environ. Microbiol. **45:**1310-1315.

26. **Lovley, D. R., and M. J. Klug.** 1983. Sulfate Reducers can Out Compete Methanogens at Fresh Water Sulfate Concentrations. Appl. Environ. Microbiol. **45:**187-192.

27. **Lu, X., J. T. Wilson, and D. H. Kampbell.** 2009. Comparison of an assay for *Dehalococcoides* DNA and a microcosm study in predicting reductive dechlorination of chlorinated ethenes in the field. Environmental Pollution. **157:**809-815.

28. **Morris, R. M., J. M. Fung, B. G. Rahm, S. Zhang, D. L. Freedman, S. H. Zinder, and R. E. Richardson.** 2007. Comparative proteomics of *Dehalococcoides* spp. reveals strain-specific peptides associated with activity. Appl. Environ. Microbiol. **73:**320-326.

29. **Nijenhuis, I., and S. H. Zinder.** 2005. Characterization of hydrogenase and reductive dehalogenase activities of *Dehalococcoides* ethenogenes strain 195. Appl. Environ. Microbiol. **71:**1664-1667.

30. **Peirson, S. N., J. N. Butler, and R. G. Foster.** 2003. Experimental validation of novel and conventional approaches to quantitative real-time PCR data analysis. Nucl. Acids Res. **31:**e73.

31. **Rahm, B. G., and R. E. Richardson.** 2008. *Dehalococcoides'* Gene Transcripts as Quantitative Bioindicators of PCE, TCE and cDCE Dehalorespiration Rates: Trends and Limitations. Environ. Sci. Technol. **42:**5099-5105.

32. **Rahm, B. G., R. M. Morris, and R. E. Richardson.** 2006. Temporal expression of respiratory genes in an enrichment culture containing *Dehalococcoides ethenogenes.* Appl. Environ. Microbiol. **72:**5486-5491.

33. **Rahm, B. G., and R. E. Richardson.** 2008. Correlation of respiratory gene expression levels and pseudo-steady-state PCE respiration rates in *Dehalococcoides ethenogenes.* Environ. Sci. Technol. **42:**416-421.

34. **Rowe, A. R., B. J. Lazar, R. M. Morris, and R. E. Richardson.** 2008. Characterization of the Community Structure of a Dechlorinating Mixed Culture and Comparisons of Gene Expression in Planktonic and Biofloc-Associated "*Dehalococcoides*" and *Methanospirillum* Species. Appl. Environ. Microbiol. **74:**6709-6719.

35. **Schefe, J., K. Lehmann, I. Buschmann, T. Unger, and H. Funke-Kaiser.** 2006. Quantitative real-time RT-PCR data analysis: current concepts and the "novel gene expression CT difference" formula. Journal of Molecular Medicine. **84:**901-910.

36. **Schink, B.** 1997. Energetics of syntrophic cooperation in methanogenic degradation. Microbiol. Mol. Biol. Rev. **61:**262-&.

37. **Seshadri, R., L. Adrian, D. E. Fouts, J. A. Eisen, A. M. Phillippy, B. A. Methe, N. L. Ward, W. C. Nelson, R. T. Deboy, H. M. Khouri, J. F. Kolonay, R. J. Dodson, S. C. Daugherty, L. M. Brinkac, S. A. Sullivan, R. Madupu, K. T. Nelson, K. H. Kang, M. Impraim, K. Tran, J. M. Robinson, H. A. Forberger, C. M. Fraser, S. H. Zinder, and J. F. Heidelberg.** 2005. Genome sequence of the PCE-dechlorinating bacterium Dehalococcoides ethenogenes. Science. **307:**105-108.

38. **Smatlak, C. R., J. M. Gossett, and S. H. Zinder.** 1996. Comparative kinetics of hydrogen utilization for reductive dechlorination of tetrachloroethene and methanogenesis in an anaerobic enrichment culture. Environmental Science and Technology. **30:**2850-2858.

39. **Stams, A. J. M.** 1994. Metabolic Interactions between Anaerobic-Bacteria in Methanogenic Environments. Anton. Leeuw. Int. J. G. **66:**271-294.

40. **Stams, A. J. M., and X. Z. Dong.** 1995. Role of formate and hydrogen in the degradation of propionate and butyrate by defined suspended cocultures of acetogenic and methanogenic bacteria. Anton. Leeuw. Int. J. G. **68:**281-284.

41. **Stojanowic, A., G. J. Mander, E. C. Duin, and R. Hedderich.** 2003. Physiological role of the F-420-non-reducing hydrogenase (Mvh) from Methanothermobacter marburgensis. Arch. Microbiol. **180:**194-203.

42. **Thauer, R. K., A. Kaster, H. Seedorf, W. Buckel, and R. Hedderich.** 2008. Methanogenic archaea: ecologically relevant differences in energy conservation. Nat. Rev. Micro. **6:**579-591.

43. **Thauer, R. K.** 2011. Hydrogenases and the Global H-2 Cycle. Eur. J. I. C. 919-921.

44. **Werner, J. J., D. Knights, M. L. Garcia, N. B. Scalfone, S. Smith, K. Yarasheski, T. A. Cummings, A. R. Beers, R. Knight, and L. T. Angenent.** 2011. Bacterial community structures are unique and resilient in full-scale bioenergy systems. Proc. Natl. Acad. Sci. U. S. A. **108:**4158-4163.

45. **Werner, J. J., A. C. Ptak, B. G. Rahm, S. Zhang, and R. E. Richardson.** 2009. Absolute quantification of *Dehalococcoides* proteins: enzyme bioindicators of chlorinated ethene dehalorespiration. Environ. Microbiol. **11:**2687-2697.

46. **Wood, G. E., A. K. Haydock, and J. A. Leigh.** 2003. Function and regulation of the formate dehydrogenase genes of the methanogenic Archaeon *Methanococcus maripaludis*. J. Bacteriol. **185:**2548-2554.

47. **Worm, P., A. J. M. Stams, X. Cheng, and C. M. Plugge.** 2011. Growth- and substrate-dependent transcription of formate dehydrogenase and hydrogenase coding genes in

Syntrophobacter fumaroxidans and *Methanospirillum hungatei*. Microbiology-Sgm. **157:**280-289.

48. **Yang, Y. R., and P. L. McCarty.** 1998. Competition for hydrogen within a chlorinated solvent dehalogenating anaerobic mixed culture. Environ. Sci. Technol. **32:**3591-3597.

CHAPTER 5

Summary and Future directions

5.A. Summary of Research Objectives

The main research objectives of this work were to develop and compare biomarkers for respiration for two hydrogen utilizing organisms, *Dehalococcoides ethenogenes* str. 195 (DET) and *Methanospirillum hungatei* (MHU), in a mixed culture fed tetrachloroethene (PCE) and butyrate. With this work we hoped to address two important questions in environmental microbiology and bioremediation**: 1) How do biomarker levels quantitatively relate to the activity of an organism?** and **2) Can we begin to understand how different activities are distributed in complex samples based on biomarkers of multiple organisms ?** Biomarker development in DET and MHU involved the following work flow.

1) Determining appropriate respiration biomarkers from genomic, transcriptomic and proteomic inference, as well as previous biomarker work (studies in DET in (4, 15, 19) and in MHU (28)).

2) Developing assays for absolute quantification of both RNA and protein biomarkers using selected nucleic acid and amino acid sequence information.

3) Assaying and quantifying biomarkers under a variety of experimental conditions that altered respiration rates

4) Assessing empirical relationships between respiration and biomarkers (i.e., mRNA vs. respiration), and between different types of biomarkers (i.e., RNA and Protein)

Selection of appropriate biomarkers for monitoring respiration in DET and MHU centered on metabolic enzymes integral to the processes being assessed. The information gained from

biomarker development work has been the basis for biomarker comparisons between DET and MHU.

5.B. Summary of Biomarker Development

5.B.1. Characterization of the Mixed Culture System

Phylogenetic characterization of the PCE and butyrate-fed mixed culture, Donna II, enriched almost two decades ago by the Gossett lab, demonstrated the presence of up to 18 microbial organizational taxanomic units (OTUs). A recent clone library constructed by the Joint Genome Institute (JGI) as part of a metagenome sequencing project, supported the overall structure of this community (all 18 OTUs were represented). Comparison with other *Dehalococcoides*-containing communities suggests a shared phylogenetic structure of these consortia. Physiologies of the nearest cultured representatives of Donna II OTUs suggest that the majority of OTUs are homologous to fermentative organisms (see Appendix IV, Table A4.1). Although the dominant OTUs involved in butyrate fermentation have not been confirmed in this culture, detection of a known butyrate-to-hydrogen fermentation pathway (homologous to *Syntrophomonas wolfei*) in Donna II metagenomic sequences (JGI), along with the detection of many of this pathway's proteins in shotgun proteomic experiments, highlight *Syntrophomonas* spp. as a candidate hydrogen producer in this system. A 16S rRNA sequence homologous to an acetogenic genera (with single fermentative representative) was also identified (*Treponema* spp.). Though acetogenesis could consume hydrogen, this process is not thermodynamically favorable under butyrate fermentation (the main donor supplied to Donna II) and so is likely not a prominent metabolic sink for hydrogen. As such, *Methanospirillum hungatei* (MHU) and

Dehalococcoides ethenogenes (DET) are the two known hydrogen-consuming organisms present in the Donna II anaerobic mixed culture.

5.B.2. Expanding *Dehalococcoides* Biomarker Work

The DET-centric respiratory biomarkers tested in this work were HupL (a hydrogenase), PceA and TceA (characterized reductive dehalogenases), and DET1545 and DET1559 (RDase homologs). DET biomarker selection, described previously (21) was predominantly based on genomic inference coupled with transcriptomic and proteomic information. Building on previous RNA work, we combined a series of electron donors and electron acceptors over variety of continuous feeding rates (pseudo-steady-state system). In this and other work (4, 10, 21), qPCR and qRT PCR assays were utilized for quantification of DET DNA and RNA biomarkers. Empirical relationships observed from these data support different trends between pseudo-steady state (PSS) mRNA expression level and respiration rate. Of particular promise as dehalorespiration biomarkers are transcript levels of TceA and HupL, both of which demonstrated strong linear correlations on a log-log scale across two orders of magnitude of respiration rates ($R = 0.83$ and 0.85, respectively).

In addition to these empirical trends, RNA exponential decay rates were described for these biomarker targets. Observed mRNA half-lives ranging from 10 to 24 hours highlight the transient nature of these biomarkers, and speak to the temporal sensitivity of these molecules in terms of assessing activity on timescales relevant to field-scale operations. These observations support data previously presented in terms of both decay (11), and PSS relationships (18, 20).

This dissertation work also advanced methods for direct quantification of peptide biomarkers. In DET, protein abundance was quantified in base culture samples (wasted from Donna II 6 L batch reactor) and two continuous-feed experiments (120 and 40 μeeq per L-hour

feeding rates). Further development of quantitative protein assays (described in Werner et al. (25)), utilizing a targeted mass spectrometry-based proteomic approach known as multiple reaction monitoring (MRM), included the incorporation of new peptide targets, as well as assessment of sources of measurement variability. Among base culture samples and continuous feed samples, few statistical differences were observed in peptide abundance per genome, suggesting a consistent, per-cell proteome. This was also observed using relative quantification proteomic approaches (iTRAQ experiments). Though relative protein abundance increased with PCE feeding rate on a per microgram total protein basis, these increases appeared to reflect an increase in total biomass. Normalization to an S-Layer protein (DET1407) in each sample demonstrated no statistically significant increases across respiration rates. Under the growth conditions and extent of protein turnover (maximum of one culture turnover) in our experiments, the monitored proteins maintained consistent levels, with TceA always the most abundant metabolic target at an average of 1100 proteins per genome copy.

Comparison of mRNA expression levels to protein abundances was performed to assess translation of biomarker targets. When time-integrated transcript abundances were compared with the net proteins produced (both over the course of a batch feed) there was a disconnect between total transcript abundance and net production of proteins for different targets. For example, TceA, though expressed at mRNA levels comparable to HupL, is on average five times more abundant at the protein level (1100 ± 450 and 167 ± 120 copies per 16S rDNA for TceA and HupL, respectively). Transcripts, such as DET1545, made up a substantial portion of the integrated mRNA pool but were not highly abundant at the protein level. This cross-target disconnect in mRNA versus protein abundance was supported by data from continuous feed experiments, where the ratio of net TceA proteins produced per hour per mRNA were two to

four times greater than other transcripts (0.4-1.2 vs. 0.03- 0.17 proteins per mRNA-hour for TceA vs. all other proteins, respectively).

Differential protein decay was highlighted as a potential source of variation in protein abundances. However, when degradation of proteins was monitored relative to a control, degradation rates mimicked cell decay; both were within a range of 0.05 to 0.09 per day. This supported the hypothesis that differences in protein abundance were not being driven by differences in protein decay. The overall consistency in per-cell enzyme content over the time course of these experiments allowed for the calculation of per protein kinetic parameters. We used the average per-cell protein content to calculate *in vivo* kinetic parameters from observed respiration rates and average substrate levels. Specifically, we calculated kinetic parameters for the previously characterized DET RDases, TceA and PceA (12, 13). Similarity between our calculated rate constants and those established during biochemical assays with purified proteins suggest that assessing the potential rates of reactions *in situ* based on quantitative measures of enzymes and metabolite data is feasible and has the potential, with further method development, to circumvent some of limitations of RNA approaches. In particular, this approach could account for strain to strain variation in enzyme abundances that are currently not resolvable using nucleic acid biomarkers, thus allowing for better prediction of *in situ* rates.

5.B.3. *Methanospirillum* Biomarkers: Potential Biomarkers for Respiration

Because hydrogen utilization is the avenue by which MHU could potentially compete with *Dehalococcoides*, biomarker development for MHU centered around hydrogen consuming enzymes (hydrogenases). Initial MHU biomarker work started prior to the acquisition of Donna II specific metagenomic and proteomic information, and so our initial task was the identification of appropriate hydrogenase sequence information. Targeting hydrogenase sequences acquired

from the *Methanospirillum hungatei JF-1* genome, degenerate primer sets were constructed from orthologous sequences for the following enzymes: energy-conserving hydrogenase subunit A (Ech A), methyl-viologen reducing hydrogenase subunit D (MvrD, the only subunit annotated in JF-1), coenzyme F_{420}-reducing hydrogenase (FrcA), and formate dehydrogenase (FdhA). With the exception of the Ech hydrogenase (which only yielded DHC sequences), all degenerate primer sets generated sequences with 90 to 95% nucleotide similarity to JF-1 homologs. The logic for identifying formate dehydrogenase sequences was based on evidence that *Methanospirillum* spp. can utilize formate in addition to hydrogen (6), and the expression of these targets might provide insight into this avenue of metabolism. However, the formation of formate as a fermentation product was not observed (<1 μM) in the Donna II culture (analysis of organic acids for n=40 experimental datasets). As such, FrcA and MvrD were the main biomarker targets studied in MHU. Assays for targeting RNA and DNA biomarkers using qPCR and qRT-PCR were developed, in addition to identification of peptide targets with transition ion pairs for MRM quantification.

Studies were performed to measure MHU mRNA biomarkers across different respiration rates. The methane produced in the Donna II culture is the result of two types of methanogenesis (acetoclastic and hydrogenotrophic), so experimental conditions that omitted acetoclastic methanogenesis were employed to robustly relate MHU biomarkers to respiration. As respiration increased so did the level of pseudo-steady state mRNA expression of both FrcA and MvrD. Respiration was strongly linearly correlated with mRNA expression on log-log plots over two orders of magnitude of respiration (1 to 150 μeeq per L-hr), (R = 0.96 for MvrD and FrcA), though far fewer experimental conditions were tested for MHU than DET. However, incorporating PSS mRNA expression data from all experiments where MHU targets were

measured corroborated the relationship with respiration. Comparing PSS mRNA levels with estimates of MHU's contribution to total methanogenesis (based on assumptions supported stoichiometrically and experimentally [using methyl fluoride to inhibit acetoclastic methanogenesis]) the data matched the trend seen in MHU-only respiration experiments.

Interestingly, while the patterns of expression were similar for both MHU biomarkers, the overall expression levels of MvrD and FrcA differed substantially. MvrD was generally two orders of magnitude less abundant than FrcA in qRT-PCR studies, and one order of magnitude lower in terms of absolute fluorescence in microarray work. Although both of these biomarkers are thought to be essential to MHU methanogenesis, the degree of difference in expression between these targets was surprising. Though both of these biomarkers have been observed in shotgun proteomic experiments, absolute quantification of protein abundance (via MRM) was sought to shed light on the implications of the differences in mRNA expression. This quantification demonstrated that MvrD and FrcA are similar in terms of per-genome abundance (60 ± 1and 42 ± 14 proteins per genome copies). Though more work is required to distinguish what factors are controlling differences in protein abundance in this organism, this work further highlights that mRNA expression data may not always be indicative of protein abundance.

5.C. Comparing Dehalococcoides and Methanospirillum Biomarkers

The biomarkers previously described for DET and MHU allow comparison of biomarker trends across differential activities in the mixed culture system. In Donna II, DET and MHU have been shown to compete for hydrogen (3, 22). These microbes were also shown to be in close physical association in that both are commonly observed in mixed culture bioflocs. One of the first avenues of comparison for DET and MHU was to observe differences in biomarker

expression between planktonic or biofloc-associated DET and MHU. In general, heterogeneity in terms of mRNA expression between mixed bioflocs and planktonic cells was not observed in DET. Physical proximity to other organisms (presumably hydrogen producers) does not appear to have a strong affect on transcription in this culture. As MHU were predominantly observed to be associated with bioflocs, it was difficult to distinguish expression differences across growth forms. However, for the mRNA targets chosen for comparison (MHU MvrD, and DET HupL), expression levels varied by almost two orders of magnitude across organisms (4×10^9 vs. 5.5×10^7 copies per mL culture for HupL and MvrD, respectively).

DET and MHU populations both demonstrate increases in mRNA expression in response to batch provision of substrates (specifically PCE and butyrate) and the onset of respiration. Consistent between work in Chapter 2 (performed in 2007) and more recent MHU biomarker work (Chapter 4), DET exhibits up-regulation of HupL transcripts within one hour of provision of substrate. Up-regulation of MHU biomarkers does not occur until later time points; at the earliest, increases in MHU transcript abundance were observed 3 hours post amendment. As described above, PSS mRNA level in both MHU and DET hydrogenases demonstrate strong linear correlations with respiration rate on a log-log scale. These data support the potential utility of these biomarkers for assessing differential activity of organisms. However, one potential problem posed by this work is that the absolute levels of biomarker targets can vary dramatically. In general, MHU FrcA expression was slightly more abundant for equivalent respiration rates than DET HupL. Both of these targets remained near two orders of magnitude greater in abundance than MvrD. The interpretation of absolute abundance of mRNA levels may depend on the particular target being monitored. This highlights the importance of understanding quantitative biomarker trends to associate abundance with activity.

In light of physiologic differences between DET and MHU, and in particular ribosome content, differences in the translation of mRNA biomarkers were expected between organisms. Higher protein production on a per mRNA-basis was expected for MHU given the higher ribosome per transcript ratio. However, more HupL proteins were observed on a per genome basis than either MHU target. Given that in general more FrcA transcripts are observed than HupL, on a per-transcript basis FrcA results in far fewer proteins. There are many potential factors that may explain these observed differences. For example, in FrcA transcripts may be translated slowly or at low levels (few proteins per mRNA), proteins may have a very rapid degradation rate post synthesis, or both (i.e., high turnover). However, this once again highlights that the relationship between mRNA abundance and protein abundances is not consistent. More work is required to further resolve protein-mRNA relationships, specifically in MHU. In addition, the utility of protein measurements for assessing differential activity of these organisms using previously described kinetic characterization has yet to be tested.

5.D. Methodological Future Directions

Though absolute quantification of proteins was achieved by the MRM approach, refining experimental methods and controls could increase the utility of this technique. One of the major experimental limitations highlighted by this work is the variability in protein measurements via MRM. Analysis of different sources of variation demonstrated that protein extraction was the largest source of variability, followed by run-to-run variation among data sets analyzed on different dates, variation in tryptic digestion and variability in injection replicates. To help correct for extraction variation an internal reference standard could be utilized. Cellular internal

standards, such as the S-Layer for DET, could serve to normalize to total population biomass. However, for absolute quantification in complex matrices, additional controls may be needed.

Bovine Serum Albumin (BSA) has been added to a subset of samples prior to extraction, and MRM transition ion pairs specific to BSA have been designed for monitoring abundance which will allow for assessment of protein recovery in future work. As BSA is added as pure protein (not part of a cell), this marker will not account for variability in cell lysis (a likely source of variability in protein extractions). If variation is still significant using BSA as an internal standard, an intracellular marker could be applied. This intracellular marker would need to be quantifiable both intra-cellularly (pre-extraction) and extra-cellularly (post-extraction). A fluorescent protein, such as GFP, could be utilized for this aim. In conjunction with design of MRM targets for absolute quantification, GFP expressing bacteria (normalized to a given fluorescent intensity) could be added pre-extraction which would allow for correction based on extraction efficiency. However, this approach has yet to be attempted and would require further method validation.

Variability in ionization and chromatography are other sources of error that potentially cause variation across analysis runs. In this work, two synthetic peptides were added across samples to allow for correction in ionization efficiency across samples. However, corrections based on reference peptides induced more variation in measurements –as evidenced by the reduced R^2 values of standard curves (data not shown). This is potentially due to errors in addition at the proteomics facility. Though internal standards were not ultimately utilized in this work, other research has supported the utility of this approach and accurate addition of reference peptides should be pursued further (9).

Though it is commonly accepted that two peptides with two corresponding transition ions are acceptable for quantification of a given protein, quantified peptide abundances often differ (9). This is likely due to post-translational modifications that affect quantitative detection of a given peptide by MRM, and thus protein quantification should be assessed from the alternate peptide (9). Given the variability in peptide measurements and the diverse sources of that variability, utilizing multiple peptides (and multiple transition ions for each peptide) for analysis of a given protein, especially in complex samples, would add confidence to quantification. In this work, certain proteins only contained one peptide that was successfully quantified. One of the DET1559 peptides, for example, contains a methionine that was oxidized by the matrix in which standards were constructed. Though this peptide was often detected in samples, it could not be confidently quantified. This and other methionine-containing peptides were omitted from quantification, and should be replaced in future MRM analyses. Other proteins quantified in this work potentially contained peptides that were post-translationally modified. For PceA, the peptide FEGAATETSYER was consistently either half the abundance of the two other PceA peptide targets or below the detection limit. Thus, adding additional peptides for other proteins where translational modification may be affecting analysis (i.e., HupL) will help ensure accurate quantification and should be incorporated.

5.E. Suggested Research Directions

Future experiments with DET and MHU in the Donna II mixed culture could help to resolve some of the questions raised by this work. In MHU, increasing the number and variety of experiments performed will help resolve biomarker trends that have been observed. Currently the range of respiration rates for which we can compare biomarker mRNA expression to MHU

methanogenesis is limited. Extending hydrogen only culturing conditions, either through the use of different materials for hydrogen diffusion studies, or construction of PSS condition that maintain different hydrogen partial pressures will help to resolve biomarker mRNA-respiration trends in MHU. In addition, other MHU biomarkers have been highlighted by mixed culture proteomic work and could be tested at both the protein and mRNA level.

Biomarker relationships for mRNA and respiration have been well characterized in DET. Determining these relationships in other *Dehalococcoides* strains would help support the robustness of these biomarkers and move them towards application in a field setting. As different biomarker targets exhibit very different trends in mRNA expression across experimental conditions (i.e., comparing HupL to DET1545 or PceA), uncovering whether these patterns are specific to a given biomarker target, or to the DET strain, is important to establish. It would also be useful to confirm mRNA-protein relationships in a different *Dehalococcoides* strains.

In addition to extending RNA work, performing experiments that facilitate understanding of 1) MHU protein production and 2) MHU protein decay, will further our understanding of what factors are controlling the observed differences in the mRNA-protein relationships for MvrD and FrcA. Two main factors could lead to observed difference in this relationship: faster translation of MvrD transcripts compared to FrcA transcripts and/or slower MvrD protein decay rates compared to FrcA. Analysis of net protein production under continuous feeding conditions would allow for the analysis of differences in MHU biomarker target net synthesis rates. With respect to protein-specific decay rates, true decay in MHU biomarkers has been difficult to observe in our culturing systems as the populations are never truly starved. Carbon dioxide is not a limiting substrate and low levels of hydrogen are released during endogenous decay. Sub-cultures amended with PCE only (and no electron donor) may help mitigate MHU's utilization of

hydrogen produced by endogenous decay and allow for more accurate estimates of MHU decay in DNA, RNA and protein. Confirming whether production or decay has a stronger influence on protein abundance could help resolve potential reasons for differences in biomarker relationships. Incorporation of additional MHU targets will potentially be useful for resolving these relationships.

As previously stated, once the current limitations of proteomic approaches (and extraction methods, see below) are overcome, these methods will provide a powerful approach to assessing activity of organisms in environmental systems. In particular, in conjunction with enzyme kinetic parameters and substrate concentrations, quantitative protein abundances could make for a direct approach for monitoring realized microbial metabolic capabilities. An important aspect of this work is to confirm that enzymatic kinetics are independent of *Dehalococcoides* strain. Quantifying enzyme abundance in different *Dehalococcoides* strains in conjunction with quantifying substrate levels and rates of conversion, will help confirm *in vivo* kinetic parameters for RDase homologs. In turn, this will help highlight the utility of direct protein measurements as *in situ* biomarkers.

The ultimate goal of biomarker research is the application to field systems where quantification of these targets would be informative of *in situ* microbial activities. As methods designed for laboratory techniques are often not applicable to environmental samples, analysis of biomarker extraction protocols for recovery of RNA and proteins should be performed. Performance of RNA extraction protocols from field systems have been steadily improving (2, 5, 14, 17, 23, 24) and several approaches have applied these techniques to quantification RNA from environmental samples including soil and ground water (11, 14, 17, 23). Several, studies have highlighted successful recovery of proteins from environmental systems (1, 8, 16, 26, 27),

though few of these approaches dealt with proteomic methods that were quantitative. A comparison of proteomic extraction protocols suggests that protocols that involve freeze thaw-lysis recovered larger quantities of bulk protein than protocols that utilize bead beating of chemical lysis (7), though quality of data recovered following different lysis approaches was not reported. In the future, testing these protein and RNA extraction protocols with quantitative analysis, and potentially internal controls will advance applicability of these methods for field quantification of biomarkers.

Assessment of microbial activities in environmental systems has many important applications for the fields of Microbiology and Environmental Engineering. This work has highlighted some of the potential strengths, as well as potential pitfalls of utilizing mRNA and protein biomarkers. It is our hope the continued research and validation of biomarkers tested will lead to an approach that is applicable directly to field systems and will help further our understanding of environmentally-relevant microbes.

REFERENCES

1. **Benndorf, D., G. U. Balcke, H. Harms, and M. von Bergen.** 2007. Functional metaproteome analysis of protein extracts from contaminated soil and groundwater. ISME J. **1:**224-234.

2. **Desai, C., H. Pathak, and D. Madamwar.** 2010. Advances in molecular and "-omics" technologies to gauge microbial communities and bioremediation at xenobiotic/anthropogen contaminated sites. Bioresour. Technol. **101:**1558-1569.

3. **Fennell, D. E., and J. M. Gossett.** 1998. Modeling the production of and competition for hydrogen in a dechlorinating culture. Environ. Sci. Technol. **32:**2450-2460.

4. **Fung, J. M., R. M. Morris, L. Adrian, and S. H. Zinder.** 2007. Expression of reductive dehalogenase genes in *Dehalococcoides ethenogenes* strain 195 growing on tetrachloroethene, trichloroethene, or 2,3-dichlorophenol. Appl. Environ. Microbiol. **73:**4439-4445.

5. **Hirsch, P. R., T. H. Mauchline, and I. M. Clark.** 2010. Culture-independent molecular techniques for soil microbial ecology. Soil Biol. Biochem. **42:**878-887.

6. **Iino, T., K. Mori, and K. Suzuki.** 2010. Methanospirillum lacunae sp. nov., a methane-producing archaeon isolated from a puddly soil, and emended descriptions of the genus *Methanospirillum* and *Methanospirillum hungatei.* Int. J. Syst. Evol. Microbiol. **60:**2563-2566.

7. **Keller, M., and R. Hettich.** 2009. Environmental Proteomics: a Paradigm Shift in Characterizing Microbial Activities at the Molecular Level. Microbiol. Mol. Biol. Rev. **73:**62-70.

8. **Lacerda, C. M. R., and K. F. Reardon.** 2009. Environmental proteomics: applications of proteome profiling in environmental microbiology and biotechnology. Brief. Func. Genom. Proteom. **8:**75-87.

9. **Lange, V., P. Picotti, B. Domon, and R. Aebersold.** 2008. Selected reaction monitoring for quantitative proteomics: a tutorial. Mol. SystBiol. **4:**222.

10. **Lee, P. K. H., D. R. Johnson, V. F. Holmes, J. Z. He, and L. Alvarez-Cohen.** 2006. Reductive dehalogenase gene expression as a biomarker for physiological activity of Dehalococcoides spp. Appl. Environ. Microbiol. **72:**6161-6168.

11. **Lee, P. K. H., T. W. Macbeth, K. S. Sorenson Jr., R. A. Deeb, and L. Alvarez-Cohen.** 2008. Quantifying genes and transcripts to assess the in situ physiology of "*Dehalococcoides*" spp. in a trichloroethene-contaminated groundwater site. Appl. Environ. Microbiol. **74:**2728-2739.

12. **Magnuson, J. K., M. F. Romine, D. R. Burris, and M. T. Kingsley.** 2000. Trichloroethene reductive dehalogenase from *Dehalococcoides ethenogenes*: Sequence of tceA and substrate range characterization. Appl. Environ. Microbiol. **66:**5141-5147.

13. **Magnuson, J. K., R. V. Stern, J. M. Gossett, S. H. Zinder, and D. R. Burris.** 1998. Reductive dechlorination of tetrachloroethene to ethene by two-component enzyme pathway. Appl. Environ. Microbiol. **64:**1270-1275.

14. **McGrath, K. C., S. R. Thomas-Hall, C. T. Cheng, L. Leo, A. Alexa, S. Schmidt, and P. M. Schenk.** 2008. Isolation and analysis of mRNA from environmental microbial communities. J. Microbiol. Methods. **75:**172-176.

15. **Morris, R. M., J. M. Fung, B. G. Rahm, S. Zhang, D. L. Freedman, S. H. Zinder, and R. E. Richardson.** 2007. Comparative proteomics of *Dehalococcoides* spp. reveals strain-specific peptides associated with activity. Appl. Environ. Microbiol. **73:**320-326.

16. **Park, C., J. T. Novak, R. F. Helm, Y. Ahn, and A. Esen.** 2008. Evaluation of the extracellular proteins in full-scale activated sludges. Water Res. **42:**3879-3889.

17. **Poretsky, R. S., N. Bano, A. Buchan, G. LeCleir, J. Kleikemper, M. Pickering, W. M. Pate, M. A. Moran, and J. T. Hollibaugh.** 2005. Analysis of microbial gene transcripts in environmental samples. Appl. Environ. Microbiol. **71:**4121-4126.

18. **Rahm, B. G., and R. E. Richardson.** 2008. *Dehalococcoides*' Gene Transcripts as Quantitative Bioindicators of PCE, TCE and cDCE Dehalorespiration Rates: Trends and Limitations. Environ. Sci. Technol. **42:**5099-5105.

19. **Rahm, B. G., R. M. Morris, and R. E. Richardson.** 2006. Temporal expression of respiratory genes in an enrichment culture containing *Dehalococcoides ethenogenes*. Appl. Environ. Microbiol. **72:**5486-5491.

20. **Rahm, B. G., and R. E. Richardson.** 2008. Correlation of respiratory gene expression levels and pseudo-steady-state PCE respiration rates in *Dehalococcoides ethenogenes.* Environ. Sci. Technol. **42:**416-421.

21. **Rahm, B. G.** 2008. Bioindicators of Reductive Dechlorination in a *Dehalococcoides ethenogenes*-Containing Mixed Culture Transcriptional Trends With Respect to Substrate Type, Substrate Concentration, and Culture Operation. Ph.D. Thesis. Cornell University.

22. **Smatlak, C. R., J. M. Gossett, and S. H. Zinder.** 1996. Comparative kinetics of hydrogen utilization for reductive dechlorination of tetrachloroethene and methanogenesis in an anaerobic enrichment culture. Environ. Sci. Technol. **30:**2850-2858.

23. **Smith, M. C., and D. P. Fries.** 2008. A field-able rna extraction and purification procedure. J. Rapid Meth. Microbiol. **16:**13-21.

24. **Stewart, F. J., E. A. Ottesen, and E. F. DeLong.** 2010. Development and quantitative analyses of a universal rRNA-subtraction protocol for microbial metatranscriptomics. ISME J. **4:**896-907.

25. **Werner, J. J., A. C. Ptak, B. G. Rahm, S. Zhang, and R. E. Richardson.** 2009. Absolute quantification of *Dehalococcoides* proteins: enzyme bioindicators of chlorinated ethene dehalorespiration. Environ. Microbiol. **11:**2687-2697.

26. **Wilkins, M. J., N. C. VerBerkmoes, K. H. Williams, S. J. Callister, P. J. Mouser, H. Elifantz, A. L. N'Guessan, B. C. Thomas, C. D. Nicora, M. B. Shah, P. Abraham, M. S. Lipton, D. R. Lovley, R. L. Hettich, P. E. Long, and J. F. Banfield.** 2009. Proteogenomic Monitoring of Geobacter Physiology during Stimulated Uranium Bioremediation. Appl. Environ. Microbiol. **75:**6591-6599.

27. **Wilmes, P., M. Wexler, and P. L. Bond.** 2008. Metaproteomics Provides Functional Insight into Activated Sludge Wastewater Treatment. Plos One. **3:**e1778.

28. **Worm, P., A. J. M. Stams, X. Cheng, and C. M. Plugge.** 2011. Growth- and substrate-dependent transcription of formate dehydrogenase and hydrogenase coding genes in *Syntrophobacter fumaroxidans* and *Methanospirillum hungatei*. Microbiology-Sgm. **157:**280-289.

APPENDIX I

Supplementary Material for Chapter 2

A1.A. Supplemental Tables

Table A1.1. Taxonomic classification of sequences obtained from the Donna II enrichment culture (this study) and other chloroethene-degrading communities containing *Dehalococcoides.* Taxonomic grouping denoted by spacing and font as indicated in title. (i.e., ***Phylum,*** **Class*,*** ***Order,*** Family, *Genus*)

Taxonomy ***Phylum*** **Class** ***Order*** Family *Genus*	**Number of Sequences**	**Number of Studies (n=12)**	**Presence in Donna II**
Firmicutes	**140**	**12**	+
Clostridia	**135**	**12**	+
Eubacteriaceae	15	8	+
Clostridiaceae	49	12	+
Peptococcaceae	25	7	
Syntrophomonadaceae	17	5	+
Bacteroidetes	**59**	**9**	+
Porphyromonadaceae	34	8	+
Bacteriodaceae	11	5	

Flavobacteraceae	5	5	+
Deltaproteobacteria	**49**	**11**	**+**
Syntrophobacterales	8	6	+
Myxococcales	6	3	+
Desulfuromonales	7	5	
Delulfovibrionaceae	15	5	
Epsilonproteobacteria	**9**	**5**	**+**
Campylobacteraceae	2	2	
Helicobacteraceae	7	4	+
Spirochaetes	**9**	**6**	**+**
Treponema	6	3	
Spirochaetae	3	3	
Nitrospira	**3**	**3**	**+**
Nitrospiraceae	3	3	+
Actinobacteria	**8**	**4**	
Actinobacterales	6	4	
Chloroflexi	**59**	**11**	**+**
Deholococcoides	29	7	+
Methanomicrobia	**21**	**5**	**+**

*identification of *Dehalococcoides sp.* not known at time of publication.

Study Author (# of 16S rDNA sequences)

Bowman et al. 2006 (28)

Dennis et al. 2003 (32)

Doijka et al. 1998 (95)*

Flynn et al. 2000 (10)

Freeborne et al. 2005 (73)

Gu et al. 2004 (14)

Lowe et al. 2002 (112)

MacBeth et al. 2004 (26)

Richardson et al. 2002 (50)

Rossetti et al. 2003 (16)

Duhamel et al. 2006 (20)

Rowe et al. 2008 (23)

Table A1.2. FISH probes used in this study, calculated overall hybridization free energy, and average fluorescence of cells of actively respiring *D. ethenogenes* Strain 195 pure cultures using different probe combinations.

Probe Name	Target Organisms	Probe Sequence 5' - 3'	Target Position E.coli numbering	Overall ΔG[a]	Average Fluorescence Intensity above background per cell	Reference Chapter 2
Dhe137R	DHC[b]	GAAGCTATCCCCCACTTAGA	137-156	-14.30	1360+/-608	this study
Dhe201R	DHC	GACGCAAGCCCCTCACCAAGCACCT	201-225	-23.34	1730+/-628	Nielson (50)
Dhe619R	DHC	GAATGACWCGTCCCGGTTAA	619-638	-7.95	107+/-89.1	this study
Dhe1259degR	DHC	AGCTCCAGTTCRCACTGTTG	1259-1278	-11.75	5700+/-1560	Yang & Zeyer (63)
Arch915	Archaea	GTGCTCCCCCGCCAATTCCT	915-934	ND	ND	Amann et al. (3)
NonEub338	none	ACTCCTACGGGAGGCAGC	338-355	ND	ND	Amann et al. (3)
Combinations						
Dhe201 + Dhe1259deg	DHC	as above	as above	as above	4190+/-674	as above
Dhe137 + 201 + 619 + 1259deg	DHC.	as above	as above	as above	5720+/-919	as above

[a] delta G as presented by model Yilmez & Noguera, 2004 (65)
[b] DHC = *Dehalococcoides* spp.
ND: Not determined

REFERENCES

1. **Bowman, K. S., W. M. Moe, B. A. Rash, H. S. Bae, and F. A. Rainey.** 2006. Bacterial diversity of an acidic Louisiana groundwater contaminated by dense nonaqueous-phase liquid containing chloroethanes and other solvents. FEMS Microbiol. Ecol. **58:**120-133.

2. **Dennis, P. C., B. E. Sleep, R. R. Fulthorpe, and S. N. Liss.** 2003. Phylogenetic analysis of bacterial populations in an anaerobic microbial consortium capable of degrading saturation concentrations of tetrachloroethylene. Can. J. Microbiol. **49:**15-27.

3. **Dojka, M. A., P. Hugenholtz, S. K. Haack, and N. R. Pace.** 1998. Microbial Diversity in a Hydrocarbon- and Chlorinated-Solvent-Contaminated Aquifer Undergoing Intrinsic Bioremediation. Appl. Environ. Microbiol. **64:**3869-3877.

4. **Duhamel, M., K. Mo, and E. A. Edwards.** 2004. Characterization of a highly enriched Dehalococcoides-containing culture that grows on vinyl chloride and trichloroethene. Appl. Environ. Microbiol. **70:**5538-5545.

5. **Flynn, S. J., F. E. Loffler, and J. M. Tiedje.** 2000. Microbial community changes associated with a shift from reductive dechlorination of PCE to reductive dechlorination of cis-DCE and VC. Environ. Sci. Technol. **34:**1056-1061.

6. **Freeborn, R. A., K. A. West, V. K. Bhupathiraju, S. Chauhan, B. G. Rahm, R. E. Richardson, and L. Alvarez-Cohen.** 2005. Phylogenetic analysis of TCE-dechlorinating consortia enriched on a variety of electron donors. Environ. Sci. Technol. **39:**8358-8368.

7. **Gu, A. Z., B. P. Hedlund, J. T. Staley, S. E. Strand, and H. D. Stensel.** 2004. Analysis and comparison of the microbial community structures of two enrichment cultures capable of reductively dechlorinating TCE and cis-DCE. Environ. Microbiol. **6:**45-54.

8. **Lowe, M., E. L. Madsen, K. Schindler, C. Smith, S. Emrich, F. Robb, and R. U. Halden.** 2002. Geochemistry and microbial diversity of a trichloroethene-contaminated Superfund site undergoing intrinsic *in situ* reductive dechlorination. FEMS Microbiol. Ecol. **40:**123-134.

9. **Macbeth, T. W., D. E. Cummings, S. Spring, L. M. Petzke, and K. S. Sorenson.** 2004. Molecular characterization of a dechlorinating community resulting from *in situ* biostimulation in a trichloroethene-contaminated deep, fractured basalt aquifer and comparison to a derivative laboratory culture. Appl. Environ. Microbiol. **70:**7329-7341.

10. **Richardson, R. E., V. K. Bhupathiraju, D. L. Song, T. A. Goulet, and L. Alvarez-Cohen.** 2002. Phylogenetic characterization of microbial communities that reductively dechlorinate TCE based upon a combination of molecular techniques. Environ. Sci. Technol. **36:**2652-2662.

11. **Rossetti, S., L. L. Blackall, M. Majone, P. Hugenholtz, J. J. Plumb, and V. Tandoi.** 2003. Kinetic and phylogenetic characterization of an anaerobic dechlorinating microbial community. Microbiology-Sgm. **149:**459-469.

12. **Rowe, A. R., B. J. Lazar, R. M. Morris, and R. E. Richardson.** 2008. Characterization of the Community Structure of a Dechlorinating Mixed Culture and Comparisons of Gene Expression in Planktonic and Biofloc-Associated "Dehalococcoides" and Methanospirillum Species. Appl. Environ. Microbiol. **74:**6709-6719.

13. **Yilmaz, L. S., and D. R. Noguera.** 2004. Mechanistic approach to the problem of hybridization efficiency in fluorescent *in situ* hybridization. Appl. Environ. Microbiol. **70:**7126-7139.

APPENDIX II

Supplementary Material Chapter 3

A2.A Supplemental materials and methods

Calculation of rates of respiration in terms of electron equivalents (eeq) were based on measured chloroethenes and utilized the following formulas forPCE:

$$r\ PCE = \frac{d\ (2 * TCE + 4 * cDCE + 6 * VC + 6 * Ethene)}{dt}$$

TCE:

$$r\ TCE = \frac{d\ (2 * cDCE + 4 * VC + 4 * Ethene)}{dt}$$

cDCE:

$$r\ PCE = \frac{d\ (2 * VC + 2 * Ethene)}{dt}$$

The eeqs for the conversion of ethene are not counted towards respiration as this step has been shown to be co-metabolic (2).

A2.B. Supplemental Tables

Table A2.1. Experimental parameters for continuous feed and batch fed Donna II sub-cultures used to study protein and RNA biomarkers. Replicate reactors listed for each experiment including information on feeding regime, respiration rates, and growth/hydraulic residence time. Specific data sets were used for Protein quantification and qRT-PCR analysis. All metabolite data utilized from these experiments were utilized for the calculation of kinetic coefficients.

Experiment Title (Continuous Feed)	Replicate Name	Electron Acceptor (EA)	EA feeding rate (μeeq/L-hr)	Electron Donor (ED)	ED:EA (H2 eeq basis)	Length of Experiment (days)	Dehalorespiration rate (μeeq/L-hr)	Hydraulic Residence time (days)	Predicted growth per hour (16S rDNA copies/day)	Protein quantification	Nucleic Acid Quantification(qPCR)
High PCE 3 rates	PCE 40 A	PCE	48	Butyrate	1.88	6.7	48	6.7	5.15E+09	√	√
	PCE 40 B	PCE	42	Butyrate	2.29	6.7	42	6.7		√	√
	PCE 120 A	PCE	126	Butyrate	1.38	1.7	99	1.7	1.67E+10	√	√
	PCE 120 B	PCE	126	Butyrate	1.49	1.7	67	1.7		√	√
PCE High	HiP1	PCE	259	Butyrate	3	1	140	1.25			√
	HiP2	PCE	231	Butyrate	3.4	1	133	1.25	2.89E+10		√
	HiP3	PCE	280	Butyrate	2.8	1	167	1.25			√
PCE High Low	High PSS (HHL3)	PCE^n	183	Butyrate	4.26	7	137.8	10	2.32E+10		√
	HLL1	PCE^n	4.9	Butyrate	1.4	7	4.9	40			√
	Low PSS (HLL2)	PCE	4.7	Butyrate	1.4	7	4.8	40	6.71E+08		√
	HLL3	PCE	5.9	Butyrate	1.1	7	5.9	40			√
PCE 10	P1	PCE^n	63	Butyrate	2.8	7	62	10	2.20E+10		√
	P2	PCE^n	44	Butyrate	4.2	7	43	10			√
TCE 10	T1	TCE^n	85	Butyrate	2.3	7	57	10	9.20E+09		√
	T2	TCE^n	82	Butyrate	2.4	7	54	10			√
PCE Half Butyrate	PHB1	PCE^n	104	Butyrate	0.29	7	85	11.1	3.49E+09		√
	PHB2	PCE^n	45	Butyrate	0.66	7	39	11.1			√
	PHB3	PCE^n	106	Butyrate	0.28	7	97	11.1			√

PCE Lact/But	PLL1	PCE	48	Lactate	0.81	7	45	10	8.07E+09	√
	PLL2	PCE	39	Lactate	0.51	7	37	10		√
PCE Hydrogen	H2PB1	PCE	10	H_2	0.5	1.5	9.7	12	2.75E+09	√
	H2PB2	PCE	8.8	H_2	0.5	1.5	7.3	12		√
PCE 0, YE, FYE	PnfyN1	PCE	3	No donor	-	7	1.3	40	9.98E+08	√
	PnfyN2	PCE	3	No donor	-	7	1.3	40		√
	PnfyF1	PCE	4.5	fermented yeast extract	-	7	4.8	40	2.20E+09	√
	PnfyF2	PCE	5.4	fermented yeast extract	-	7	6.5	40		√
	PnfyY1	PCE	4.9	yeast extract	-	7	4.5	40	2.21E+09	√
	PnfyY2	PCE	4.7	yeast extract	-	7	4.3	40		√
PCE 3 Rates	P3A1	PCE	25	Butyrate	1.5	4	25	10	5.97E+08	√
	P3A2	PCE	22.6	Butyrate	1.7	4	23	10		√
	P3B1	PCE	4.3	Butyrate	1.9	4	4.5	10	1.34E+08	√
	P3B2	PCE	4.8	Butyrate	1.7	4	4.9	10		√
	P3C1	PCE	0.9	Butyrate	2.3	4	1	10	4.30E+07	√
	P3C2	PCE	0.9	Butyrate	2.2	4	0.9	10		√
TCE 3 Rates	T3A1	TCE	51	Butyrate	3.2	4	34	10	1.59E+09	√
	T3A2	TCE	35	Butyrate	2.7	2	23	10		√
	T3B1	TCE	10	Butyrate	3.5	4	6.9	10	3.38E+08	√
	T3B2	TCE	11	Butyrate	3.3	4	7.3	10		√
	T3C1	TCE	2.2	Butyrate	3.9	4	1.5	10	7.27E+07	√
	T3C2	TCE	2.1	Butyrate	4.1	4	1.4	10		√
DCE 3 Rates	D3A1	DCE	30	Butyrate	2.2	1	30	10	1.68E+09	√
	D3A2	DCE	32	Butyrate	2.6	4	32	10		√
	D3B1	DCE	8.8	Butyrate	2	4	8.9	10	5.26E+08	√
	D3B2	DCE	8.2	Butyrate	2.2	4	8.2	10		√
	D3C1	DCE	2.3	Butyrate	1.9	4	2.3	10	1.06E+08	√

	D3C2	DCE	2.3	Butyrate	1.8	4	2.3	10			√
Decay	Time Zero 3	-	-	-	-	0	-	-	-	√	√
	DecayA1	-	-	-	-	7	-	-	-		√
	DecayB1	-	-	-	-	7	-	-	-		√
	DecayB2	-	-	-	-	3	-	-	-		√
iTRAQ Protein PSS	PCE 10 A	PCE	9.096	Butyrate	6	6	9	10	ND	√	
	PCE 30 A	PCE	28.272	Butyrate	3.9	3	28	5	ND	√	
	PCE 60 A	PCE	52.224	Butyrate	3.2	1.5	52	2.5	ND	√	

Experiment Title (Batch Feed)	**Replicate Name**	**Electron Acceptor (EA)**	**Total EA fed (µM)**	**Electron Donor (ED)**	**ED:EA (H2 eeq basis)**	**Length of Experiment**	**Dehalorespiration products (µeeq/L)**	**Hydraulic Residence time**	**Predicted growth per cycle (16S rDNA copies)**	**Protein quantification**	**Nucleic Acid quantification (qPCR)**
Batch	Time Zero 1	PCE	220	Butyrate	2	7	1320	70	1.80E+11	√	√
	TS 2	PCE	220	Butyrate	2	7	1320	70	1.80E+11		√
	TS 3	PCE	220	Butyrate	2	7	1320	70	1.80E+11		√
	Time Zero 2	PCE	220	Butyrate	2	7	1320	70	2.40E+11	√	√

[n] refers to addition of neat substrates rather than substrate dissolved or saturated in media.

Table A2.2. Quantitative PCR primer sets and qPCR annealing temperatures for DET metabolic gene targets.

Organism	Gene ID	Gene Name	Annotation	Primmer Sequence	Annealing temp	Reference
Dehalococcoides ethenogenes st. 195	DET_DE16S	16S rRNA	16S ribosomal RNA	GGAGCGTGTGGTTTAATTCGATGC (sense) GCCCAAGATATAAAGGCCATGCTG (anti-sense)	60ºC	(1)
	DET0079	TceA	reductive dehalogenase	TAATATATGCCGCCACGAATGG (sense) AATCGTATACCAAGGCCCGAGG (anti-sense)	60ºC	(1)
	DET0110	HupL	[Ni/Fe] hydrogenase, group 1, large subunit (EC:1.12.99.6)	TGACGTTATTGCAGTAGCTGAGT (sense) CACACCATAGCTGAGCAGGTT (anti-sense)	55ºC	(1)
	DET0318	PceA	reductive dehalogenase	ATGGTGGATTTAGTAGCAGCGGTC (sense) ATCATCAAGCTCAAGTGCTCCCAC (anti-sense)	60ºC	(1)
	DET1545	DET 1545	reductive dehalogenase, putative	ATACTTACCGGTCAAGGGCGTTAG (sense) ATGGTCACGATGTTCCTGGGTAAG(anti-sense)	60ºC	(1)
	DET1559	DET 1559	reductive dehalogenase, putative	CAATTAAAGTGGGTGGTTGGGCTG (sense) ATCTGTGCCCATATCATCTTGCGG (anti-sense)	60ºC	(1)

Table A2.3. Coefficients of variation (CVs) for each MRM run. "Run" indicates analysis of complete experimental set including samples and standard curves. Abundance of MRM targets were based on standard curves generated during each run. Individual samples were used to measure reproducibility of injection replicates, protein digest replicates, and sample extraction replicates. ND refers to no data collected for this sample for given run. Average CV ± standard deviation (St. Dev.) is based on individual CVs of all detected peptides.

Injections Replicates									
	Sample 1			Sample 2			Sample 3		
	Average CV		St. Dev.	Average CV		St. Dev.	Average CV		St. Dev.
Run 1	12.3	±	12.3	15.3	±	18.9	11.2	±	7.4
Run 2	11.1	±	8.9		ND		33.8	±	18.3
Run 3	15.2	±	13.7	14.6	±	16.5	14.4	±	12.0
Digest Replicates									
	Sample 1			Sample 2			Sample 3		
	Average CV		St. Dev.	Average CV		St. Dev.	Average CV		St. Dev.
Run 1	25.11	±	17.64	21.75	±	16.29	18.31	±	14.98
Run 2	22.86	±	15.56	24.97	±	12.05	14.62	±	8.08
Run 3	32.44	±	14.12	25.11	±	17.64	15.87	±	24.82
Extraction Replicates									
	Sample 1			Sample 2			Sample 3		
	Average CV		St. Dev.	Average CV		St. Dev.	Average CV		St. Dev.
Run 1	44.1	±	20.7		ND			ND	
Run 2	38.2	±	15.1	31.6		19.0	50.2	±	25.2
Run 3	32.4	±	14.1	33.0	±	8.0	33.7	±	17.7
Analysis Run Replicates									
	Sample 1			Sample 2			Sample 3		
	Average CV		St.Dev	Average CV		St.Dev	Average CV		St.Dev
Average of Runs	36.4	±	32	40.6	±	32.9	40.3	±	27.4

Table A2.4. Comparison of peptide per cell data between previous experimental data set (3) and current work. Peptides per 16S rDNA calculated using qPCR on DNA extracted either in parallel from a separate cell pellet using protocol described in methods ([a]) or directly from French press supernatant ([b]). ND represents not determined.

	Peptide	Time Zero Average (Peptide per 16S rDNA)[a]	± St.Dev.	PSS Average (Peptide per 16S rDNA)[a]	± St.Dev	PSS Average (Peptides per 16S rDNA)[b]	± St.Dev.	Werner, 2009 (Peptides per 16S rDNA)[b]
TceA 1	DEWWASENPIR	**7.2E+02**	± 3.3E+02	**1.6E+03**	± 1.8E+02	**4.1E+04**	± 1.1E+04	2.0E+04
TceA 2	VSSIIEPR	**1.5E+03**	± 1.6E+03	**8.8E+02**	± 3.3E+02	**2.0E+04**	± 1.3E+04	ND
TceA 3	WEGTPEENLLIMR							3.1E+04
PceA 1	YQGTPEDNLR	**9.2E+01**	± 4.9E+01	**9.4E+01**	± 5.0E+01	**2.1E+03**	± 1.9E+03	2.2E+04
PceA 2	YFGGEDVGALELDDK	**7.8E+01**	± 3.4E+01	**1.4E+02**	± 2.5E+01	**2.8E+03**	± 1.9E+03	ND
PceA 3	FEGAATETSYER						±	8.5E+02
HupL 1	IEATVDGGEVK	**4.6E+01**	± 1.5E+01	**7.4E+01**	± 2.2E+01	**1.6E+03**	± 4.0E+01	1.2E+03
HupL 2	DNDNPFELVR	**2.9E+02**	± 1.4E+02	**1.8E+02**	± 3.3E+00	**4.4E+03**	± 1.0E+03	ND
HupL 3	IVADEMVK							3.0E+03
S-Layer 1	FDNIGILEWNADK	**6.4E+02**	± 6.8E+02	**1.5E+03**	± 5.3E+02	**4.0E+04**	± 2.2E+04	1.8E+04
S-Layer 2	VNTANSTSEWFPAVFTTVK	**9.0E+02**	± 2.8E+02	**1.7E+03**	± 8.2E+02	**4.2E+04**	± 2.9E+04	1.1E+04
GroEL 1	AQIEETESAFDR	**2.3E+02**	± 7.7E+01	**1.7E+02**	± 7.8E-01	**4.2E+03**	± 1.9E+03	1.4E+04
GroEL 2	GYISAYFVTDPGR	**2.8E+02**	± 1.1E+02	**2.4E+02**	± 2.8E+01	**7.1E+03**	± 3.1E+03	1.3E+04
DET1545 1	LYTLTPEYGAPGR	**2.4E+00**	± 1.4E+00	**2.1E+00**	± 3.8E-01	**3.6E+01**	± 2.0E+01	<350
DET1545 2	TASNYPGYTYR	**9.0E+00**	± 5.5E+00	**6.5E+00**	± 3.7E+00	**1.1E+02**	± 9.0E+01	ND
DET1545 3	LYGVLTDLPLEPTHPIDAGIYR							<180

EF-TU 1	ILDSAEPGDAVGLLR	**5.6E+02**	±	3.8E+02	**2.7E+02**	±	5.6E+01	**6.9E+03**	±	3.4E+03	ND
EF-TU 2	NSFPGDEIPIVR	**6.6E+02**	±	3.1E+02	**1.5E+02**	±	1.0E+01	**3.7E+03**	±	7.7E+02	ND
Rp L7/L12 1	ALEAAGATIEIK	**9.0E+02**	±	1.2E+03	**1.4E+02**	±	1.3E+01	**3.2E+03**	±	6.3E+02	ND
Rp L7/L12 2	TVIELSELVK	**1.8E+02**	±	8.6E+01	**1.2E+02**	±	4.7E+01	**2.0E+03**	±	2.4E+03	ND

Table A2.5. Comparison of percent *Dehalococcoides ethenogenes* cell protein represented by the average protein measured through MRM. Peptides per 16S rDNA calculated using qPCR on DNA extracted either in parallel from a separate cell pellet using protocol described in methods ([a]) or directly from french press supernatant ([b]). Total per cell DET protein based on values from pure culture *Dehalococcoides ethenogenes* (2).

Protein Target	Percentage of Protein based on Werner, 2009[b]	Percentage of Protein based average per 16S rDNA[b]	Percentage of Protein based on average per 16S rDNA[a]
DET0079 (TceA)	9.29	11.25	0.46
DET0318 (PceA)	3.74	0.79	0.04
DET110 (HupL)	0.72	1.06	0.04
DET1545 (putative, Rdase)	ND	0.02	0.001
DET1407 (putative, S-Layer)	9.07	25.53	1.01
DET1428 (GroEL)	4.49	1.96	0.07
DET0990 (rp L7/L12)	ND	0.95	0.05
DET0997 (EF-TU)	ND	11.43	0.01

A2.C. Supplemental Figures

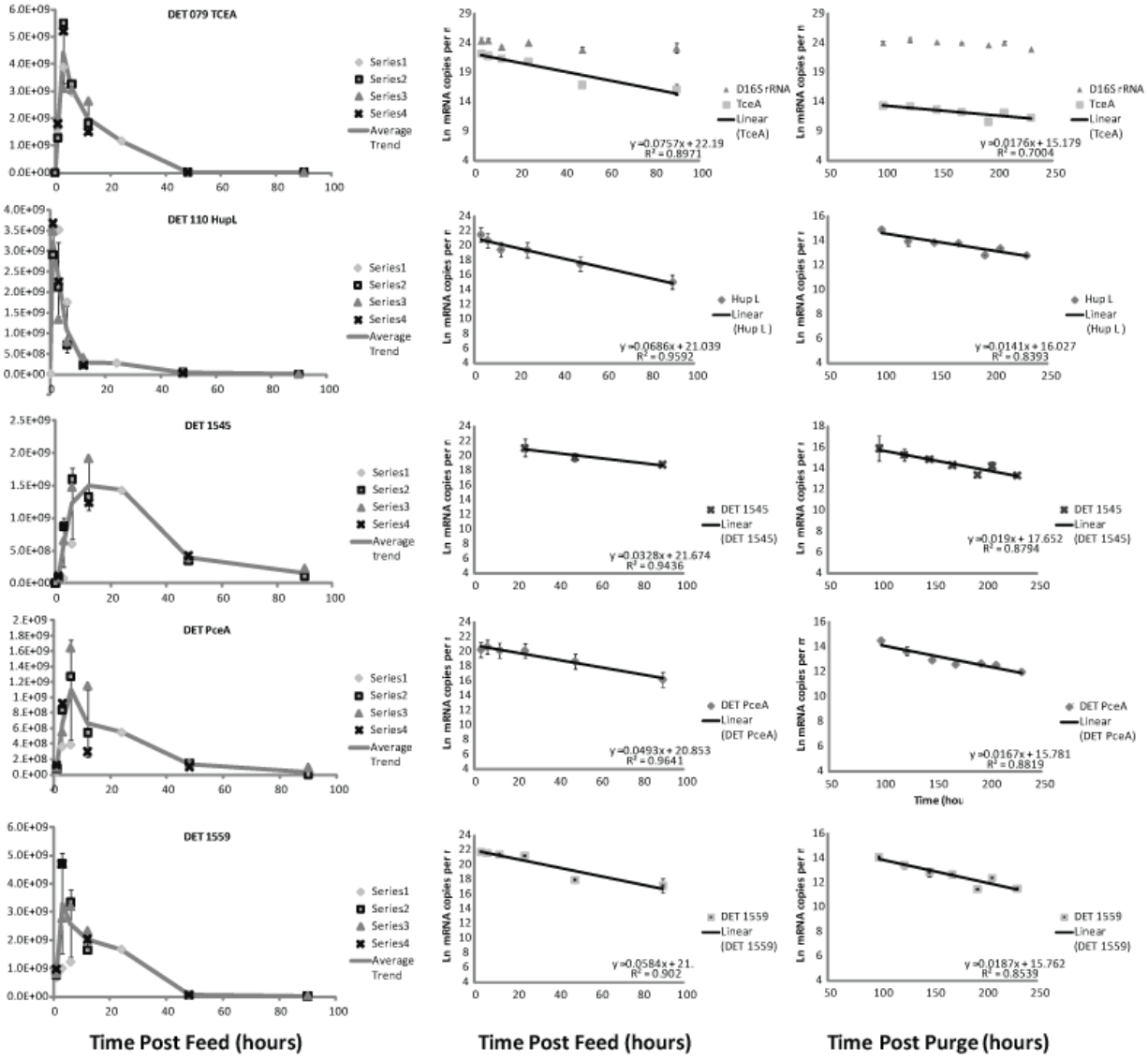

Figure A2.1. Quantification of mRNA biomarkers in batch reactor following addition of PCE (110 µM) and butyrate (440 µM) (left). PCE respiration is complete after six hours. Exponential decay fits (Ln mRNA vs. time) for period following peak expression (active mRNA degradation) (center) and post purging of reactors of chloroethenes (three to four days following PCE and butyrate feed) (right) demonstrating endogenous mRNA degradation. Error bars represent standard deviations based on biological replicates.

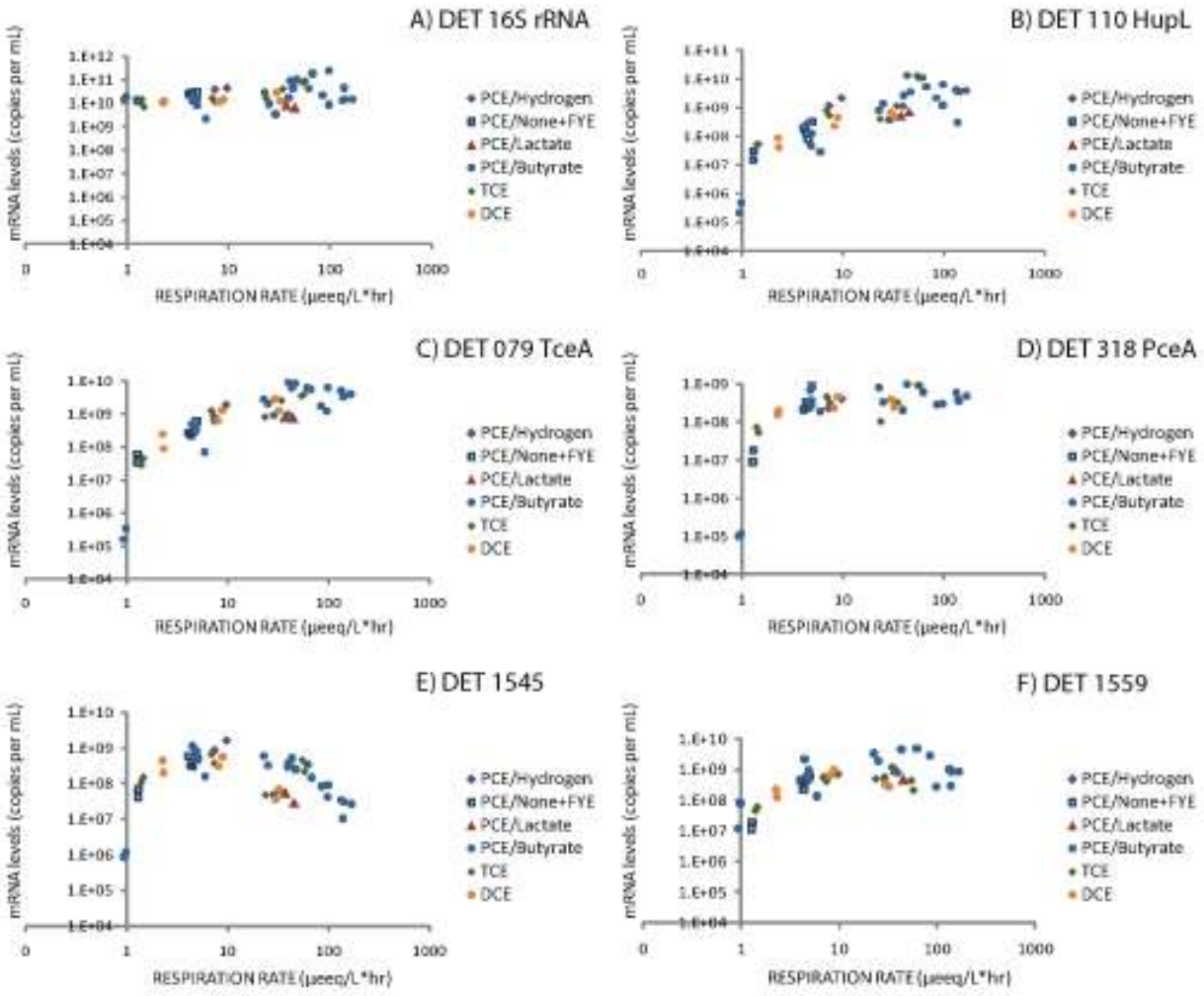

Figure A2.2. Pseudo-steady state RNA expression levels of DET targets with respiration rate: (A) 16S rRNA, (B) HupL, (C) TceA, (D) PceA, (E) DET1545, and (F) DET1559. Replicate reactors plotted as separate points for each experiment. Experimental conditions separated into provision of different electron donors (No Donor(ND)/Fermented Yeast Extract (FYE)/Yeast Extract (YE), Hydrogen only, Butyrate, or Lactate) and/or electron acceptors (PCE, TCE, cDCE). Specific experimental parameters listed in Table A2.1.

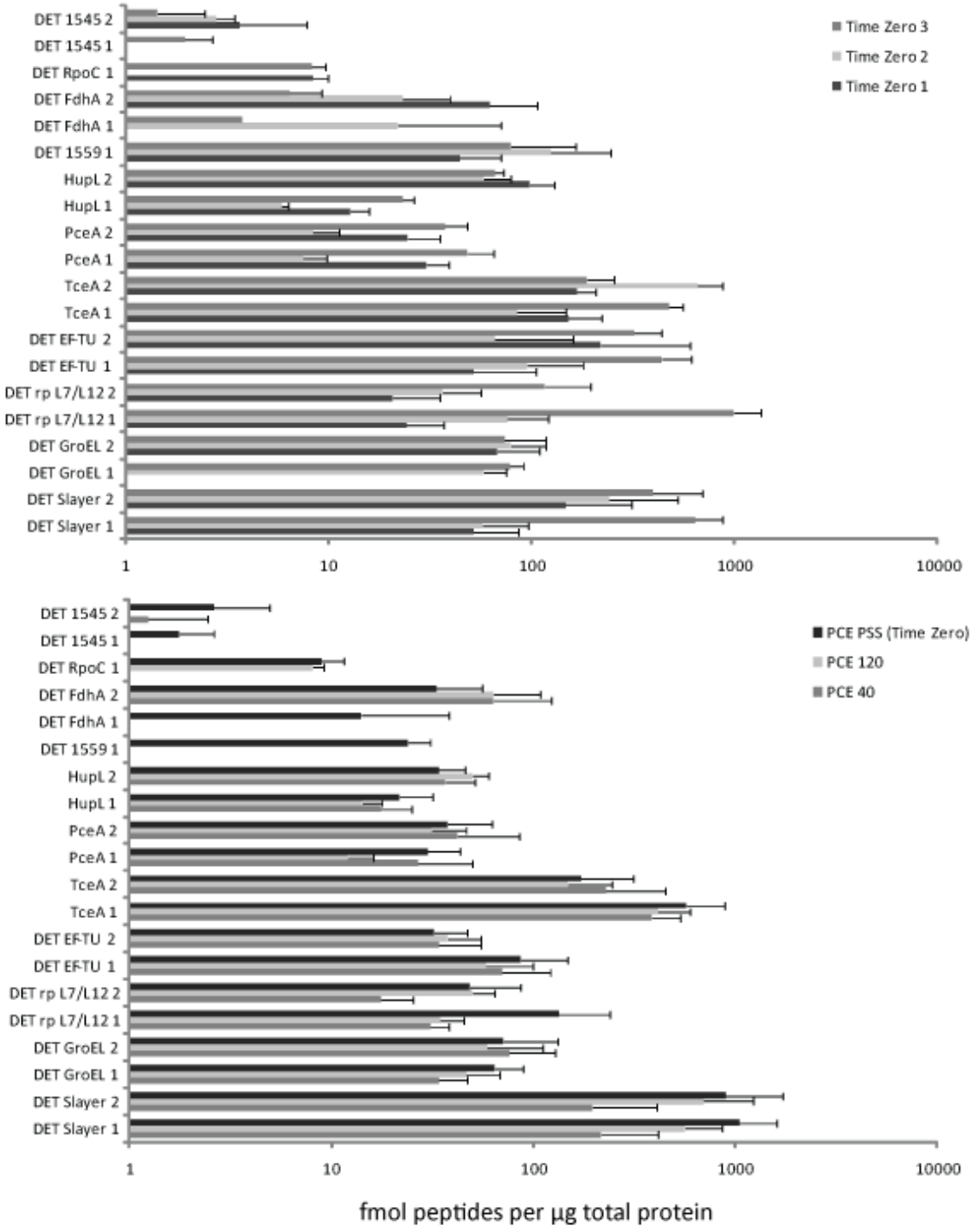

Figure A2.3. Absolute quantification of DET peptides per microgram total protein using multiple reaction monitoring (MRM). Each data point represents the average value generated from at least two transition ions measured in three to four runs for each peptide. Error bars represent standard deviation of value observed during replicate runs.

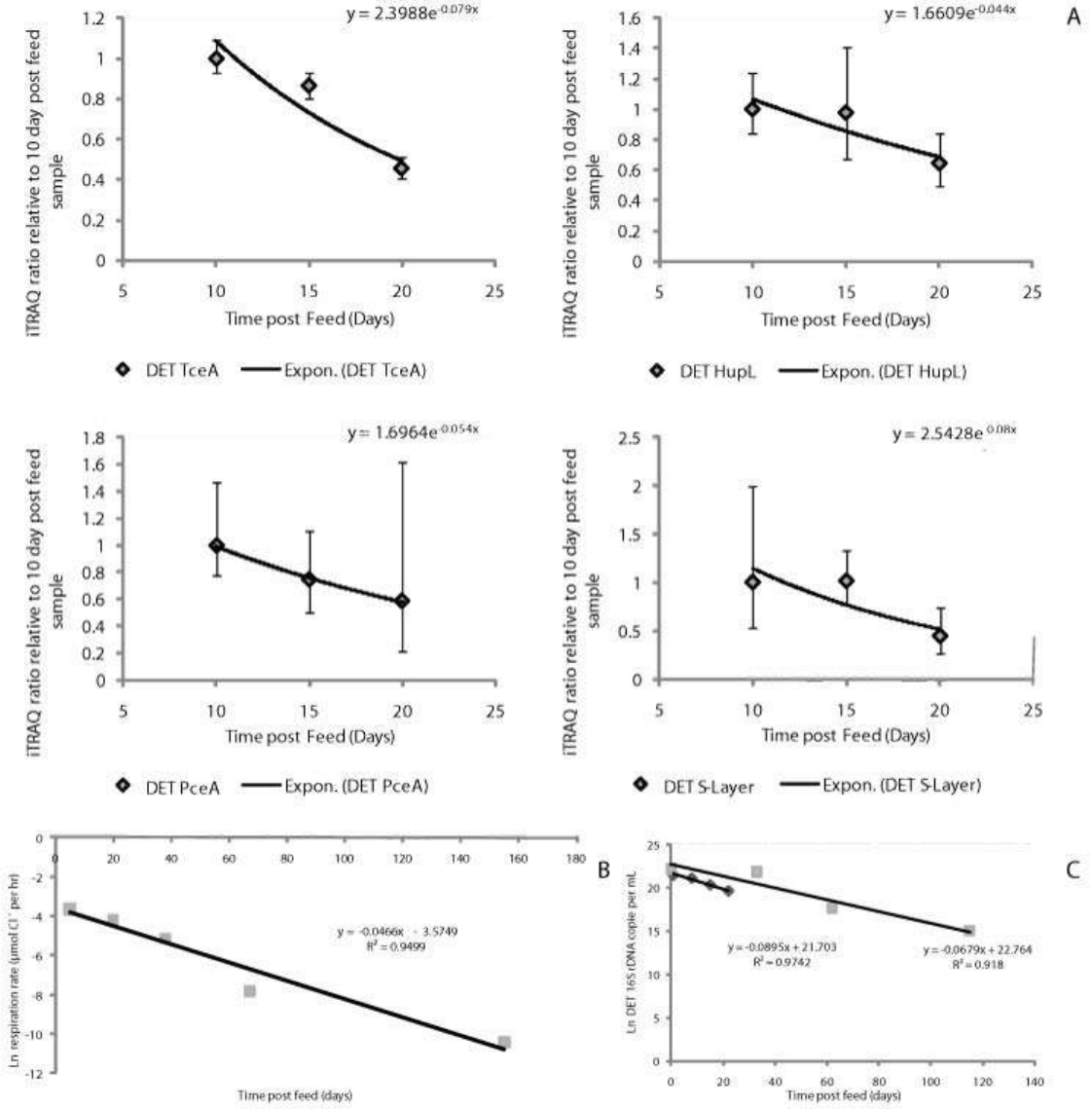

Figure A2.4. Relative quantification of protein degradation in samples purged post PCE and butyrate batch feed and allowed to starve for a period of 5-15 days post purge. Error bars represent 95% confidence intervals of iTRAQ ratios. Decay in reductive dechlorination rate was also modeled through exponential decay and observed to decrease by 4-5 %, while the DNA measurements suggested higher cell decay rates between 7-9%.

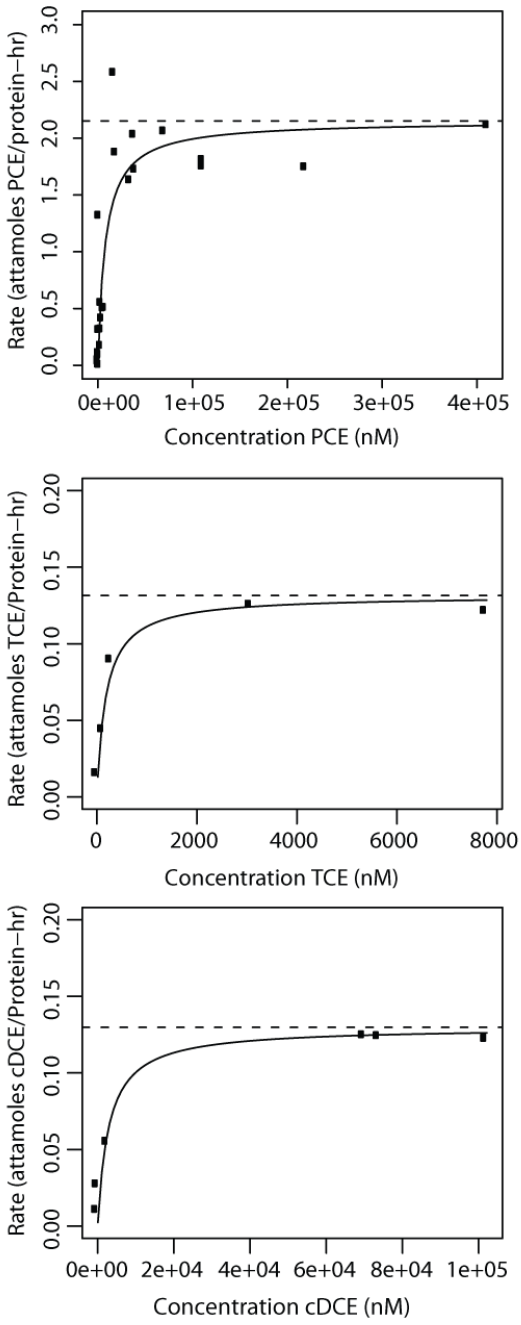

Figure A2.5. Non-linear regression of per-enzyme rates for PceA (A) and TceA (B&C) calculated from substrate levels and reaction rates observed in PSS data sets (See Supplemental Table A2.1). Enzyme protein levels for each study were calculated based on measured 16S rDNA/L and measured enzyme protein per 16S rDNA copies. Rates were also corrected for hydrogen limitation (see methods). Dashed line indicates calculated k_{max} based on non-linear regression (See Table 3.3, Chapter 3 for more information).

REFERENCES

1. **Fung, J. M., R. M. Morris, L. Adrian, and S. H. Zinder.** 2007. Expression of reductive dehalogenase genes in Dehalococcoides ethenogenes strain 195 growing on tetrachloroethene, trichloroethene, or 2,3-dichlorophenol. Appl. Environ. Microbiol. **73:**4439-4445.

2. **Maymo Gatell, X., Y. T. Chien, J. M. Gossett, and S. H. Zinder.** 1997. Isolation of a bacterium that reductively dechlorinates tetrachloroethene to ethene. Science (Washington D C). **276:**1568-1571.

3. **Werner, J. J., A. C. Ptak, B. G. Rahm, S. Zhang, and R. E. Richardson.** 2009. Absolute quantification of *Dehalococcoides* proteins: enzyme bioindicators of chlorinated ethene dehalorespiration. Environ. Microbiol. **11:**2687-2697.

APPENDIX III

Supplementary Material Chapter 4

A3.A. Supplemental materials and Methods

A3.A1 Microarray Design:

The microarray designed for this experiment was an Agilent Technologies© two-color, 15k, 60 mer, 8 plex array. The specific designs of the probes utilized a modified method provided by the eArray© software suite (1). The probe set design employed a base-composition (BC) technique for designing and scoring the best probe for each transcript (1). The probe set includes all *Dehalococcoides ethenogenes* str. 195 predicted open reading frames, non-protein encoding RNA transcripts (rRNAs, tRNAs), community member 16S rDNA and hydrogenase sequences and a luciferase control. A modified temperature matching (Tm) method developed the probe set for array. The Tm method searched for an optimal design with a consistent melting point temperature (80° C) without sacrificing the overall quality of the individual probe (1). However, if a BC score of 3,4, or poor was reported for a transcript, multiple probes around the melting temperature of 80° C were designed. The probe with the best base composition score nearest to the 80° C temperature was selected. The designed probes were searched using the Basic Local Alignment Search Tool (BLAST) (3) against both the National Center for Biotechnology Information (NCBI) nucleotide collection and the assembled mixed community metagenome (metagenome data not reported, currently being compiled by the Joint Genome Institute) to confirm the specificity of all probe sets. The microarray platform is uploaded and freely available at the NCBI Gene Expression Omnibus (GEO) database (http://www.ncbi.nlm.nih.gov/geo/).

A3.A2. RNA-cDNA Handling for Microarray Monitoring

50 mL of liquid culture samples were centrifuged at 14190 *g*. The centrifuged sample was split into 8 individual RNA extractions with each sample following the RNeasy Mini Kit (Qiagen) extraction previously outlined (5). The 8 distinct RNA extractions were recombined on the spin filter before the first RW1 buffer wash. The Superscript I DNAse RNA cleanup, amino-allyl cDNA formation, cDNA cleanup, and cDNA labeling with Cy3 or Cy5 followed the method outlined (7). The quality and quantity of the RNA was determined using the RNA 6000 Nano assay on an Agilent 2100 bioanalyzer (Agilent Technologies). The quantity of resulting cDNA was determined by using the Quant-IT OliGreen ssDNA Assay Kit (Invitrogen). A common control RNA pool sampled from the main Donna II reactor after 3 days of starvation was labeled with Cy3.

A3.A3. Microarray Hybridization and Scanning:

For each experiment, Cy5 labeled cDNA from the mixed community mRNA pool was hybridized against an aliquot of common control of Cy3 labeled cDNA from 3-day starved culture. The hybridization, washing, and scanning of the microarray samples was performed by the Cornell University Microarray Core Facility (http://cores.lifesciences.cornell.edu/brcinfo/) and followed the methods outlined by the manufacturer (1). The general procedure mixed 25 µl (~400 ng) of the labeled cDNA sample with 25 µl 2x Gene Expression (GEx) Hybridization Buffer HI-RPM (1), hybridized the sample to the microarray slide at 65° C for 17 hours, washed with GEx Wash Buffer 1 and 2 (1) at room and elevated (37° C) temperatures, and scanned with an Agilent Technologies Scanner G2505C with a 5 µm resolution.

A3.A4. Statistical Treatment of the Data Set:

Microarray image analysis was conducted using Agilent Feature Extraction 10.5 Image Analysis Software. The Feature Extraction Software was also utilized to perform a within-array

modified LOESS normalization between the Cy5 and Cy3 signals, to calculate a log ratio between the Cy5 and Cy3 channels, and to calculate a modified Student t-test p-value between the Cy5 and Cy3 signal distributions (8). The more detailed treatment the Agilent Feature Extraction employed can be found in the user manual (2). Replicate spots for the same probe (ranging from 6-20 spots/probe) were geometrically averaged. The raw and normalized data is freely available at the NCBI GEO database.

A3.B. Supplementary Tables

Table A3.1. Experimental parameters for continuous feed and batch fed Donna II sub-cultures used to study protein and RNA biomarkers. Replicate reactors listed for each experiment including information on feeding regime, respiration rates and hydraulic residence time. Datasets used for qRT-PCR analysis indicated for MHU only (ᴍ) or both DET and MHU (√). Protein quantification performed on replicates named Time Zero 1-3.

Experiment Title (Continu-ous Feed)	Replicate Name	Chloroethene electron Acceptor (EA)	EA feeding rate (μeeq/ L-hr)	Electron Donor (ED)	ED:EA (H2 equivale nts)	Length of Experiment (days)	Dehalo-respiratio n rate (μeeq/L-hr)	Methano genesis rate (μeeq/L-hr)	Hydraulic Residence time (days)	Nucleic Acid Quantification (qPCR, qRT-PCR)
Decay	Time Zero 3	-	-	-	-	0	-	-	-	√
	DecayA1	-	-	-	-	7	-	1.2	-	√
	DecayB1	-	-	-	-	7	-	1.5	-	√
	DecayB2	-	-	-	-	3	-	2.4	-	√
Butyrate	B1	-	-	Butyrate	-	1	-	281	14	ᴍ
	B2	-	-	Butyrate	-	1	-	277	14	ᴍ
Butyrate MF experiments	BMF1	-	-	Butyrate	-	1	-	74	14	ᴍ
	BMF2	-	-	Butyrate	-	1	-	54	14	ᴍ
	Control1	-	-	-	-	1	-	-	-	ᴍ
	Control2	-	-	-	-	1	-	-	-	ᴍ
Hydrogen	HH1	-	-	H_2	-	1	-	173	16.7	ᴍ
	HH2	-	-	H_2	-	1	-	170	16.7	ᴍ
	HH3	-	-	H_2	-	1	-	157	16.7	ᴍ
	H2A1	-	-	H_2	-	1.5	-	0.5	12	ᴍ
	H2A2	-	-	H_2	-	1.5	-	2.5	12	ᴍ
PCE Hydrogen	H2PB1	PCE	10	H_2	0.5	1.5	9.7	1.1	12	√
	H2PB2	PCE	8.8	H_2	0.5	1.5	7.3	1.4	12	√
PCE Butyrate High	HiP1	PCE	259	Butyrate	3	1	140	124	1.25	√
	HiP2	PCE	231	Butyrate	3.4	1	133	127	1.25	√
	HiP3	PCE	280	Butyrate	2.8	1	167	172	1.25	√

PCE Butyrate High Low	High PSS (HHL3)	PCE	183	Butyrate	4.26	7	137.8	390	10	√
	HLL1	PCE	4.9	Butyrate	1.4	7	4.9	94	40	√
	Low PSS (HLL2)	PCE	4.7	Butyrate	1.4	7	4.8	92	40	√
	HLL3	PCE	5.9	Butyrate	1.1	7	5.9	119	40	√
PCE Half Butyrate	PHB1	PCE	104	Butyrate	0.29	7	85	387	11.1	√
	PHB2	PCE	45	Butyrate	0.66	7	39	466	11.1	√
	PHB3	PCE	106	Butyrate	0.28	7	97	389	11.1	√
PCE Lactate	PLL1	PCE	48	Lactate	0.81	7	45	516	10	√
	PLL2	PCE	39	Lactate	0.51	7	37	358	10	√
PCE No Donor	PnfyN1	PCE	3	-	-	7	1.3	0.6	40	√
	PnfyN2	PCE	3	-	-	7	1.3	0.7	40	√
	PnfyF1	PCE	4.5	fermented yeast extract	-	7	4.8	38.7	40	√
	PnfyF2	PCE	5.4	fermented yeast extract	-	7	6.5	51.8	40	√
	PnfyY1	PCE	4.9	yeast extract	-	7	4.5	42.4	40	√
	PnfyY2	PCE	4.7	yeast extract	-	7	4.3	39.5	40	√
PCE Butyrate	P3A1	PCE	25	Butyrate	1.5	4	25	469	10	√
	P3A2	PCE	22.6	Butyrate	1.7	4	23	394	10	√
	P3B1	PCE	4.3	Butyrate	1.9	4	4.5	331	10	√
	P3B2	PCE	4.8	Butyrate	1.7	4	4.9	357	10	√
	P3C1	PCE	0.9	Butyrate	2.3	4	1	329	10	√
	P3C2	PCE	0.9	Butyrate	2.2	4	0.9	317	10	√
TCE Butyrate	T3A1	TCE	51	Butyrate	3.2	4	34	473	10	√
	T3A2	TCE	35	Butyrate	2.7	2	23	368	10	√
	T3B1	TCE	10	Butyrate	3.5	4	6.9	169	10	√
	T3B2	TCE	11	Butyrate	3.3	4	7.3	205	10	√
	T3C1	TCE	2.2	Butyrate	3.9	4	1.5	73	10	√
	T3C2	TCE	2.1	Butyrate	4.1	4	1.4	92	10	√

DCE Butyrate	D3A1	DCE	30	Butyrate	2.2	1	30	185	10	√
	D3A2	DCE	32	Butyrate	2.6	4	32	101	10	√
	D3B1	DCE	8.9	Butyrate	2	4	8.9	165	10	√
	D3B2	DCE	8.2	Butyrate	2.2	4	8.2	158	10	√
	D3C1	DCE	2.3	Butyrate	1.9	4	2.3	58	10	√
	D3C2	DCE	2.3	Butyrate	1.8	4	2.3	82	10	√
Experiment Title (Batch Feed)	Replicate Name	Electron Acceptor (EA)	Total EA fed (µM)	Electron Donor (ED)	ED:EA (H2 equivalents)	Length of Experiment (day)	Dehalorespiration products (µeeq/L)	Methane Production (µeeq/L)	Hydraulic Residence time	Nucleic Acid quantification
Batch	Time Zero 1	PCE	220	Butyrate	2	7	1320	1920	70	√
	TS 2	PCE	220	Butyrate	2	7	1320	1920	70	√
	TS 3	PCE	220	Butyrate	2	7	1320	1920	70	√
	Time Zero 2	PCE	220	Butyrate	2	7	1320	1920	70	√

Table A3.2. Proteins identified in Donna II mixed culture Shotgun proteomics that are assignable to *Methanospirillum hungatei* sequences in either the publically available genomes or available metagenomic sequences. . Each gene locus is relative to the *Methanospirillum hungatei* JF-1 genome (http://img.jgi.doe.gov) with corresponding sequence description, and enzyme commission number. ProtScores are determined by Protein Pilot 2.0^{TM} software and are indicative of sum of contributing high confidence peptides (see methods for further details). G.O. assignments and E.C. numbers generated with the software Blast2GO (4). * indicates protein best hit was a homolog in the Donna II metagenome.

ProtScore Unused	ProtScore Total	%Protein Cov(95)	Gene Locus (JF-1)	Sequence Description	a.a.seq. length	Gene Ontology	Enzyme Codes
43.47	43.47	26.3	Mhun_2513	hypothetical protein Mhun_2513	847	C:ribosome; F:structural constituent of ribosome; P:translation	EC:3.6.5.3
23.05	25.06	22.2	Mhun_2148	methyl-coenzyme M methylreductase alpha subunit	567	P:methanogenesis; F:metal ion binding; F:coenzyme-B sulfoethylthiotransferase activity	EC:2.8.4.1
22.25	22.25	58.1	Mhun_2147*	methyl-coenzyme M methylreductase gamma subunit	222	F:structural constituent of ribosome; C:small ribosomal subunit; P:translation; F:coenzyme-B sulfoethylthiotransferase activity; F:rRNA binding; P:methanogenesis	EC:3.6.5.3; EC:2.8.4.1
18.12	18.12	15.4	Mhun_0996	tpr repeat-containing protein	634	F:binding	
16.76	16.83	10.4	Mhun_2023	formate dehydrogenase alpha subunit	685	F:formate dehydrogenase activity; C:formate dehydrogenase complex; P:oxidation reduction; F:electron carrier activity; P:transcription; P:formate metabolic process; F:molybdenum ion binding	EC:1.2.1.2
15.99	15.99	16.2	Mhun_2257*	Coenzyme F420-dependent N(5),N(10)-methenyltetrahydromethanopterin	328	F:coenzyme F420-dependent N5,N10-methenyltetrahydromethanopterin reductase activity; P:oxidation reduction	EC:1.5.99.11

14.98	14.98	28.2	Mhun_2255	methylenetetrahydromethanopterin dehydrogenase	280	C:cytoplasm; F:tetrahydromethanopterin S-methyltransferase activity; C:vesicle membrane; P:oxidation reduction; P:one-carbon metabolic process; F:methylenetetrahydromethanopterin dehydrogenase activity; F:ferredoxin hydrogenase activity; C:integral to membrane; P:methanogenesis; P:sodium ion transport	EC:2.1.1.86; EC:1.5.99.9; EC:1.12.7.2
14.4	15.7	17.7	Mhun_2144*	methyl-coenzyme M methylreductase beta subunit	435	P:cysteine metabolic process; F:pyridoxal phosphate binding; F:cysteine desulfurase activity; F:transaminase activity; F:coenzyme-B sulfoethylthiotransferase activity; P:methanogenesis	EC:2.8.1.7; EC:2.6.1.0; EC:2.8.4.1
10.6	10.6	12.6	Mhun_2332*	coenzyme f420-reducing hydrogenase alpha subunit	358	F:FAD binding; C:membrane; P:oxidation reduction; F:iron-sulfur cluster binding; F:ferredoxin hydrogenase activity; F:nickel ion binding; F:coenzyme F420 hydrogenase activity	EC:1.12.7.2; EC:1.12.98.1
10.58	10.83	10.8	Mhun_0128	chaperone protein	610	P:auxin biosynthetic process; P:protein folding; P:response to stress; P:oxidation reduction; F:ATP binding; F:unfolded protein binding; F:2-alkenal reductase activity	EC:1.3.1.74
10.1	10.1	15.6	Mhun_2175*	tetrahydromethanopterin s-methyltransferase subunit h	340	F:tetrahydromethanopterin S-methyltransferase activity; P:one-carbon metabolic process	EC:2.1.1.86
9.94	16.56	9.2	Mhun_2021	formate dehydrogenase alpha subunit	686	F:formate dehydrogenase activity; C:formate dehydrogenase complex; P:oxidation reduction; F:electron carrier activity; P:transcription; P:formate metabolic process; F:molybdenum ion binding	EC:1.2.1.2

8.64	8.64	10.7	Mhun_1272	carbon monoxide dehydrogenase catalytic subunit	628	P:oxidation reduction; C:cytoplasm; F:carbon-monoxide dehydrogenase (acceptor) activity; P:generation of precursor metabolites and energy; F:4 iron, 4 sulfur cluster binding; F:nickel ion binding	EC:1.2.99.2
6.39	6.39	3.6	Mhun_1838	4fe-4s ferredoxin iron-sulfur binding domain protein	671	F:iron-sulfur cluster binding; F:electron carrier activity; F:CoB--CoM heterodisulfide reductase activity; F:FAD binding; P:methanogenesis; P:tRNA processing	EC:1.2.7.1
6.27	6.7	7.6	Mhun_2549	thermosome	552	P:protein folding; F:unfolded protein binding; F:ATP binding; P:auxin biosynthetic process	
6.18	6.18	10.4	Mhun_0521	abc transporter tungsten-binding protein	307	F:transporter activity; C:integral to membrane; C:membrane; P:molybdate ion transport; F:hydrolase activity; P:transport; F:molybdate transmembrane-transporting ATPase activity; F:molybdate ion transmembrane transporter activity; C:plasma membrane	EC:2.7.4.3
5.88	9.27	8.3	Mhun_2332	coenzyme F420 hydrogenase subunit alpha	469	F:FAD binding; P:oxidation reduction; F:iron-sulfur cluster binding; F:ferredoxin hydrogenase activity; C:plasma membrane; F:nickel ion binding; F:coenzyme F420 hydrogenase activity	EC:1.6.5.3
5.83	5.83	11.1	Mhun_1835	4Fe-4S ferredoxin iron-sulfur binding domain protein	388	F:4 iron, 4 sulfur cluster binding; P:oxidation reduction; F:metal ion binding; F:electron carrier activity; F:formylmethanofuran dehydrogenase activity	EC:1.6.5.3
5.77	5.77	10.8	Mhun_2329	coenzyme F420-reducing hydrogenase subunit beta	288	F:acetate kinase activity; F:ATP binding; C:cytoplasm; P:organic acid metabolic process; P:phosphorylation	

5.16	5.16	8.8	Mhun_1837	heterodisulfide reductase subunit b	296	P:methanogenesis; P:oxidation reduction; F:CoB--CoM heterodisulfide reductase activity; P:cofactor metabolic process	
4.47	4.47	8.3	Mhun_1990	formylmethanofuran dehydrogenase subunit c	266	F:electron carrier activity; F:iron-sulfur cluster binding	EC:4.2.1.33
4.41	4.41	23.8	Mhun_0131	ferritin dps family protein	164	F:ferric iron binding; P:oxidation reduction; F:oxidoreductase activity; P:cellular iron ion homeostasis	EC:6.1.1.20
4.25	4.25	11.4		flagellin	175	F:electron carrier activity; F:iron-sulfur cluster binding	EC:2.7.6.1
4.04	4.04	11.6	Mhun_1554*	beta-lactamase domain protein	216	F:metal ion binding; F:signal transducer activity; P:oxidation reduction; F:hydrolase activity; F:oxidoreductase activity; P:signal transduction; F:electron carrier activity; F:FMN binding	
4	4	8.1	Mhun_2330	coenzyme F420-reducing hydrogenase gamma subunit	262	F:quinone binding; F:electron carrier activity; F:NADH dehydrogenase (ubiquinone) activity; P:transport; F:nickel ion binding; F:4 iron, 4 sulfur cluster binding; F:coenzyme F420 hydrogenase activity; F:FAD binding; P:electron transport chain	
3.96	3.96	8.3	Mhun_0085	aliphatic sulfonate binding protein precursor	350	F:signal transducer activity; P:signal transduction; P:regulation of transcription, DNA-dependent	
3.94	3.95	3.7	Mhun_0148	pas pac sensor protein	299	F:formylmethanofuran dehydrogenase activity; P:oxidation reduction; P:methanogenesis	
3.92	3.92	7.9	Mhun_1988	formylmethanofuran dehydrogenase subunit b	443	C:cytoplasm; P:auxin biosynthetic process; F:peptidase activity; P:protein metabolic process; F:ATPase activity; F:DNA binding; F:protein binding; F:nuclease activity; F:ATP binding; P:nucleotide-excision repair	

3.43	3.48	2.6	Mhun_1813*	formate dehydrogenase alpha subunit	688	C:intracellular; F:formate dehydrogenase activity; F:electron carrier activity; C:formate dehydrogenase complex; F:molybdenum ion binding; P:oxidation reduction; P:formate metabolic process; F:transcription factor activity; P:regulation of transcription, DNA-dependent	EC:2.7.7.4; EC:3.6.5.1; EC:3.6.5.2; EC:3.6.5.3; EC:3.6.5.4
0	3.47	2.6	Mhun_1813	formate dehydrogenase alpha subunit	688	C:intracellular; F:formate dehydrogenase activity; F:electron carrier activity; C:formate dehydrogenase complex; F:molybdenum ion binding; P:oxidation reduction; P:formate metabolic process; F:transcription factor activity; P:regulation of transcription, DNA-dependent	EC:2.4.2.19
0.03	1.73	1.3	Mhun_1833	formate dehydrogenase alpha subunit	687	F:formate dehydrogenase activity; C:formate dehydrogenase complex; P:oxidation reduction; F:electron carrier activity; P:transcription; P:formate metabolic process; F:molybdenum ion binding	
0.03	2.49	1.3	Mhun_3238	formate dehydrogenase alpha subunit	687	F:formate dehydrogenase activity; C:formate dehydrogenase complex; P:oxidation reduction; F:electron carrier activity; P:transcription; P:formate metabolic process; F:molybdenum ion binding	EC:2.7.7.4; EC:3.6.5.1; EC:3.6.5.2; EC:3.6.5.3; EC:3.6.5.4
3.27	3.28	2.1	Mhun_2022	formate dehydrogenase beta subunit	383	F:pseudouridine synthase activity; F:iron-sulfur cluster binding; F:formate dehydrogenase activity; F:electron carrier activity; F:RNA binding; P:oxidation reduction; F:pseudouridylate synthase activity;	

						P:tRNA pseudouridine synthesis	
3.26	3.27	1	Mhun_1406	methyl-accepting chemotaxis sensory transducer	1091	F:translation elongation factor activity; P:two-component signal transduction system (phosphorelay); F:sulfate adenylyltransferase (ATP) activity; P:peptidyl-histidine phosphorylation; P:regulation of transcription, DNA-dependent; P:translational elongation; F:ATP binding; P:signal transduction; F:GTPase activity; F:two-component sensor activity; C:cytoplasm; C:membrane; F:GTP binding	
3.26	3.27	2.4	Mhun_1592	translation elongation factor ef-subunit alpha	425	F:translation elongation factor activity; P:two-component signal transduction system (phosphorelay); F:sulfate adenylyltransferase (ATP) activity; P:peptidyl-histidine phosphorylation; P:regulation of transcription, DNA-dependent; P:translational elongation; F:ATP binding; P:signal transduction; F:GTPase activity; F:two-component sensor activity; C:cytoplasm; C:membrane; F:GTP binding	EC:1.4.1.2
2.77	2.91	4.43	Mhun_2174	tetrahydromethanopterin s-methyltransferase subunit a	248	P:mRNA catabolic process; F:3'-5'-exoribonuclease activity; F:RNA binding; F:polyribonucleotide nucleotidyltransferase activity; C:mitochondrion; P:RNA processing	
2.57	29.47	17.1	Mhun_2263	hypothetical protein Mhun_2263	862	P:oxidation reduction; F:oxidoreductase activity; F:electron carrier activity; F:transition metal ion binding	EC:6.3.4.3
0.02	1.54	4.7	Mhun_1311	rubrerythrin	190	P:oxidation reduction; F:oxidoreductase activity; F:electron	

						carrier activity; F:transition metal ion binding	
2.39	2.39	5.6	Mhun_0613	peptidase m50	377	F:oxidoreductase activity; F:iron-sulfur cluster binding; P:oxidation reduction	
2.36	2.36	2.7	Mhun_2840	surface layer protein	963	C:light-harvesting complex; P:oxidation reduction; F:L-erythro-3,5-diaminohexanoate dehydrogenase activity; P:protein-chromophore linkage; C:chloroplast; F:zinc ion binding	
2.21	2.21	2.1	Mhun_2610	phosphoenolpyruvate synthase	762	F:structural constituent of ribosome; C:small ribosomal subunit; P:translation	
2.18	2.18	4.3	Mhun_0248	periplasmic binding protein	375	F:iron-sulfur cluster binding; F:formate dehydrogenase activity; F:electron carrier activity; P:pseudouridine synthesis; P:oxidation reduction; F:lyase activity	
2.17	2.53	2.2	Mhun_1814	formate dehydrogenase beta subunit	414	F:iron-sulfur cluster binding; F:formate dehydrogenase activity; F:electron carrier activity; P:pseudouridine synthesis; P:oxidation reduction; F:lyase activity	
2.16	2.16	10.4	Mhun_2063	protein	212	C:cytoplasm; P:auxin biosynthetic process; F:P-P-bond-hydrolysis-driven protein transmembrane transporter activity; F:metal ion binding; C:plasma membrane; P:protein import; P:intracellular protein transmembrane transport; F:ATP binding; P:protein targeting; P:protein secretion	EC:3.6.3.6; EC:3.6.3.14; EC:5.99.1.3
2.15	2.15	1.8	Mhun_1989	formylmethanofuran dehydrogenase subunit a	571	F:catalytic activity	
2.1	2.1	2.9	Mhun_1181	v-type atp synthase subunit c	351	P:biological_process; C:cellular_component	

0	1.9	12.9	Mhun_1839	methyl-viologen-reducing hydrogenase delta subunit	62	F:receptor activity	EC:5.4.99.2
2.1	2.1	5.7	Mhun_1842	methyl-viologen-reducing hydrogenase delta subunit	140	P:methanogenesis; F:metal ion binding; P:electron transport chain; F:oxidoreductase activity; F:2 iron, 2 sulfur cluster binding; P:transport	EC:5.4.99.2
2.09	2.09	6.4	Mhun_0672	branched-chain amino acid aminotransferase	297	P:branched chain family amino acid biosynthetic process; F:branched-chain-amino-acid transaminase activity; F:D-alanine:2-oxoglutarate aminotransferase activity; F:lyase activity	
2.08	3.79	4.4	Mhun_0023	serine hydroxymethyltransferase	436	P:auxin biosynthetic process; P:protein folding; F:ATPase activity; P:response to stress; P:oxidation reduction; F:ATP binding; F:unfolded protein binding; F:2-alkenal reductase activity	EC:3.6.5.3
2.08	2.08	7.9	Mhun_3015	30S ribosomal protein s19e	140	C:ribosome; F:structural constituent of ribosome; F:RNA binding; P:ribosome biogenesis; P:translation	
2.08	2.08	7.4	Mhun_1601	50S ribosomal protein l7ae	122	F:structural constituent of ribosome; C:cytosolic small ribosomal subunit; P:translation	
2.02	15.95	41.7	Mhun_2147	methyl-coenzyme M methylreductase gamma subunit	252	F:iron-sulfur cluster binding; F:electron carrier activity; F:NADH dehydrogenase (ubiquinone) activity; F:iron ion binding; F:ferredoxin hydrogenase activity; P:ATP synthesis coupled electron transport; C:membrane	
2.01	2.6	2.7	Mhun_1981	formylmethanofuran dehydrogenase subunit c	332	C:cytoplasm; F:sulfurtransferase activity; F:protein binding; P:tRNA processing	
2	2	6.8	Mhun_2237	50S ribosomal protein l6p	176	P:glutamine metabolic process; P:cobalamin biosynthetic process; F:cobalamin-transporting ATPase	EC:2.7.2.1

						activity; F:amidase activity
2	2	5.3	Mhun_2229	adenylate kinase	190	F:transporter activity; P:transport

A3.C. Supplemental Figures

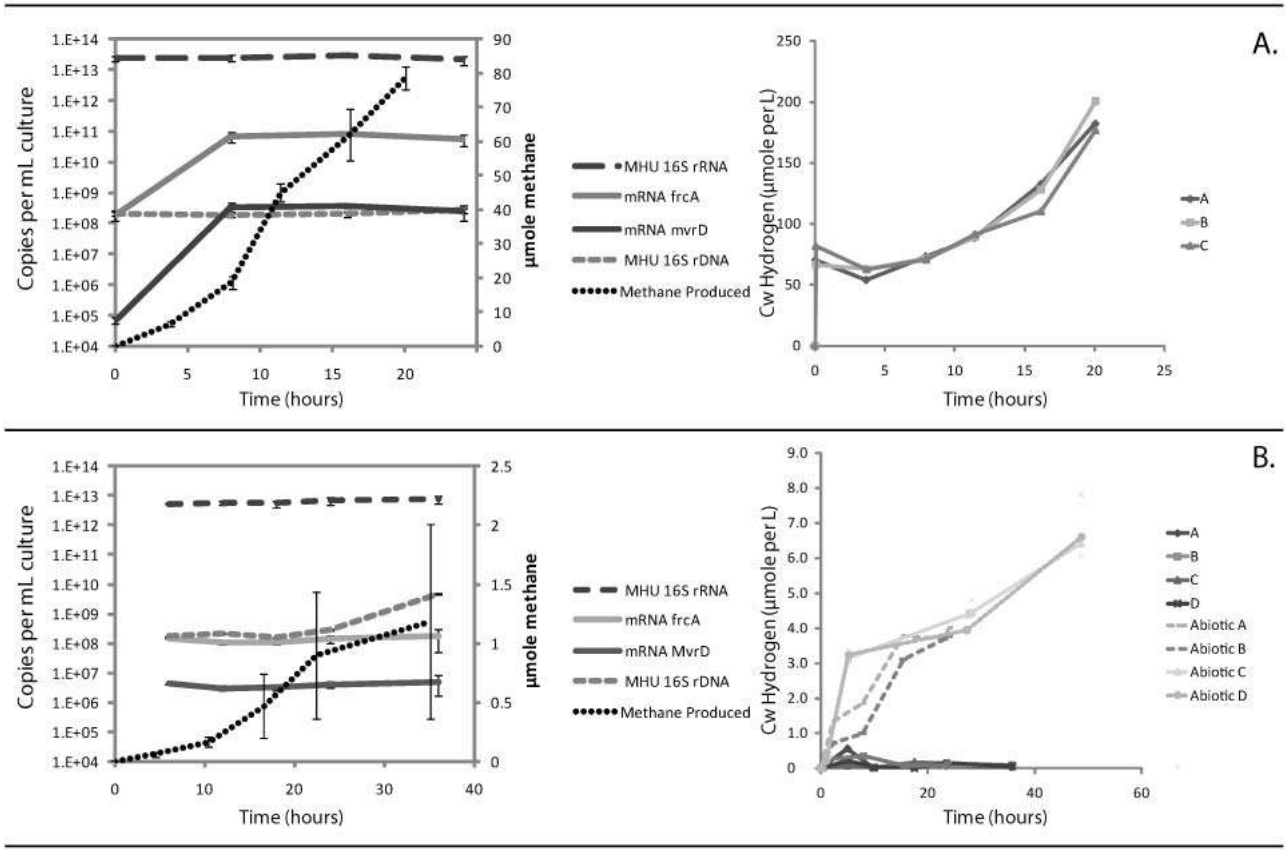

Figure A3.1. Pseudo-steady state expression of MHU biomarkers under two hydrogen feeding conditions. Hydrogen added in batch every four hours to maintain a hydrogen concentration over ten times the reported half velocity constant K_S (A) (6). One hundred µM hydrogen was added at six hour intervals for this experiment. Hydrogen diffusion across a LDPE tubing was used to administer a slow hydrogen feeding rate (B). Abiotic controls were used to calculate rates of hydrogen addition. Error bars represent standard errors of biological replicates. C_w stands for hydrogen concentration in water at equilibrium with headspace readings.

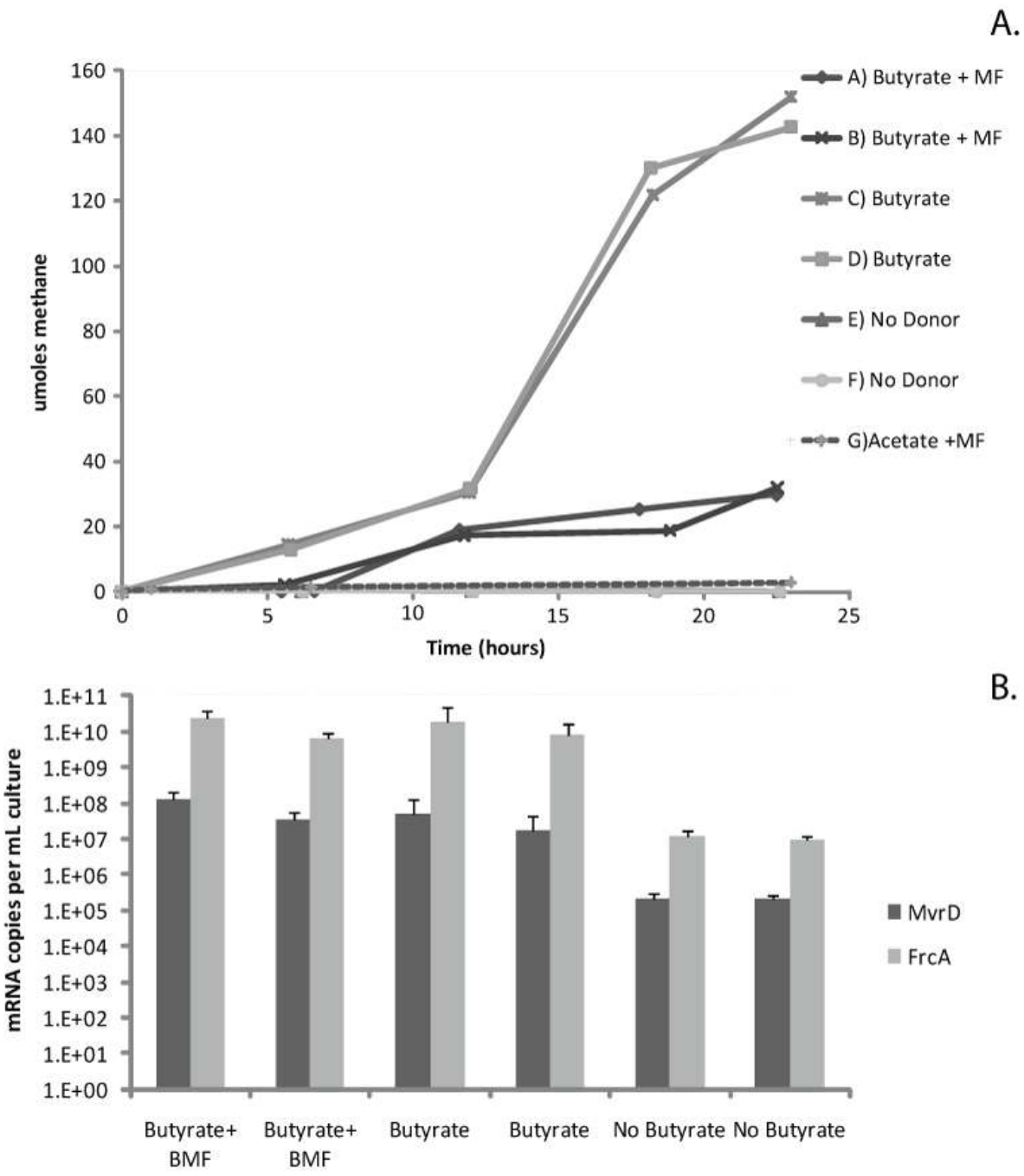

Figure A3.2. Inhibition of acetoclastic methanogenesis through inhibition with methyl fluoride (MF). Methane production under butyrate, butryrate + MF, no-donor added and acetate +MF controls (A). Average mRNA expression from hour six to 24, of MHU biomarker targets (B). Error bars indicate standard errors of biological replicates.

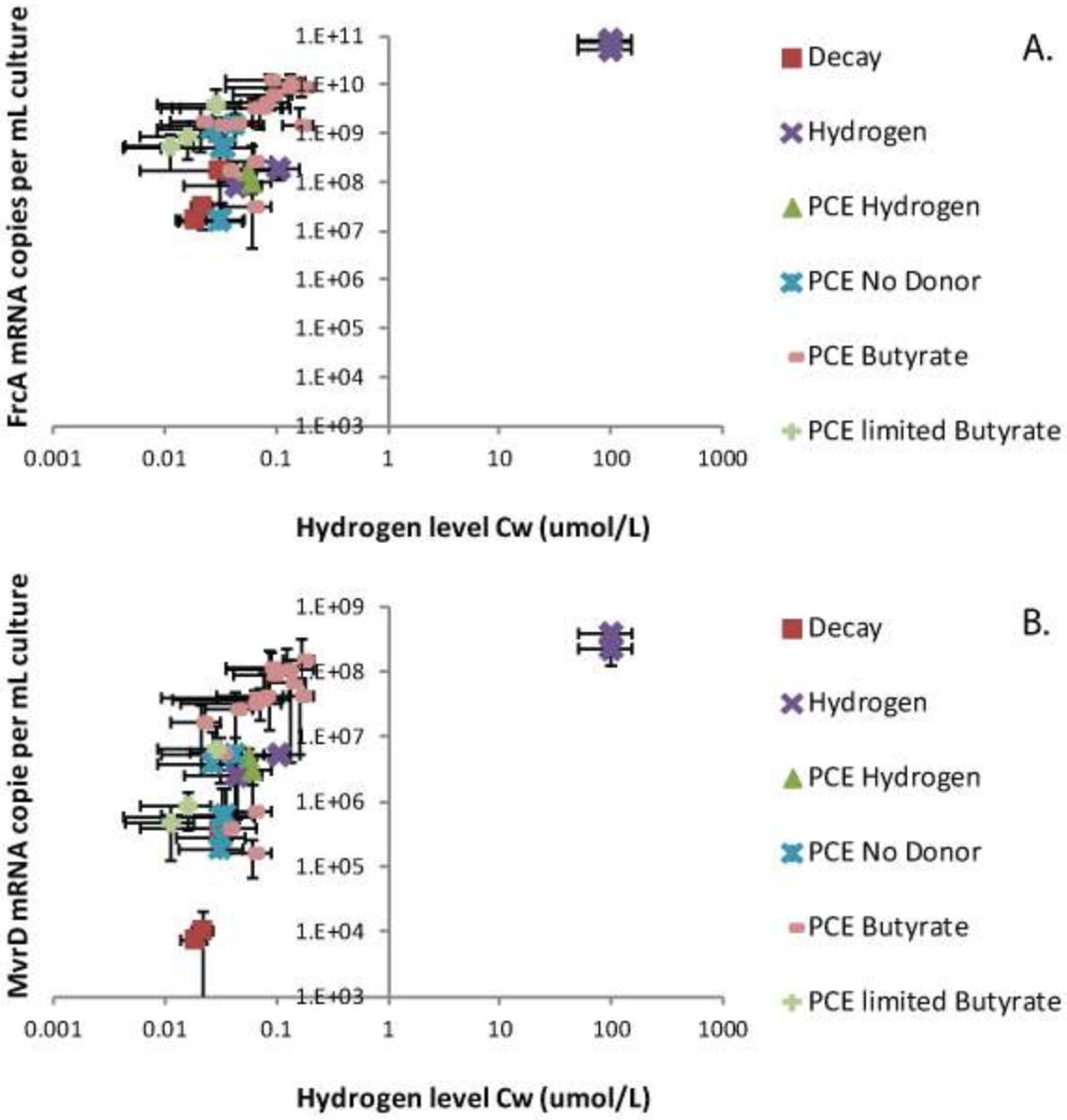

Figure A3.3. Pseudo-steady state expression levels for subset of experiments listed in Table A3.1, compared with average dissolved hydrogen level (C_W) for FrcA (A) and MvrD (B). Experiments are grouped based on the type of electron donor and presence of PCE. X-error bars represent the standard deviation of average hydrogen levels over the course of the experiment. Y-error bars represent the standard deviation of PSS mRNA expression level over the course of the experiment.

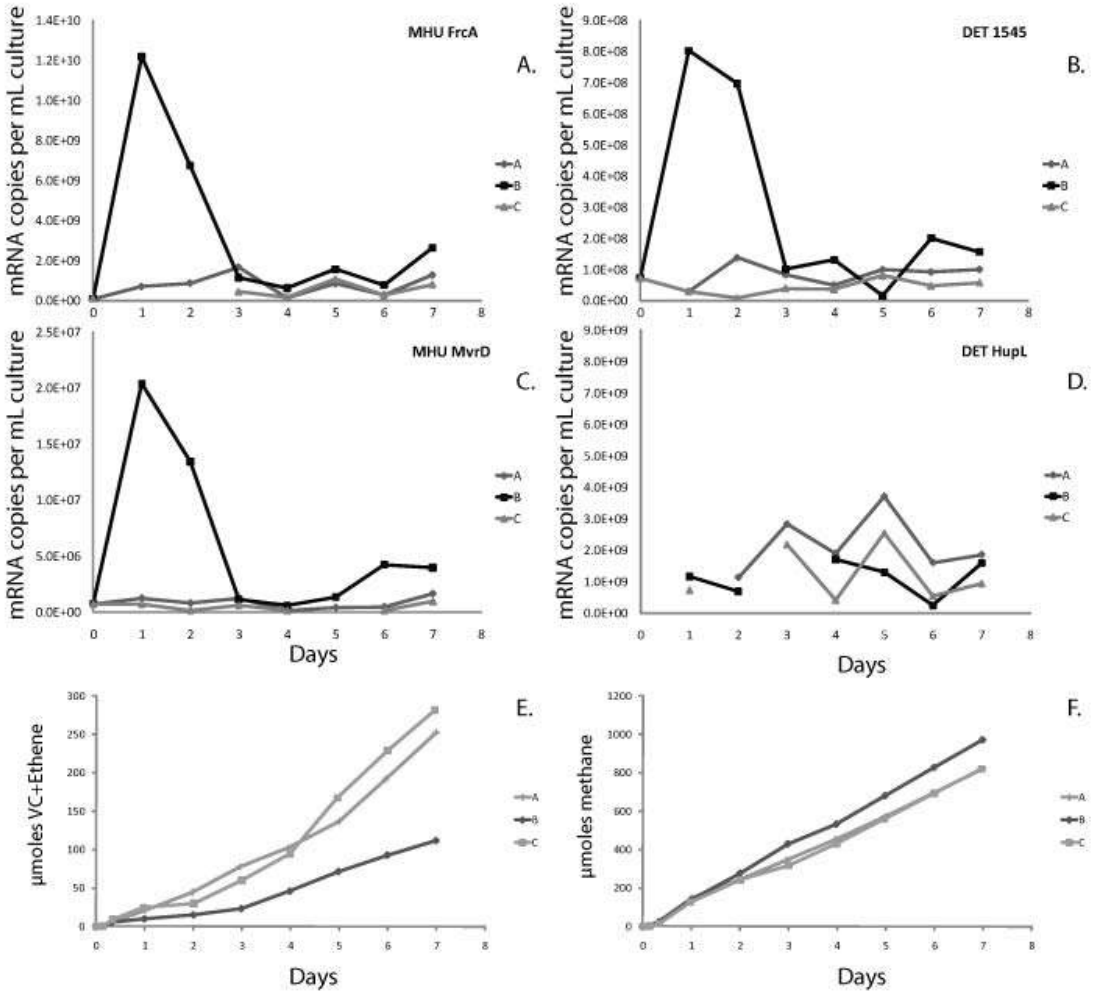

Figure A3.4. Expression time course of DET and MHU mRNAs during donor limited butyrate and PCE fed experiment (ratio of 0.5 to 1 ED to EA) (A-D). Each individual time course represents a biological replicate. Metabolites: PCE respiration products VC and Ethene (E), and methane (F) for these time courses. A syringed clog in replicate B caused decreased PCE addition, (butyrate syringe was not affected). Methane produced during these experiments is the result of acetoclastic and hydrogenotrophic methanogenesis.

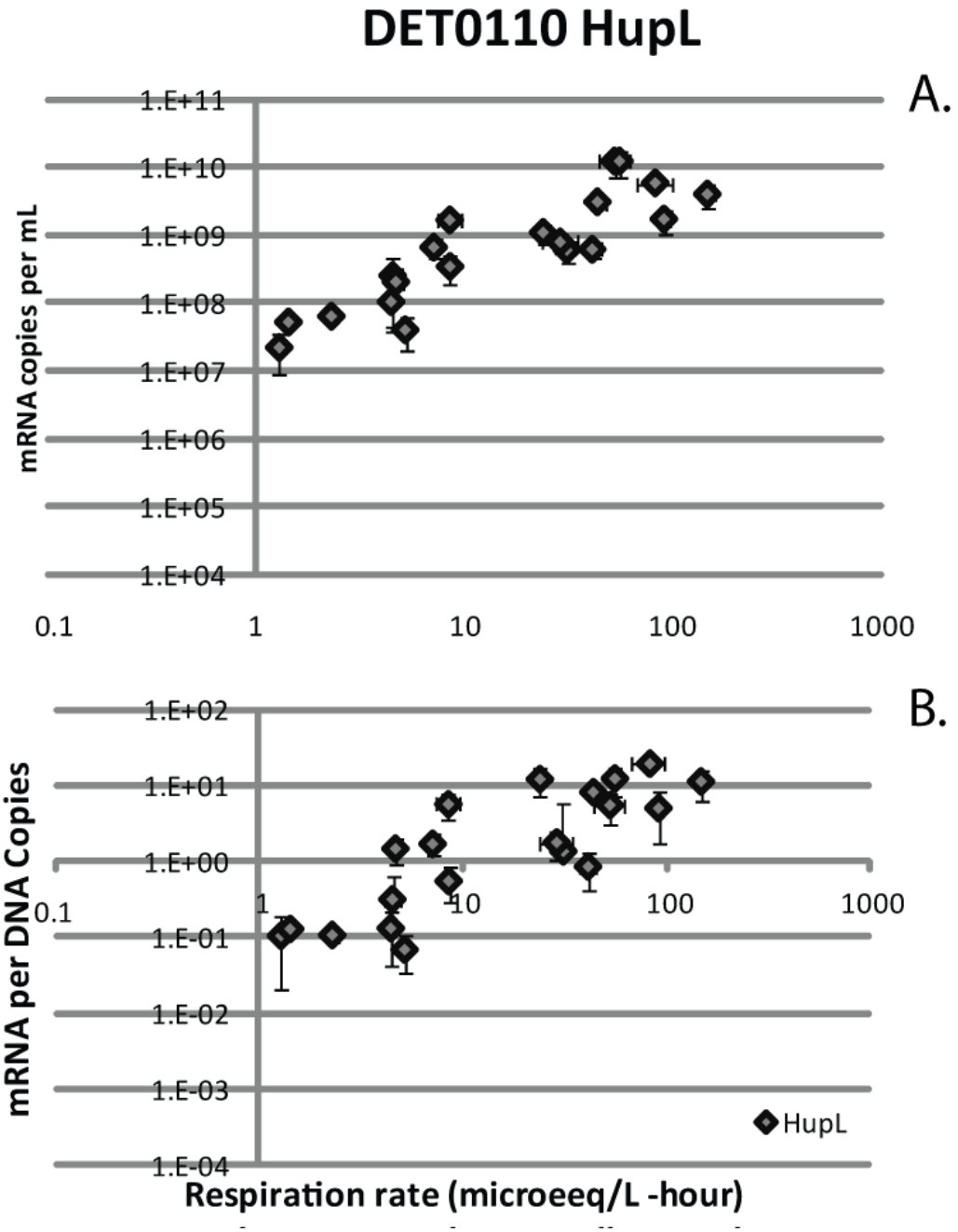

Figure A3.5. Pseudo-steady state respiration rates vs. mRNA concentrations of specific DET hydrogenase DET0110 HupL. Transcripts reported on a per mL (A), and a per 16S rDNA copy (B). Error bars represent standard error of average respiration rates between replicates (x-error bars) and standard deviations of PSS mRNA measurements over time for replicate reactors (y-error bars). For experimental conditions see Table A3.1.

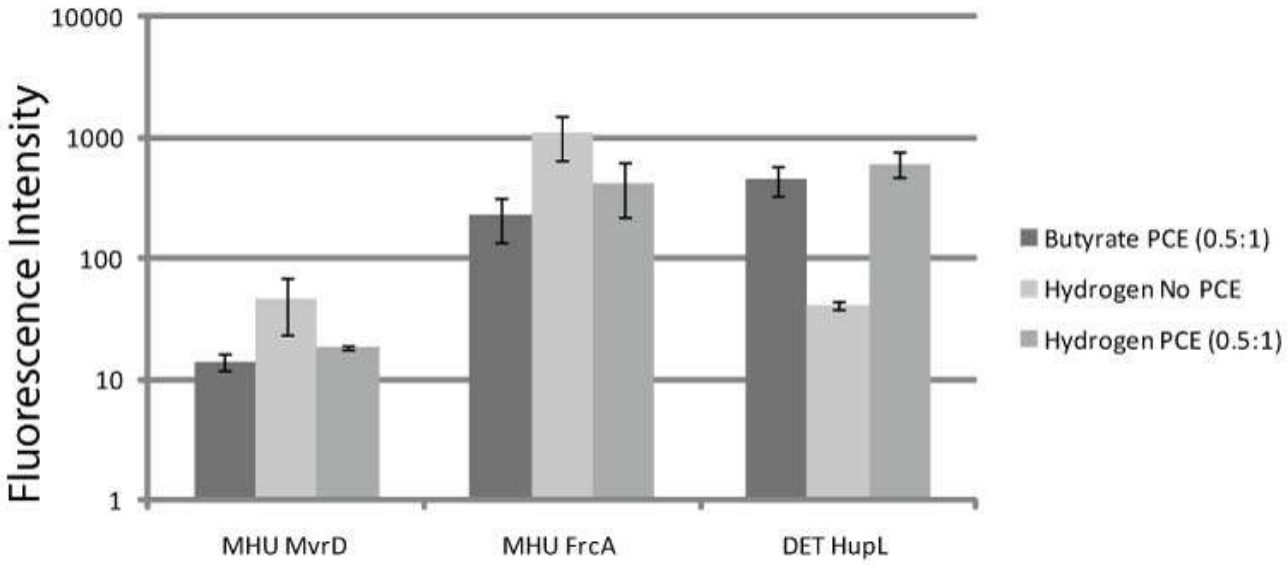

Figure A3.6. Absolute intensity based on mixed culture microarray experiments. Error bars indicate the average intensity measured from 6 to20 replicate probe spots. Data are from experiments with and without PCE added.

REFERENCES

1. **Agilent Technologies**. 2009. Agilent Feature Extraction Software (v10.7) Reference Guide. Santa Clara, CA.

2. **Agilent Technologies.** 2010. Agilent Genomic Workbench 6.0 User Guide. Santa Clara, CA.

3. **Camacho, C., G. Coulouris, V. Avagyan, N. Ma, J. Papadopoulos, K. Bealer, and T.L. Madden**. 2008. BLAST+: architecture and applications. BMC Bioinformatics **10**:421.

4. **Gotz, S., J. M. Garcia-Gomez, J. Terol, T. D. Williams, S. H. Nagaraj, M. J. Nueda, M. Robles, M. Talon, J. Dopazo, and A. Conesa.** 2008. High-throughput functional annotation and data mining with the Blast2GO suite. Nucleic Acids Res. **36:**3420-3435.

5. **Rahm, B.G., R.M. Morris, and R.E. Richardson**. 2006. Temporal expression of respiratory genes in an enrichment culture containing Dehalococcoides ethenogenes. Appl. Environ Microbiol. **72**: 5486–5491.

6. **Smatlak, C. R., J. M. Gossett, and S. H. Zinder.** 1996. Comparative kinetics of hydrogen utilization for reductive dechlorination of tetrachloroethene and methanogenesis in an anaerobic enrichment culture. Environmental Science and Technology. **30:**2850-2858.

7. **Waller A. S.** 2009. Molecular Investigation of Chloroethene Reductive Dehalogenation by the Mixed Microbial Community KB1. Ph.D. Thesis. University of Toronto

8. **Zahurak M., G. Parmigiani, W. Yu, R. B. Scharpf, D. Berman, E. Schaeffer, S. Shabbeer, and L. Cope**. 2007. Pre-processing Agilent microarray data. BMC bioinformatics **8**:142.

APPENDIX IV

Clone Library Blast Analysis

Table A4.1. Nearest cultured neighbors of sequences obtained from Donna Culture clone library as determined by BLAST analysis of 16S rRNA gene.

Clone Designation	Nearest Cultured Neighbor	% Max Identity based on BLAST	Literature-Predicted Physiology
Chlorflexi			
D2CL_Dehalococcoides ethenogenes	*Dehalococcoides ethenogens str. 195*	100	**Reductive Dechlorination**[1]
D2CL_Anaerolinea like sp.	*Anaerolinea thermophila, Longilinea arvoryzae*	92	Carbohydrate fermentation in the presence of yeast extract[2]
Firmicutes			
D2CL_Clostridia/Acetovibrio like sp.	*Clostridium straminisolvens*	86	Cellulose degradation[3]
D2CL_Clostridia like sp.	*Eubacterium acidaminophilum, Clostridium litorale, Alkaliphilus metalliredigens QYMF*	97, 92, 88	Anaerobic fermentation[4]
D2CL_Clostridia/Thermoven abulum like sp	*Tepidanaerobacter syntrophicus*	99	Syntrophic alcohol/lactate fermentation[5]
D2CL_Soehngenia like sp.	*Soehngenia saccharolytica*	98	Fermentation of carbohydrates and yeast extract[6]
D2CL_Anaerovorax like sp.	*Anaerovorax odorimutans*	94	Amino acid fermentation[7]
D2CL_Syntrophomonad/ Aminomonas like sp.	*Aminomonas paucivorans*	89	Asaccharolytic, amino acid fermentation[8]
D2CL_Syntrophomonas like sp.	*Syntrophomonas cellicola, Syntrophomonas wolfei* subsp. *Saponavida*	100, 98	Syntrophic Fatty acid/aromatic acid-degradation[9]
Proteobacteria			
D2CL_Deltaproteobacteria, Smithella/Syntrophus like sp.	*Syntrophus aciditrophicus, Smithella proprianica*	93	Anaerobic Fermentation, propionate degradation[10,11]
D2CL_Epsilon-Proteobacteria, Sulfricurvum like sp.	*Sulfuricurvum kujiense*	96	Nitrate reduction, sulfur or H2 donor[12]
Nitrospira			
D2CL_Nitrospiralers, Magnetobacterium like sp.	*Candidatus Magnetobacterium*	86	Speculated sulfur oxidation and/or iron reduction[13]

	bavaricum		
Spirochetes			
D2CL_Spirochetes, Treponema like sp.	*Treponema azonutricium*	87	Anaerobic fermentation, non homo acetogneic[14]
Bacteriodetes			
D2CL_Bacteroidetes	*Petrimonas sulfuriphila*	99	Anaerobic Fermentation or Sulfur, nitrate and Fe reduction[15]
Thermotogales			
D2CL_Thermotoga like sp.	*Fervidibacterium islandicum, Thermosipho melanesiensis BI429, Thermotoga petrophila*	86, 86, 85	Keritin degrader, deep sea hydrothermal vent organism, fatty acid degrader[16]
Methanomicrobia			
D2CL_Methanosatea like sp.	*Methanosaeta thermophila*	97	**Acetoclastic methanogenesis[17]**
D2CL_Methanospirillum hungatei like sp.	*Methanospirillum hungatei JF1*	97	**Hydrogenotrophic methanogenesis[17]**

References:

1. MaymoGatell, X; *et al.* Sci. **1997**, 276 (5318): 1568- 1571.
2. Sekiguchi, Y.; *et al.* IJSEM. **2003**, 53: 1843-1851.
3. Kato, S.; *et al*. ISJEM. **2004**, 54: 2043-2047.
4. Paredes, C.J .; *et al.* Nat.Rev.Micro., **2005**, 3, 969-978.
5. Sekiguchi, Y.: *et al.* ISJEM. **2006,** 56: 1621-1629.
6. Parshina, S.; *et al.* ISJEM. **2003**, 53: 1791-1799.
7. Matthies, C.; *et al.* IJSB. **2000**, 50: 1591-1594.
8. Beana, S.; *et al.* IJSB. **1999**, 49: 975-982.
9. Wu, C.; *et al*. ISJEM. **2006, 56**: 2331-2335.
10. McInerney, M.; *et al*. PNAS. **2007**, 104(18): 7600-7605.
11. Liu, Y.; *et al.* IJSB. **1999**, 49: 545-556.
12. Kodama, Y.; *et al.* ISJEM. **2004**, 54: 2297-2300.
13. Spring, S.; *et al.* AEM. **1993,** 59(8): 2397-2403.
14. Graber, J.; *et al.* AEM. **2004,** 70(3): 1315-1320.
15. Grabowski, A.; *et al.* ISJEM. **2005**, 55: 1113-1121.
16. Conners, S.; *et al.* FEMS Rev.Micro**. 2006**, 30(6): 872-905.
17. Garcia, J.; *et al.* Anaerobe. **2000**, 6(4): 205-226

APPENDIX V

Multiple Reaction Monitoring Standard Curves for Peptide Quantification

NOTE: “Jeff’s” refers to standard curve from 2008 and reported in Werner et al. (2009, Environmental Microbiology). “tsX” refers to the specific transition ion (parent ion/fragment ion pair)

A5.1. TceA Peptide Standard Curves

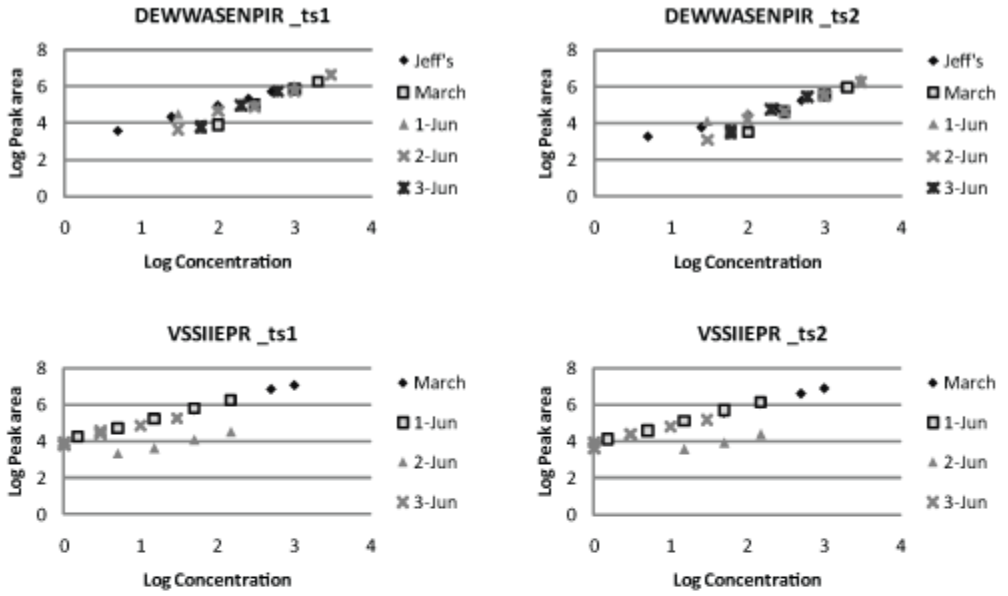

A5.2. HupL Peptide Standard Curves

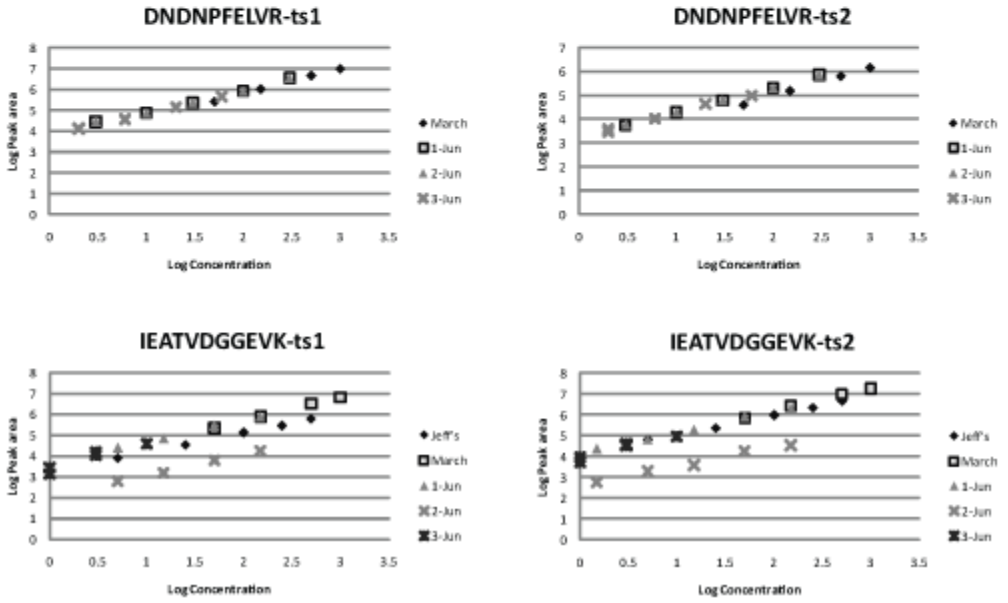

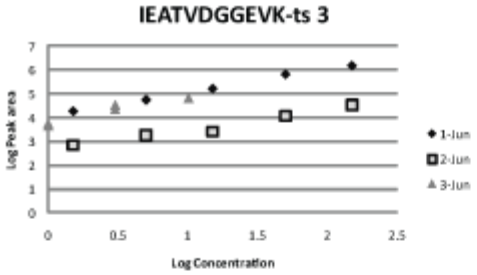

A5.3. S-Layer Peptide Standard Curves

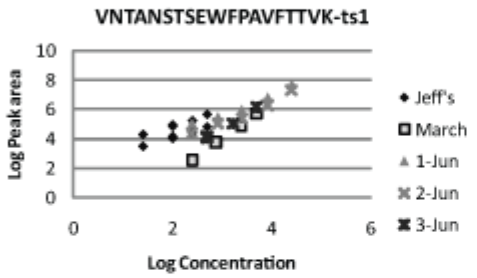

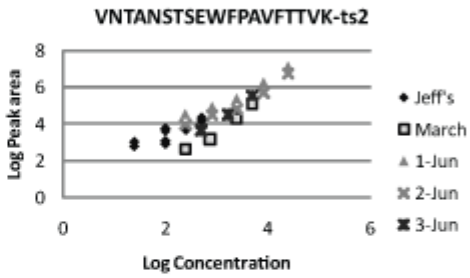

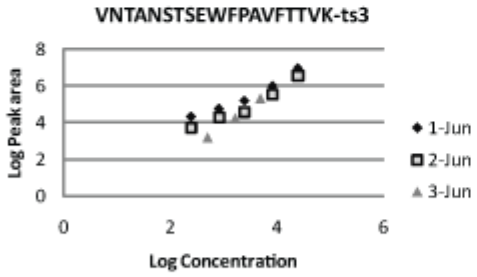

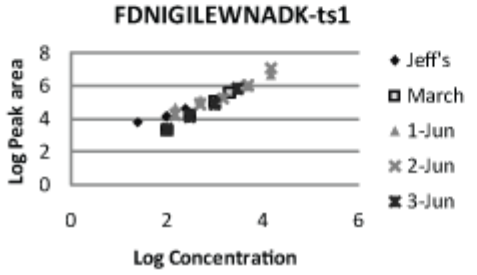

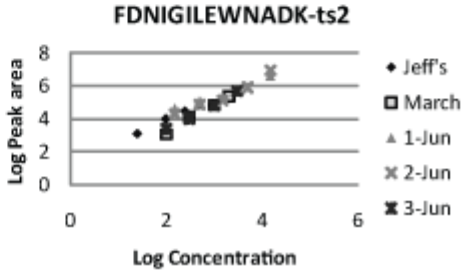

A5.4. DET EF-TU Peptide Standard Curves

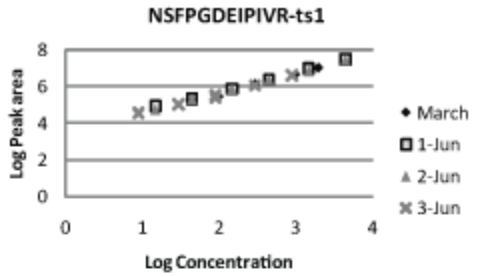

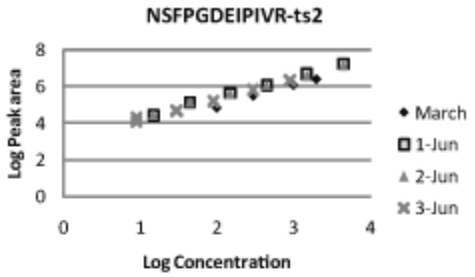

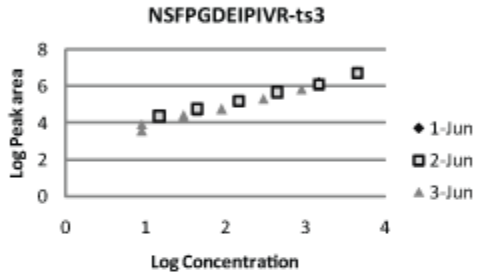

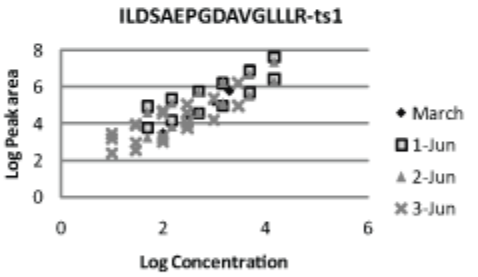

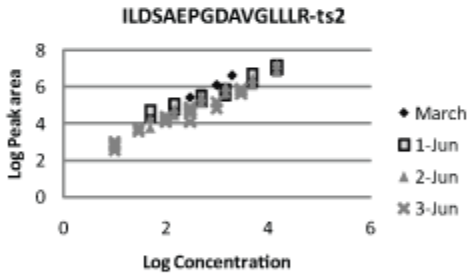

A5.5. PceA Peptide Standard Curves

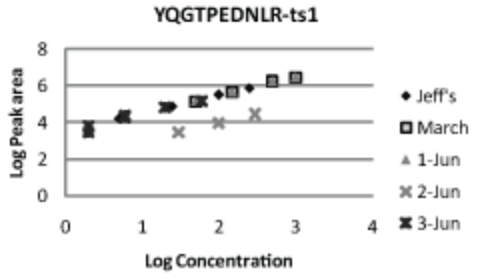

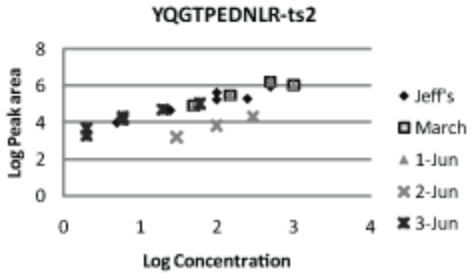

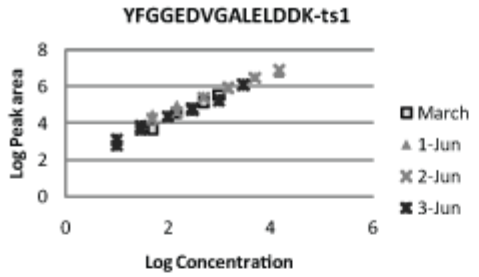

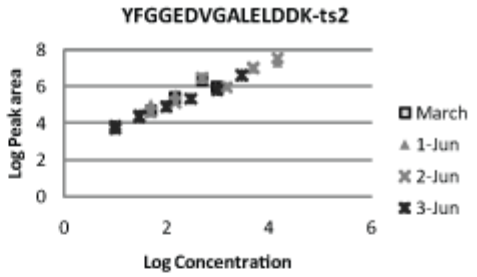

A5.6. DET1545 Peptide Standard Curves

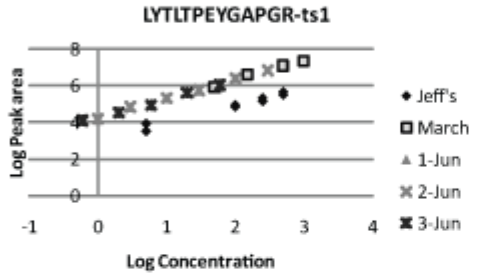

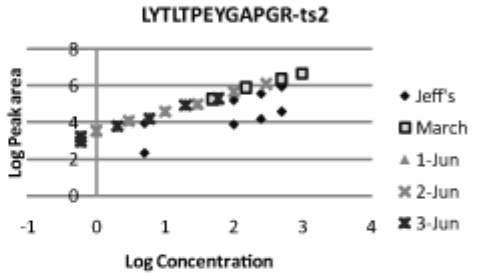

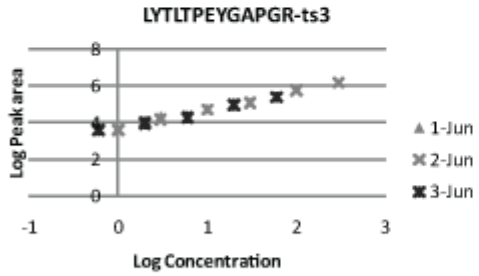

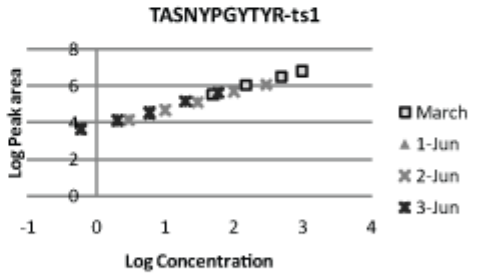

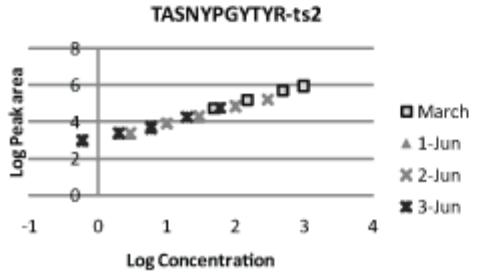

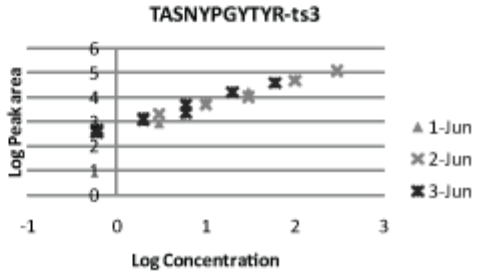

A5.7. DET1559 Peptide Standard Curves

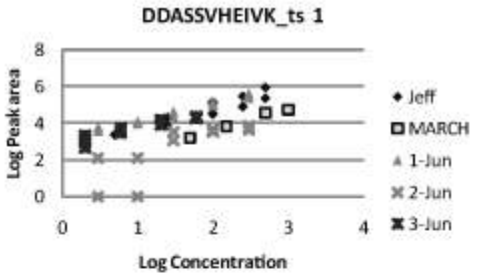

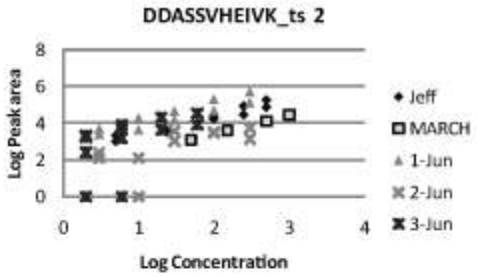

A5.8. GroEL Peptide Standard Curves

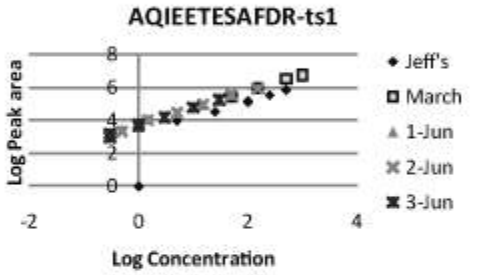

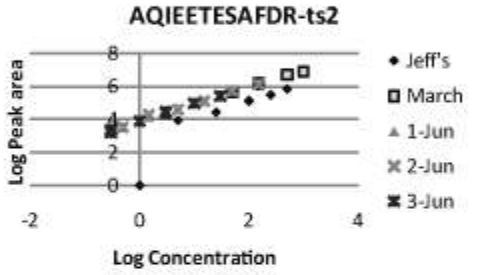

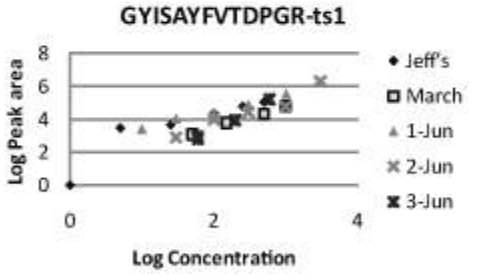

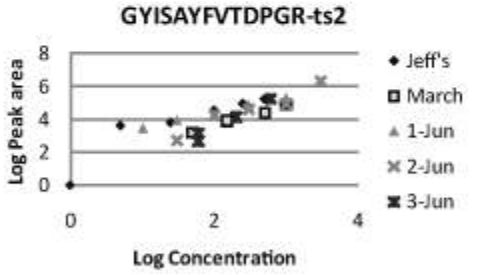

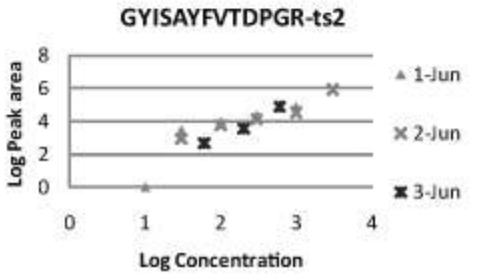

A5.9. DET rp L7 Peptide Standard Curves

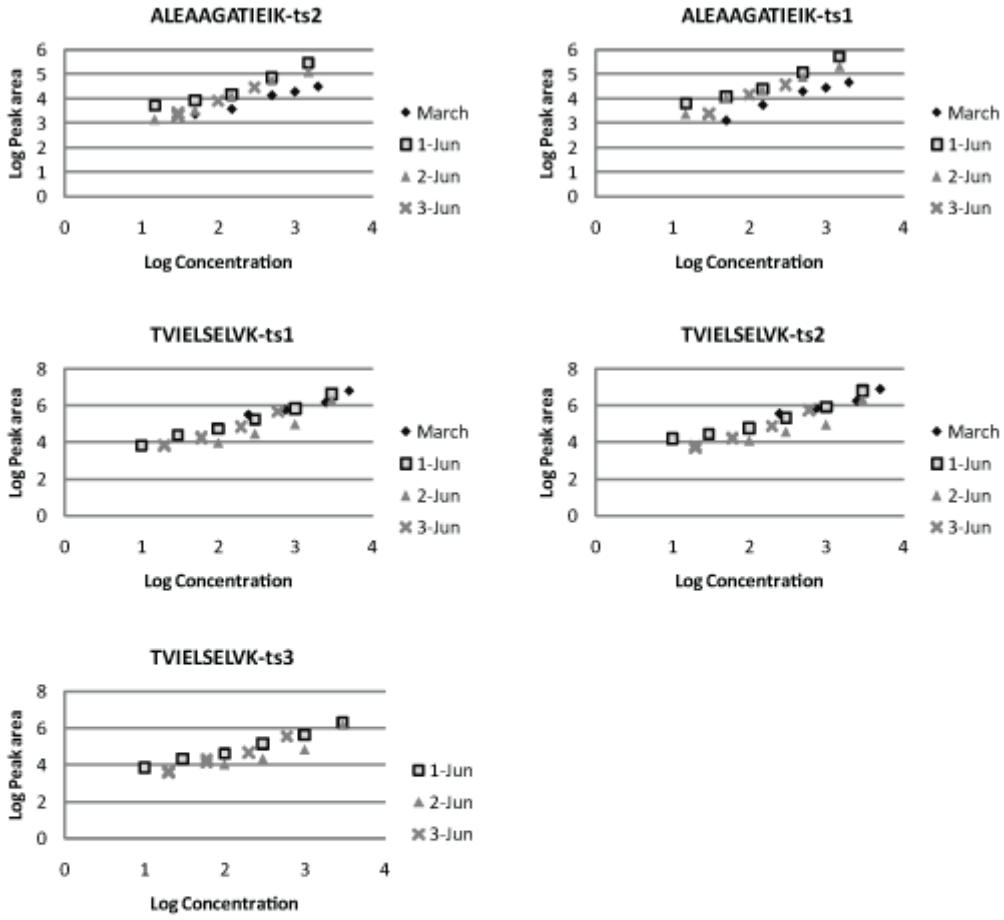

A5.10. RpoC Peptide Standard Curves

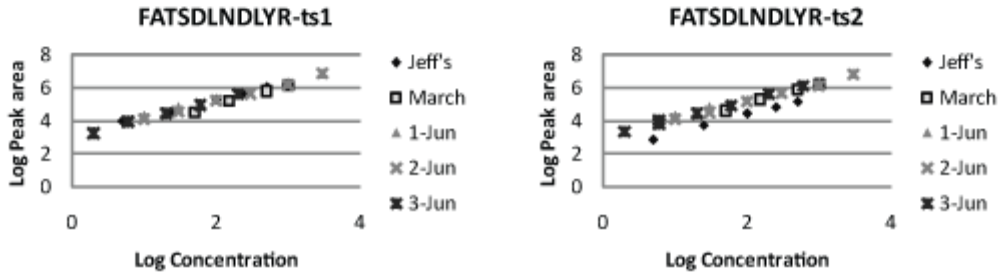

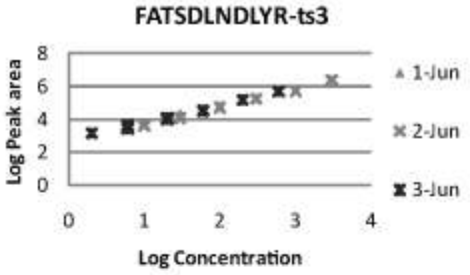

A5.11. MHU EF-1 alpha Peptide Standard Curves

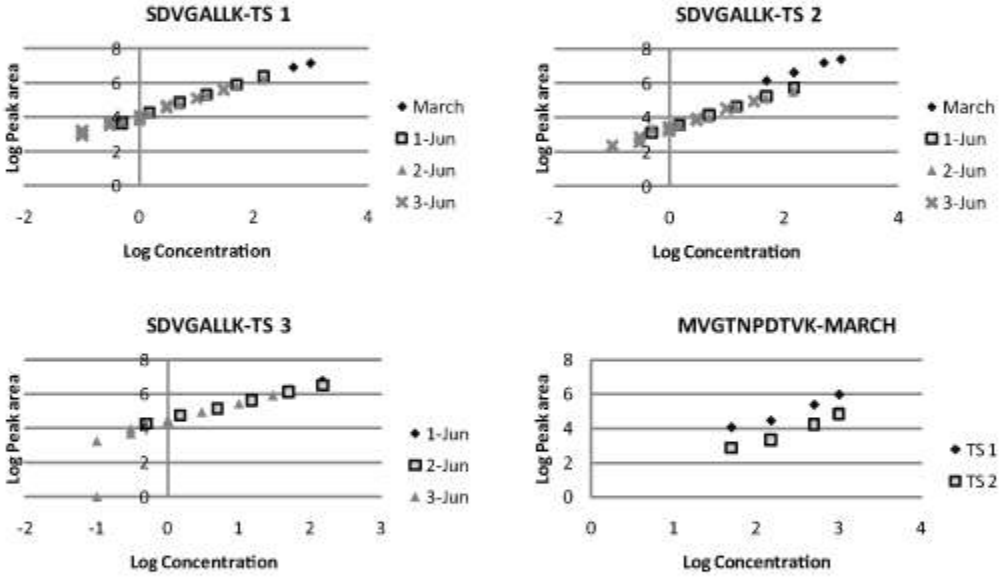

A5.12. MHU rp L12AE/ rp L7AE Peptide Standard Curves

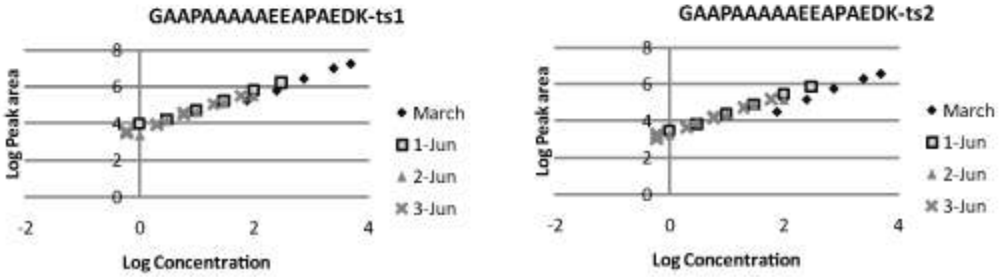

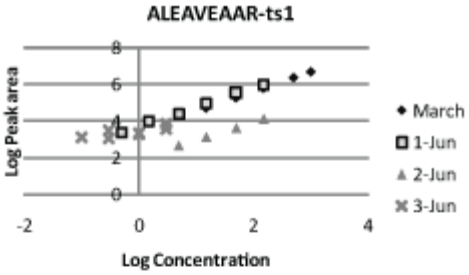

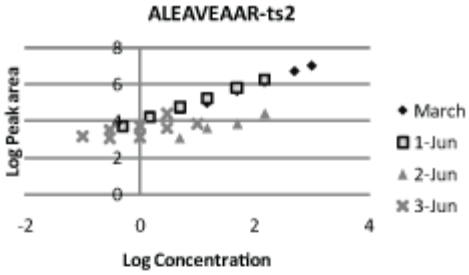

A5.13. MHU FrcA Peptide Standard Curves

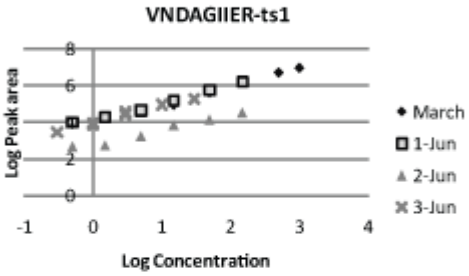

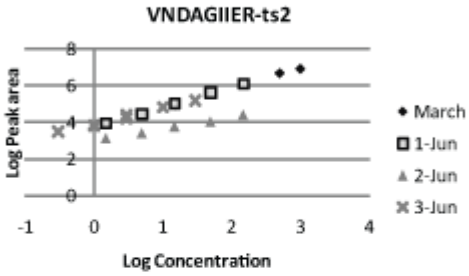

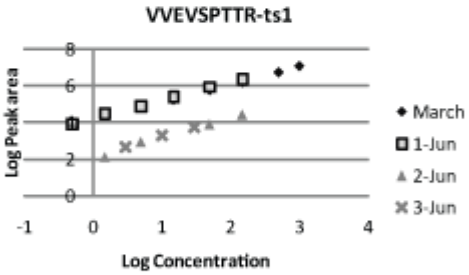

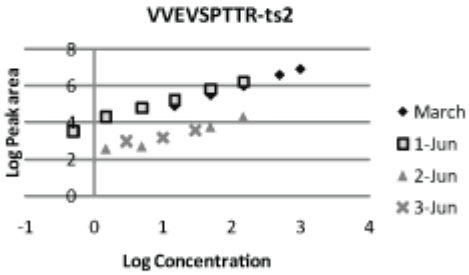

A5.14. MHU MvrD Peptide Standard Curves

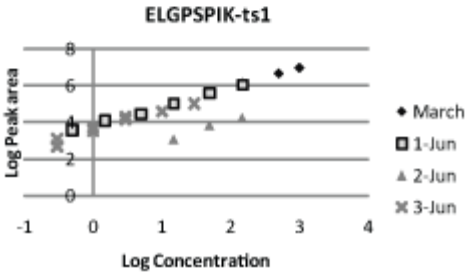

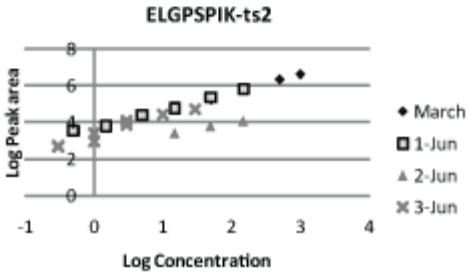

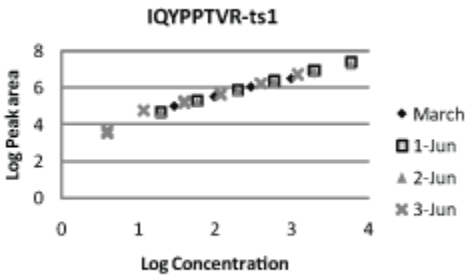
IQYPPTVR-ts1
Log Peak area
Log Concentration
March
1-Jun
2-Jun
3-Jun

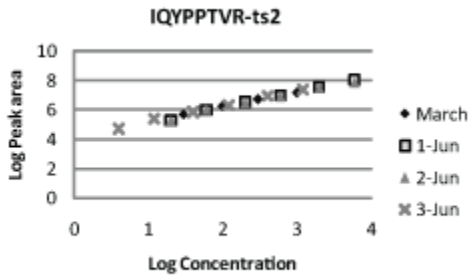
IQYPPTVR-ts2
Log Peak area
Log Concentration
March
1-Jun
2-Jun
3-Jun

APPENDIX VI

Sample Chromatograms for MRM Peptide Targets

Sample coding: AR_XXX_YY.
XXX= sample ID and digest replicate
YY= injection # on specific run day.

A6.1. TceA Peptide Example Chromatograms

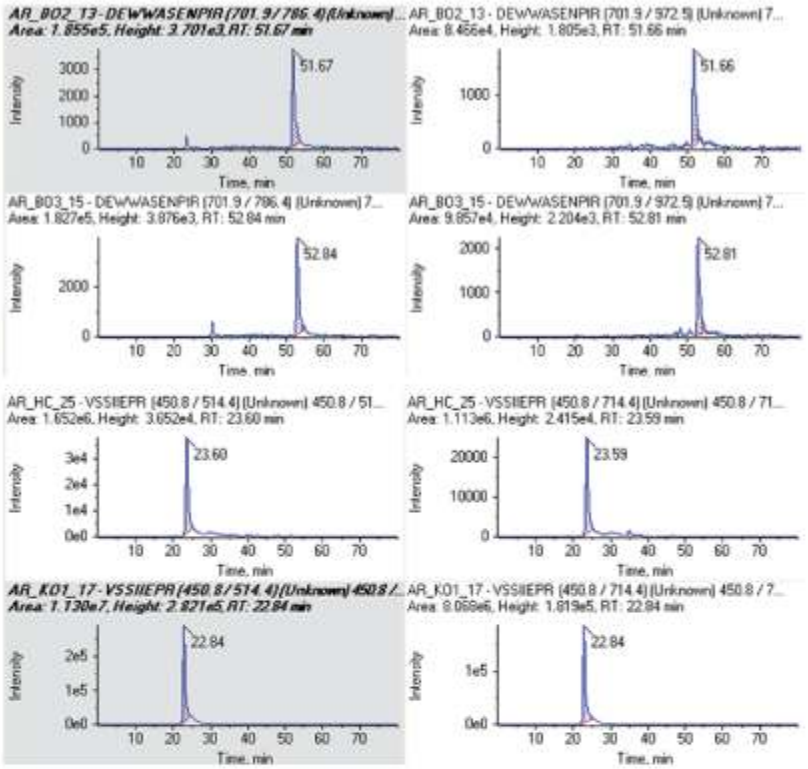

A6.2. HupL Peptide Example Chromatograms

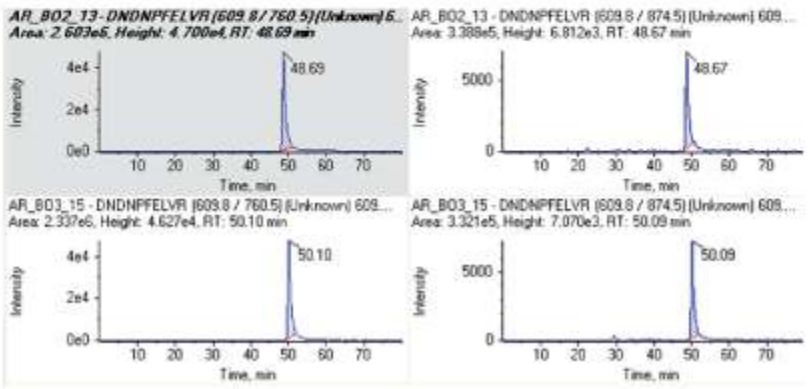

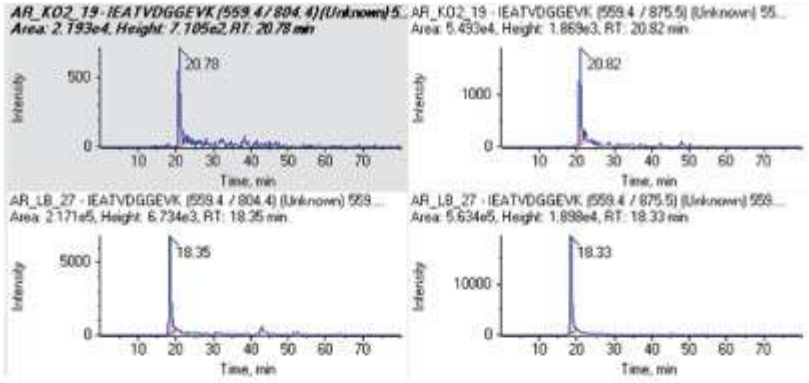

A6.3. S-Layer Peptide Example Chromatograms

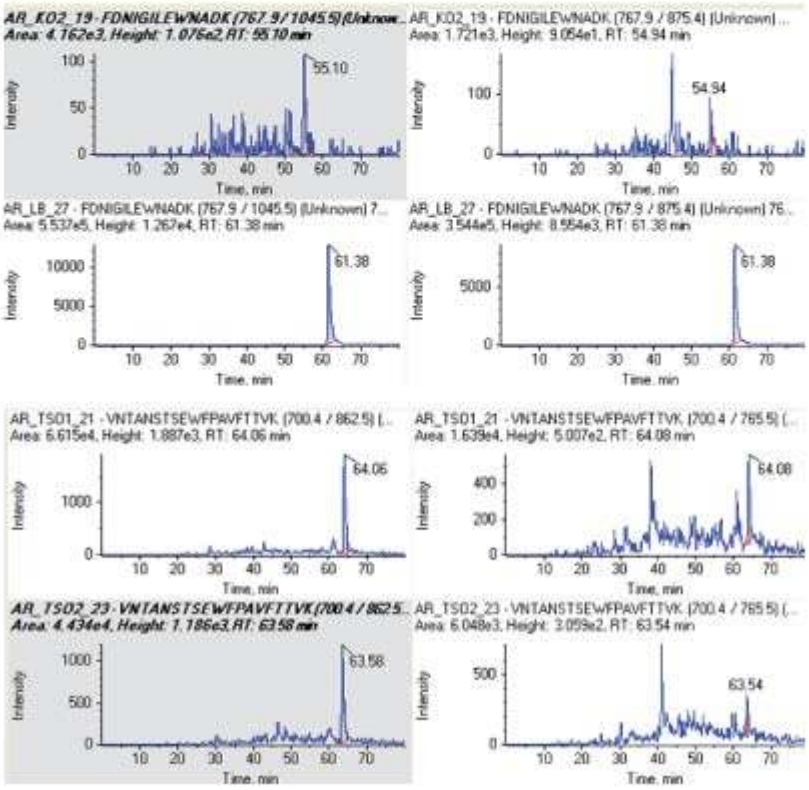

A6.4. DET EF-TU Peptide Example Chromatograms

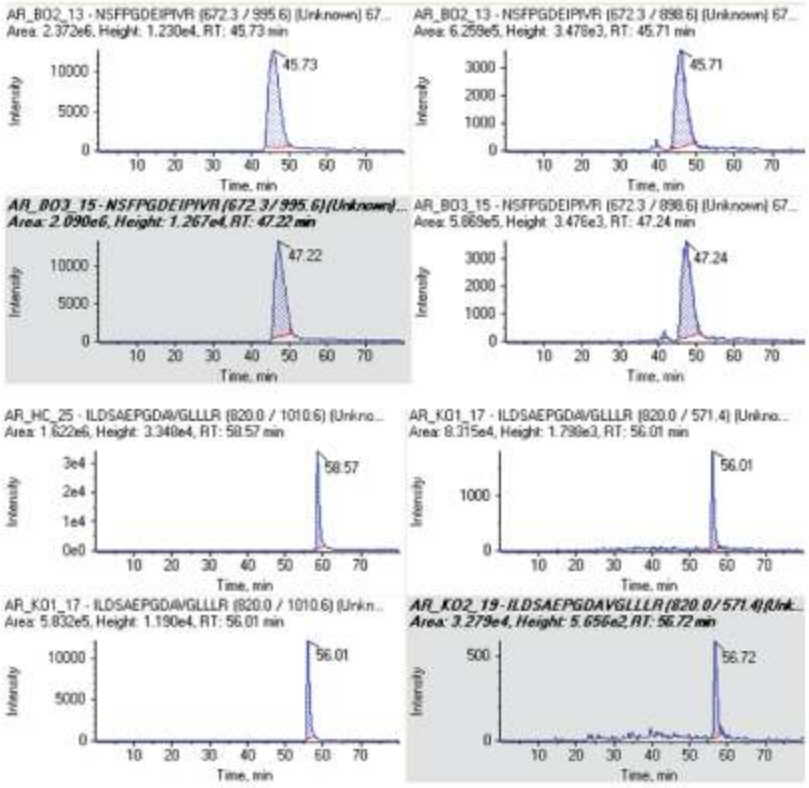

A6.5. PceA Peptide Example Chromatograms

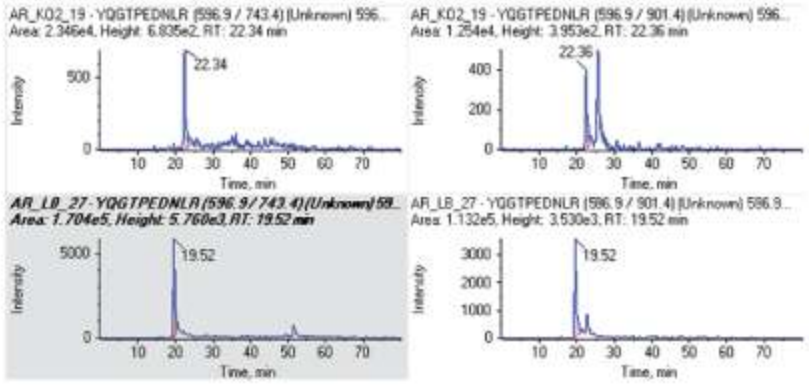

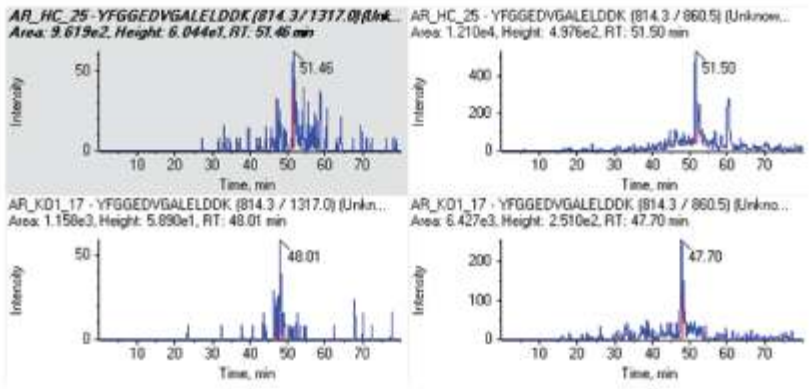

A6.6. DET1545 Peptide Example Chromatograms

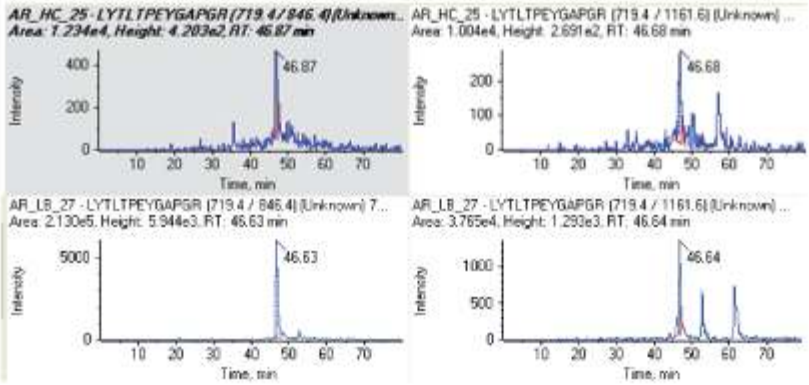

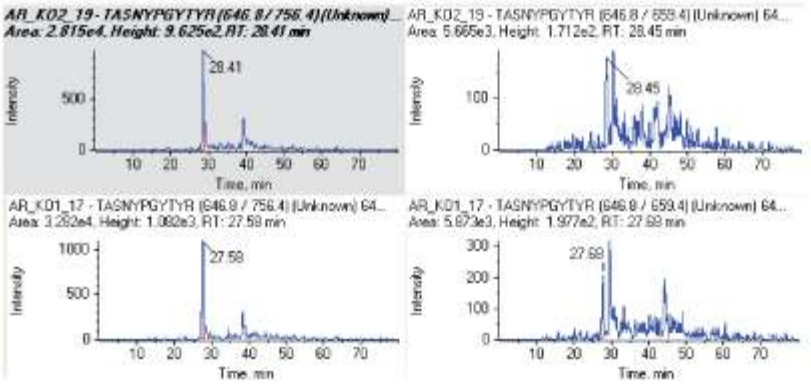

A6.7. DET1559 Peptide Example Chromatograms

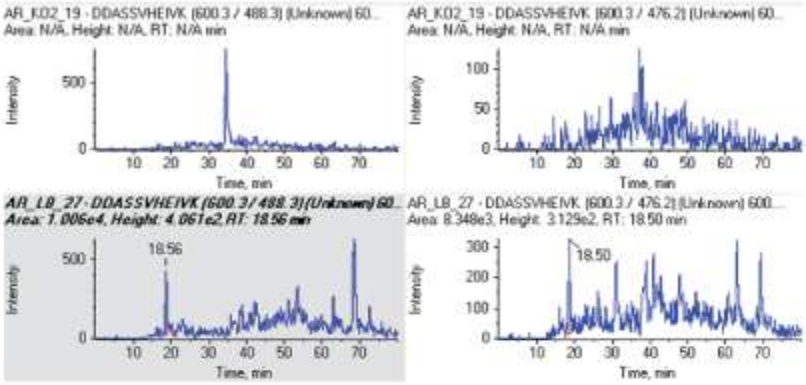

A6.8. GroEL Peptide Example Chromatograms

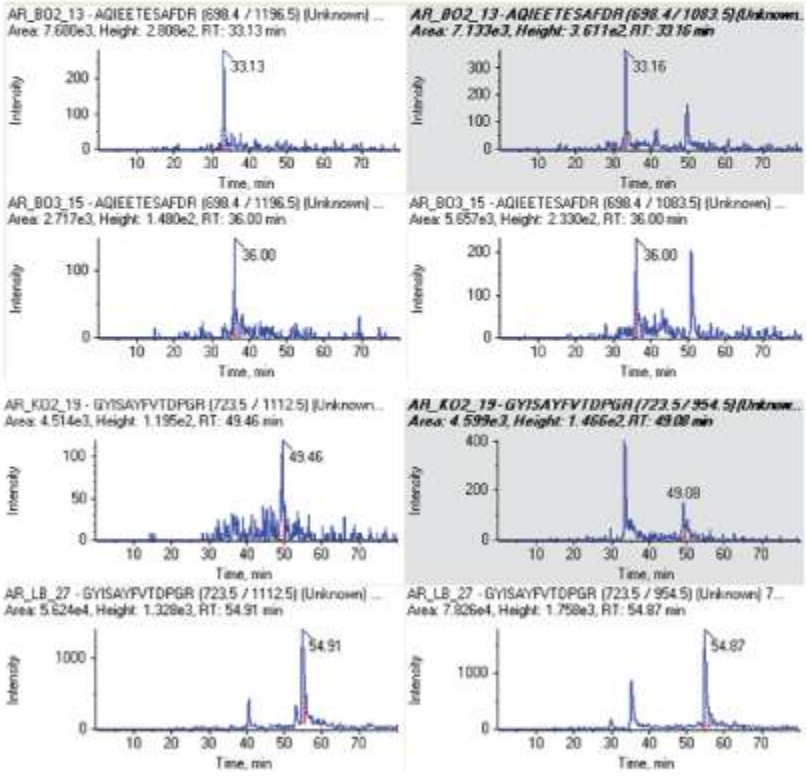

A6.9. DET rp L7 Peptide Example Chromatograms

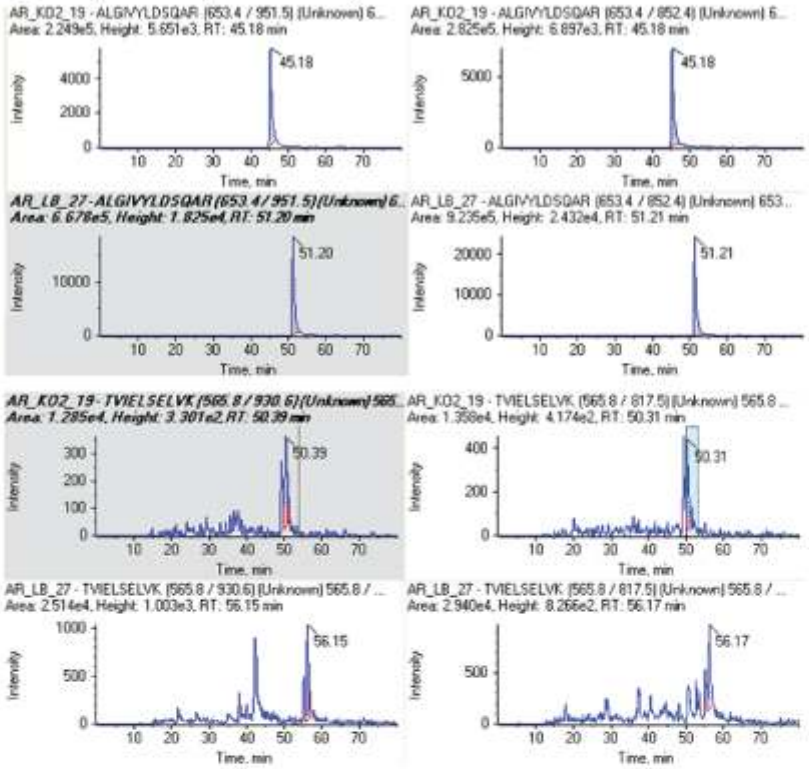

A6.10. RpoC Peptide Example Chromatograms

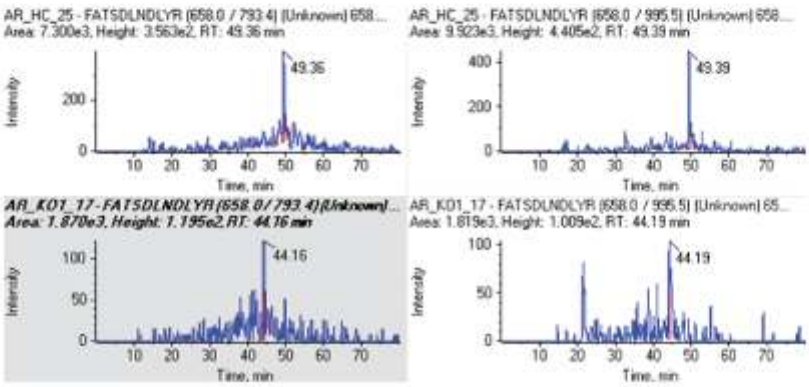

A6.11. MHU EF-1 alpha Peptide Example Chromatograms

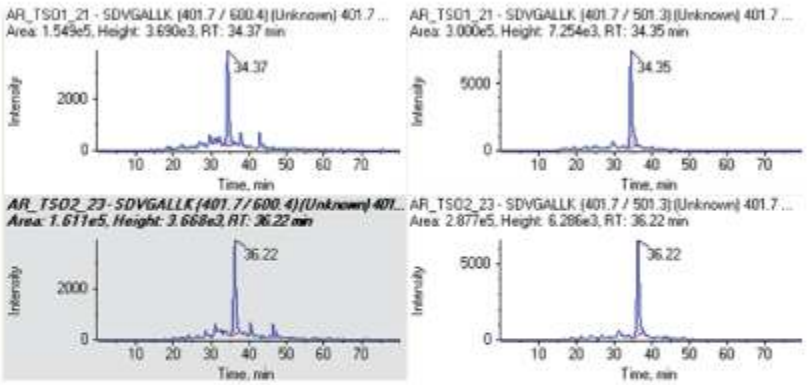

A6.12. MHU rp L12AE/ rp L7AE Peptide Example Chromatograms

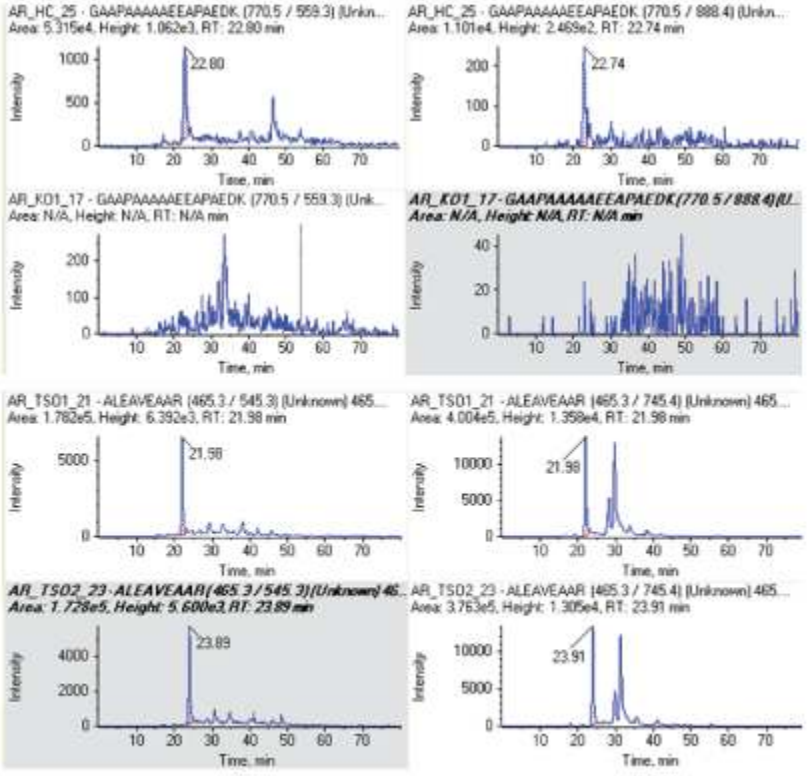

A6.13. MHU FrcA Peptide Example Chromatograms

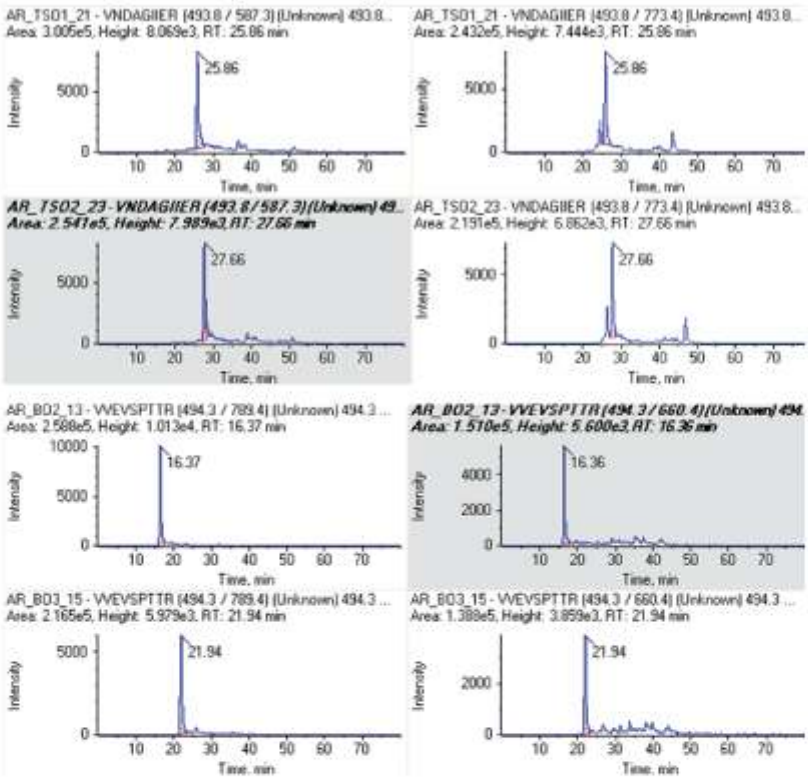

A6.14. MHU MvrD Peptide Example Chromatograms

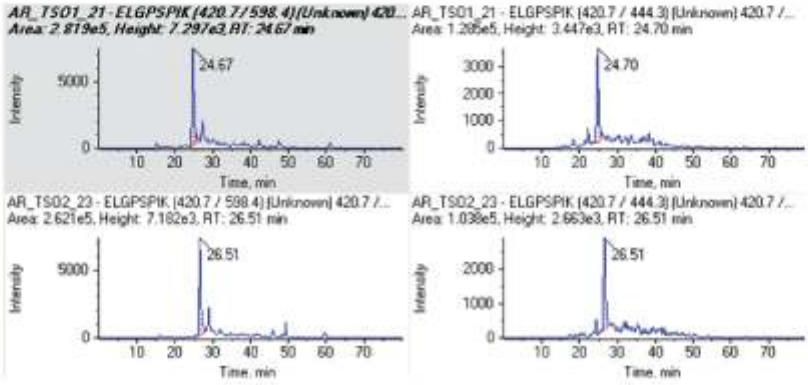

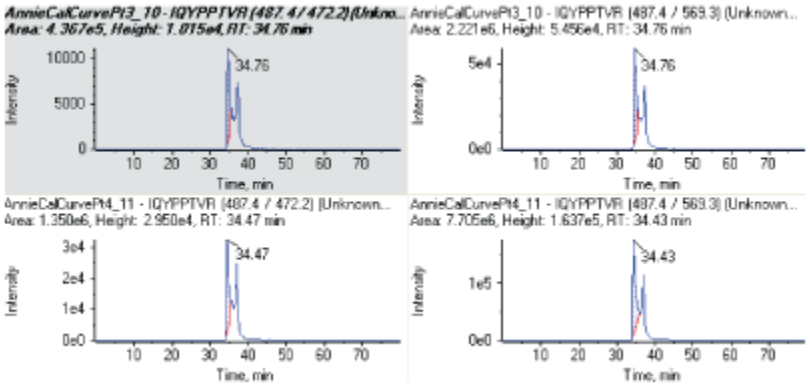
AnnieCalCurvePt3_10 - IQYPPTVR (487.4 / 472.2) (Unkno...
Area: 4.367e5, Height: 1.015e4, RT: 34.76 min
Intensity
10000
5000
0
34.76
10 20 30 40 50 60 70
Time, min
AnnieCalCurvePt3_10 - IQYPPTVR (487.4 / 569.3) (Unknown...
Area: 2.221e6, Height: 5.456e4, RT: 34.76 min
Intensity
5e4
0e0
34.76
10 20 30 40 50 60 70
Time, min
AnnieCalCurvePt4_11 - IQYPPTVR (487.4 / 472.2) (Unknown...
Area: 1.350e6, Height: 2.950e4, RT: 34.47 min
Intensity
3e4
2e4
1e4
0e0
34.47
10 20 30 40 50 60 70
Time, min
AnnieCalCurvePt4_11 - IQYPPTVR (487.4 / 569.3) (Unknown...
Area: 7.705e6, Height: 1.637e5, RT: 34.43 min
Intensity
1e5
0e0
34.43
10 20 30 40 50 60 70
Time, min